

Chloride diffusion in concrete/prediction of the onset of corrosion in reinforced concrete structures

Navaz Cheriya Malikakkal

Civil Engineering

December, 1994

Abstract

Deterioration of concrete structures due to the corrosion of reinforcement is the major problem of durability in the Gulf countries. It is necessary to study the diffusion of chloride ions in concrete, to determine the time for the onset of corrosion in concrete structures. This research was aimed at determining the diffusion coefficients for chloride ions in Type V Sulphate Resisting Cement concrete made from local materials, using two approaches: (a) Sustained chloride exposure test, assuming the applicability of Fick's laws of diffusion for the transport of chloride ions, and (b) Gas diffusion tests which have never been applied to concrete before.

The results indicate that the effective diffusion coefficients (D_e) for chloride ions in concrete is dependent on the water-cement ratio, cement content and exposure conditions, but are independent of the exposure chloride concentrations. From a non-linear regression analysis of the test results, D_e is expressed in terms of w/c ratio and cement content. The gas diffusion test appears to be a promising rapid technique for evaluating D_e for chloride ion in concrete. It is also observed that under idealized conditions, the solution to Fick's second law for the appropriate boundary conditions can be used to reasonably predict the time to initiation of corrosion.

Chloride Diffusion in Concrete / Prediction of the Onset of Corrosion in Reinforced Concrete Structures

by

Navaz Cheriya Malikakkal

A Thesis Presented to the

FACULTY OF THE COLLEGE OF GRADUATE STUDIES

KING FAHD UNIVERSITY OF PETROLEUM & MINERALS

DHAHRAN, SAUDI ARABIA

In Partial Fulfillment of the
Requirements for the Degree of

MASTER OF SCIENCE

In

CIVIL ENGINEERING

December, 1994

INFORMATION TO USERS

This manuscript has been reproduced from the microfilm master. UMI films the text directly from the original or copy submitted. Thus, some thesis and dissertation copies are in typewriter face, while others may be from any type of computer printer.

The quality of this reproduction is dependent upon the quality of the copy submitted. Broken or indistinct print, colored or poor quality illustrations and photographs, print bleedthrough, substandard margins, and improper alignment can adversely affect reproduction.

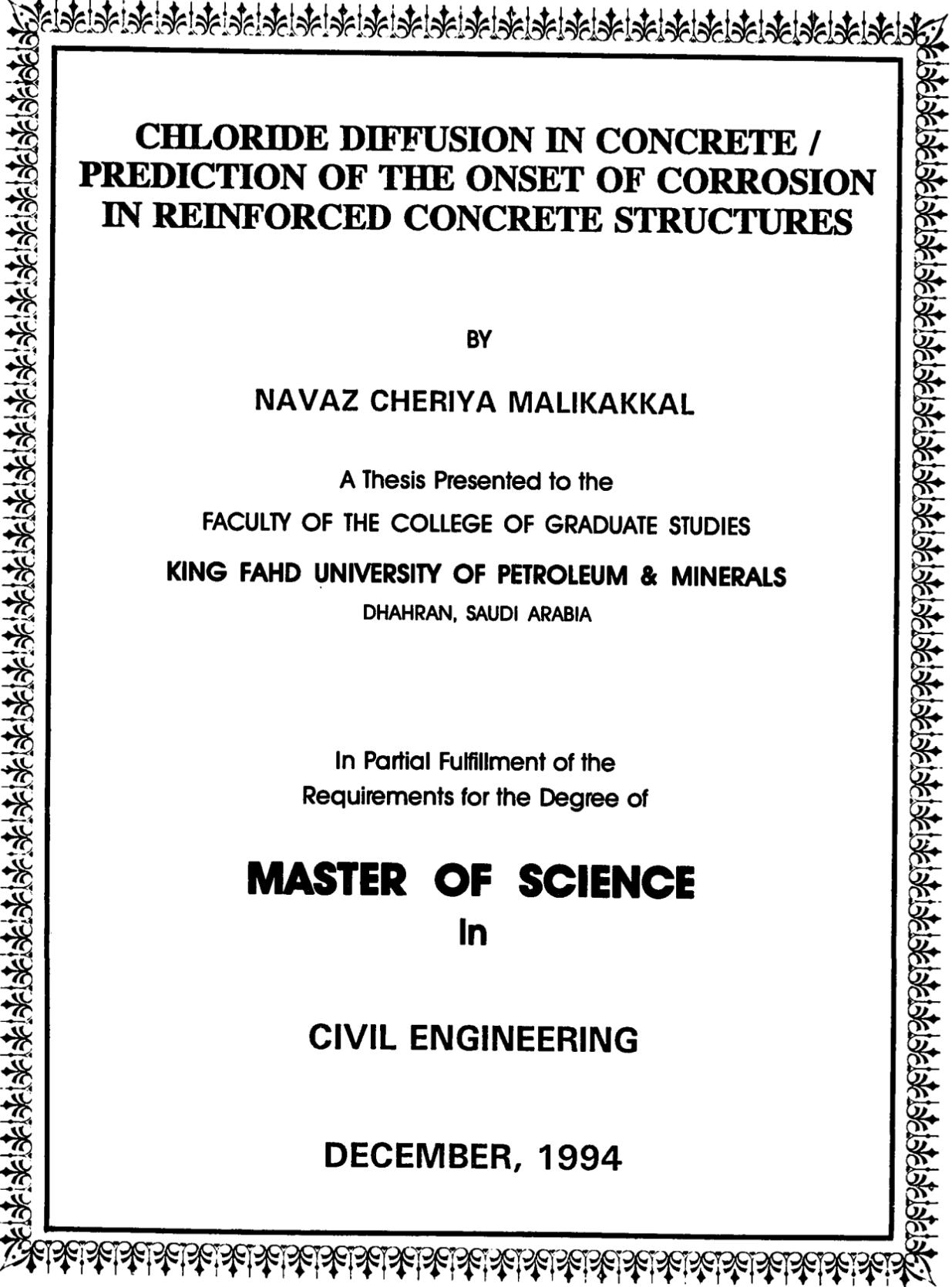
In the unlikely event that the author did not send UMI a complete manuscript and there are missing pages, these will be noted. Also, if unauthorized copyright material had to be removed, a note will indicate the deletion.

Oversize materials (e.g., maps, drawings, charts) are reproduced by sectioning the original, beginning at the upper left-hand corner and continuing from left to right in equal sections with small overlaps. Each original is also photographed in one exposure and is included in reduced form at the back of the book.

Photographs included in the original manuscript have been reproduced xerographically in this copy. Higher quality 6" x 9" black and white photographic prints are available for any photographs or illustrations appearing in this copy for an additional charge. Contact UMI directly to order.

UMI

A Bell & Howell Information Company
300 North Zeeb Road, Ann Arbor, MI 48106-1346 USA
313/761-4700 800/521-0600



**CHLORIDE DIFFUSION IN CONCRETE /
PREDICTION OF THE ONSET OF CORROSION
IN REINFORCED CONCRETE STRUCTURES**

BY

NAVAZ CHERIYA MALIKAKKAL

A Thesis Presented to the
FACULTY OF THE COLLEGE OF GRADUATE STUDIES
KING FAHD UNIVERSITY OF PETROLEUM & MINERALS
DHAHRAN, SAUDI ARABIA

In Partial Fulfillment of the
Requirements for the Degree of

MASTER OF SCIENCE
In

CIVIL ENGINEERING

DECEMBER, 1994

UMI Number: 1362020

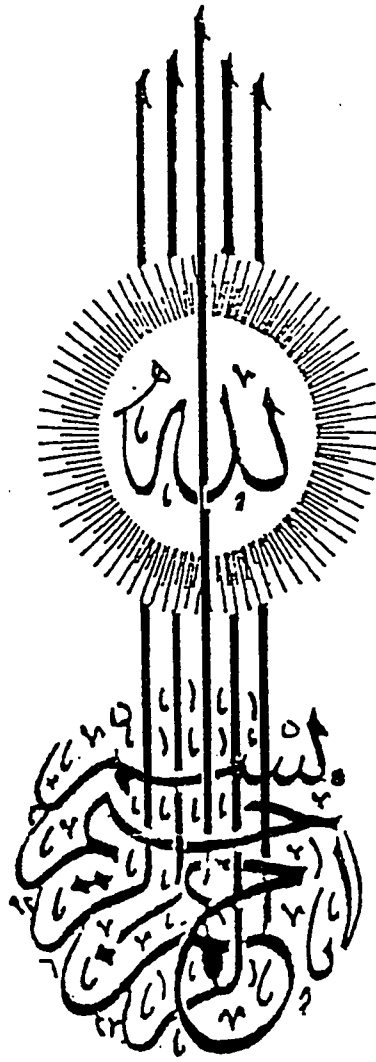
UMI Microform 1362020

Copyright 1995, by UMI Company. All rights reserved.

**This microform edition is protected against unauthorized
copying under Title 17, United States Code.**

UMI

**300 North Zeeb Road
Ann Arbor, MI 48103**



سُبْحَانَكَ لَا عِلْمَ لَنَا إِلَّا مَا عَلَّمْتَنَا إِنَّكَ أَنْتَ الْعَلِيمُ الْحَكِيمُ

(Glory to Thee: Of knowledge we have none, save what Thou hast taught us: In truth; it is Thou who art perfect in knowledge and wisdom.)

(2:32)

KING FAHD UNIVERSITY OF PETROLEUM & MINERALS
DHAHRAN, SAUDI ARABIA

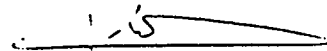
This thesis, written by

Navaz Cheriya Malikakkal

*under the direction of his Thesis Advisor, and approved by his Thesis committee, has
been presented to and accepted by the Dean, College of Graduate Studies, in partial
fulfillment of the requirements for the degree of*

MASTER OF SCIENCE IN CIVIL ENGINEERING (Structures)

Thesis Committee:



Chairman (Dr. Alfarabi M. Sharif)



Co-Chairman (Prof. Abul Kalam Azad)



Member (Dr. Husain Jubran Al-Gahtani)



Member (Dr. Kevin F. Loughlin)



Dr. Alfarabi M. Sharif
Department Chairman



Dr. Ala H. Rabeh
Dean, College of Graduate Studies

Date: 5-2-05



To

my dearest Uppava & Umma

for their love, sacrifices, prayers and understanding

ACKNOWLEDGEMENTS

All thanks are to ALLAH SUBHANAHU WATALA for having made it possible for me to complete this research successfully. Acknowledgements are due to King Fahd University of Petroleum & Minerals for having given me the opportunity to pursue my graduate study here, for the facilities extended and finally for the financial support provided.

I am extremely thankful and deeply indebted to my thesis Committee Chairman Dr. Alfarabi Sharif, Co-chairman Prof. Abul Kalam Azad, and Committee Member Dr. Kevin F. Loughlin for their constant guidance, help and attention throughout this research. Thanks are also due to Committee Member Dr. Husain Jubran Al-Gahtani for his valuable comments and suggestions. I am also thankful to Dr. Mohammed Malehuddin for his help during various stages of this work. I take this opportunity to express my sincere appreciation and thanks to Mr. Ibrahim Asi for his constant help throughout my course of study here and for having allowed me to use the department vehicles and his PC. Thanks to Mr. Cudapah Niyazi Sadath for teaching me to use the set up for corrosion potential and corrosion current measurements, Dr. Omar Bagabrah for his suggestions on the slides for presentation, Mr. Omar for his help at various occasions, especially in drawing the flow-charts,

Mr. Abdullappa, the Late Mr. Essam, Mr. Mohammed Nahash, Mr. Hasan Zakariya and other staff of the civil engineering laboratories for their help during various stages of this work. I would like to express my thanks to Mr. John and Mr. Romeo of the chemical engineering workshop for fabricating the gas diffusion test set up.

I also express my thanks for my dear friend Vinu for his care and help at certain critical points. Thanks to my friend Rauf for his help and company right from the very first day of classes. Special thanks are to Abbas Qureshi (goli) for his concern, help, understanding, unlimited (goal) fundaes and above all his support at all difficult times.

Last but not the least, I thank my parents, sisters, K.A., in-laws, my brothers Riza and Ashraf, all my friends, teachers, colleagues and well-wishers. These three years in fact will always be cherished.

ABSTRACT

Deterioration of concrete structures due to the corrosion of reinforcement is the major problem of durability in the Gulf countries. It is necessary to study the diffusion of chloride ions in concrete, to determine the time for the onset of corrosion in concrete structures. This research was aimed at determining the diffusion coefficients for chloride ions in Type V Sulphate Resisting Cement concrete made from local materials, using two approaches: (a) Sustained chloride exposure test, assuming the applicability of Fick's laws of diffusion for the transport of chloride ions, and (b) Gas diffusion tests which have never been applied to concrete before.

The results indicate that the effective diffusion coefficients (D_e) for chloride ions in concrete is dependent on the water-cement ratio, cement content and exposure conditions, but are independent of the exposure chloride concentrations. From a non-linear regression analysis of the test results, D_e is expressed in terms of w/c ratio and cement content. The gas diffusion test appears to be a promising rapid technique for evaluating D_e for chloride ion in concrete. It is also observed that under idealized conditions, the solution to Fick's second law for the appropriate boundary conditions can be used to reasonably predict the time to initiation of corrosion.

ملخص

إن صدأ حديد التسليح يعتبر أحد العوامل الرئيسية في تدهور متانة المباني الخرسانية بدول الخليج. ولتحديد الوقت الزمني الذي يبدأ فيه صدأ حديد التسليح يجب دراسة إنشاء أيون الكلوريد في الخرسانة. يقوم هذا البحث بتقييم عامل إنشاء أيون الكلوريد في الخرسانة المصنوعة من المواد المحلية والأسمنت المقاوم للسلفات بطريقتين:

أ - اختبار تعرض الخرسانة للكلوريد وإفترض أن قوتين فيكس للإشعاع يمكن تطبيقها علي إنتشار أيون الكلوريد في الخرسانة.

ب - اختبار إنشاء الغاز في الخرسانة والذي لم يستعمل سابقاً.

إن نتائج هذا البحث أكدت أن عامل الإنشاء الحقيقي لأيون الكلوريد في الخرسانة يعتمد على نسبة الماء للأسمنت وكمية الأسمنت والأجواء المحيطة ولكن لا يعتمد على مدى تركيب محلول الكلوريد المعرض له الخرسانة. باستخدام التحليل الإرتدادي غير الخطي لنتائج الإختبارات المعملية أمكن إيجاد معادلة لعامل الإنشاء الحقيقي لأيون الكلوريد بمعلومية نسبة الماء للأسمنت وكمية الأسمنت. كما أن استخدام اختبار إنتشار الغاز كطريقة سريعة لمعرفة إنتشار الكلوريد في الخرسانة أعطى نتائج جيدة. وقد إستنتج أيضاً أن إستعمال القانون الثاني لفيكس تحت الظروف المخبرية من الممكن معرفة بداية صدأ حديد التسليح بعد التقييم الصحيح للظروف المحيطة.

TABLE OF CONTENTS

TITLE PAGE	i
FINAL APPROVAL	ii
ACKNOWLEDGEMENTS	iv
ABSTRACT (English)	vi
ABSTRACT (Arabic)	vii
TABLE OF CONTENTS	viii
LIST OF TABLES	xii
LIST OF FIGURES	xiii
 CHAPTER 1: INTRODUCTION	 1
General.....	1
Scope of this Research.....	5
 CHAPTER 2: LITERATURE REVIEW	 7
General.....	8
Solution of Fick's Second Law of Diffusion	14
Measurement of Diffusion Coefficient	15
Field Studies	16
Threshold Chloride Concentration	17
Summary.....	18
 CHAPTER 3: THEORETICAL BACKGROUND	 22
Chloride Exposure Test	22
Fick's First Law.....	22
Fick's Second Law.....	23

Gas Diffusion Test.....	24
Molecular Diffusion	25
Knudsen Diffusion.....	27
Mass Balance Equations.....	27
Effective Diffusion Coefficients	35
CHAPTER 4: EXPERIMENTAL PROGRAM	39
General.....	39
Materials.....	40
Cement.....	40
Aggregates.....	40
Mix Design	40
Specimens	41
Specimen Preparation	42
Mixing and Casting.....	42
Curing	42
Experimental Technique	43
Part 1: Chloride Exposure Test	43
Analysis for Total Chlorides	43
Spectrophotometry	44
Part 2: Gas Diffusion Test	45
Dynamic Experiment on a Single Pellet	46
Static Experiment on a Single Pellet.....	47
Part 3: Reinforcement Corrosion.....	48
Linear Polarization Resistance Technique	49

Auxiliary Tests	51
Mercury Intrusion Porosimetry	51
Concrete Permeability	52
Compressive Strength.....	53
CHAPTER 5: RESULTS & DISCUSSION.....	80
Mercury Intrusion Porosimetry	80
Concrete Permeability	80
Compressive Strength.....	81
Chloride Exposure Test	81
Effect of Water Cement Ratio	84
Effect of Cement Content.....	86
Effect of Exposure Condition	86
Effect of Surface Chloride Concentration.....	88
Gas Diffusion Test.....	89
Result Comparison of the Exposure and the Gas Diffusion Test.....	90
Reinforcement Corrosion	91
CHAPTER 6: PREDICTION OF CORROSION INITIATION	166
General.....	166
Basic Prediction Equation	166
Surface Chloride Concentration.....	167
Threshold Chloride Concentration	168
Expression for Effective Diffusion Coefficient.....	168
Results and Discussion.....	169

MIX DESIGN CONSIDERATION	170
CHAPTER 7: CONCLUSIONS AND RECOMMENDATIONS....	174
Conclusions	174
Recommendations	176
REFERENCES	177
APPENDIX A: VOLUMETRIC CALIBRATION OF THE	
DIFFUSION CELL	188
Top Half Cell with Sensor.....	188
Bottom Half Sensor	191
APPENDIX B: OPTIMIZATION OUTPUT.....	196
APPENDIX C: SAMPLE CALCULATION FOR THE STATIC	
TEST	199
Molecular Diffusion Coefficient	199
Knudsen Diffusion Coefficient	201
Evaluation of epsilon / tau.....	201
APPENDIX D: SAS PROGRAM AND OUTPUT	215
SAS Program	215
SAS Output for the Regression Analysis	218
VITAE	219

LIST OF TABLES

1.	Threshold Chloride Concentration	20
2.	Absorption and Sp. Gravity of Coarse Agg.	54
3.	Grading of Coarse Agg.	54
4.	Absorption and Sp. Gravity of Fine Agg.	54
5.	Specimen Description	55
6.	Porosity and Effective Pore Radius of Concrete	94
7.	Water Penetration in cms.	94
8.	Diffusion Coefficients from the Exposure Test After Optimization	97
9.	Knudsen Diffusivity Values	98
10.	Diffusion Coefficients from the Gas Diffusion Test	98
11.	Comparison of the Exposure and the Gas Diffusion Test Results	99
12.	Results of the Reinforcement Corrosion Study	100
13.	Measured Chloride Concentration at Rebar Level	101
14.	Summary of the Parameters Used for Prediction	172
15.	Predicted Time to Initiation of Corrosion	173
16.	Test on the Top Chamber	189
17.	Test on the Bottom Chamber	191
18.	Computer Generated Theta Values	206
19.	Table Collectively Showing the epsilon/tau Values.	208

LIST OF FIGURES

1.	Commonly Used Diffusion Cell	21
2.	Diffusion With Perturbation (ref.39)	21
3.	A Typical Chloride Concentration Profile	36
4.	Sketch Showing the Diffusion Cell	37
5.	Chart Obtained from the Gas Diffusion Test	38
6.	Concentration Ratio Versus mV Plot	38
7.	Experimental Parameters Considered in Part 1	56
8.	Experimental Parameters Considered in Part 2	57
9.	Experimental Parameters Considered in Part 3	58
10.	Photograph Showing the Discs Used for Gas Diffusion Tests	59
11.	Photograph Showing the Close-up of The Disc	60
12.	Photograph Showing the Blocks Used for the Corrosion Study	61
13.	Photograph Showing the Bar Used in the Corrosion Specimens	62
14.	Photograph Showing the Samples used for MIP	63
15.	Photograph Showing Some of the Cylinders Tested for Comp. Str.	64
16.	Photograph Showing the Curing of Specimens	65
17.	Photograph Showing the Specimens Exposed Indoors	66
18.	Photograph Showing the Specimens Exposed Outdoors	67
19.	Photograph Showing the Holes Filled after Coring	68
20.	Photograph Showing Some of the Cores Extracted	69
21.	Photograph Showing the Interval of Slicing	70
22.	Photograph Showing the Set up Used for Chloride	

	Analysis	71
23.	Photograph Showing the Close-up of Cell Used for Dy. Test	72
24.	Photograph Showing the Set-up of The Dynamic Test	73
25.	Photograph of the Cell used for the Static Diffusion Test	74
26.	Photograph Showing the Set-up for the Static Diffusion Test	75
27.	Photograph Showing the Diffusion Cell and the Reference Cell	76
28.	Photograph Showing the Set-up for LPT	77
29.	Photograph Showing the Set-up for Water Impermeability Test	78
30.	Photograph Showing a Cube Being Split Open	79
31.	Photograph Showing Some Typical Cubes Tested for Permeability	93
32.	Results of the DIN 1048 Water Impermeability Test	95
33.	28 day Cylinder Compressive Strength	96
34.	Chloride Profiles: (CC=350 kg/cum., W/C=0.4, 4% Chloride, Indoors)	102
35.	Chloride Profiles: (CC=350 kg/cum., W/C=0.4, 4% Chloride, Outdoors)	103
36.	Chloride Profiles: (CC=350 kg/cum., W/C=0.4, 8% Chloride, Indoors)	104
37.	Chloride Profiles: (CC=350 kg/cum., W/C=0.4, 8% Chloride, Outdoors)	105
38.	Chloride Profiles: (CC=350 kg/cum., W/C=0.55, 4% Chloride, Outdoors)	106
39.	Chloride Profiles: (CC=350 kg/cum., W/C=0.55, 8% Chloride, Indoors)	107
40.	Chloride Profiles: (CC=350 kg/cum., W/C=0.55, 8% Chloride, Outdoors)	108

41.	Chloride Profiles: (CC=350 kg/cum., W/C=0.7, 4% Chloride, Indoors)	109
42.	Chloride Profiles: (CC=350 kg/cum., W/C=0.7, 4% Chloride, Outdoors)	110
43.	Chloride Profiles: (CC=350 kg/cum., W/C=0.7, 8% Chloride, Indoors)	111
44.	Chloride Profiles: (CC=350 kg/cum., W/C=0.7, 8% Chloride, Outdoors)	112
45.	Chloride Profiles: (CC=300 kg/cum., W/C=0.4, 4% Chloride, Indoors)	113
46.	Chloride Profiles: (CC=400 kg/cum., W/C=0.4, 4% Chloride, Indoors)	114
47.	Chloride Profiles: (CC=300 kg/cum., W/C=0.55, 4% Chloride, Indoors)	115
48.	Chloride Profiles: (CC=400 kg/cum., W/C=0.55, 4% Chloride, Indoors)	116
49.	Effect of W/C Ratio on Chloride Diffusion: (CC=300 Kg/cum., 140 Days, 4% Chloride, Indoors)	117
50.	Effect of W/C Ratio on Chloride Diffusion: (CC=400 Kg/cum., 140 Days, 4% Chloride, Indoors)	118
51.	Effect of W/C Ratio on Chloride Diffusion: (CC=350 Kg/cum., 105 Days, 4% Chloride, Indoors)	119
52.	Effect of W/C Ratio on Chloride Diffusion: (CC=350 Kg/cum., 70 Days, 4% Chloride, Outdoors)	120
53.	Effect of W/C Ratio on Chloride Diffusion: (CC=350 Kg/cum., 175 Days, 8% Chloride, Indoors)	121
54.	Effect of W/C Ratio on Chloride Diffusion: (CC=350 Kg/cum., 70 Days, 8% Chloride, Outdoors)	122
55.	Variation of Effective Diffusion Coefficient with W/C Ratio	123
56.	Effect of Cement Content on Chloride Diffusion: (W/C=0.4, 140 Days, 4% Chloride, Indoors)	124
57.	Effect of Cement Content Chloride Diffusion: (W/C=0.55, 140 Days, 4% Chloride, Indoors)	125

58.	Effect of Exposure Conditions on Chloride Diffusion: (CC=350 kg/cum., W/C=0.4, 4% Chloride, 175 Days)	126
59.	Effect of Exposure Conditions on Chloride Diffusion: (CC=350 kg/cum., W/C=0.4, 8% Chloride, 175 Days)	127
60.	Effect of Exposure Conditions on Chloride Diffusion: (CC=350 kg/cum., W/C=0.55, 8% Chloride, 175 Days)	128
61.	Effect of Exposure Conditions on Chloride Diffusion: (CC=350 kg/cum., W/C=0.7, 4% Chloride, 70 Days)	129
62.	Effect of Exposure Conditions on Chloride Diffusion: (CC=350 kg/cum., W/C=0.7, 8% Chloride, 70 Days)	130
63.	Effect of Exposure Solution Concentration on Chloride Diffusion: (W/C=0.4, 175 Days, Indoors)	131
64.	Effect of Exposure Solution Concentration on Chloride Diffusion: (W/C=0.4, 175 Days, Outdoors)	132
65.	Effect of Exposure Solution Concentration on Chloride Diffusion: (W/C=0.55, 70 Days, Outdoors)	133
66.	Effect of Exposure Solution Concentration on Chloride Diffusion: (W/C=0.7, 105 Days, Indoors)	134
67.	Effect of Exposure Solution Concentration on Chloride Diffusion: (W/C=0.7, 70 Days, Outdoors)	135
68.	Fit for $\ln(1-2x)$ Vs t : (CC=350 kg/cum., W/C=0.4)	136
69.	Fit for $\ln(1-2x)$ Vs t : (CC=350 kg/cum., W/C=0.55)	137
70.	Fit for $\ln(1-2x)$ Vs t : (CC=350 kg/cum. W/C=0.7)	138
71.	Corrosion Potentials: (W/C=0.4, 4% Chloride, Cover=4")	139
72.	Corrosion Potentials: (W/C=0.4, 4% Chloride, Cover=3")	140
73.	Corrosion Potentials: (W/C=0.4, 4% Chloride, Cover=1.5")	141
74.	Corrosion Potentials: (W/C=0.55, 4% Chloride, Cover=4")	142
75.	Corrosion Potentials: (W/C=0.55, 4% Chloride, Cover=3")	143
76.	Corrosion Potentials: (W/C=0.55, 4% Chloride, Cover=1.5")	144

77.	Corrosion Potentials: (W/C=0.4, 8% Chloride, Cover=4") . .	145
78.	Corrosion Potentials: (W/C=0.4, 8% Chloride, Cover=3") . .	146
79.	Corrosion Potentials: (W/C=0.4, 8% Chloride, Cover=1.5")	147
80.	Corrosion Potentials: (W/C=0.55, 8% Chloride, Cover=4") . .	148
81.	Corrosion Potentials: (W/C=0.55, 8% Chloride, Cover=3") . .	149
82.	Corrosion Potentials: (W/C=0.55, 8% Chloride, Cover=1.5")	150
83.	Corrosion Current Densities: (W/C=0.4, 4% Chloride, Cover=4")	151
84.	Corrosion Current Densities: (W/C=0.4, 4% Chloride, Cover=3")	152
85.	Corrosion Current Densities: (W/C=0.4, 4% Chloride, Cover=1.5")	153
86.	Corrosion Current Densities: (W/C=0.55, 4% Chloride, Cover=4")	154
87.	Corrosion Current Densities: (W/C=0.55, 4% Chloride, Cover=3")	155
88.	Corrosion Current Densities: (W/C=0.55, 4% Chloride, Cover=1.5")	156
89.	Corrosion Current Densities: (W/C=0.4, 8% Chloride, Cover=4")	157
90.	Corrosion Current Densities: (W/C=0.4, 8% Chloride, Cover=3")	158
91.	Corrosion Current Densities: (W/C=0.4, 8% Chloride, Cover=1.5")	159
92.	Corrosion Current Densities: (W/C=0.55, 8% Chloride, Cover=4")	160
93.	Corrosion Current Densities: (W/C=0.55, 8% Chloride, Cover=3")	161
94.	Corrosion Current Densities: (W/C=0.55, 8% Chloride, Cover=1.5")	162

95.	Specimens Showing no Signs of Corrosion: (W/C=0.4, 8% Chloride, Cover=1.5")	163
96.	Block Showing Initiation: (W/C=0.4, 8% Chloride, Cover=1.5")	164
97.	Blocks Showing Active Corrosion: (W/C=0.55, Cover=1.5")	165
98.	Experimental and Calculated Values of De	171
99.	Flow Diagram for the Gas Expansion Test	195
100.	Diffusion Curve Obtained From the Static Test	204
101.	Plot of Concentration Ratio Vs Time	205

Chapter I

INTRODUCTION

1.1 General

Concrete structures in the Arabian Gulf countries show severe deterioration after a very short span of 10 or 15 years after construction. This is mainly due to the hot, humid and aggressive environment in which they exist. Due to the corrosion of reinforcement, it has been observed that even buildings designed and constructed according to well established codes and practices develop signs of deterioration quite early in this prevailing harsh environment.

The process by which a metal returns to its native state is referred to as corrosion. Steel is manufactured by the reduction of ores. This process of reduction requires a large amount of energy. Because of this large amount of intrinsic energy, the metal tends to revert to a lower energy state and this reversal is accomplished through corrosion.

The highly alkaline environment in concrete normally provides an excellent degree of protection to the reinforcing steel. The tight gamma ferric oxide film formed around the bar because of the high pH of the

pore solution passivates the steel against corrosion. But a reduction in the pH of the pore solution by carbonation or by the ingress of aggressive ions like chloride ions, disrupts the protective film and renders the bar vulnerable to corrode. But carbonation is a slow process and carbonation induced corrosion is not quite as common as chloride induced corrosion in the gulf region.

Chloride ions are quite often unintentionally induced through the constituent materials like salt contaminated aggregates or water and sometimes intentionally in the form of chemicals to accelerate the setting of concrete. Moreover chloride ions penetrate hardened concrete if exposed to aggressive environment. Typical cases are concrete exposed to a marine environment or bridge decks or parking garages exposed to de-icing salts in winter or structures situated in salt-laden environments. In the case of structurally damaged concrete, the diffusion of chlorides is made even more easy.

According to the ACI Committee Report [1] on the corrosion of metals in concrete, there are three modern theories to explain the effect of chloride ions on corrosion of concrete reinforcement: i) Oxide Film Theory; ii) Adsorption Theory; and iii) Transitory Complex Theory

While the entry of chlorides through constituent materials can be controlled by strict adherence to better construction practices, the ingress of chloride ions from external sources can only be controlled by having a good quality concrete which is impermeable and/or coating with some impermeable membranes.

According to Figg [2], in addition to having the ability to migrate within the concrete to produce differential concentration cells, the harmful effects caused by chlorides are

1. Increase in the electrical conductivity of the concrete, thereby accelerating the corrosion
2. Even at high pH levels, if chloride ions are present in sufficient quantities, they can overcome the passivating effect
3. Chloride ions have an adverse effect on the hydration of the calcium silicates and thus on the long term strength improvement and impermeability

In order to evaluate the performance of concrete structures with respect to durability, a greater understanding of the rate of migration of the chloride ion is necessary. The main factor of interest when it comes to such a study is the chloride diffusion coefficient in concrete. Though there is no universally accepted criteria for the process of attack of chloride ions, the process of transportation of chloride ions in concrete by the mechanism of Fick's laws of diffusion is agreed upon universally.

An assumption underlying the application of Fick's Laws to the diffusion of chloride ions in concrete is that of no reaction between the diffusing aggressive ion and tricalcium aluminate (C_3A) in concrete. So far, the application of Fick's Law to the diffusion of chloride ions even in Type

I ordinary portland cement (OPC) concrete with a high C_3A has been under this assumption. But it is quite reasonable to say that comparatively, the assumption is more valid in the case of Type V sulphate resisting portland cement (SRPC) as the C_3A content is much lower in this cement, which will lead to a lesser degree of binding of the chloride ions.

Estimating the diffusion coefficient will help to predict the depth of chloride penetration in concrete over a period of time. So, knowing a certain threshold level of chloride, for a particular concrete, the time required for the chloride concentration to exceed the threshold value at the rebar level can be estimated.

In order to plan for the likely consequences of corrosion damage, it is of vital interest to engineers to know the expected time or age of the structure at which corrosion will be initiated. This knowledge about the initiation time to corrosion is essential from the view point of serviceability of a structure and also to allocate the resources, planning ahead for a repair or a demolition.

Several studies have been conducted to evaluate the chloride diffusion in cement paste and/or concrete. However, the diffusion of these ions under arid and semi-arid conditions, as in the Arabian Gulf, has not been evaluated. The thermal incompatibility between the aggregate fraction and the hardened cement paste provides considerable micro-cracks

at the aggregate-paste interface, which significantly influences the chloride diffusion in such concretes [3,4]. Moreover, the poor quality of the aggregates in this part of the world further is expected to enhance the diffusion of chloride ions. Clearly, there is a need to evaluate the chloride diffusion coefficients in concretes made with local aggregates and exposed to such hot-humid environment.

1.2 Scope of this Research

The primary aim of this research is to investigate the diffusion of chloride ions in Type V Sulphate Resisting Cement concrete in laboratory and outdoor conditions.

The broad objectives are

1. To determine the diffusion coefficient for chloride ions in concrete using the conventional procedure of applying a constant concentration of chloride exposure for concretes of different mix design. The effect of the following parameters on the diffusion of chloride ions are considered:
water-cement ratio, cement content, chloride concentration and exposure conditions
2. To use a new experimental set-up based on gas diffusion through concrete discs to determine the porosity and tortuosity

of concrete, which is then to be related to the diffusion of chloride ions in the concrete.

3. To predict the onset of corrosion in reinforced concrete structures, on the basis of the laboratory generated test data.

The scope of the work is limited to the use of only one type of portland cement, namely Type V, and to the widely used Riyadh aggregates.

Chapter II

LITERATURE REVIEW

The corrosion of steel reinforcement in concrete and its damaging impact have generated significant research interest in the area of chloride penetration or diffusion in concrete. Voluminous work has been devoted to the various aspects of chloride ingress and the factors influencing it, the bulk of these studies addressing the problem as diffusion through porous solids. Literature is well stocked with experimental work as well as mathematical modelling for the diffusion of chloride ions through cementitious materials.

It is not intended to review all of the past work which is extensive, as some of these works are not critically important to this research. It is sufficient to provide an in-depth highlight of the important observations, findings and conclusions covering a broad cross-section of the work carried out upto date. For clarity of presentation, the literature review is divided into the following subsections.

2.1 General

Garrels et al. [5] from their study on diffusion through water saturated rocks reported, that using a potassium chloride solution renders the progress rate of chloride ion concentration front compatible with Fick's diffusion law. Later, Collepardi et al. [6] first calculated meaningfully the diffusion coefficient from laboratory tests for various cement paste mixes using Fick's second law of diffusion for the appropriate boundary conditions and concluded that chloride penetration proceeds by ionic diffusion. Gjorv and Vennesland [7] studied the diffusion of chloride ions into concrete from seawater. The test variables were w/c ratio, type of cement, cement content, polarization potential and aggregate type. Results showed that porosity and permeability, which increase with w/c ratio, affect the diffusion only in the exterior layers while in the interior, the diffusion is affected by chloride binding and ion exchange. The lower diffusion in blended cements was attributed to the lower amount of calcium hydroxide present, which means a lower capacity for ion exchange and therefore lower penetration of chlorides. The tricalcium aluminate (C_3A) content was seen to have no significant effect on chloride diffusion provided its percentage was less than 8.6%.

The study of diffusion through hardened cement pastes of various compositions has received considerable attention [8-11]. Increase in diffusion rate with increased w/c is noted by Page et al [8]. Page et al, [10] concluded that sulphate resisting cement performs poorly against

corrosion and diffusion of chlorides. Diffusion cells were used in the experimental determination of chloride diffusivity by Goto and Roy [9], Page et al [10], Diab et al [11] and Dhir et al [12]. Dhir et al. [12] observed that for OPC concrete, on increasing the exposure temperature from 20 to 40⁰C, the diffusivity value shot up by almost 2.8 times. The effect of silica fume and fly ash on diffusion characteristics was explored by Byfors [13]. Midgley and Illston [14] investigated the effect of chloride concentration by considering two solutions of NaCl with different concentrations. Test results showed that the depth of penetration at a given time increases with the w/c ratio and the concentration of chloride ions. The study also concluded that the presence of chloride ions alters the pore-size distribution of the hardened cement paste with smaller pores are associated with higher chloride ions. Ost and Monfore [15] looked into the chloride migration rate into aggregates of concrete by comparing the rate of migration in concrete and cement paste. Experimental data indicated that chloride migrated into concrete more readily than into the cement paste.

To study the effect of cation type associated with chloride ions on the corrosion of rebar, Hansson et al. [16] made OPC mortar prisms with mild steel rod and used calcium chloride, sodium chloride and potassium chloride as exposures. Results indicate that, of the three salts calcium chloride had the most deleterious effect. It creates a more open structure, which aids diffusion, higher electrical conductivity and reduces the pH level of the pore water. Sodium and potassium ions also increase

the porosity, but to a lesser extent; however they increase the pH level. It was also inferred that the total chloride ion content of the pore solution does not alone account for the corrosion rate, but the rate of corrosion is also controlled by other factors that include porosity, pH level and the availability of oxygen.

Concerns have been raised with regard to the applicability of diffusion as an appropriate modelling of chloride ingress, as there are several mechanisms by which chloride ions can be transported within the concrete [17-19]. Several processes may be combined, making it difficult to identify a single mechanism. One of the mechanisms for surface penetration is intrusion of chloride-bearing water into capillary pores of unsaturated (dry) concrete by capillary action. Alternate wetting and drying can lead to buildup of chloride ions through absorption. If a structure is not dried to a high degree for a prolonged period of time, chloride penetration into concrete by absorption and capillary suction is basically restricted to a small depth below the surface. If there is a differential head of chloride-bearing water, permeability will also influence the ingress of chlorides for which higher permeability coefficient will permit higher rate of flow.

The other dominant mechanism of the chloride ion transport is the diffusion which takes place under a concentration gradient. If the outside concentration is higher than the inside of concrete, the migration of chloride ions through pore water in concrete will take place by diffusion.

The relative importance of the two major mechanisms of chloride transport, namely diffusion and absorption, depend on the moisture content of concrete. Absorption may be dominant if a dry concrete with significant loss of pore water is wetted with chloride-bearing water, whereas for a reasonably moist concrete (sufficient level of pore water exists) diffusion process will prevail. However, researchers tend to agree that in most cases diffusion can be assumed to be the basic transport mechanism of chloride ions for reasonably moist structures [20,21].

Another argument against the validity of pore diffusion of chloride ingress [22] is that some part of the chloride is chemically bound in concrete due to reaction with cement and remains immobilized [23]. The chloride concentration profile therefore depends to some extent upon the type of cement used in concrete.

As part of the chloride in concrete is chemically bound due to reaction of chloride ions with constituents of cement, the free chloride concentration is of importance for corrosion initiation [21]. Raharinaivo and Jean-Marie [24] arrived at a formulation to find the apparent diffusivity considering the reaction of the chloride ions with the constituents of cement. The study concluded, among others, that the chloride penetration can be modelled by Fick's diffusion law without the reaction component when the concrete pores are wide enough, so that the solid bodies around the pores (traps) may be neglected. Gau and Cornet [25] have considered a reaction rate between chloride ions, cement paste

and a chloride convection coefficient for the solution of Fick's law. However, as the convection effect over long term with large area is small, it can be ignored to obtain a reasonable solution of Fick's law [34]. According to researchers [25,34], the reaction between Cl^- and cement can be accounted for by considering an effective diffusion as $D_e = D / \{(K+1)(K+p)\}$, where K represents slope of chloride adsorption isotherm and p is the porosity of concrete.

From their study on chloride penetration and Cl^- / OH^- ratio in cement pastes, Kayyali and Haque [26] concluded that the critical ratio of Cl^- / OH^- for depassivation exceeded the set limit of 0.6 by Hausmann. [24,44]. The influence of w/c ratio, pozzolanic admixture and temperature on chloride ion diffusion was conducted by Weyers and Smith [27] who used a non-linear regression analysis to determine diffusion coefficient. They concluded that Fick's law was applicable in all cases except for silica fume mixture. The values of the diffusion coefficient ranged from 1×10^{-8} to $4 \times 10^{-8} \text{ cm}^2/\text{sec}$. Relationship between w/c and diffusion coefficient was suggested for two exposure conditions.

The penetration of wind-blown chlorides into concrete was looked into by Jaegerman [28] by considering the effect of w/c ratio and curing regimes on such penetration for specimens exposed to Mediterranean Sea conditions. This study showed that chloride penetration increases with an increase in w/c ratio and is influenced by the curing regime. Diffusion coefficients are calculated using Fick's law.

Dhir et al. [29] from their tests on concrete cube specimens made out of ordinary Portland cement and cured under different conditions, found that the diffusivity calculated by applying Crank's relationship [30] to Fick's second law approached a value found by a rapid test devised by them. A method is suggested and nomograms were provided to estimate the time required to reach a certain chloride concentration for a constant diffusivity. The calculated values of diffusivity ranged from 0.5×10^{-8} to $8.3 \times 10^{-8} \text{ cm}^2/\text{sec}$.

Mustafa and Yusof [31], from their study on OPC concrete specimens exposed to marine environment confirmed the dependency of chloride content on the time of exposure. It was also observed that the surface concentrations and the apparent diffusion coefficient varied with time of exposure. The variation of the reported diffusion coefficients was from 4.4×10^{-8} to $5.0 \times 10^{-8} \text{ cm}^2/\text{sec}$.

In their study of diffusion of chloride ions and hydroxyl ions into concrete, Sergi et al. [32] concluded that total and free chloride profiles could be interpolated to a good approximation by Fick's law. The study also confirmed that the relationship between free and bound chloride could be represented by Langmuir adsorption isotherm.

Teng and Lee [33] have proposed a different numerical technique to find apparent diffusion coefficient of chloride in concrete which is claimed to be more suitable for non-steady state of diffusion. The meth-

od uses nonlinear chi-square and Newton's (NCSN) method to determine the diffusion coefficient.

2.2 Solution of Fick's Second Law of Diffusion

Literature review shows that, for the application of Fick's second law of diffusion, several techniques have been used to find solution of the partial differential equation for Fick's second law for the appropriate boundary conditions. The commonly applicable form (Eqn.3.4, Chapter 3) involves concentration of chloride ions C_s as ppm at the exposed surface (at $x=0$) and the concentration at a distance x from the surface, C_x . As C_x is conveniently measured as percentage by weight of cement (or concrete), the direct application of Fick's law is therefore not possible. Sergi et al. [32] have measured chloride content as ppm by extracting the pore water in concrete. Weyers and Smith [27] adopted a nonlinear regression analysis and a finite difference method was used to determine the diffusion coefficient by Miki [34]. Numerical integration is pursued by Midgley and Illston [14] and an iterative program has been used to determine the value of diffusion coefficient which best fits the data of chloride concentration by Liam et al. [35]. The diffusion coefficient ranged from 2.13×10^{-8} to $5.5 \times 10^{-8} \text{ cm}^2/\text{sec}$. Nagano and Naito [36] provides a solution of Fick's law with stepwise uniform (periodic) functions for C_s at the boundary. The values of the diffusion coefficient reported here were in the range from 1.4×10^{-8} to

$$2.2 \times 10^{-8} \text{ cm}^2/\text{sec.}$$

2.3 Measurement of Diffusion Coefficient

Generally, diffusion coefficients have been determined either by using the conventional method of subjecting specimens to known concentrations of chloride solutions and then chemically measuring the chloride concentration at different depths of the samples [7,8,29,32] or by using diffusion cells as shown in Fig. 1. Each of these concentration gradient type tests requires a long duration, to get meaningful results prompting researchers to look for rapid methods.

In order to expedite the diffusion process in a diffusion cell experiment, a small potential difference of 2 V (DC) has been applied as perturbation [9], on the assumption that such a small disturbance, which expedites diffusion, does not critically affect the measured values. Whiting's Coulomb test [37] for rapid measurement of chloride permeability, developed for bridge deck testing, has been adopted by AASHTO Standard [38]. Unfortunately, This test does not provide information on diffusion of chloride ion itself in concrete. Andrade and Sanjuan [39] compared the method with the normal diffusion test and found that the diffusion from migration experiments were different from those calculated from normal diffusion tests. Dhir et al. [40] have proposed a simple rapid test using diffusion cell to determine diffusion coefficient. In this method, a small potential difference is applied at a

low current across a concrete specimen in a diffusion cell (Fig. 2). Even then, about a week would be required to obtain an estimate of diffusion coefficient from this experiment. Tang and Nilsson [41] proposed a new rapid method by applying an electric field by which chloride penetration profile can be obtained in much shorter time (several hours or a few days depending on the type of concrete). Several advantages of this method have been highlighted [39].

2.4 Field Studies

The interest of researchers to gather field data on the chloride penetration and to see how the penetration can be modelled has led to numerous studies of insitu chloride profiles for old concrete structures [19,34,35,36,42]. From the best fitting plots of the measured data, diffusion coefficient of chloride was calculated. All have reaffirmed in principle the general applicability of Fick's law and based on insitu findings, advocated the use of diffusion law to predict corrosion initiation time for a given threshold value of chloride concentration [34,35]. Nagano and Naito [36] have considered three different types of chloride exposures at the boundary, including stepwise uniform concentration, and have provided the solution to Fick's law. Furthermore, they have examined the effect of coating on concrete on the chloride ingress. Masuda [42] has considered the effect of chloride exposure on structures which are indirectly exposed to the seawater by taking into account the chloride concentration in atmosphere. Fick's law has been

used again with new boundary condition. The predicted profile with an assumed diffusivity of $2 \times 10^{-8} \text{ cm}^2/\text{sec.}$ was found to have a good correlation with that of the actual structures.

2.5 Threshold Chloride Concentration

Estimation of the threshold level of chloride ion concentration at the rebar location has received widespread attention. However, unanimity on an universal value is far from close, due to the complexity of corrosion process which is dependent upon a number of interactive factors such as pH of concrete, water-cement ratio and amount of water soluble chloride [43]. Representative samples of numerous works in this area which have examined various influential parameters, including the ratio of Cl^-/OH^- in pore solution and pH level are reported [44-56]. Consequently, a wide range of chloride ion concentrations has been reported for corrosion.

The reported values of the threshold range from 0.39 kg/m^3 [47] to 1.65 kg/m^3 of concrete [48]. European state-of-the-art report concludes that there is no consensus on the permissible limits of chloride concentration but a concentration level of 0.35-1 % by weight of cement content may initiate corrosion process [45]. For the Middle East environment, the reported range is 0.05-0.7 % [46]. Some of results are reproduced in Table 1 [46]. Based on a survey of a large number of buildings in Britain, Everett and Treadway [54], proposed a classifica-

tion for assessing the risk of corrosion in terms of acid-soluble chloride content by weight of cement: low (less than 0.4%), medium (0.4-1.0%) and high (greater than 1 %). A review of suggested values indicates that in general, corrosion may occur with chloride content exceeding 0.35% by weight of cement.

2.6 Summary

This literature review indicates that researchers generally have agreed, in the absence of a better model, that Fick's second law of diffusion can approximately be applied to the modelling of chloride diffusion into concrete for most cases having a prolonged exposure period. Based on an assumed level of concentration of chloride ions at the rebar location which will initiate corrosion, diffusion equations can be used to predict corrosion initiation time. The onus then falls on the determination of an appropriate value of diffusion coefficient for chloride ingress, and a mathematical representation of the chloride exposure. It is imperative therefore that for the development of a reliable time prediction model for corrosion-free service life of reinforced concrete structures in this local region, extensive experimental work must be carried out to determine diffusion coefficients of chloride for different concrete mixes and to model the existing environment.

Evidently several studies have been conducted to evaluate the chloride diffusion in cement paste and/or concrete. However, the diffusion of

these ions under arid and semi-arid conditions, as in the Arabian Gulf, has not been evaluated. The thermal incompatibility between the aggregate fraction and the hardened cement paste provides considerable micro-cracks at the aggregate-paste interface, which significantly influences the chloride diffusion in such concretes [3,4]. Moreover, the poor quality of the aggregates in this part of the world further enhances the diffusion of chloride ions. Therefore, there is a need to evaluate the chloride diffusion coefficients in concretes made using such aggregates and exposed to such hot-humid environment.

Moreover, no work has yet been carried out so far to see if the concepts of molecular diffusion and Knudsen diffusion, as applied to porous catalyst [57] , can be applied to concrete for chloride penetration. From a laboratory setup, the ratio of porosity to tortuosity, which is assumed to be constant for a porous solid medium [57], can be calculated using gas diffusion experiment as proposed in this work and this can then be used to determine chloride diffusion coefficient.

**Table 1. Chloride Threshold Values for the Onset of Corrosion
(reproduced from Rasheeduzzafar et al [46])**

Source	Percentage by weight of cement	kg /m ³ (lb/yd ³) of concrete for typical concrete mixtures
ACI Committee 201 on Durability of Concrete in Service[47]	0.15 (moist environment, but not exposed to chlorides)	0.39 (0.65)
	0.10 (moist environment, but exposed to chlorides)	
BS CP 110 : 1972 (latest amendment 1979)	0.36	1.47 (2.45)
Weigler and Segmuller [48]	0.40	1.65 (2.75)
Stratfull et al [49]	0.15	0.60 (1.00)
Clear (FHWA) [50]	0.20	0.81 (1.35)
Knofel [51]	0.20	0.81 (1.35)
Hausmann [52]	0.05 (for pH=12.5)	0.20 (0.34) (for pH=12.5)
	0.70 (for pH=13.2)	2.83 (4.72) (for pH=13.2)
Lewis [53]	0.15	0.60 (1.0)

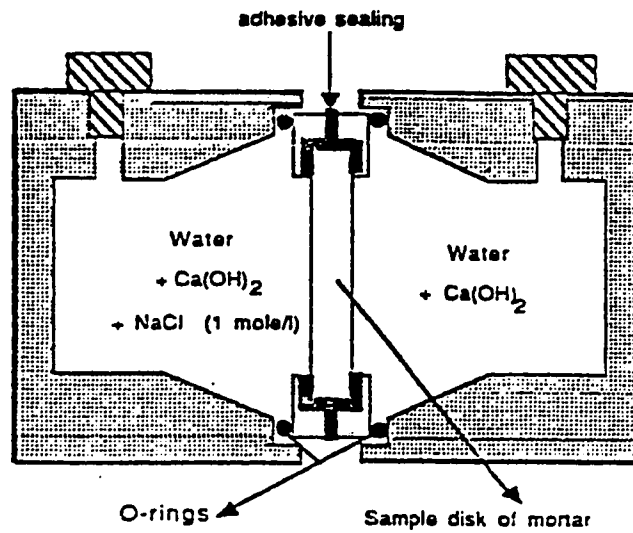


Figure 1: Commonly Used Diffusion Cell

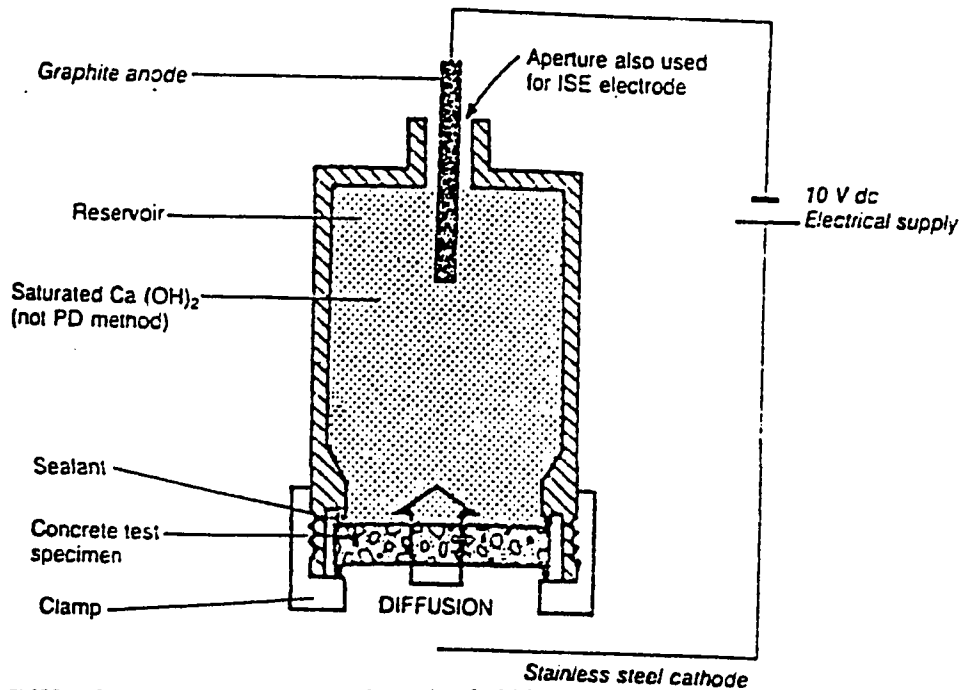


Figure 2: Diffusion With Perturbation (ref.39)

Chapter III

THEORETICAL BACKGROUND

In this chapter the theoretical background for the determination of the diffusion of chloride ions into concrete are provided for two distinctively different approaches: (a) Chloride Exposure Test and (b) Gas Diffusion Test. While the former is a conventional method which has been widely used in the past, the second method is the first attempt of its kind for concrete like materials.

3.1 Chloride Exposure Test

The assumption underlying the application of Fick's laws to concrete and its validity has already been explained in Chapter 1. The following sections briefly states the necessary mathematical formulae involved. No attempt is made to derive the well known form of the Crank's solution [30] to Fick's second Law.

3.1.1 Fick's First Law

Ionic diffusion in a porous media is governed by Fick's first law [57], which deals with the mass flux due to a concentration gradient,

$$J = -D_c \frac{\partial C}{\partial x} \quad (3.1)$$

where

J is the mass flux

D_c is the diffusion coefficient

C is the concentration

x is the distance

$\frac{\partial C}{\partial x}$ is the concentration gradient in one dimension

3.1.2 Fick's Second Law

For unsteady state in one dimensional diffusion, Fick's second law [57] is

$$\frac{\partial C}{\partial t} = - \frac{\partial J}{\partial x} \quad (3.2)$$

Substituting for J from (3.1)

$$\frac{\partial C}{\partial t} = D_c \frac{\partial^2 C}{\partial x^2} \quad (3.3)$$

Where D_c has been assumed to be constant

The applicable boundary conditions for the solution of this differential equations for a semi-infinite domain are

$$C_x = C_i \text{ at } t = 0 \text{ when } 0 < x < \infty$$

$$C_x = C_i \text{ at } x = 0 \text{ when } 0 < t < \infty$$

$$C_x = C_i \text{ at } x = \infty \text{ when } 0 < t < \infty$$

By combination of variables, the solution for Eq. (3.3) is

$$\frac{C_x - C_i}{C_s - C_i} = 1 - \operatorname{erf} \frac{x}{2\sqrt{D_e t}} \quad (3.4)$$

where

C_i is the initial chloride concentration

C_x is the chloride concentration at a depth x

C_s is the surface chloride concentration

erf is the error function

D_e is the effective diffusion coefficient

t is the time elapsed

Using the above solution, when the initial chloride concentration, the surface chloride concentration and the chloride concentration at a particular depth x at a time t are known the effective diffusion coefficient D_e can be determined. For a given time period t , the variation of concentration of chloride ions across the depth as determined from Eq. 3.4 is shown in Fig. 3.

3.2 Gas Diffusion Test

Gas diffusion in a porous media could be molecular diffusion, Knudsen diffusion or a combination of the two, depending on the size of the pores [58]. In concrete there exists large pores as well as small sized

pores. So here, the diffusion process is a combination of molecular and Knudsen diffusion. An experiment can be set up in the laboratory using a thin concrete disc as the separating medium between two gas chambers as shown in Fig. 4. Using helium (He) and nitrogen (N_2) in the two chambers, the diffusion of these gases through the porous concrete can be observed by measuring the concentration of the gases in any one chamber. A steady state will be attained when the concentration of gases in each of the chambers becomes 50 %. Before arriving at the mass balance equations for the static test the molecular diffusion and the Knudsen diffusion will be defined first in the following paragraphs.

3.2.1 Molecular Diffusion

If the pores of the medium are relatively large molecular diffusion may occur. Here, the collision of molecules with each other is predominant when compared to that with the pore walls.

Hirschfelder, Bird and Spotz [59], presented the following equation for the molecular diffusion coefficient

$$D_{12} = \frac{0.001858 T^{3/2} \left[\frac{1}{M_1} + \frac{1}{M_2} \right]^{1/2}}{P \sigma_{12}^2 \Omega_p} \quad (3.5)$$

where

D_{12} is the molecular diffusivity of 1 in 2 in cm^2/sec

T is the absolute temperature in Kelvin

M_1 & M_2 are the molecular weights of 1 and 2

P is the absolute pressure

σ_{12} is the "collision diameter", a Lennard-Jones parameter in Angstroms.

For the binary system 1/2, σ_{12} is defined as

$$\sigma = \frac{\sigma_1 + \sigma_2}{2}$$

where

σ_1 and σ_2 are the collision diameters for the components 1 and 2 respectively.

Ω_p is the "collision integral" for molecular diffusion, a dimensionless parameter. The value of Ω is tabulated against kT/ϵ_{12} , k being the Boltzmann Constant and ϵ_{12} , is the energy of molecular interaction for the binary system 12, which is defined as

$$\epsilon_{12} = \sqrt{\epsilon_1 \epsilon_2}$$

ϵ_1 and ϵ_2 are both tabulated

3.2.2 Knudsen Diffusion

If the pores are quite small, the molecules will collide with the pore walls much more frequently than with each other then Knudsen diffusion will dominate. Knudsen diffusivity is not applicable to liquids. It is given by the following expression

$$D_k = 9700 \, r_p \sqrt{\left(\frac{T}{M}\right)} \quad (3.6)$$

where

D_k is the Knudsen diffusion coefficient in cm^2/sec

r_p is the mean pore radius in cms.

T is the temperature in Kelvin

M is the molecular weight.

3.2.3 Mass Balance Equations

Referring to Fig. 4, a mass balance equation can be deduced for the known concentration of gases recorded from the experiment. In deriving the necessary equations, the following assumptions are made:

(1). *Both chambers have the same volume:*

A gas expansion test was conducted on the diffusion cells to determine the volume of the two chambers. The two chambers were found to have almost the same volume and an average value of 84.88 cc. was adopted. The calculations are reported in Appendix A.

(2). The film resistance is negligible:

The gas diffusing through concrete specimens encounters two resistances. The resistance of a thin layer of film of gas formed on the surface of the disc because of the diffusion of the gas from the other chamber and the resistance offered by the body of the concrete. It was observed that on injecting the pulse, no peak response was detected. From this it can be concluded that the resistance offered by the body of the concrete to the gas diffusion is so large that the film resistance can be considered to be negligible.

(3). The diffusion is in a quasi-steady state

The diffusion through concrete is so slow that the diffusion through the bulk of the body can be considered instead of diffusion through elemental thicknesses, validating the assumption of the quasi-steady state diffusion.

(4). The pressure is constant

The system is closed and so the pressure can be assumed to be constant.

Overall mass balance in chamber A for species 1 (1 is He, 2 is N_2)

Accumulation = Input - Output

$$\frac{d[VC_1]}{dt} = 0 - AN_1 \quad (3.7)$$

$$V \frac{dC_1}{dt} = -AN_1 \quad (3.8)$$

As P is constant

$$C_1 = Cx_1 \quad (3.9)$$

Therefore

$$VC \frac{dx_1}{dt} = -AN_1 \quad (3.10)$$

or

$$\frac{dx_1}{dt} = -\frac{A}{VC} N_1 \quad (3.11)$$

To find the flux, we must use Stefan-Maxwell relations [60]. At constant pressure, these relations are:

$$-C \nabla x_1 = \left[\frac{x_2 \tau}{D_{12}^E} + \frac{\tau}{D_{1k}^E} \right] N_1 - \frac{x_1 \tau}{D_{12}^E} N_2 \quad (3.12)$$

and

$$-C \nabla x_2 = -\frac{x_2 \tau}{D_{12}^E} N_1 + \left[\frac{x_1 \tau}{D_{12}^E} + \frac{\tau}{D_{2k}^E} \right] N_2 \quad (3.13)$$

Multiplying both sides by $\frac{D_{12}^e}{\tau}$

$$-\frac{CD_{12}^e}{\tau} x_1 = \left[x_2 + \frac{D_{12}}{D_{1k}} \right] N_1 - x_1 N_2 \quad (3.14)$$

$$-\frac{CD_{12}^e}{\tau} x_2 = -x_2 N_1 + \left[x_1 + \frac{D_{12}}{D_{2k}} \right] N_2 \quad (3.15)$$

Due to quasi-steady state assumptions and equal volumes, we may assume that the gradients are linear, equal and opposite

$$\nabla x_2 = -\nabla x_1 \quad (3.16)$$

Adding (3.14) and (3.15)

$$\left[x_2 + \frac{D_{12}}{D_{1k}} \right] N_1 - x_1 N_2 - x_2 N_1 + \left[x_1 + \frac{D_{12}}{D_{2k}} \right] N_2 = 0 \quad (3.17)$$

or

$$\frac{N_1}{D_{1k}} + \frac{N_2}{D_{2k}} = 0 \quad (3.18)$$

$$N_2 = -\frac{D_{2k}}{D_{1k}} N_1 \quad (3.19)$$

Substitute into (3.14)

$$-\frac{CD_{12}^e}{\tau} \nabla x_1 = \left[x_2 + \frac{D_{12}}{D_{1k}} \right] N_1 + x_1 \frac{D_{2k}}{D_{1k}} N_1 \quad (3.20)$$

and for chamber A,

$$x_1 + x_2 = 1$$

therefore

$$x_2 = 1 - x_1 \quad (3.21)$$

$$-\frac{CD_{12}^E}{\tau} \nabla x_1 = \left[1 - x_1 + \frac{D_{12}}{D_{1K}} + x_1 \frac{D_{2K}}{D_{1K}} \right] N_1 \quad (3.22)$$

or

$$N_1 = \frac{-\frac{CD_{12}^E}{\tau} (x_1)}{1 + \frac{D_{12}}{D_{1K}} - x_1 \left[1 - \frac{D_{2K}}{D_{1K}} \right]} \quad (3.23)$$

For assumptions specified

$$\nabla x_1 = \frac{2(0.5 - x_1)}{L} = \frac{1 - 2x_1}{L} \quad (3.24)$$

$$N_1 = \frac{-\frac{CD_{12}^E}{\tau L} (1 - 2x_1)}{1 + \frac{D_{12}}{D_{1K}} - x_1 \left[1 - \frac{D_{2K}}{D_{1K}} \right]} \quad (3.25)$$

Substitute into (3.10)

$$\frac{dx_1}{dt} = \frac{\left[-\frac{A}{V C} \right] \left[-\frac{CD_{12}^E}{\tau L} \right] [1 - 2x_1]}{1 + \frac{D_{12}}{D_{1K}} - x_1 \left[1 - \frac{D_{2K}}{D_{1K}} \right]} \quad (3.26)$$

$$\int_{x_{1,0}}^{x_1} \frac{\left[1 + \frac{D_{12}}{D_{1K}} - x_1 \left[1 - \frac{D_{2K}}{D_{1K}} \right] \right] dx_1}{1 - 2x_1} = \int_0^t \frac{AD_{12}^E}{V \tau L} dt \quad (3.27)$$

$$-\frac{1}{2}\left[1 + \frac{D_{12}}{D_{1K}}\right]\ln\left[\frac{1 - 2x_1}{1 - 2x_{1_0}}\right] - \left[1 - \frac{D_{2K}}{D_{1K}}\right]\int_{x_{1_0}}^{x_1} \frac{x_1}{1 - 2x_1} dx_1 = \frac{AD_{12}ct}{V\tau L}$$

(3.28)

$$\text{But, } \int_{x_{1_0}}^{x_1} \frac{x_1}{1 - 2x_1} dx_1 = -\frac{1}{4}\ln\left[\frac{1 - 2x_1}{1 - 2x_{1_0}}\right] + \frac{1}{2}[x_{1_0} - x_1]$$

(3.29)

$$-\frac{1}{2}\left[1 + \frac{D_{12}}{D_{1K}}\right]\ln\left[\frac{1 - 2x_1}{1 - 2x_{1_0}}\right] + \frac{1}{4}\left[1 - \frac{D_{2K}}{D_{1K}}\right]\ln\left[\frac{1 - 2x_1}{1 - 2x_{1_0}}\right]$$

$$- \frac{1}{2}\left[1 - \frac{D_{2K}}{D_{1K}}\right][x_{1_0} - x_1] = \frac{AD_{12}ct}{V\tau L}$$

(3.30)

$$\text{Define } 0 = \frac{AD_{12}ct}{V\tau L} \text{ and } x_{1_0} = 0$$

(3.31)

Therefore

$$0 = -\frac{1}{2}\left[1 + \frac{D_{12}}{D_{1K}}\right]\ln[1 - 2x_1] + \frac{1}{4}\left[1 - \frac{D_{2K}}{D_{1K}}\right]\ln[1 - 2x_1]$$

$$+ \frac{1}{2}\left[1 - \frac{D_{2K}}{D_{1K}}\right](x_1)$$

(3.32)

where

C_1 is the concentration of helium in chamber A at any instant of time in moles/cc.

x_1 is the mole fraction of helium in chamber A at any instant of time

x_{1_0} is the mole fraction of helium in chamber A initially ($t=0$)

- N_1 is the molar flux of helium into chamber A at any instant of time
in *moles/sec.cm²*
- ∇x_1 is the concentration gradient for helium in the concrete
- C_2 is the concentration of nitrogen in chamber B at any instant of
time in *moles/cc.*
- x_2 is the mole fraction of nitrogen in chamber B at any instant of
time
- N_2 is the molar flux of nitrogen in chamber B at any instant of time
in *moles/sec.cm²*
- ∇x_2 is the concentration gradient for nitrogen in the concrete
- D_{1k} is the Knudsen diffusion coefficient for helium in *cm²/sec.*
- D_{2k} is the Knudsen diffusion coefficient for nitrogen in *cm²/sec.*
- D_{12} is the molecular diffusion coefficient for the helium/nitrogen in
cm²/sec. system
- V is the volume of the chambers in *cm³*
- C is the concentration of helium/nitrogen mixture at any instant
in *moles/cc.*
- L is the thickness of the concrete disc specimen used in *cms.*
- A is the cross sectional area of the disc in *cm²*
- ϵ is the porosity of the concrete sample expressed as a fraction

τ is the tortuosity factor to account for the sinuosity of the pores along the path of diffusion

On conducting the static test, the output obtained is a chart which records the concentration difference as mV versus distance in cms as shown in Fig. (5). Knowing the speed at which the chart advances, the distance can be converted to time. Initially ($t=0$), the diffusion chamber contains only nitrogen, for which $x_1 = 0$ and the corresponding concentration difference (mV) is known. Similarly, at the time when the system attains steady state, $x_1 = 0.5$. and the corresponding concentration difference (mV) is also known. A graph is plotted for mV versus x_1 for the two points defined. From the straight line plot, shown in Fig. (6), the values of x_1 are recorded for the different mV readings corresponding to the time instants. From Eqns. 3.5 and 3.6 the molecular diffusion coefficient and the Knudsen diffusion coefficients for helium and nitrogen for that concrete are evaluated. Using Eqn.3.32, the value of θ can be calculated for any instant of time. A computer program is developed to generate θ versus x_1 . Substituting the value of θ in Eqn. 3.31, the corresponding value of the ratio $\frac{\epsilon}{\tau}$ is evaluated. Finally the average value of $\frac{\epsilon}{\tau}$ is determined, which represent a constant parameter for the particular concrete.

3.2.4 Effective Diffusion Coefficient

The diffusion through the pores takes place only through the tortuous pores of concrete. As the pores are not straight, the diffusion effectively takes place over longer distance than it would be in homogenous medium. Also, the solids being impermeable, diffusion occurs over a smaller cross sectional area than that available in a homogenous material.

The effects of the longer diffusion path and smaller areas can be lumped together in the definition of the effective diffusion coefficient [61].

$$D_e = \frac{\epsilon}{\tau} D \quad (3.33)$$

where

ϵ is the total porosity of the material

τ is the tortuosity factor, which accounts for the sinuosity of the pores along the path of diffusion

D is the diffusion coefficient of NaCl in water $1.26 \times 10^{-5} \text{ cm}^2/\text{sec}$.
at the specific temperature of 19°C .

From equation (3.32), once the value of $\frac{\epsilon}{\tau}$ is established for different concretes, effective diffusion coefficient for Cl^- ion in concrete can be computed using Eqn. (3.33).

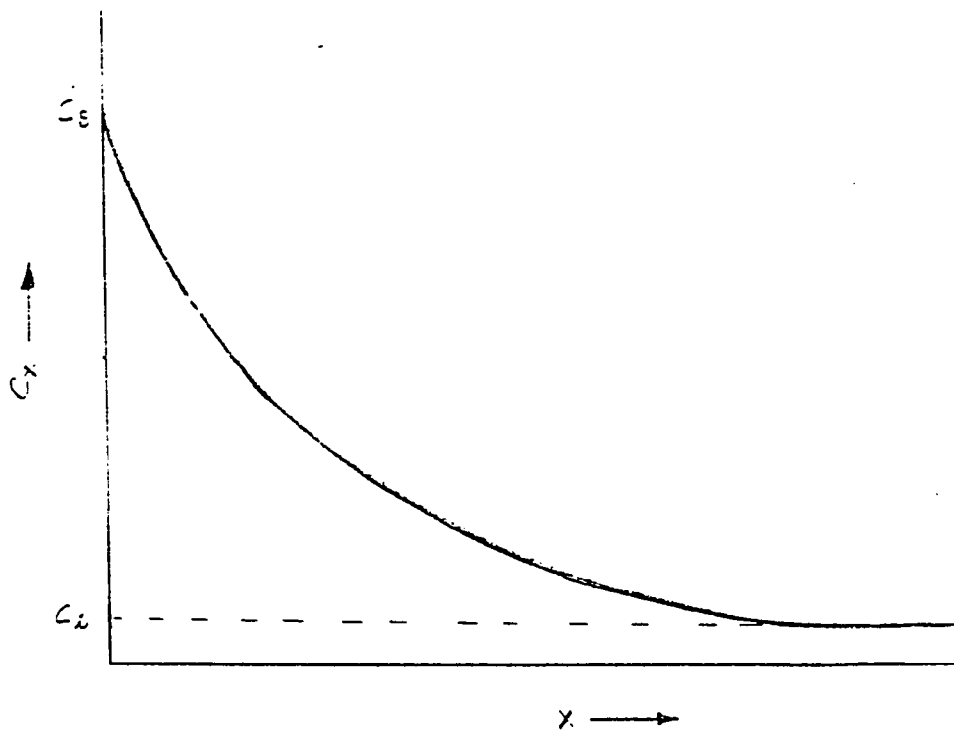


Figure 3: A Typical Chloride Concentration Profile

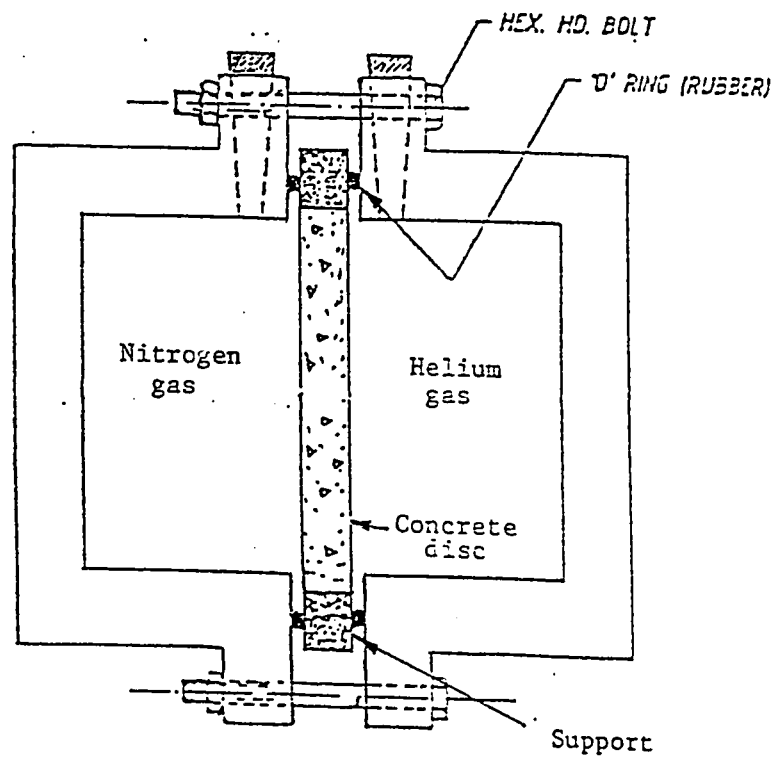


Figure 4: Sketch Showing the Diffusion Cell

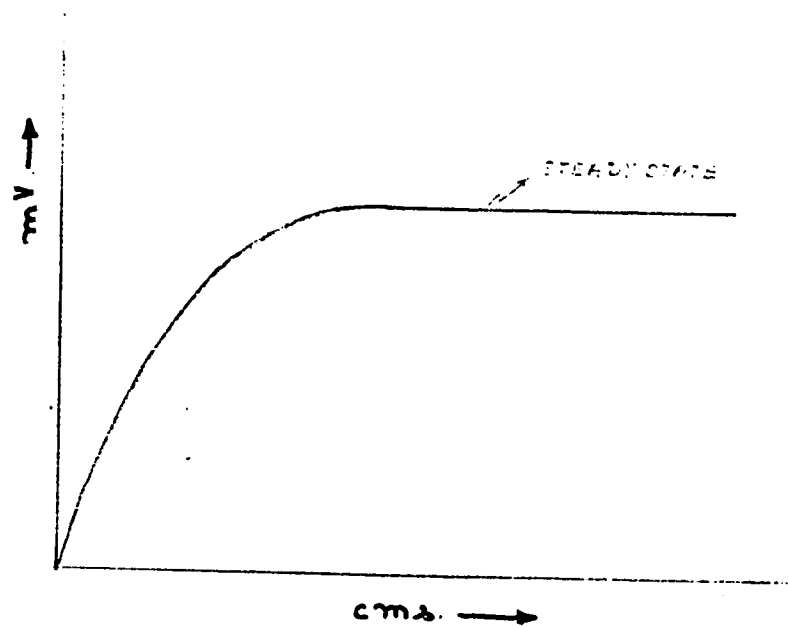


Figure 5: Chart Obtained from the Gas Diffusion Test

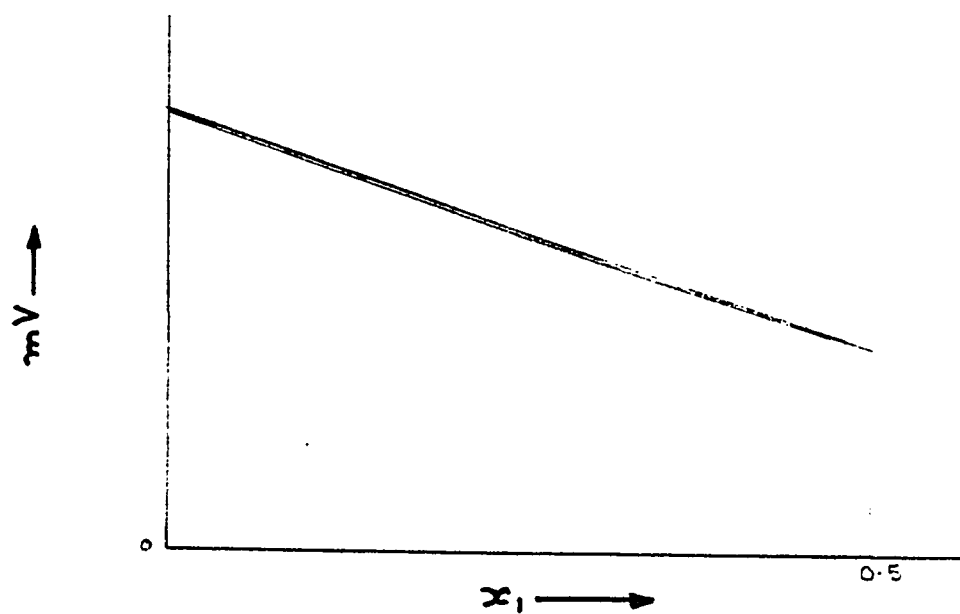


Figure 6: Concentration Ratio Versus mV Plot

Chapter IV

EXPERIMENTAL PROGRAM

4.1 General

An experimental program was planned to derive test data on the following items of interest .

1. Diffusion Coefficients for Chloride Ions in Concrete
2. Initiation of Chloride Induced Corrosion of Steel Reinforcement

For item (1), two different experimental techniques were pursued, namely:(a)Chloride Exposure Test and (b)Gas Diffusion Test. So, in order to achieve the research objectives, the program was subdivided into three major experimental programs:

Part 1. Chloride Exposure Test

Part 2. Corrosion Initiation Test

Part 3. Gas Diffusion Test

Figs. 7-9 indicates the details of the different parameters considered in each part.

4.2 Materials

4.2.1 Cement

ASTM C 150 Type V Sulphate Resisting Portland Cement which is extensively used in the Kingdom was used for this study

4.2.2 Aggregates

The coarse aggregates used in this study was the crushed limestone procured from the quarries in Riyadh. The specific gravity and absorption of coarse aggregates were determined in accordance with ASTM C-127 and are shown in Table 2. The grading of coarse aggregates was selected confirming to ASTM C-33 and is shown in Table 3.

Medium coarse sand was used as fine aggregate. The specific gravity and absorption of the fine aggregates are given in Table 4.

For mixing the constituents, potable water was used for all specimens.

4.3 Mix Design

The absolute volume method was used for the mix design of the specimens used in this research. The different parameters considered were

Cement Content = 300, 350 and 400 kg/m^3

Coarse / Fine Aggregate ratio = 1.6

Effective Water / Cement ratio = 0.4, 0.55 and 0.7

4.4 Specimens

The type, size and the number of specimens used to determine the different parameters are shown collectively in Table 5. Slabs, blocks, discs, cubes and cylinder concrete specimens were used in all experiments for the measurement of different items. The slabs were used to determine the diffusion coefficients of chloride ions for different concretes mixes and exposure conditions. The gas diffusion test is conducted on concrete disc specimens 1 cm thick. Figs. 10 and 11 indicates the specimens tested for gas diffusion. For the corrosion initiation tests, block specimens of varying cover to reinforcements were used under indoor exposure conditions only. A typical specimen tested for rebar corrosion is shown in Fig. 12. To prevent inconvenience that would be caused during coring, the slabs were cast without any reinforcement. The block specimens were cast with a central bar at a constant cover of 2" from the bottom. Leading wires were soldered to the bar as shown in Fig. 13. 5 gms of representative concrete samples were used for the pore radius measurements by mercury intrusion. Some of the samples used for pore radius measurements and the cylinders tested for compressive strength are shown in Figs. 14 and 15 respectively.

4.5 Specimen Preparation

4.5.1 Mixing and Casting

The constituents were mixed in a revolving drum type mixer. The mixing was done for approximately 3 to 5 minutes till the concrete was uniform. For the mixes with w/c ratio of 0.4, a super-plasticizer CP 430 was added at a dose of 9 ml per kg of cement for the cement contents of 300 and 350 kg/m^3 to enhance the workability. The moulds were filled in 3 layers and vibrated for compaction.

4.5.2 Curing

The specimens were demoulded 24 hrs. after casting and covered with wet burlap/towel to cure at lab temperature of 18 - 20⁰C. Fig. 16. The towels were wetted from time to time. Curing was done for a period of 2 weeks. Following the curing period, the dykes made to allow ponding and as per plan one set of specimens were kept at controlled conditions inside the laboratory and the other set was exposed outdoors as indicated in Figs. 17 and 18 respectively.

4.6 Experimental Technique

4.6.1 Part 1: Chloride Exposure Test

In this series, a set of slab specimens (details in Table 5)were ponded with chloride solutions. The different variables considered were the water/cement ratio, exposure chloride concentration and exposure conditions. The details of the different parameters are indicated in Fig. 7. Unidirectional diffusion of chloride is ensured by ponding the chloride solution on the top of the slabs in dykes made of cement mortar. The joint and the sides of the dyke was properly sealed to prevent any leakage. To maintain constant chloride concentration, the ponded solution was changed daily for the specimens.

Periodically, cores were taken from each slab for chloride analysis along the depth of the slabs. The chloride contents at different depths of the extracted cores were measured using a spectrophotometric method. After coring, the holes so formed were filled cement mortar upto a depth of 5.5" and the remaining 0.5" was filled with an epoxy sealant to ensure that no leakage would take place through the holes [Fig. 17].

4.6.1.1 Analysis for Total Chlorides

To determine the chloride profile, at an interval of 35 days, 1" diameter cores were extracted from all slabs [Fig. 20]. The coring was done using sweet water as the lubricant. Then the cores were sliced dry at different intervals [Fig. 21] using a carbide saw.

After slicing, the specimens were ground to a fine power passing #100 sieve. 3gms of the powdered sample was taken and washed into a beaker with distilled water, to which 3ml of concentrated nitric acid was added and then shaken for thorough mixing. The volume was made upto approximately 50ml by adding distilled water and was left to boil for 1 minute. This completes the digestion. Now, the solution was filtered for the extract and the filtrate was made upto 100ml with distilled water. Spectrophotometric method [62] was used to find the chloride content of the extract.

4.6.1.2 Spectrophotometry

In this method, 0.5ml of the chloride extract was diluted to 10ml using distilled water, to which was added 2ml of mercuric thiocyanate saturated in ethanol (A) and a mixture of 9M nitric acid + 0.25M of ferric ammonium sulfate (B) [144ml of HNO_3 + 106ml of distilled water + 30.14gm of ferric ammonium sulfate]. A reference solution (blank) is also prepared by mixing 10ml of de-ionized water with A and B. The absorbance of the chloride solution and the blank was measured at a wave length of 460nm. The difference between the two readings gives the net absorbance for the chloride. Now, from the calibration curve for chloride concentration against absorbance, the concentration of the extract was determined as % by weight of concrete. The apparatus and the set up is presented in Fig. 22.

The chloride profile so obtained was used to evaluate the diffusion coefficient directly by using the solution to the Fick's second law, subject to appropriate boundary conditions.

4.6.2 Part 2: Gas Diffusion Test

Conventionally, the chloride diffusion coefficient is determined using a 2 chamber diffusion cell as shown in Fig. 1, Chapter 1. One chamber filled with sodium chloride solution and the other with calcium chloride. The test requires a longer duration to complete the diffusion measurements and so the practical application is limited. Hence an attempt has been made to seek an alternative method to determine the diffusion coefficient using a gas diffusion test which is much faster and may be more general in application.

From the gas diffusion test, using helium and nitrogen, the ratio of porosity to tortuosity e/τ , which is a constant for a porous medium can be determined. From this constant the effective diffusivity of any fluid in concrete can be evaluated. The different parameters considered for the test are presented in Fig. 8.

4.6.2.1 Dynamic Experiment on a Single Pellet

The first attempt in gas diffusion test was a dynamic experiment using a single pellet apparatus. This experiment basically involves injecting a pulse into a system where a carrier gas flows across the concrete pellet, and the peak response detected at the other side of the pellet is analyzed [63]. The dynamic experiment is a very fast technique for evaluating the diffusion coefficient.

Apparatus

The apparatus consists of a single pellet cell, carrier and sample flow lines, a detector and a recorder [Figs. 23-24].

Procedure

The carrier gas (He) flows through the upper and lower chambers. The tracer (N_2) is introduced into the upper gas stream by means of a gas sampling valve. The detector is a thermal conductivity cell, which measure the thermal conductivity of the carrier and the tracer, giving pronounced peaks, which are recorded by a strip chart recorder.

Now by solving the appropriate mass balance equation for the above system in the Laplace domain using the moment theory and numerically integrating the resulting chromatographic curves, the diffusion coefficient can be determined.

In spite of making several attempts, on injecting the pulse into the system, no peak response could be detected by the recorder. This was attributed to the low porosity of the concrete specimens, which offered considerable amount of resistance to the pulse, thereby making the process of diffusion quite slow. So, when compared to the resistance offered by the bulk of the concrete specimen to the diffusing gas, the film resistance can be considered negligible. So, an alternative approach involving a static test was devised based on the conclusion of negligible film resistance.

4.6.2.2 Static Experiment on a Single Pellet

The static diffusion test though comparatively slower than the dynamic test is still much faster than the conventional diffusion test [64].

Apparatus

The apparatus consists of a single pellet cell [Fig. 25], gas flow lines, a detector and a recorder.

Procedure

One chamber is filled with helium and the other with nitrogen. The test set up is shown in Fig. 26. The gases diffuse countercurrently

through the concrete specimen. The concentration of nitrogen in chamber 2 is recorded continuously. The reference is another chamber filled with pure helium as shown in Fig. 27. As the gaseous diffusion progresses, the concentration change in the diffusion cells leads to a change in the electrical resistance. The thermisters attached to the diffusion cell detects such change in resistance with respect to the reference cell. The change of concentrations are automatically recorded in terms of millivolts on a strip chart. These diffusion curves are later converted to another plot of concentration difference against time. Now, from the plot of the concentration difference against time, the diffusivity can be determined as discussed in Chapter 3.

4.6.3 Part 3: Reinforcement Corrosion

To monitor the initiation of corrosion, concrete block specimens are used. The detailed dimensions for these specimens are given in Table 5. The parameters considered were water/cement ratio, cover to reinforcement and exposure chloride concentration. The block specimens were cast with a central 12mm bar at a constant cover of 2" from the bottom. The bars were soldered to a wire and were later coated with epoxy to prevent galvanic corrosion. The specimens were ponded with chloride solutions of 4% and 8% concentrations and exposed under controlled laboratory conditions. At regular intervals, half cell potentials

and corrosion current density measurements were monitored using the linear polarization technique. From these measurements, the initiation time of corrosion in these specimens were detected. At the end of the monitoring period, all the blocks are split open for visual observation. The chloride contents at the rebar level are also determined.

4.6.3.1 Linear Polarization Resistance Technique

Linear polarization resistance technique is used to measure the rate of corrosion of steel reinforcement [65,66].

The test procedure is based on the Stern-Geary Characterization of the typical polarization curve for the corroding metal. Here, a linear relationship is described mathematically for a region on the polarization curve in which slight changes in the current applied to the corroding metal in a ionic solution causes corresponding changes in the potential of the metal. In other words, if a large current is required to change the potential by a given amount, the corrosion rate is high and on the other hand, if only a small current is required, the corrosion rate is slow [67].

In this test, three electrodes are used to measure the resistance to polarization using a potentiostat/galvanostat. The steel rod is connected to the working electrode terminal while a steel plate and a reference electrode are connected to the respective terminals of the potentiostat. The steel is polarized by applying a potential of $\pm 10mV$ of the open

circuit potential and the resulting current between the counter and working electrodes are measured [68]. The set up used is shown in Fig. 28. The potentials are changed at a rate of 6 mV/min. and the resulting current is measured. The slope of the potential-current curve is the resistance to the polarization, R_p . The corrosion current density is then calculated using the following relationship [69]

$$I_{corr} = \frac{B}{R_p}$$

where

I_{corr} is the corrosion current density, $\mu A/cm^2$

R_p is the linear polarization resistance, $\frac{\Delta E}{\Delta I}$, ohm cm^2

$$B = \frac{\beta_a \beta_c}{2.3 (\beta_a + \beta_c)}$$

where

β_a is the anodic tafel constant

β_c is the cathodic tafel constant

The Tafel constants can be determined by polarizing steel to ± 250 mV of the rest potential or corrosion potential. In the absence of sufficient data on tafel constants, a value of 100 mV are to be used for steel in a highly resistant medium [70]. A good correlation between the weight loss determined by gravimetric methods and linear polarization technique was observed by Gonzalez et al [71] by using a $B=26$ mV for steel in

the active state and $B=52$ mV for steel in the passive state. In our investigation, $\beta_o = \beta_c = 120$ mV was used throughout, which corresponds to a $B=26$ mV.

4.7 Auxiliary Tests

4.7.1 Mercury Intrusion Porosimetry

In order to determine the mean radius of the pores and the total porosity of the concrete specimens, Mercury Intrusion Porosimetry (MIP) was conducted. The test is conducted according to ASTM D-4284.

In MIP, mercury, a non wetting liquid is forced into the pores of the material at high pressure. Pore size and volume quantification are accomplished by submerging the sample under a confined quantity of mercury and then increasing the pressure of mercury hydraulically. As the applied pressure is increased, the radius of the pores which can be filled with mercury decreases and consequently, the total amount of mercury intruded decreases. The data obtained gives the pore volume distribution directly, from which the porosity and the mean pore radius can be determined [72].

In this study, the porosity tests were carried out by Imperial Chemical Industries, U.K., using a Micrometrics 9220 Mercury Porosimeter. Intrusion was carried upto 6000 psia. For the test, a value of surface tension γ equal to 485 dynes and contact angle θ equal to 140° was

used. In addition to the applied pressure and the total pore volume recorded, the approximate pore diameter ranges and the pore volumes are also obtained. The soft ware in the porosimeter calculates a surface area from the intrusion curve.

4.7.2 Concrete Permeability

The test for water impermeability was done in accordance with DIN 1048 PART 1 [73]. The 6" cube specimens were tested at an age of 28 days. The apparatus and test set up is shown in Fig. 29. Water pressure is applied on one face only such that the pressure is acting in a direction perpendicular to the direction of casting of the cube.

As per the specification, first a pressure of 1 bar was applied for 48 hours, then 3 bars for 24 hours and lastly 7 bars for 24 hours, one after the other. Immediately after the test, the test specimen was split in the middle by applying compression on 2 steel rods lying on opposite sides above and below the specimen [Fig. 30]. The specification requires that when splitting, the face of the specimen subjected to water pressure should face downwards.

The greatest water penetration depth, measured on the test concrete was taken as the average value of the greatest penetration depth on 3 test specimens.

4.7.3 Compressive Strength

The details of the specimens are shown in Table 5. The cylinders were tested at an age of 28 days. Then after providing sulphur capping, according to ASTM C-39, using a hydraulic compression testing machine of $\pm 0.1kN$ accuracy, the cylinders were tested for strength.

Table 2: Absorption and Specific Gravity of Coarse Aggregates

Size	Absorption (%)	Bulk Sp. Gravity
3/16"	1.621	2.607
3/8"	1.477	2.605
1/2"	1.034	2.643
Overall Grading	1.497	2.610

Table 3: Grading of Coarse Aggregates

Size	Wt. Retained	Cum. Weight. Retained	% Passing	ASTM C-33 No.7
3/4"	0	0	100	100
1/2"	10	10	90	90-100
3/8"	45	55	45	40-70
3/16"	45	100	0	0-15
3/32"	0	100	0	0-5

Table 4: Absorption and Specific Gravity of Fine Aggregates

Absorption (%)	Bulk Specific Gravity
1.562	2.55

Table 5: Specimen Description

Parameter	Specimen		
	Type	Size	Number
<i>Diffusion</i>	Slab	30"x18"x6"	16
	Disc	1" ϕ , t=0.394"	
<i>Corrosion</i>	Block 1	12"x6"x6"	4
	Block 2	12"x6"x5"	4
	Block 3	12"x6"x3.5"	4
<i>Permeability</i>	Cube	6"x6"x6"	30
<i>Strength</i>	Cylinder	d=3", h=6"	30
<i>Porosity</i>	Concrete	small pieces	upto 5 gms

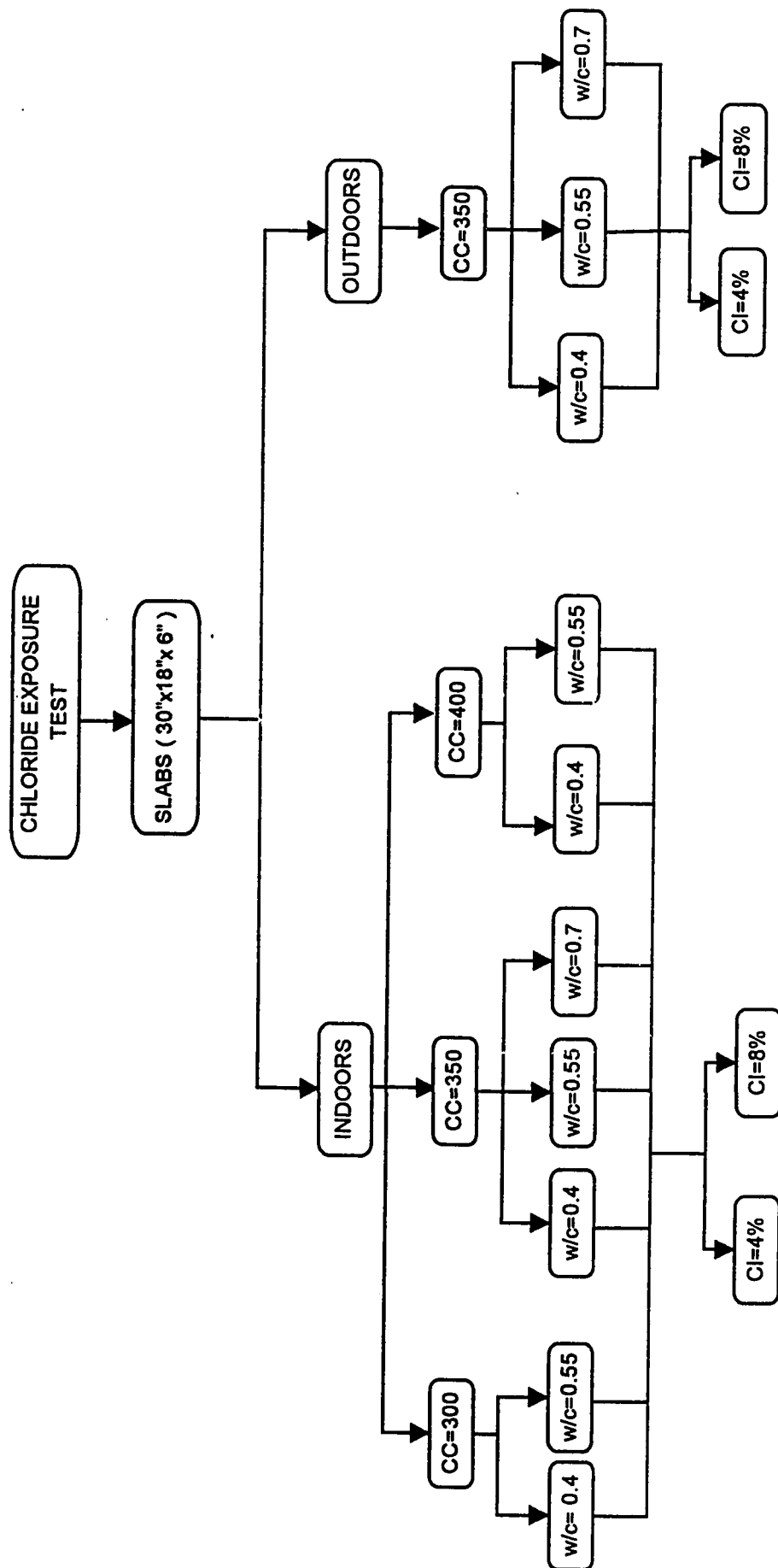


Figure 7: Experimental Parameters for Part 1

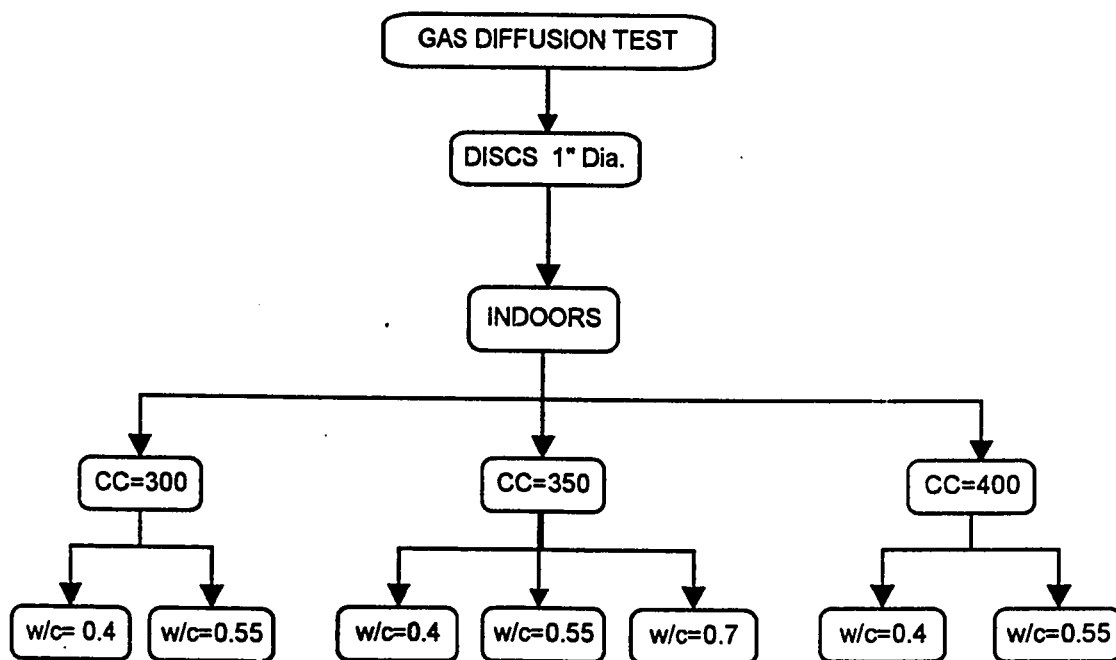


Figure 8: Experimental Parameters for Part 2

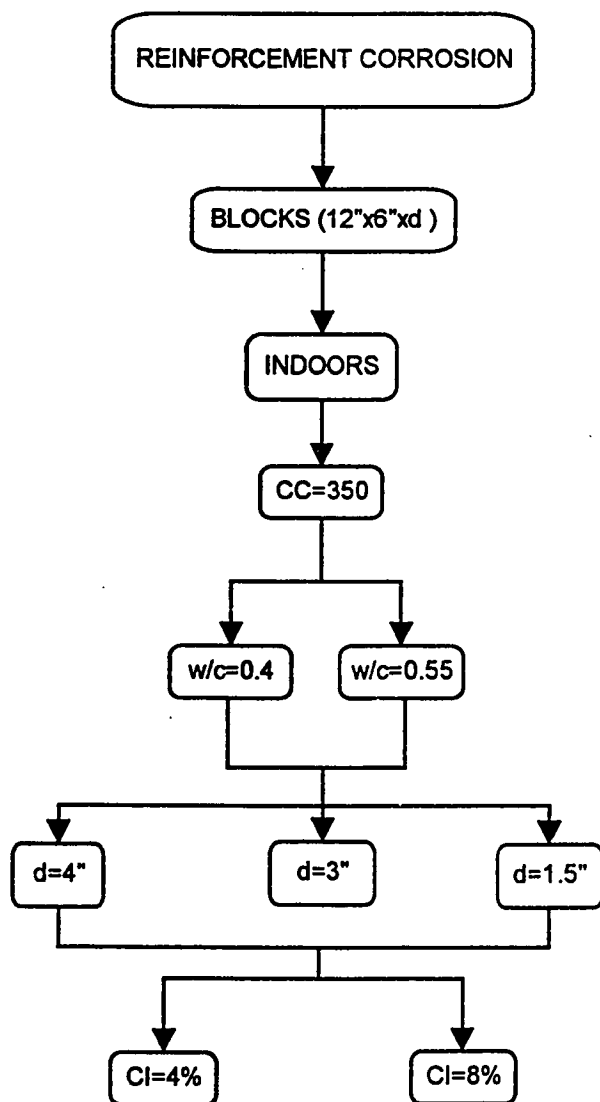


Figure 9: Experimental Parameters for Part 3



Figure 10: Photograph Showing the Discs Used for Gas Diffusion Tests

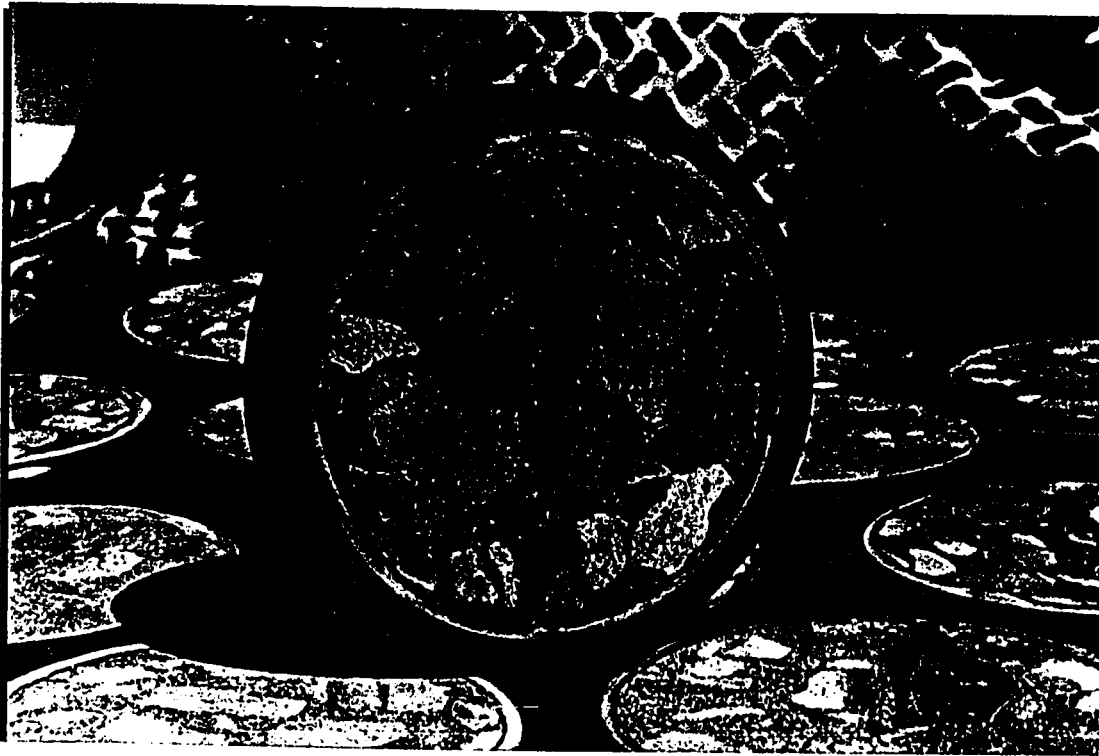


Figure 11: Photograph Showing the Close-up of The Disc

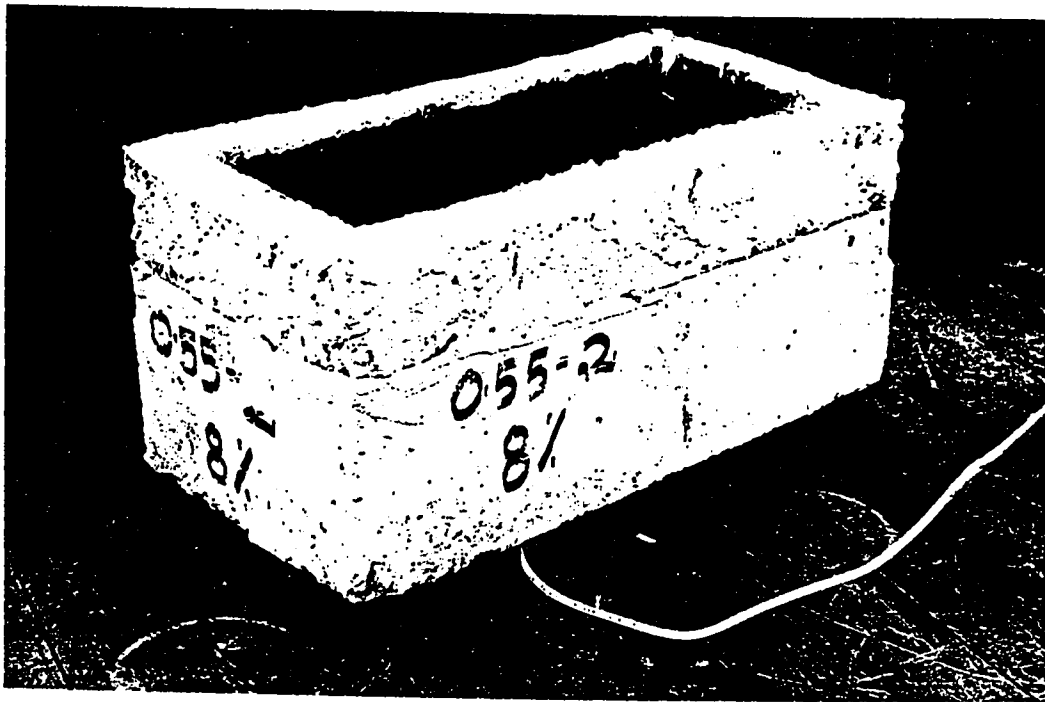


Figure 12: Photograph Showing the Blocks Used for the Corrosion Study

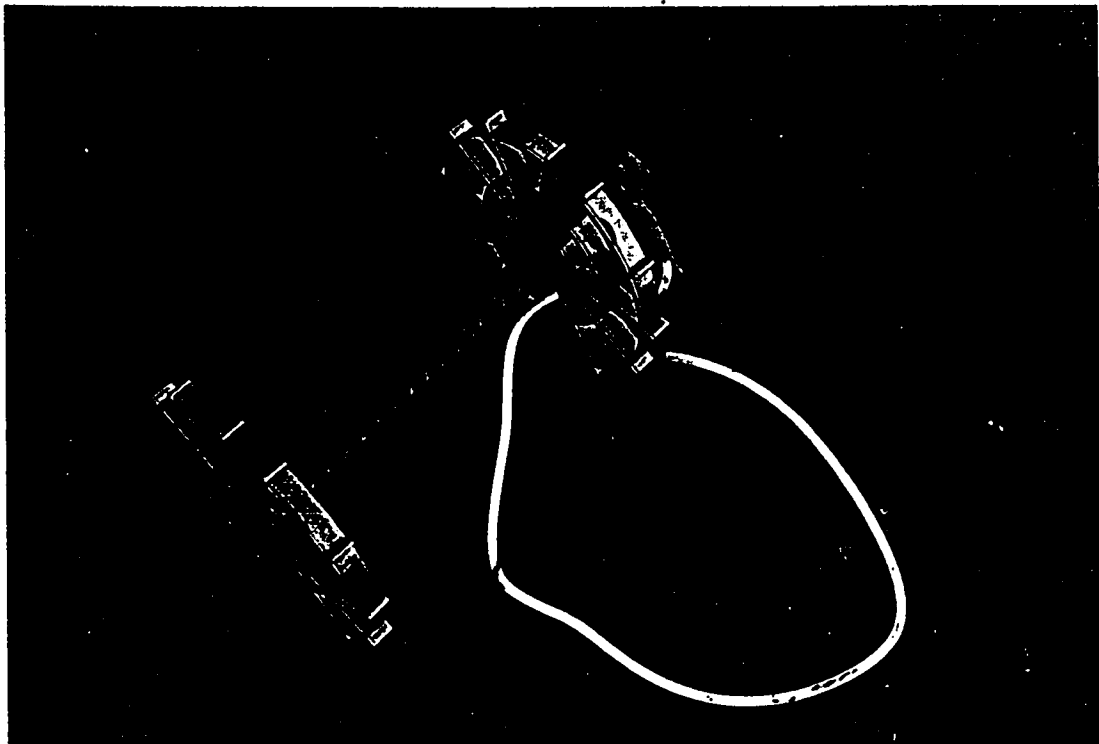


Figure 13: Photograph Showing the Bar Used in the Corrosion Specimens

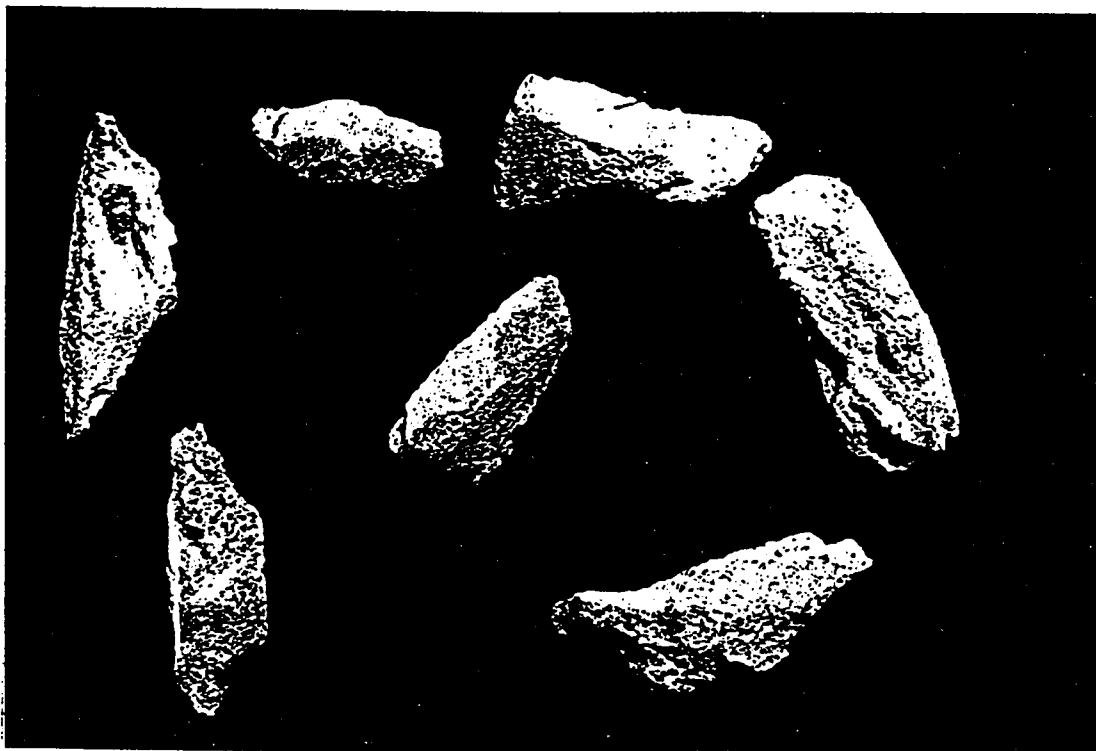


Figure 14: Photograph Showing the Samples used for MIP

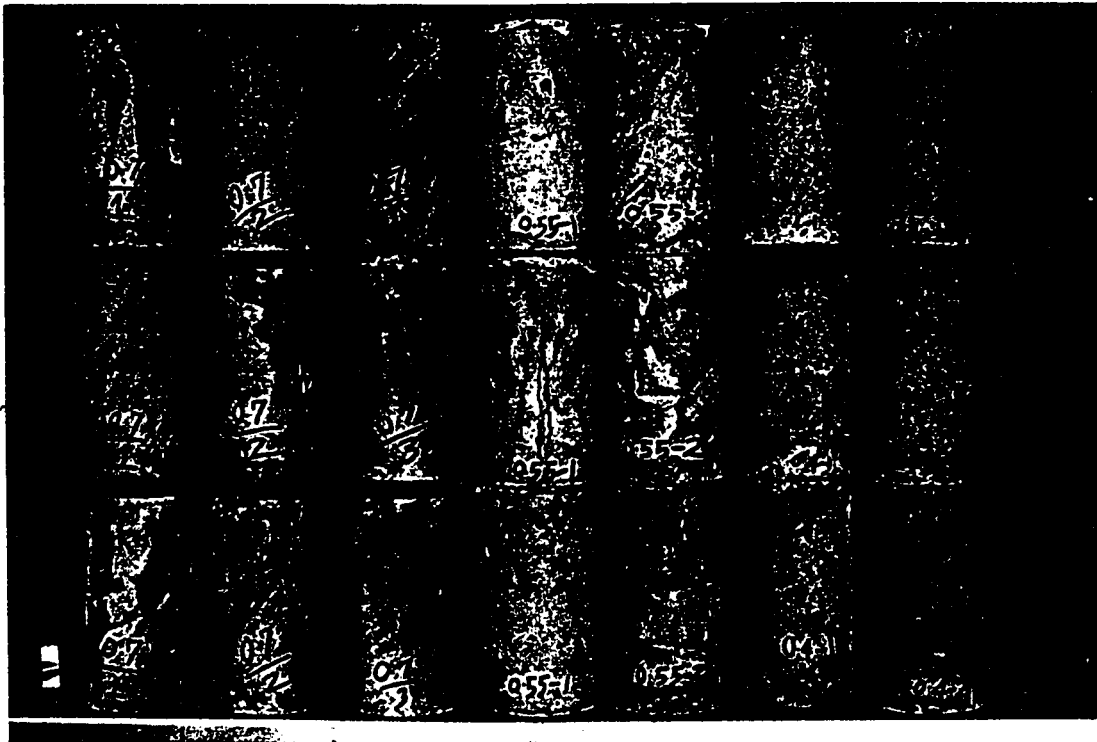


Figure 15: Photograph Showing Some of the Cylinders Tested for Comp. Str.



Figure 16: Photograph Showing the Curing of Specimens

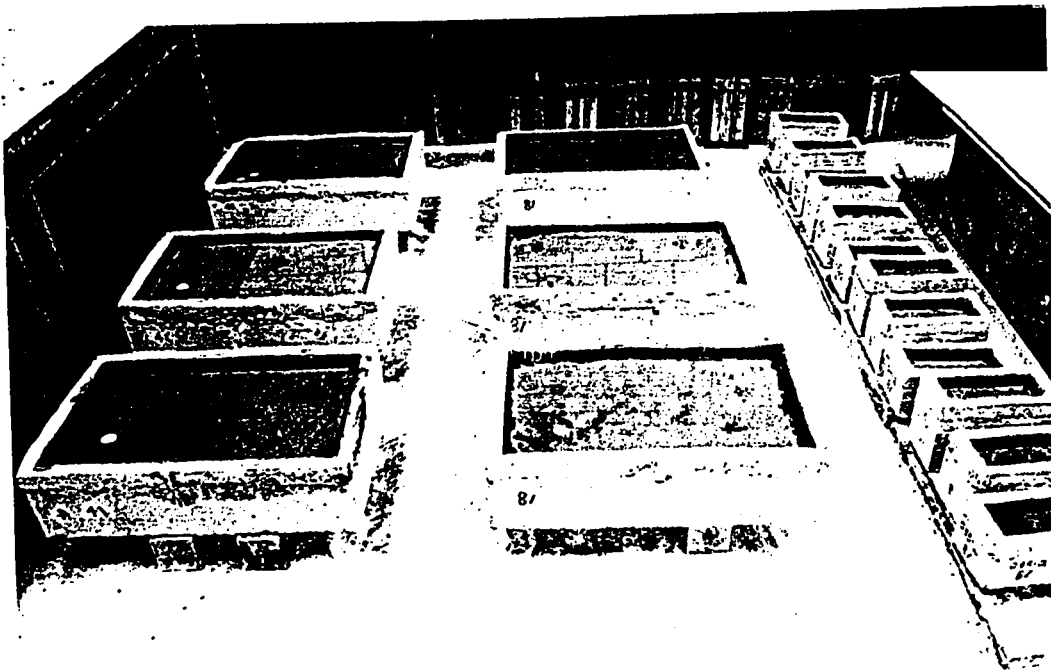


Figure 17: Photograph Showing the Specimens Exposed Indoors



Figure 18: Photograph Showing the Specimens Exposed Outdoors

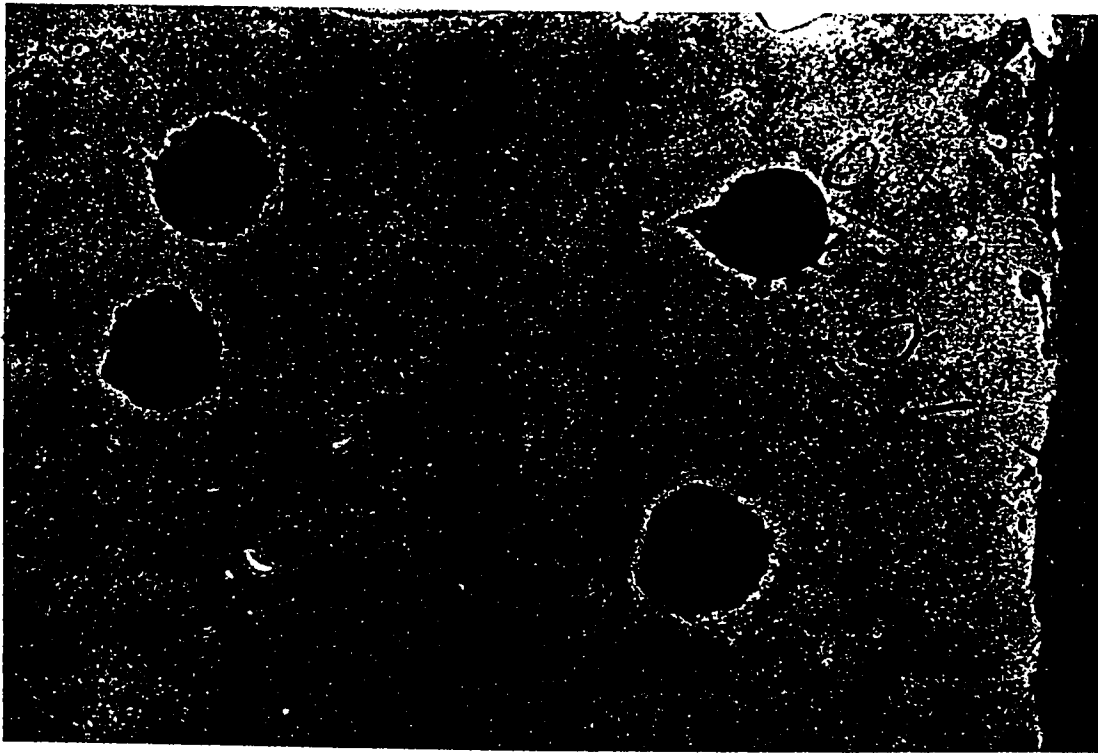


Figure 19: Photograph Showing the Holes Filled after Coring

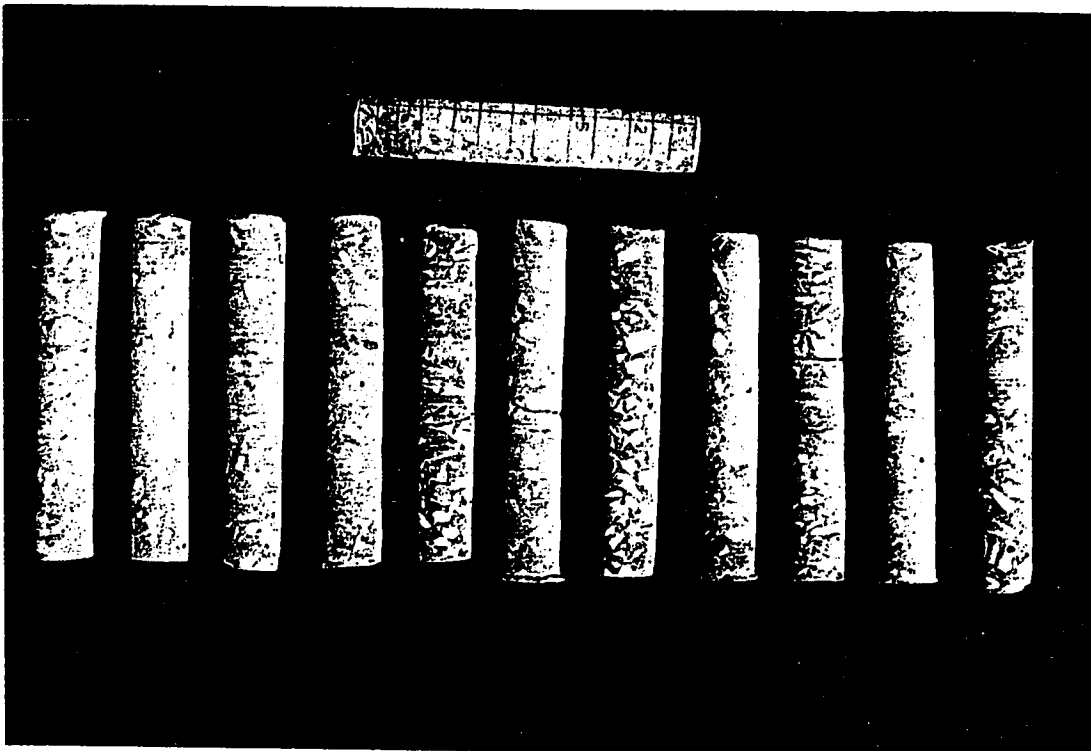


Figure 20: Photograph Showing Some of the Cores Extracted

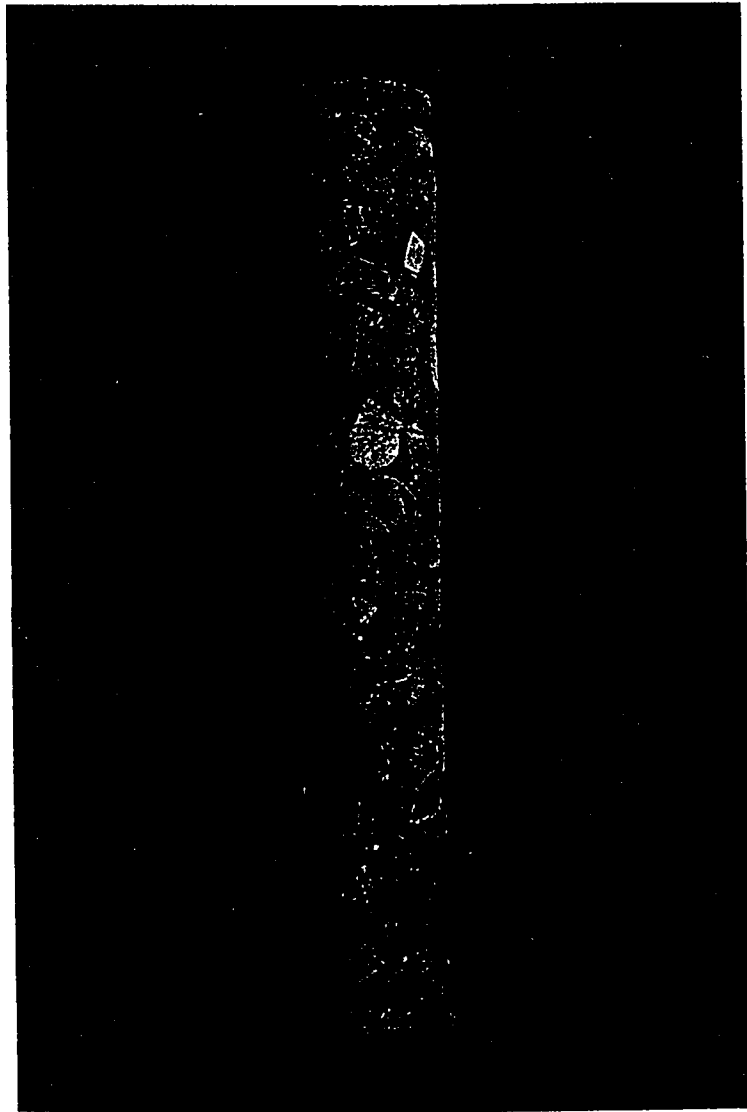


Figure 21: Photograph Showing the Interval of Slicing



Figure 22: Photograph Showing the Set up Used for Chloride Analysis

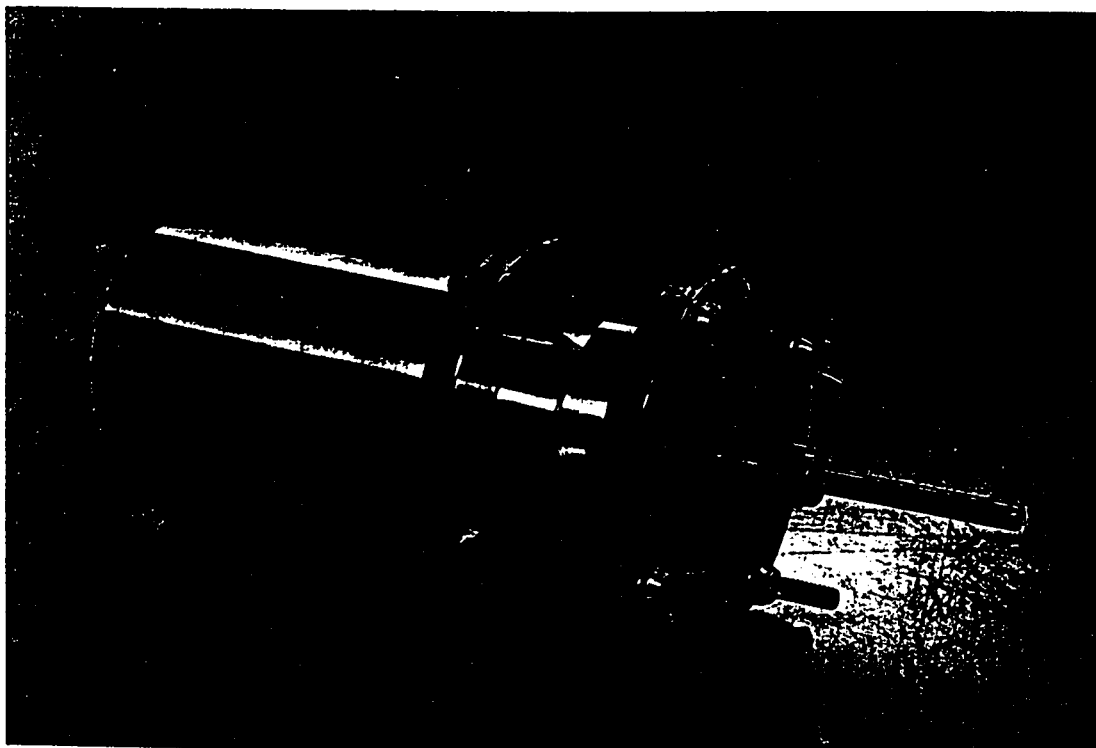


Figure 23: Photograph Showing the Close-up of Cell Used for Dy. Test

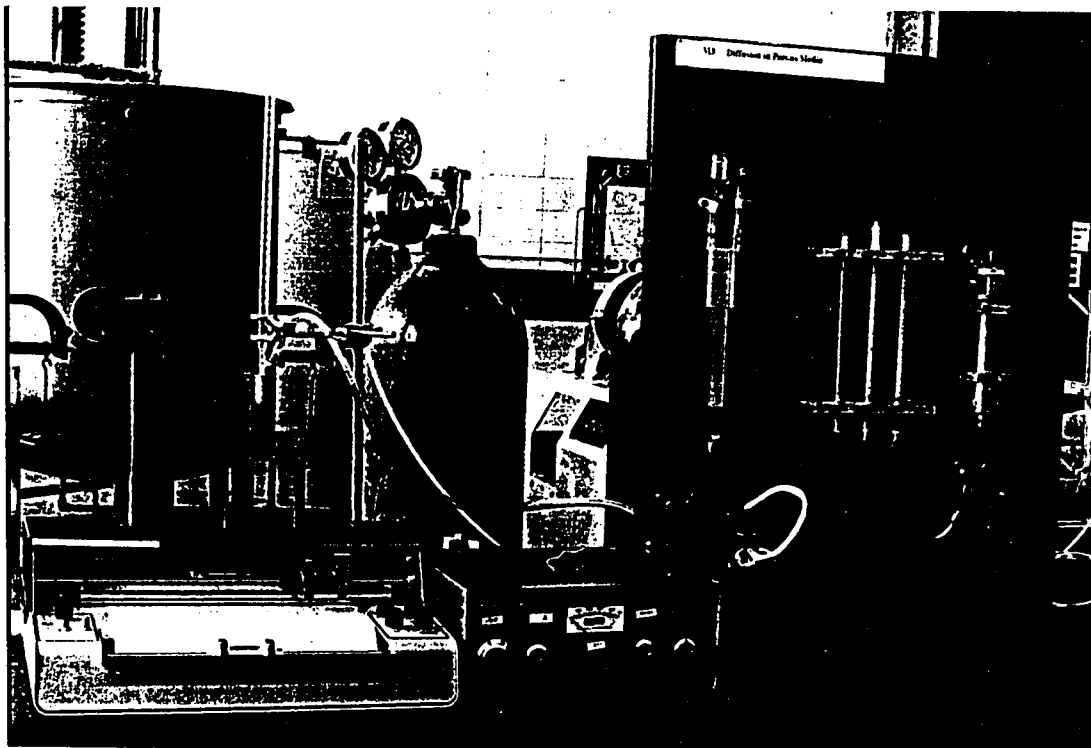


Figure 24: Photograph Showing the Set-up of The Dynamic Test

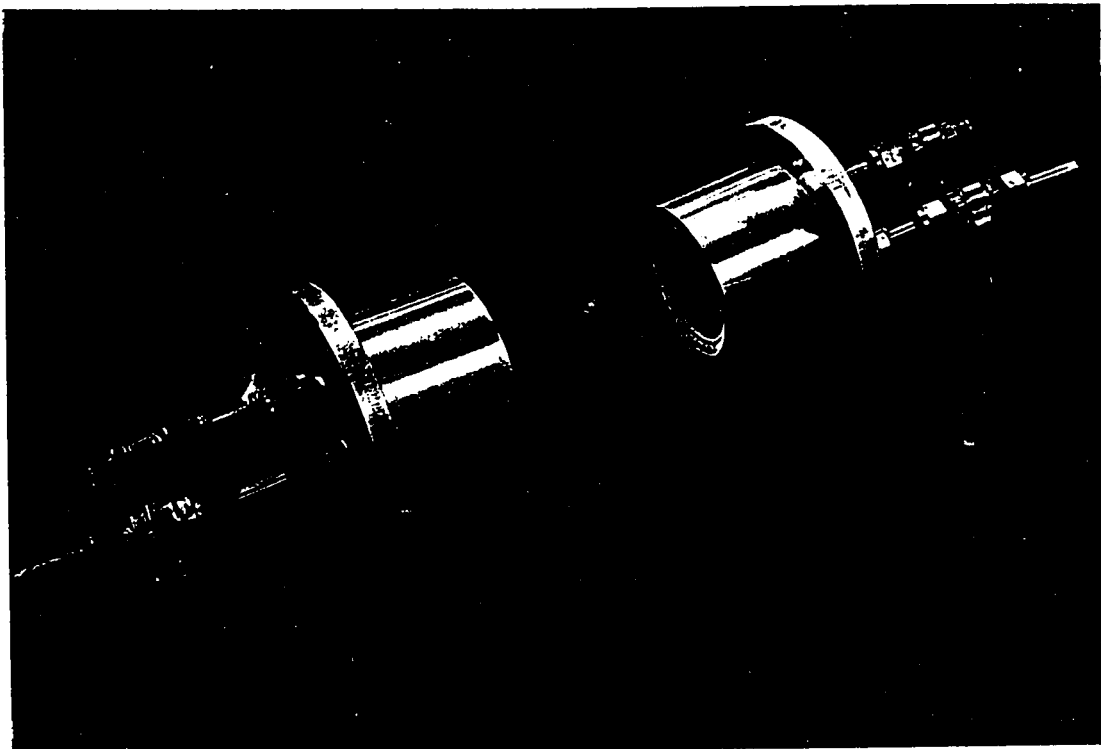


Figure 25: Photograph of the Cell used for the Static Diffusion Test

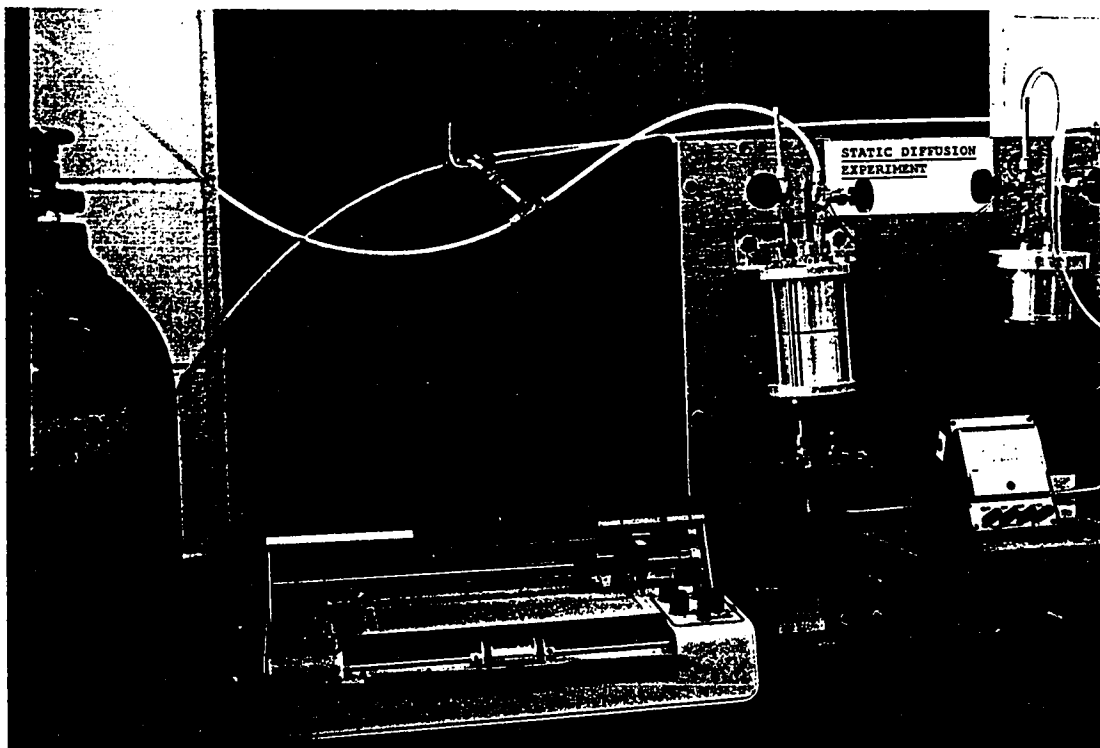


Figure 26: Photograph Showing the Set-up for the Static Diffusion Test

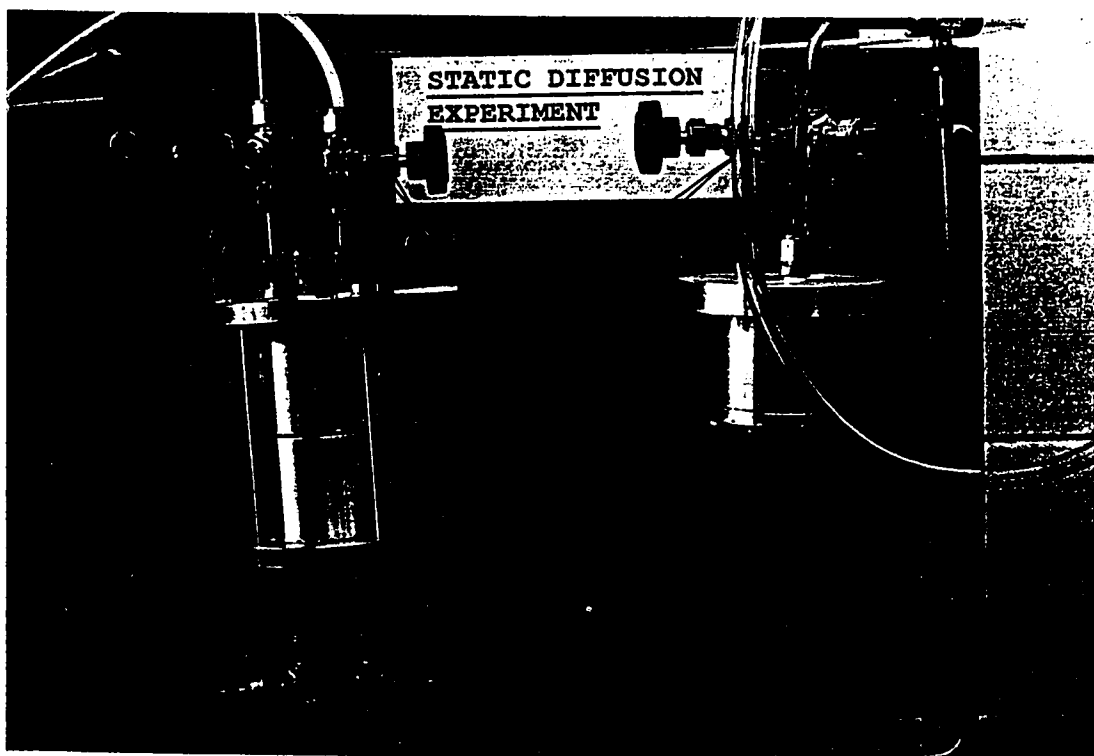


Figure 27: Photograph Showing the Diffusion Cell and the Reference Cell

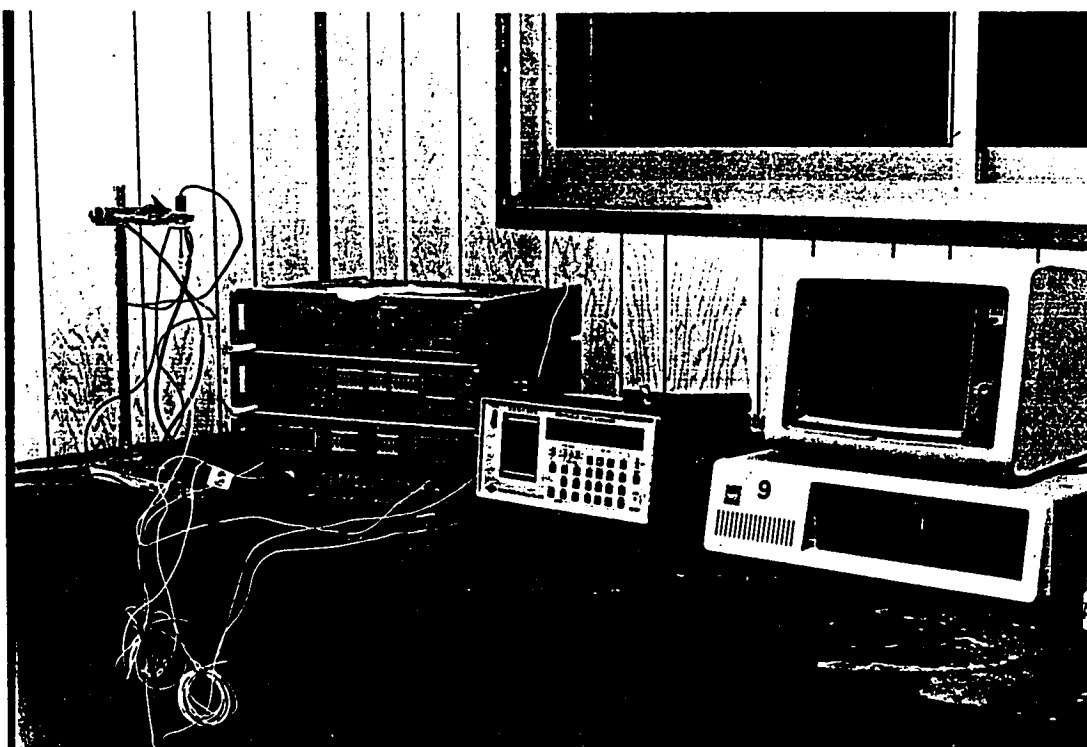


Figure 28: Photograph Showing the Set-up for LPT

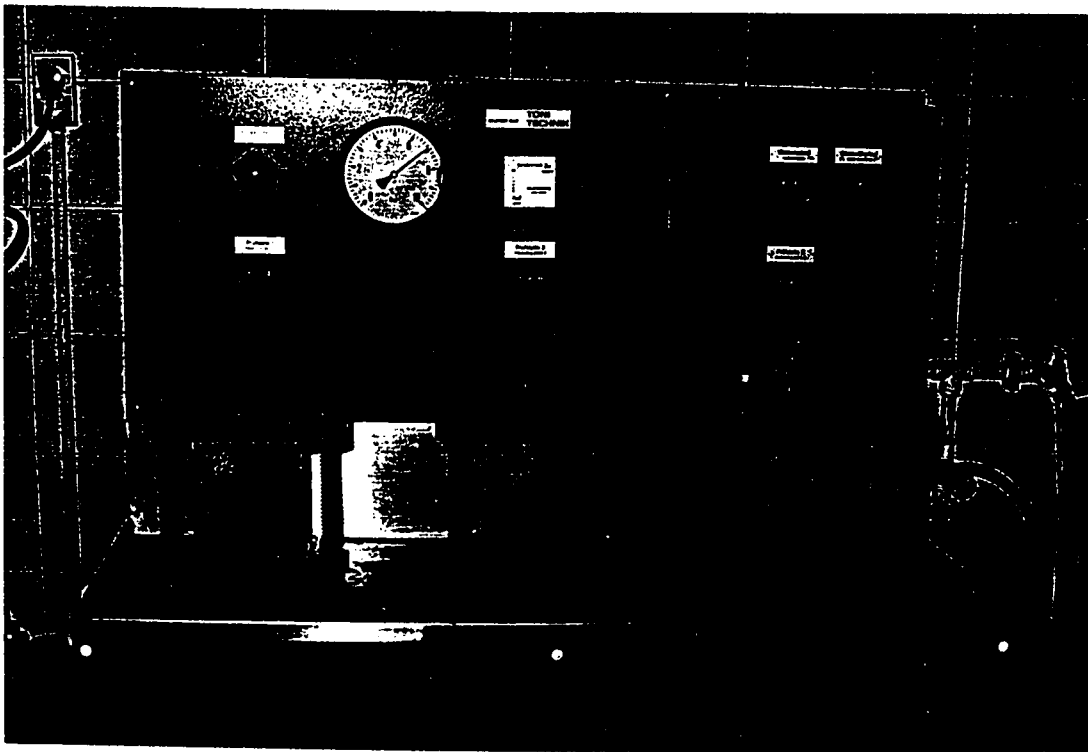


Figure 29: Photograph Showing the Set-up for Water Impermeability Test



Figure 30: Photograph Showing a Cube Being Split Open

Chapter V

RESULTS & DISCUSSION

The results of the auxilliary test are presented in sections 5.1 to 5.3 first, as they will be needed for the results and discussion of the diffusion coefficient evaluation and the effect of the different parameters presented in sections 5.4 to 5.7.

5.1 Mercury Intrusion Porosimetry

The total porosity (ϵ) and the effective pore radius (r_p) measurements of the concrete samples tested are shown in Table 6. As expected, it can be observed that generally, both ϵ and r_p increased with an increase in w/c ratio and decreased with an increase in the cement content. The effect of w/c ratio on ϵ and r_p is more predominant relative to that of cement content.

5.2 Concrete Permeability

Some typical cubes after being tested for permeability are shown in Fig. 30. Water permeability measured as the depth of water penetration from the DIN 1048 Water Impermeability test is shown in Table 7 and Fig. 32.

The depth of water penetration was found to increase with higher w/c ratio and decrease with lower cement content. In the case of w/c = 0.7, the test had to be stopped after 2 days only as water penetrated the full depth of the specimen, showing the poor quality of the concrete

5.3 Compressive Strength

The 28 day compressive strength of cylinders tested are shown in Fig. 33. It can be observed that the compressive strength increased marginally with an increase in cement content, but the strength decreased rapidly with higher w/c ratio.

5.4 Chloride Exposure Test

The solution to Fick's second law [Eqn.(3.4)] can be used to determine the effective chloride diffusion coefficient (D_c) from the chloride profiles experimentally determined. As previously stated in Chapter 3, Eqn. 3.4, contains the following parameters, the chloride concentration (C_x) at any particular depth (x), the initial or the primary chloride concentration (C_i), the chloride concentration at the surface of the concrete (C_s) and the time period (t) at which the chloride concentration was measured. If all the above parameters are known, Eqn. 3.4 could be used directly to find the value of D_c corresponding to each measured concentration along the depth of the core, and then averaged for a

constant value. But in our case the surface chloride concentration (C_s) is not available. Even though the concrete specimens were ponded with 4% and 8% NaCl solutions, this cannot be considered as the surface concentration for two reasons. First, because of the incompatibility of units i.e. the ponded solutions are expressed as % by weight of Cl in water, whereas the chloride concentration in concrete is expressed as % by weight of concrete. Second, experimentally determining the chloride concentration at $x=0$ is practically impossible. The solution to Fick's law contains 2 unknowns now, the surface concentration (C_s) and the effective diffusion coefficient (D_e). This necessitates the use of an iterative procedure to solve Eqn 3.4. So, an interactive optimization computer program was used to arrive at the best fit for the experimentally determined chloride profiles.

In order to use the optimization program to arrive at the values of C_s and D_e , a reasonable range has to be specified for the two unknowns. For a specified range of the two unknowns, given the value of all other parameters, the program back calculates the value of C_s for each combination of C_s and D_e . The iteration is continued within the range of the values specified for the two unknowns. The best fit for the experimentally determined chloride concentration profile is determined based on the minimum sum of square of errors between the calculated and the actual values of C_x . The efficiency of the program very much depends on the accuracy in prescribing the appropriate range of the unknowns.

In order to arrive at a suitable range for C_s and D_e , the following procedure was adopted. Manually, the experimentally obtained chloride profiles were extrapolated to $x=0$. This gives an idea about the approximate value of C_s . Observing the trend in the experimentally obtained data, a suitable margin is decided for the extrapolated C_s . Now, the range for the D_e value has to be decided. The optimization program used for the analysis of the data, on completing the run, gives a plot showing the optimized curve and the actual experimental values. First, a few blind tries are done with random ranges of D_e . Based on the observation for the converging trend, a reasonable range D_e is also selected.

The optimization criteria is based on the minimum sum of squares of error for a reasonable value of C_s . The program gives the best fit for the experimental values along with the optimum values of C_s and D_e . The values of C_s and D_e and the sum of squares of error (SSE) for each concrete arrived at after the optimization run are shown in Table 8. A typical output obtained from the optimization run is given in Appendix B.

As expected, with time, the chloride concentration was seen to build up gradually within the concrete. The diffusion coefficient was found to be influenced by the w/c ratio, the cement content and the exposure conditions, among which, the most influential factors were the w/c ratio

and the exposure condition. Results also indicated that the diffusion coefficients were independent of the exposure chloride concentration.

The chloride profiles obtained from the optimization run are shown in Figs. 34 to 48 for different periods. In case of $w/c = 0.7$, for the outdoor exposed specimens, when the cores were analysed after 105 days of exposure, it was seen that chloride had already passed through the full depth of the slab. The assumed boundary conditions for the solution to the Fick's law are no longer valid since the depth of the member can no longer be considered infinite. As expected, the chloride concentration increases with time and so the progressive movement of the chloride front can be observed in all the cases.

The difference in chloride concentrations between the surface and the concrete body sets up a concentration gradient which will result in the diffusion of the chlorides into the body of the concrete. This process of diffusion will continue till both concentrations are equal i.e. the gradient becomes zero. The effect of each of the experimental parameters on diffusion are discussed in detail in the following sections.

5.4.1 Effect of Water Cement Ratio

The chloride diffusion and hence the diffusion coefficient was found to be strongly influenced by the w/c ratio and exposure conditions. The effect of w/c ratio on chloride diffusion are shown in Figs. 49 to 54. For the same cement content, for a change in w/c ratio from 0.40 to

0.55 and 0.70 the corresponding change in diffusivity was from 8.52×10^{-8} to 28.1×10^{-8} and $66.3 \times 10^{-8} \text{ cm}^2/\text{sec}$ respectively. The variation of D_r with w/c ratio for a particular cement content is shown in Fig. 55. The range of 3-8 times increase in diffusivity may be attributed to the increased porosity and permeability of the concrete with higher w/c ratio.

For a cement content of 350 kg/m^3 , the porosity values corresponding to a w/c ratio of 0.40, 0.55 and 0.70 are 7.39%, 10.64% and 13.52% respectively. As mentioned previously, the concrete permeability test results also indicated a higher permeability for mixes with w/c = 0.55 and 0.70. Moreover, in the case of w/c = 0.70, the test had to be stopped after 2 days since water passed through the full depth of the specimen. This substantiates the very high values of diffusion coefficient obtained for w/c = 0.70.

The increase in diffusion with w/c ratio is in agreement with previously reported data [7,8,27,28,74] From their study on OPC mortar, Gjorv and Vennesland [7] reported the effect of higher w/c ratio to be confined only to top surfaces (i.e. upto a depth less than 10 mm) and the diffusion in the interior portions to be affected by other factors like chloride binding. However, for SRPC concrete, it is seen that the effect of w/c on diffusion is not only limited to the surface layers only but also occurs in the interior layers. It can be observed from Figs. 46 to 51 that an increase in the w/c from 0.4 to 0.7, after 175 days of

exposure, the chloride penetration depth increased from 4 cms to 10 cms, respectively.

5.4.2 Effect of Cement Content

The effect of cement content on chloride diffusion is shown in Figs. 56 & 57. As the cement content is increased from 300 to 400 kg/m^3 , diffusivity was marginally reduced from $(10.32 \times 10^{-8}$ to $7.63 \times 10^{-8} cm^2/sec.)$ for $w/c = 0.4$. However for $w/c = 0.55$, the diffusivity decreased by 51% (33.70×10^{-8} to $16.46 \times 10^{-8} cm^2/sec.$). The decrease in chloride diffusion with an increase in cement content is attributed to the development of a denser concrete. An increase in cement content results in an increase in the volume of the cement paste, which helps in two ways. First, the increased amount of paste helps to achieve better compaction and secondly it leads to a much refined pore structure. From Table 6, it can be observed that for a w/c of 0.4, when the cement content was increased from 300 to 400 kg/m^3 , the effective pore radius decreased from 224 Angstroms to 177 Angstroms.

5.4.3 Effect of Exposure Condition

The effect of the two exposure conditions, viz. indoors and outdoors on chloride diffusion are shown in Figs. 58 to 62. The indoor exposure of control laboratory conditions was at an average temperature of $19^{\circ}C$. The outdoor exposure period ranged from August to March, during

which time the ambient temperature ranged from 8 to 50°C. Only the specimens made with a cement content of 350 kg/m³ were subjected to both exposure conditions. For all concrete mixes, there was a marked difference in the values of the diffusion coefficients between the two exposures. The diffusion coefficient for specimens exposed to outdoor conditions was 3 times that of the value for indoor specimens made with w/c ratio of 0.40 (8.03×10^{-8} to 24.45×10^{-8} cm²/sec). However the difference between the outdoor and the indoor is reduced for higher w/c ratios. The sharp difference in the values of diffusion coefficient between the two exposure conditions may be attributed mainly to the effect of temperature on the kinetics of diffusion and the associated factors.

An increase in temperature will lead to a decrease in the viscosity of the pore water in concrete, through which the diffusion takes place and consequently an increase in ionic diffusion. Moreover at higher temperatures, for example 55°C and above, C₃A does not react with chloride ions to form stable chloro-aluminates [75]. So, the assumption of no reaction taking place can be valid in this case. The formation of micro-cracks at the aggregate paste interface due to the high temperature fluctuations in the exposure condition is another factor. Such micro-cracks develop due to the thermal incompatibility between the aggregates and the cement paste [3,4]. So at elevated temperatures, the minimal binding effects together with the development of micro-cracks

would lead to a higher chloride diffusion in concrete exposed to harsh outdoor environment as observed in this research.

5.4.4 Effect of Surface Chloride Concentration

The effect of surface chloride concentration on the diffusivity is shown in Figs. 63 to 67. The values of surface concentrations obtained from the optimization run are shown in Table 8. As expected, in all the cases, the ingress of chloride ions increased considerably for higher exposure chloride concentration. However, the diffusion coefficient were almost unchanged for the same w/c ratio, irrespective of the ponded solution concentration. For example, in the case of w/c = 0.40, the diffusivity values in concrete ponded with 4 and 8% chloride solutions are $8.03 \times 10^{-8} \text{ cm}^2/\text{sec.}$ and $8.52 \times 10^{-8} \text{ cm}^2/\text{sec.}$, respectively

Even though the diffusivity values were independent of the exposure chloride concentration, the effect of high exposure concentrations is detrimental from the durability point of view, as the diffusion of larger amount of chloride ions into concrete exceeding the threshold level at an early stage and will consequently lead to an early initiation of corrosion.

5.5 Gas Diffusion Test

From the expression of molecular diffusion, the value of D_{12} was calculated to be $0.485 \text{ cm}^2/\text{sec}$. The Knudsen diffusivity values for each concrete for He and N_2 are shown in Table 9. For the mass balance equation developed for the He/N_2 system, a computer program was used to generate the values of θ for increment value of $x_1 = 0.005$ as shown in Table 18. From Eqn. (3.31), the ratio ϵ/τ can be directly calculated once the value of θ is known. The average value of ϵ/τ and the standard deviation (SD) for each mix are shown in Table 18.

Once the value of ϵ/τ which is a constant for each mix is established, the effective diffusion coefficient D_e of chloride in concrete can be determined using Eqn. (3.33), and is listed in Table 10. A typical calculation for obtaining the effective diffusion coefficient of chloride ion in concrete for $W/C = 0.55$ and $CC = 350 \text{ kg/m}^3$ is given in Appendix C. The results of the static test for all the mixes are also tabulated in Appendix C.

To check the fit of the average ϵ/τ values relative to the experimental values, a plot of $\ln(1-2x_1)$ Vs time is developed as shown in Figs. 68 to 70. In all the cases a good correlation was observed. From Table 10, it can be observed that the diffusion coefficient is influenced by

the w/c ratio and cement content, however the effect of w/c ratio is found to be more dominant.

5.6 Result Comparison of the Exposure and the Gas Diffusion Test

The values of the different parameters calculated from the exposure tests and the gas diffusion tests are shown in Table 11. On the whole, exposure and the gas test results exhibit an excellent correlation. However, in the case of w/c = 0.7, it can be observed that the diffusion coefficient obtained by the gas diffusion test is approximately just half of that obtained by the exposure test. Such deviations between the two test results can only be attributed to the error in the pore radius measurements.

It was mentioned earlier that concrete samples were used for the mercury intrusion studies instead of mortar or paste. The main problem encountered here was the selection of approximately 5 gms. of a representative sample of concrete. Due to financial constraints, not many samples could be sent for testing. However from the limited data available, the results compare excellently close.

This is the first time ever that the $\frac{\epsilon}{\tau}$ ratio has been evaluated for concrete. The static diffusion test is a very fast method to determine the diffusion coefficients, it can be completed in 3 to 4 hours in comparison

to the conventional diffusion test, which requires several weeks for its completion.

5.7 Reinforcement Corrosion

The corrosion specimens were cast with a view to arrive at a correlation between the diffusivity values and the time to initiation of corrosion. The corrosion potentials and the corrosion current density values for the blocks specimens are shown in Figs. 71 to 94. The time to initiation of corrosion for the various concretes as inferred from the half cell and the corrosion density measurements are collectively shown in Table 12. To examine the actual state of the rebars after 300 days of exposure to chlorides, all the block specimens were split open. Table 13 shows the chloride contents at rebar level measured after 300 days of exposure.

It was observed that in the case of $w/c = 0.4$, the 4% chloride solution ponded specimens did not show any signs of corrosion for the 4", 3" and 1.5" cover after 300 days of exposure. A typical specimen showing no signs of corrosion is shown in Fig. 95. The 8% solution ponded specimens were also passive for the 4" and 3" cover, but for 1.5" cover, specimen, the signs of corrosion initiation was noted after approximately 280 days as shown in Fig. 96. For $w/c = 0.55$, the 4" cover specimens exposed to both, 4% and 8% chloride solution showed no signs of corrosion initiation after 300 days of exposure. However signs of

corrosion initiation were noticed after 285 days for the 3" cover specimen subjected to 8% chloride solution. Specimens with 1.5" cover exhibited active corrosion as shown in Fig. 97. From the corrosion potential readings as well as the corrosion current density figures, it can be seen that the initiation was after 200 and 120 days for the 4% and 8% solutions respectively.

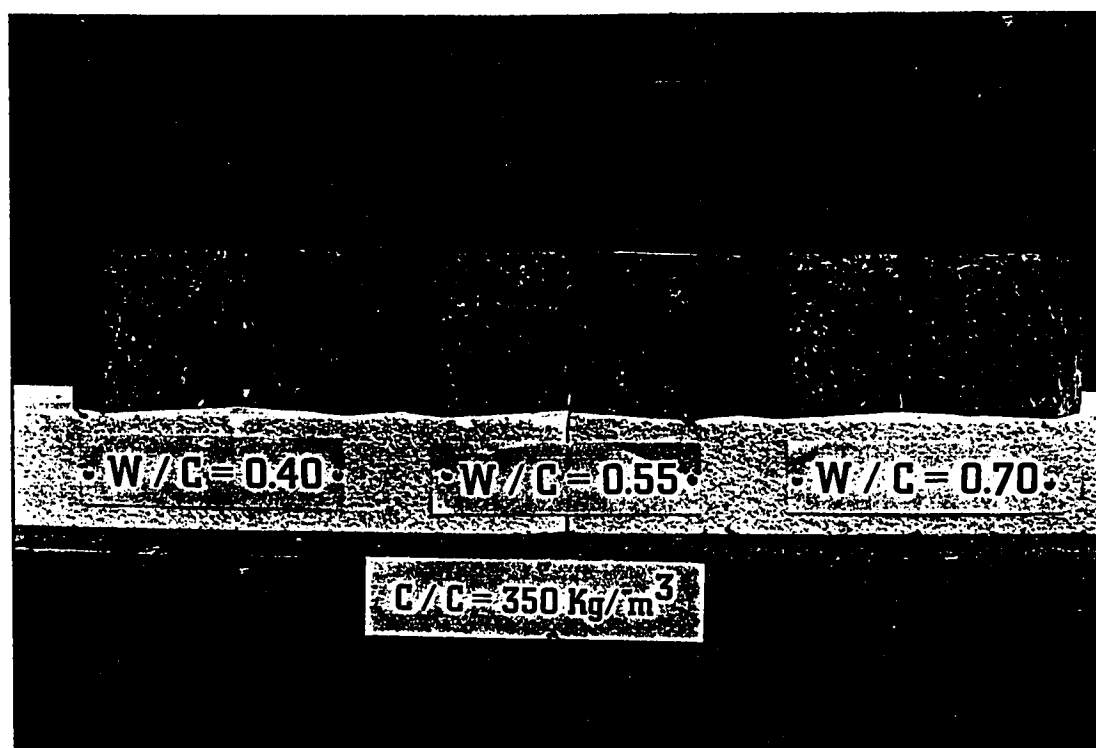


Figure 31: Photograph Showing Some Typical Cubes Tested for Permeability

Table 6: Mercury Intrusion Test Results (Porosity % / Pore Radius A)

	Cement Content		
W / C	300	350	400
0.4	7.57 / 224	7.39 / 127	8.39 / 177
0.55	8.3 / 122	10.64 / 135	8.52 / 175
0.7		13.52 / 151	

Table 7: Concrete Permeability

C C →	300	350	400
W/C	Water Penetration (cms.)		
0.4	9.84	10.65	9.93
0.55	12.8	11.9	11.17
0.7	----	14.2	----

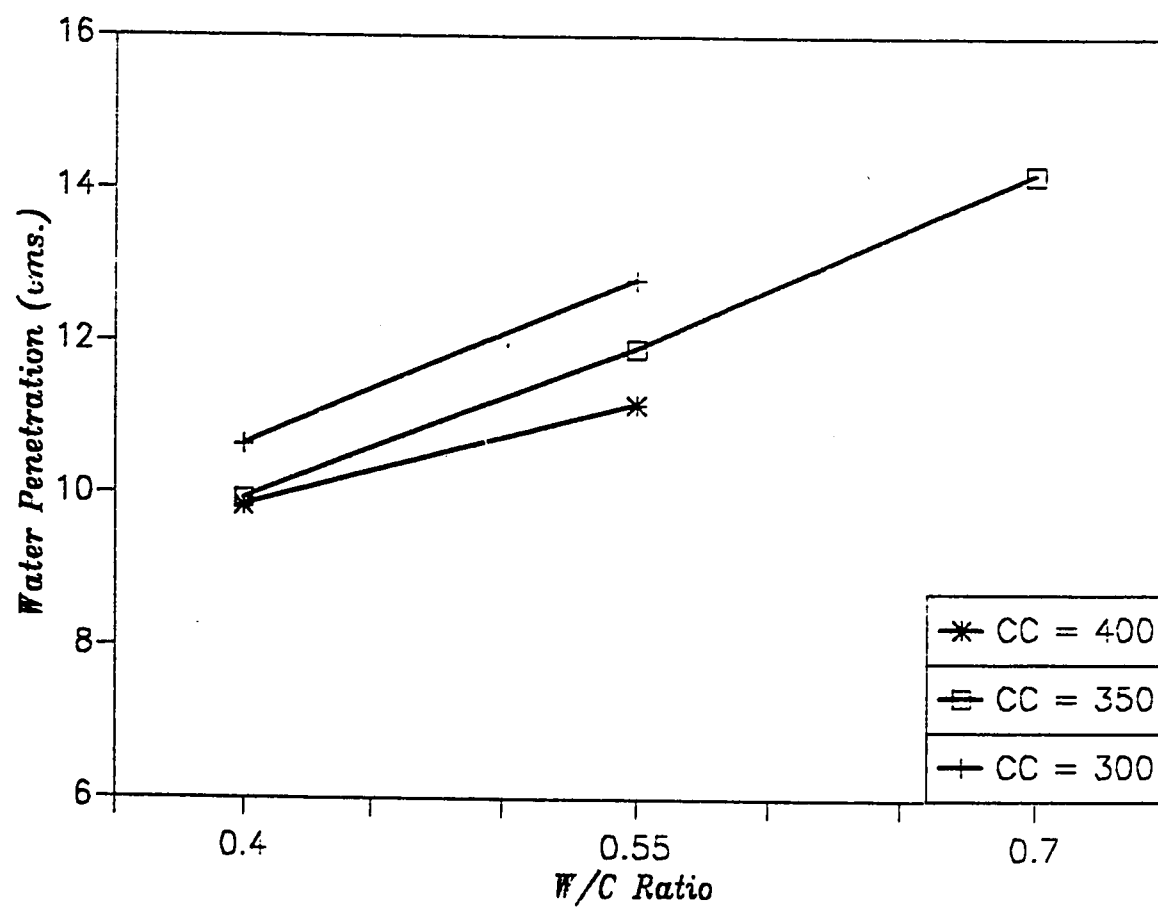


Figure 32: Results of the DIN 1048 Water Impermeability Test

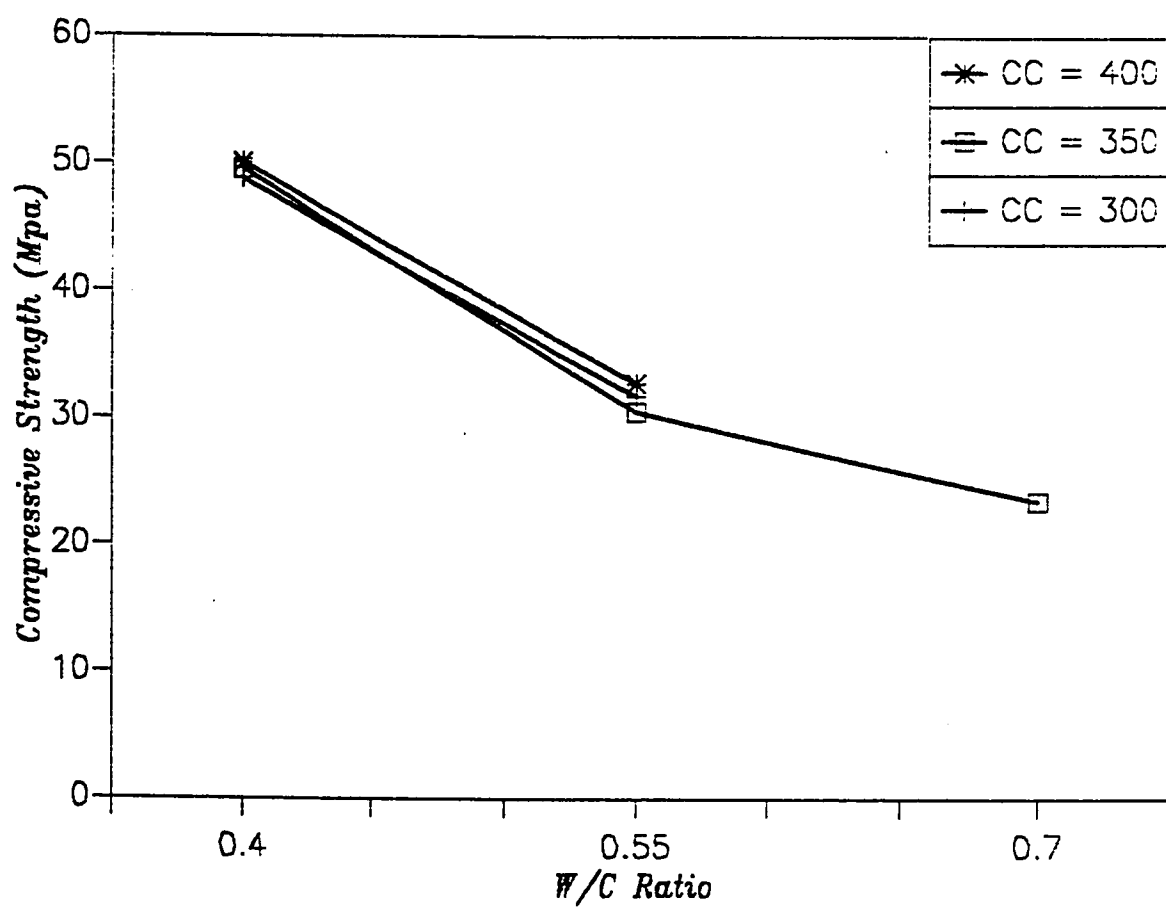


Figure 33: 28 day Cylinder Compressive Strength

Table 8 : Results of the Chloride Exposure Test

W/C	Cl	CC = 350 kg/m ³					
		Indoors			Outdoors		
		D _e [*]	C _s [^]	SSE	D _e [*]	C _s [^]	SSE
0.40	4 %	8.03	0.32	0.0015	24.45	0.362	0.0031
	8 %	8.52	0.56	0.0019	27.54	0.748	0.0262
0.55	4 %	---	---	----	78.00	0.950	0.0263
	8 %	28.10	0.760	0.0165	73.50	1.250	0.0703
0.70	4 %	68.45	0.580	0.0055	165.0	0.832	0.0411
	8 %	66.30	0.815	0.0178	170.3	1.950	0.1204
W/C	Cl	Indoors			Indoors		
		CC = 300 kg/m ³ .			CC = 400 kg/m ³ .		
0.40	4 %	10.32	0.49	0.0022	7.63	0.38	0.0036
0.55	4 %	33.70	0.54	0.0100	16.46	0.49	0.0010

* x 10⁸ cm²/sec.

^ % by weight of concrete

Table 9 : Values of Knudsen Diffusion Coefficient

98

CC →	300	350	400	300	350	400
	D_k^*			D_k^*		
W/C	Helium			Nitrogen		
0.40	0.185	0.104	0.146	0.070	0.040	0.055
0.55	0.101	0.112	0.144	0.038	0.042	0.055
0.70		0.125			0.047	

* $\text{cm}^2/\text{sec.}$

Table 10 : Results of the Gas Diffusion Test

CC	W/C	ϵ / τ	D_e^*	S.D
300	0.40	0.0090	11.34	0.0021
	0.55	0.0263	33.14	0.0042
350	0.40	0.0077	9.70	0.0011
	0.55	0.0192	24.19	0.0046
	0.70	0.0296	37.33	0.0052
400	0.40	0.0070	8.82	0.0023
	0.55	0.0110	13.86	0.0023

* $10^8 \text{ cm}^2/\text{sec.}$

Table 11: Comparison of the Exposure and the Gas Diffusion Test

CC	W / C	Chloride Exposure	Gas Diffusion
		D_e *	D_e
300	0.40	10.32	11.34
	0.55	33.70	33.14
350	0.40	8.28	9.70
	0.55	28.10	24.19
	0.70	67.38	37.33
400	0.40	7.63	8.82
	0.55	16.46	13.86

* $10^8 \text{ cm}^2 / \text{sec.}$

Table 12: Results of the Corrosion Study

		Cover to Reinforcement		
		4 "	3 "	1.5 "
W / C	Chloride	Initiation of Corrosion		
0.40	4 %	Nil	Nil	Nil
	8 %	Nil	Nil	280
0.55	4 %	Nil	Nil	200
	8 %	Nil	285	120

Table 13: Chloride Contents Measured at Rebar Level

		4 % Solution	8 % Solution
W/C	Cover	Chloride Content *	
0.40	4 "	0.003	0.003
	3 "	0.003	0.003
	1.5 "	0.0031	0.051
0.55	4 "	0.0048	0.012
	3 "	0.010	0.048
	1.5 "	0.125	0.244

* % by weight of concrete

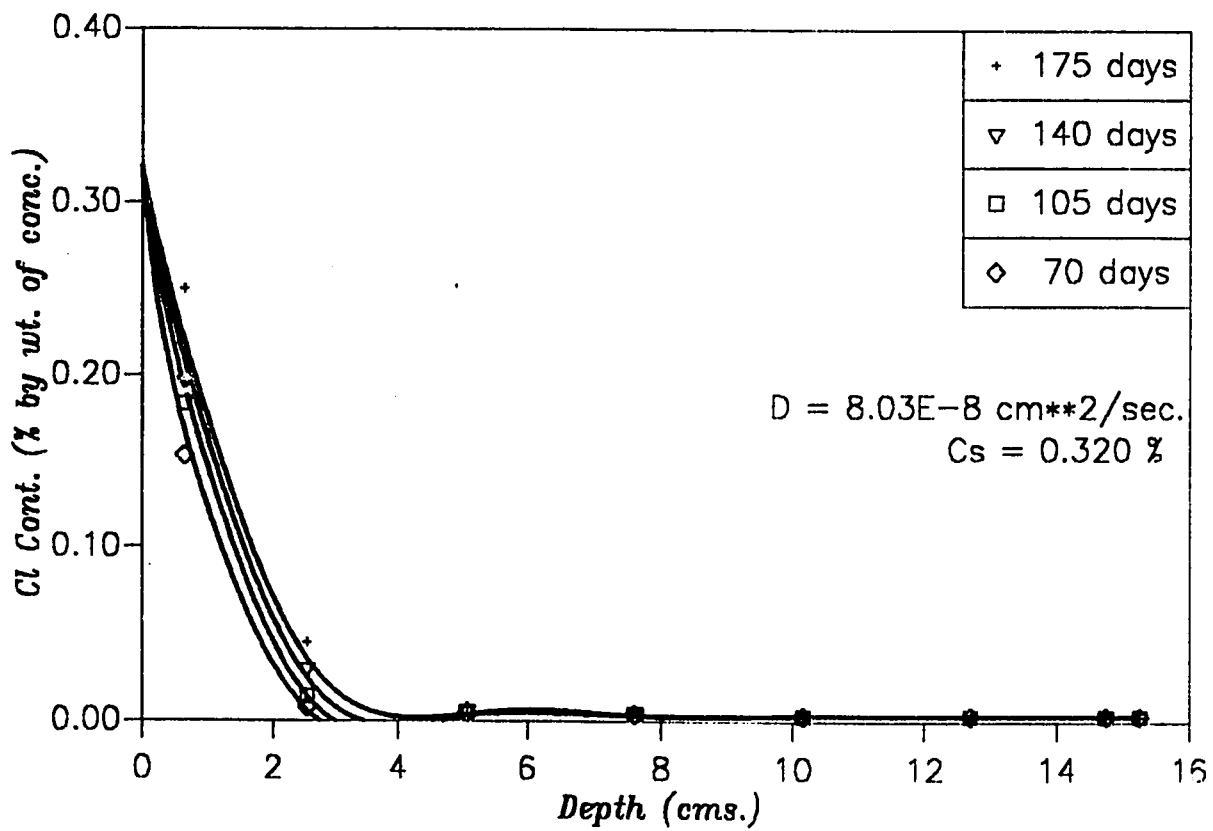


Figure 34: Chloride Profiles: (CC=350 kg/cum., W/C=0.4, 4% Chloride, Indoors)

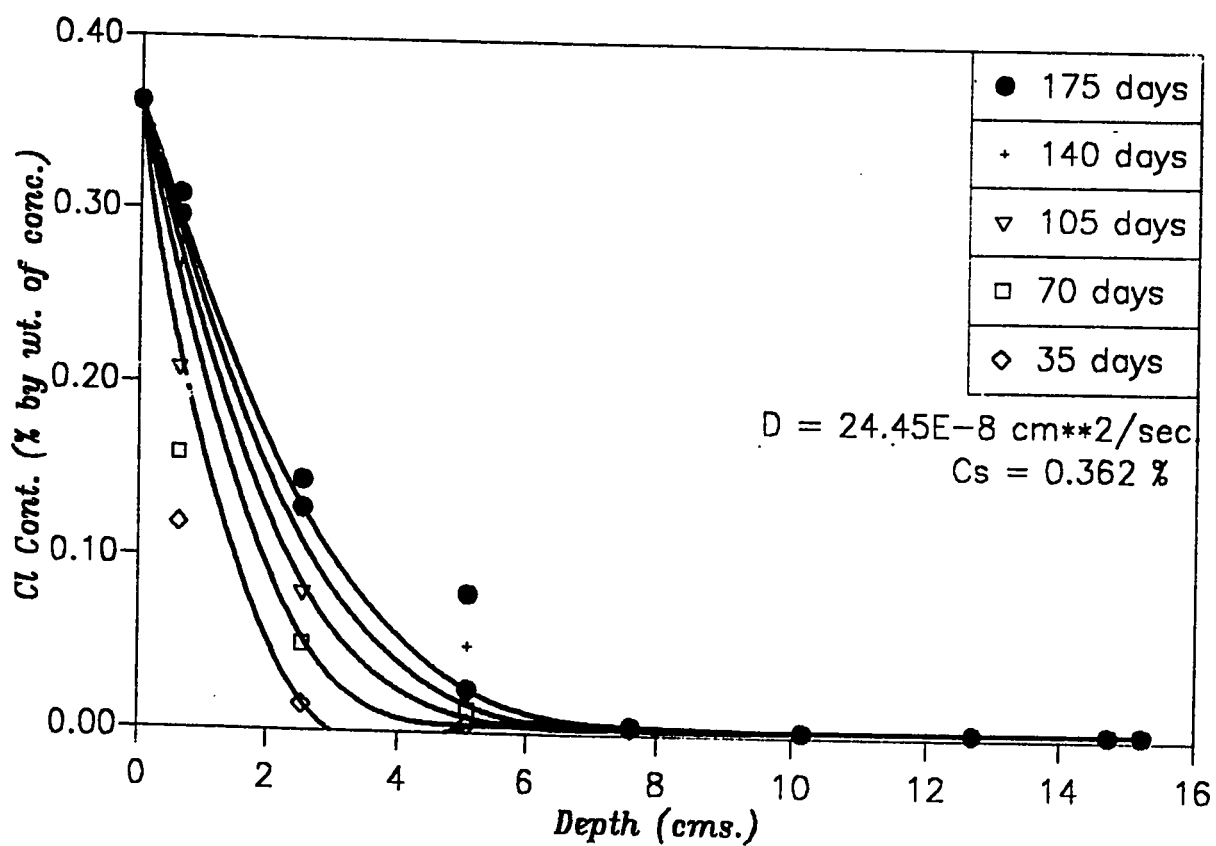


Figure 35: Chloride Profiles: (CC=350 kg/cum., W/C=0.4, 4% Chloride, Outdoors)

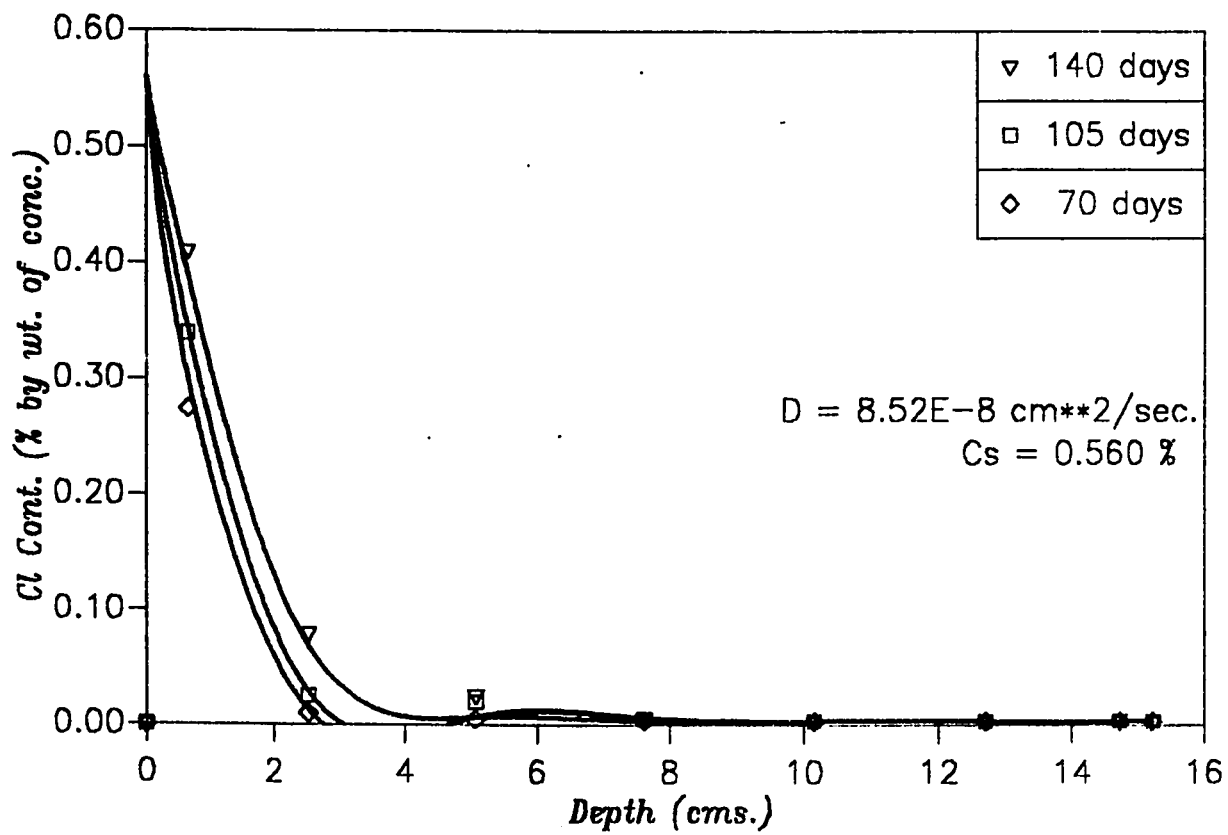


Figure 36: Chloride Profiles: (CC=350 kg/cum., W/C=0.4, 8% Chloride, Indoors)

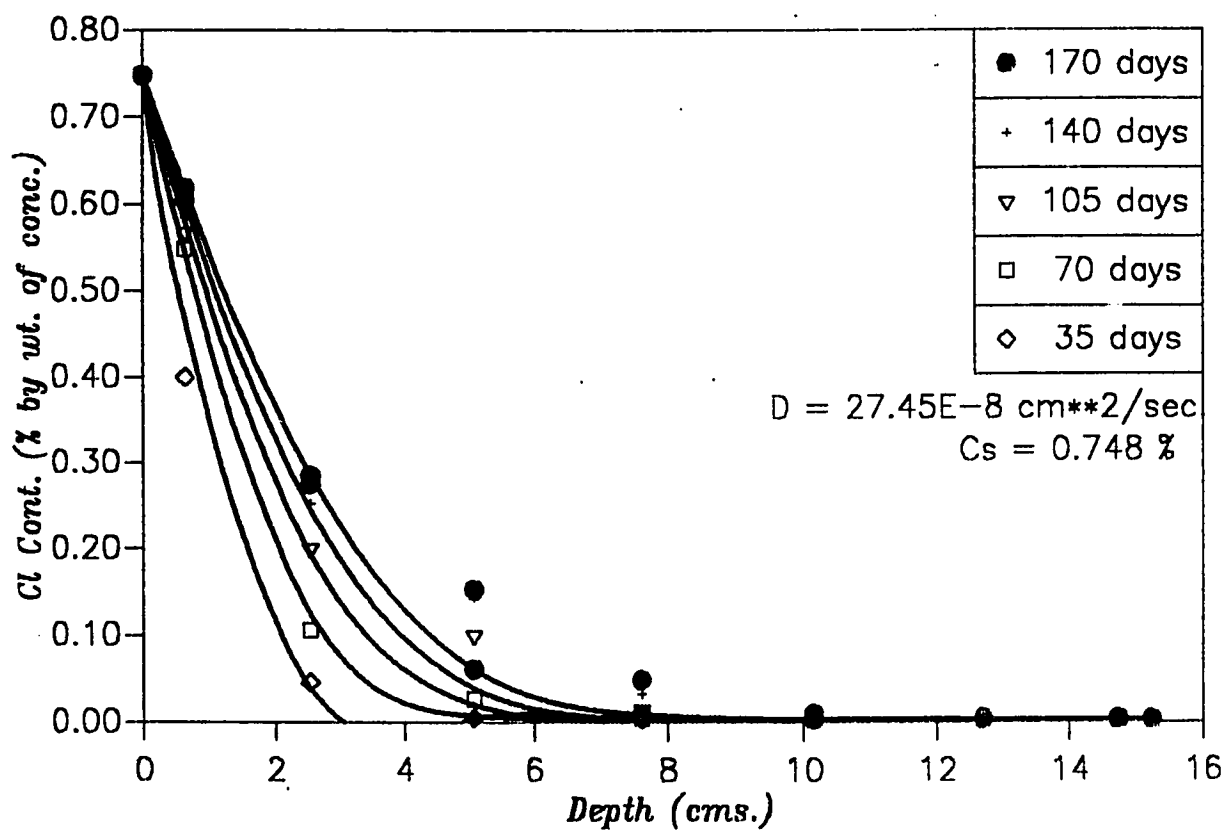


Figure 37: Chloride Profiles: (CC=350 kg/cum., W/C=0.4, 8% Chloride, Outdoors)

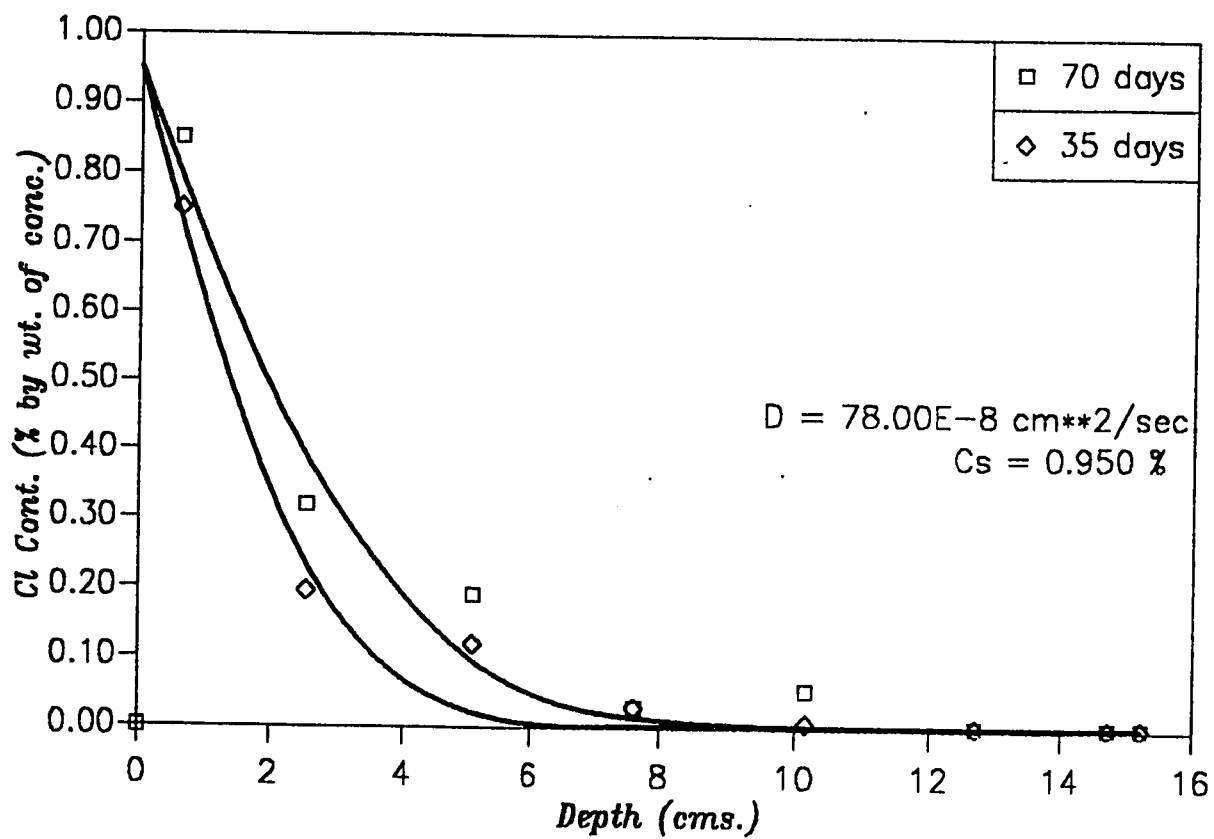


Figure 38: Chloride Profiles: (CC=350 kg/cum., W/C=0.55, 4% Chloride, Outdoors)

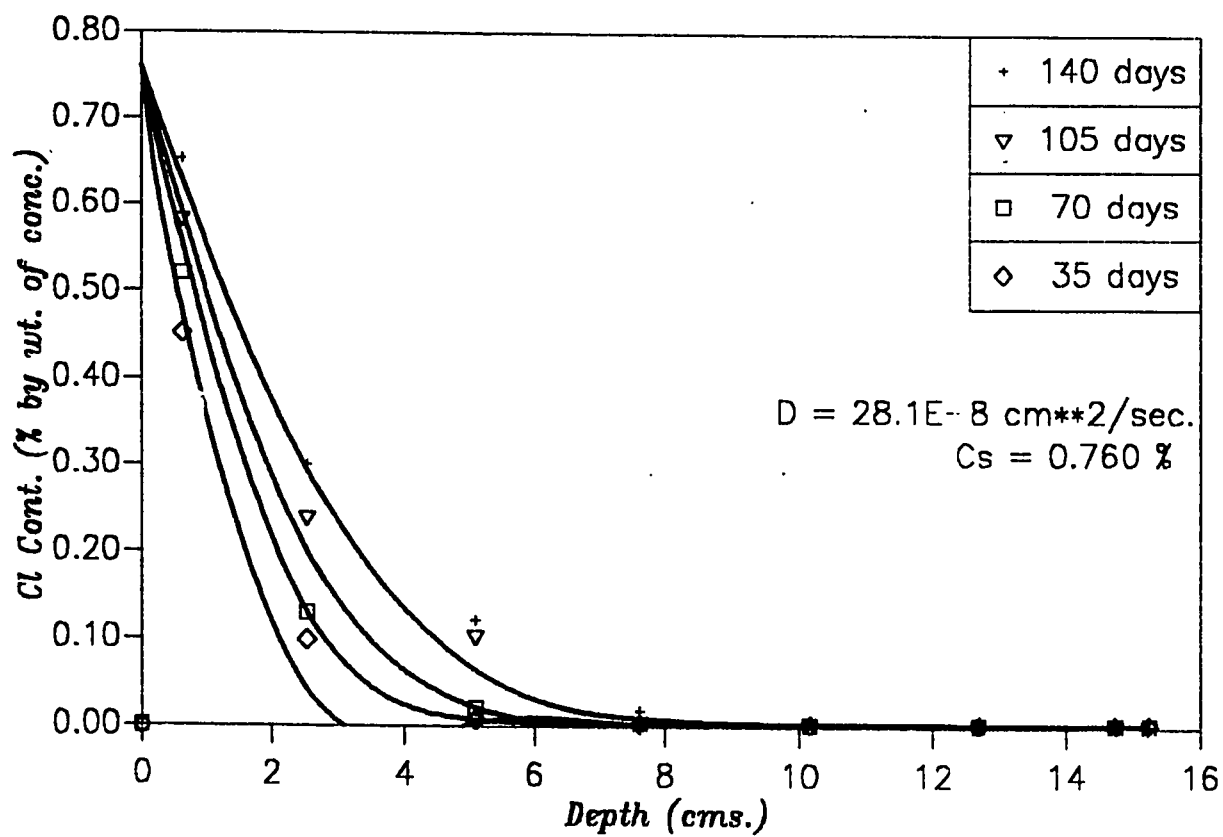


Figure 39: Chloride Profiles: (CC=350 kg/cum., W/C=0.55, 8% Chloride, Indoors)

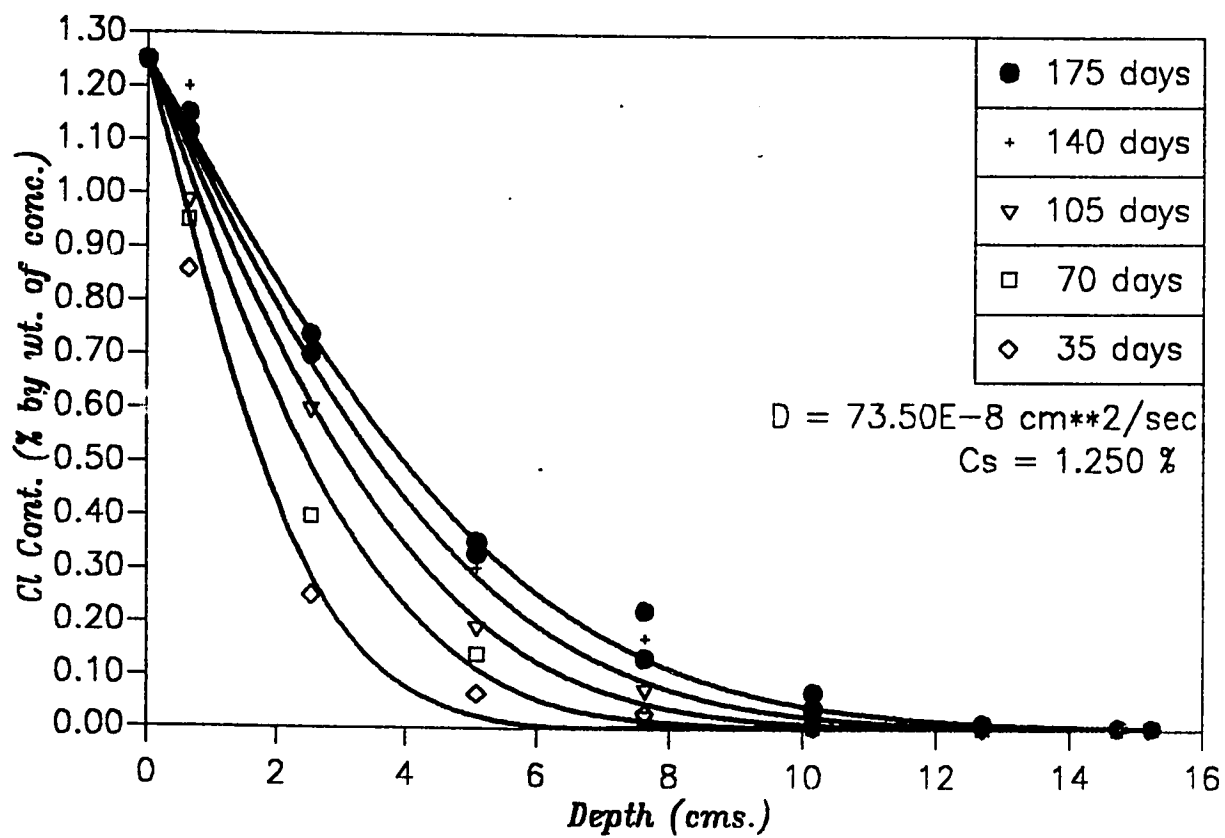


Figure 40: Chloride Profiles: (CC=350 kg/cum., W/C=0.55, 8% Chloride, Outdoors)

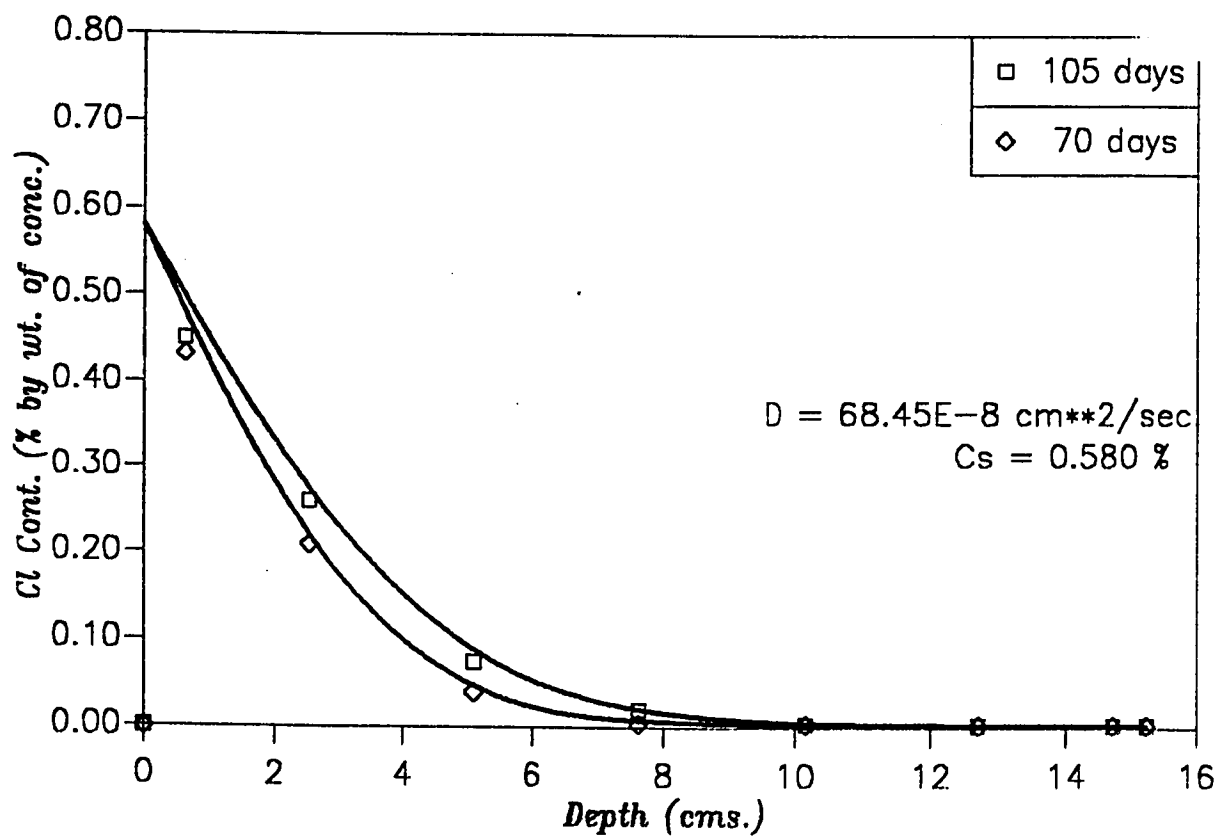


Figure 4/ : Chloride Profiles: (CC=350 kg/cum., W/C=0.7, 4% Chloride, Indoors)

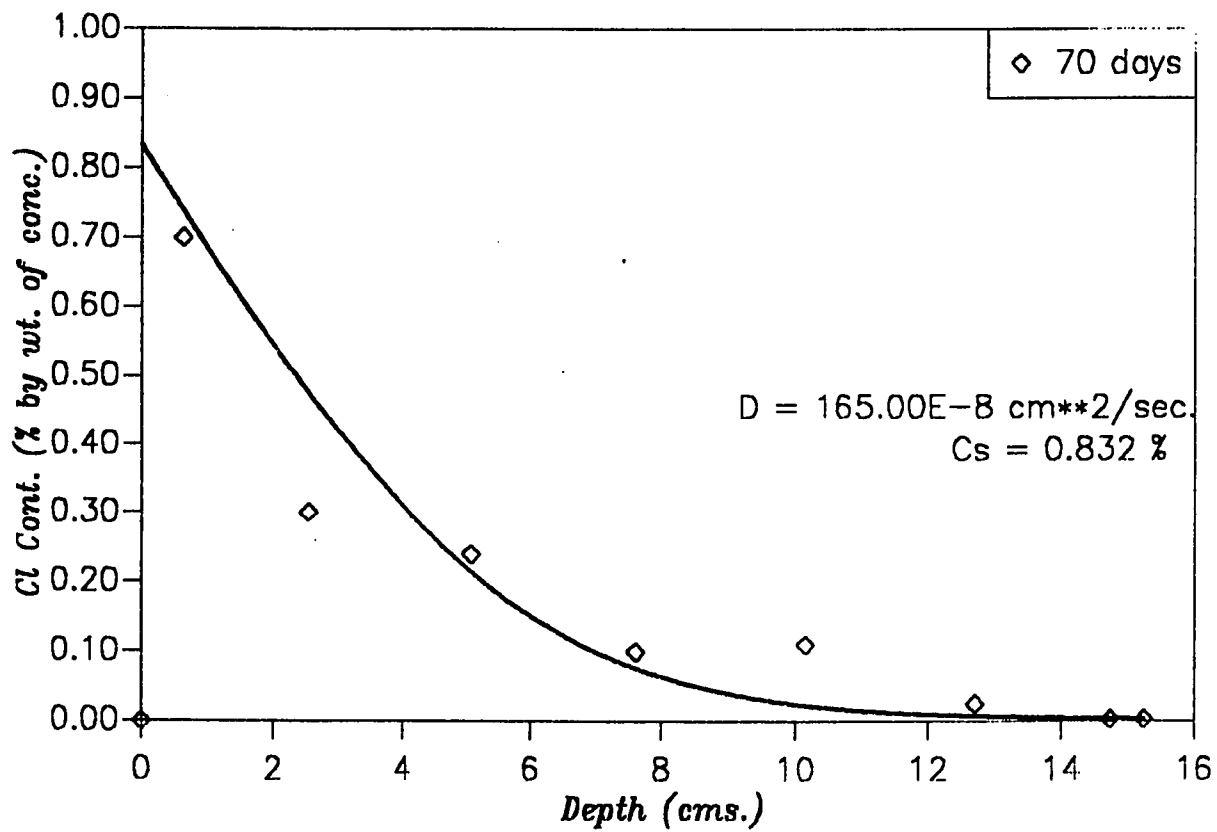


Figure 42: Chloride Profiles: (CC=350 kg/cum., W/C=0.7, 4% Chloride, Outdoors)

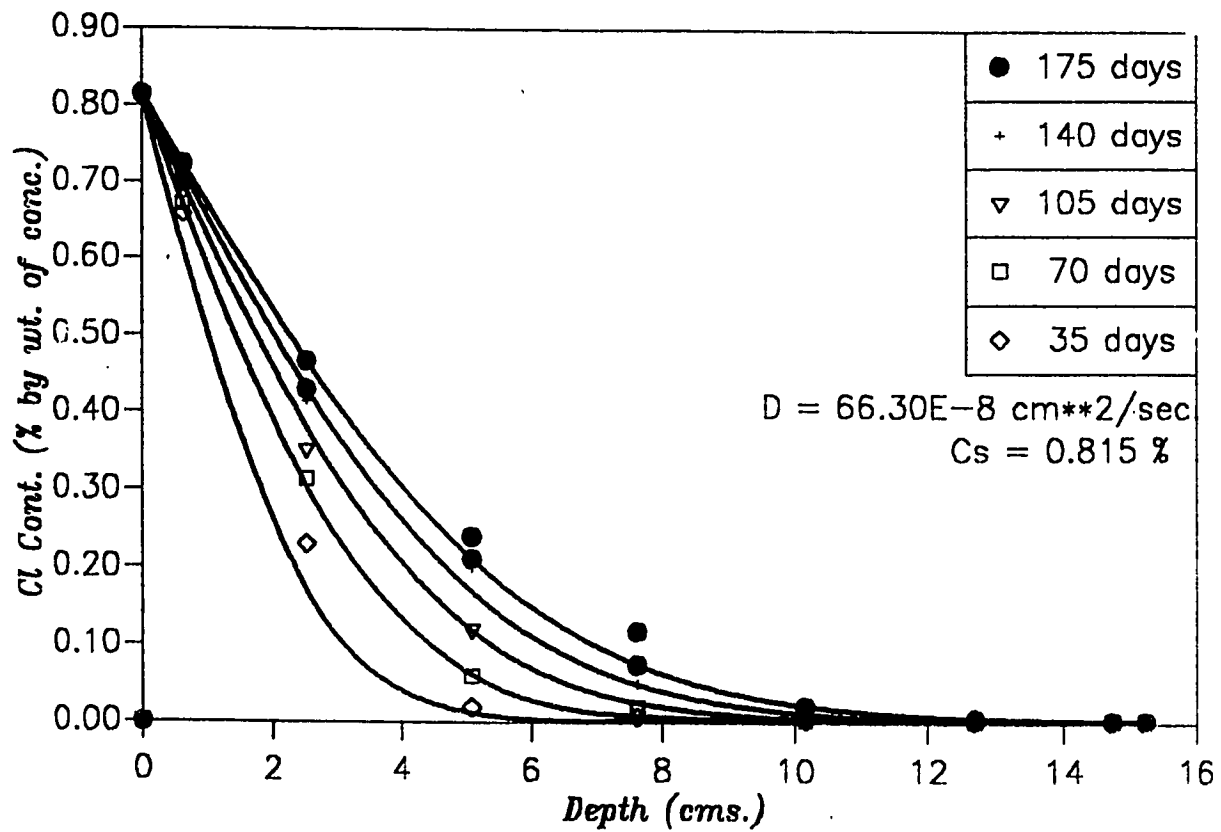


Figure 43: Chloride Profiles: (CC=350 kg/cum., W/C=0.7, 8% Chloride, Indoors)

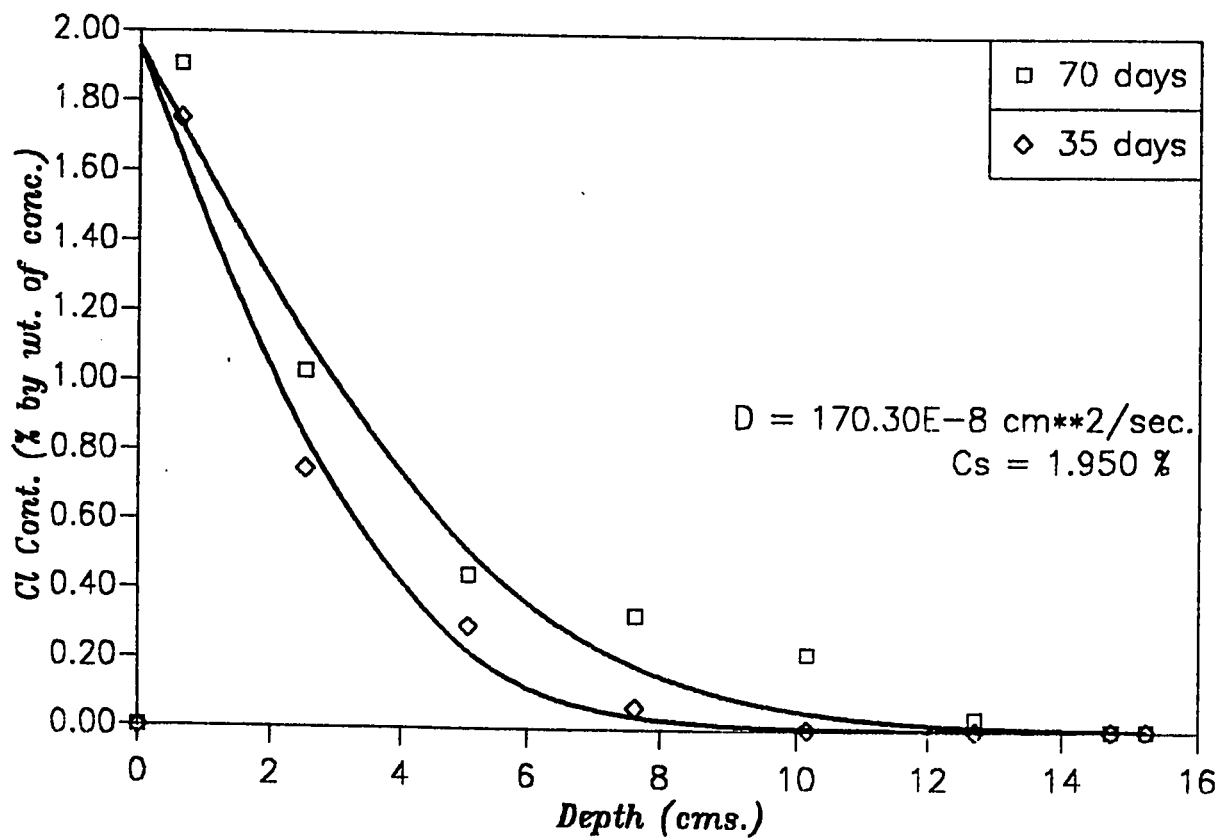


Figure 44: Chloride Profiles: (CC=350 kg/cum., W/C=0.7, 8% Chloride, Outdoors)

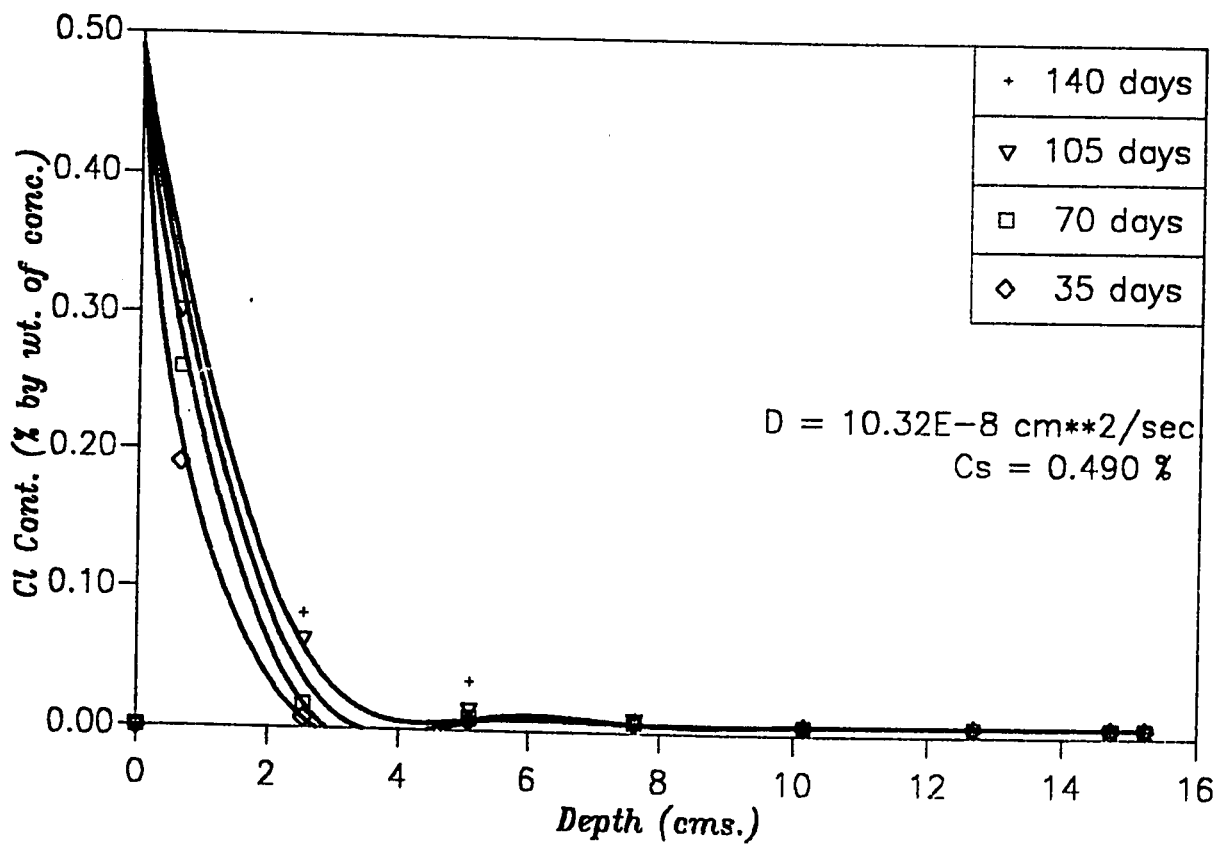


Figure 45: Chloride Profiles: (CC=300 kg/cum., W/C=0.4, 4% Chloride, Indoors)

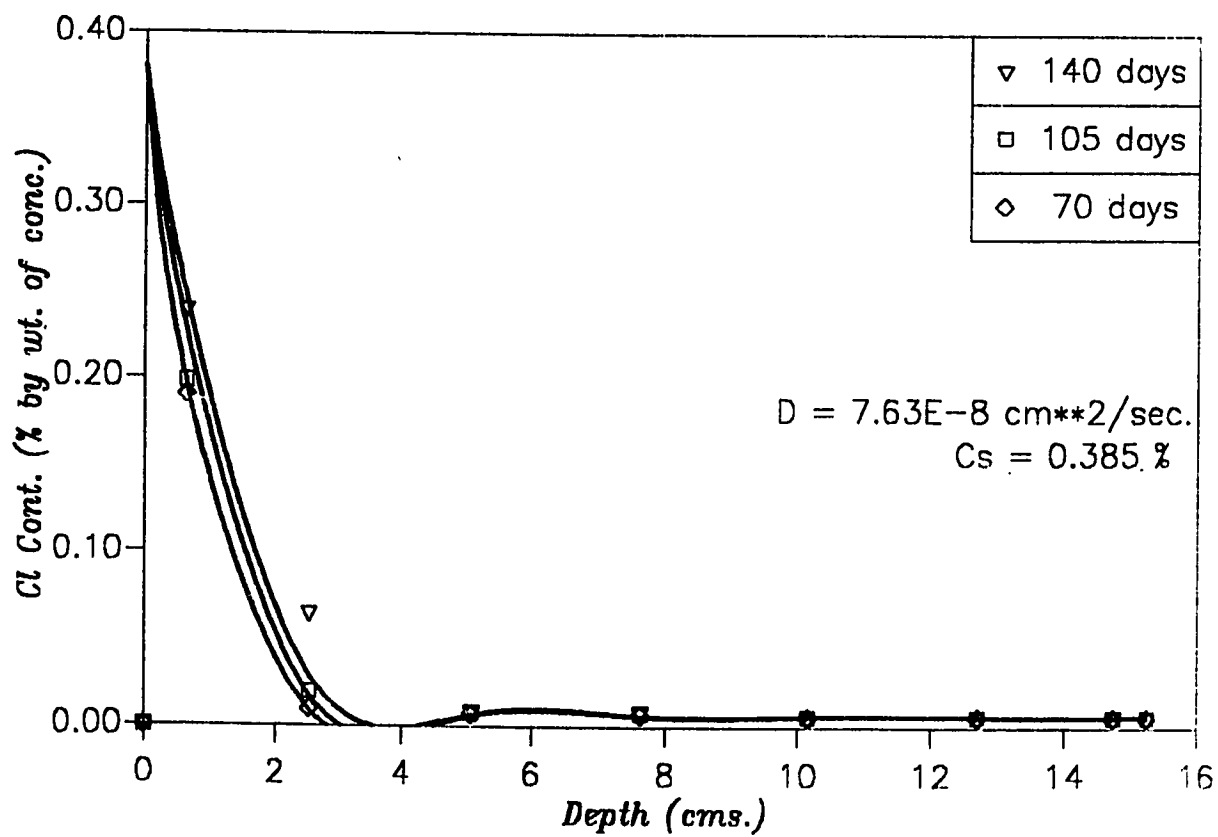


Figure 46: Chloride Profiles: (CC=400 kg/cum., W/C=0.4, 4% Chloride, Indoors)

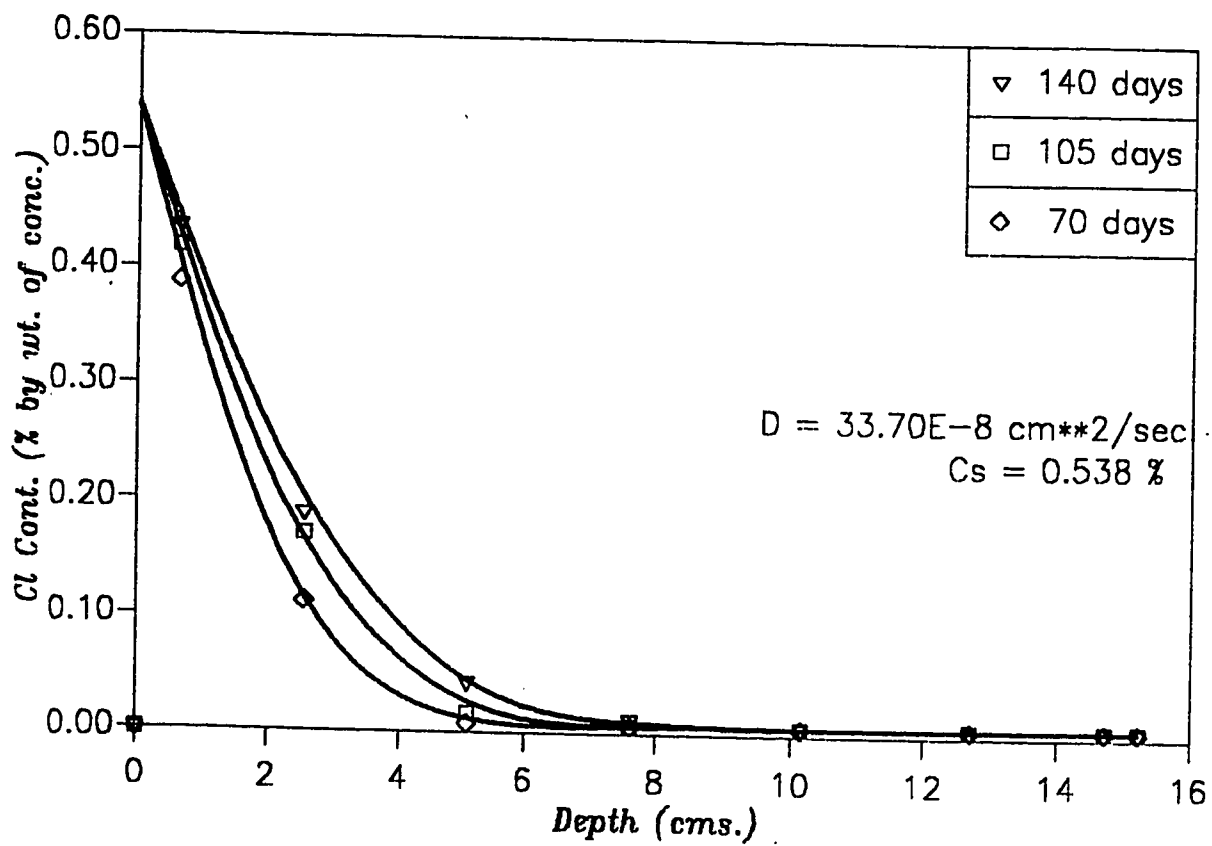


Figure 47: Chloride Profiles: (CC=300 kg/cum., W/C=0.55, 4% Chloride, Indoors)

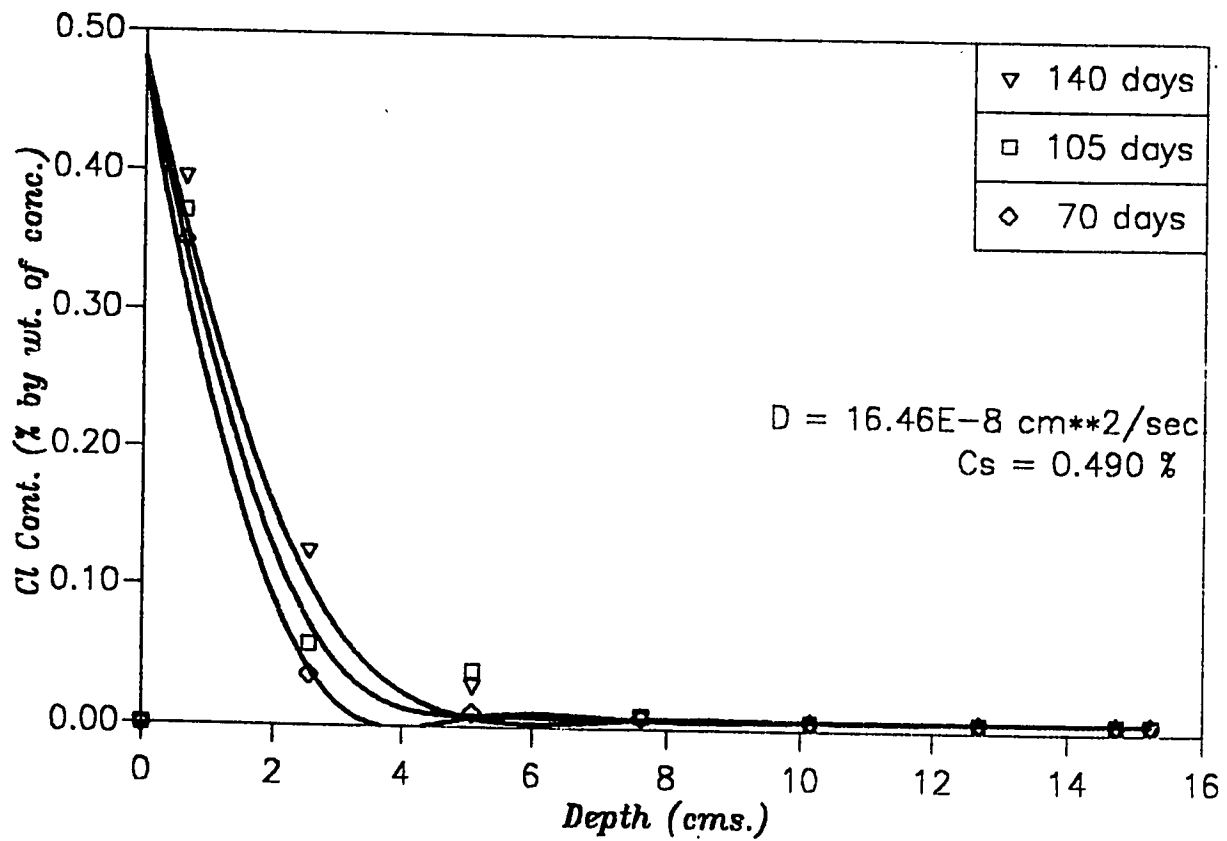


Figure 48: Chloride Profiles: (CC=400 kg/cum., W/C=0.55, 4% Chloride, Indoors)

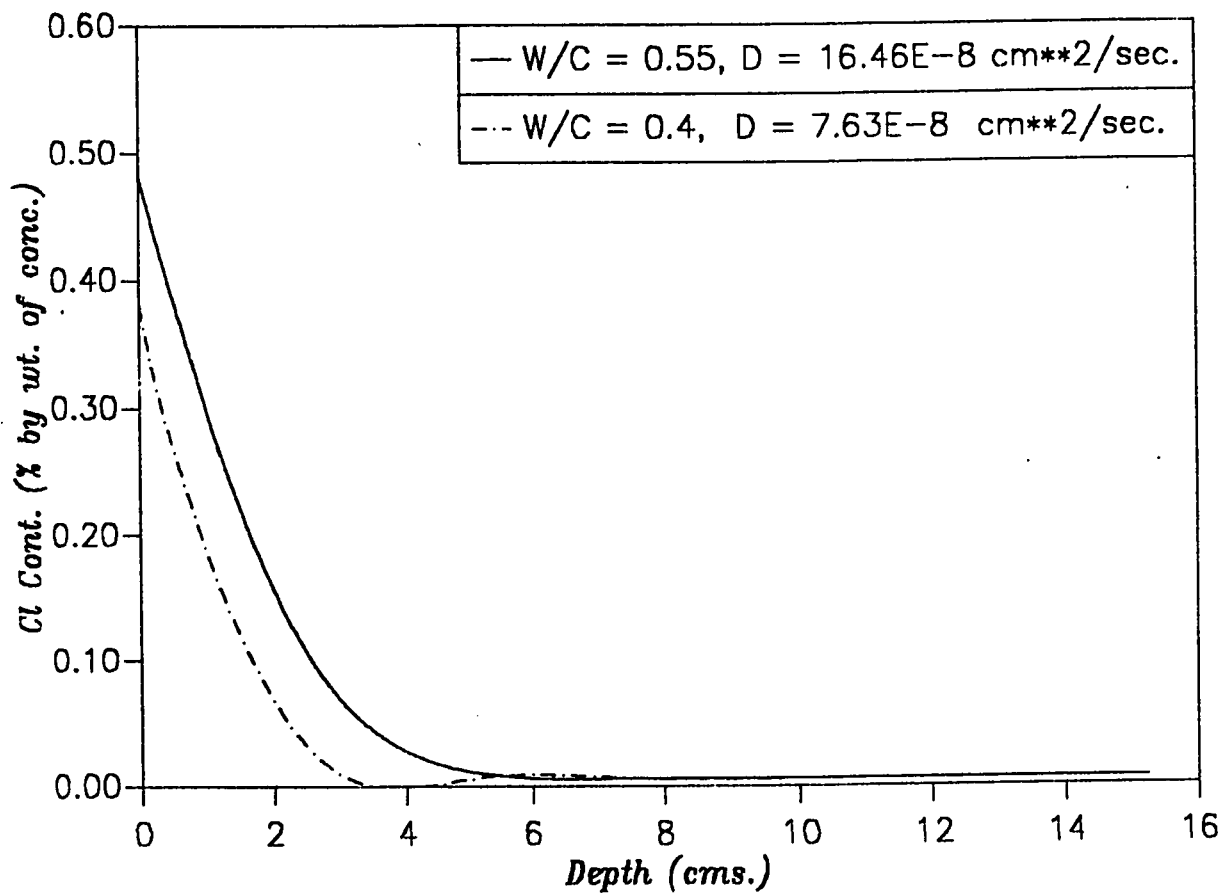


Figure 49: Effect of W/C Ratio on Chloride Diffusion: (CC=300 Kg/cum., 140 Days, 4% Chloride, Indoors)

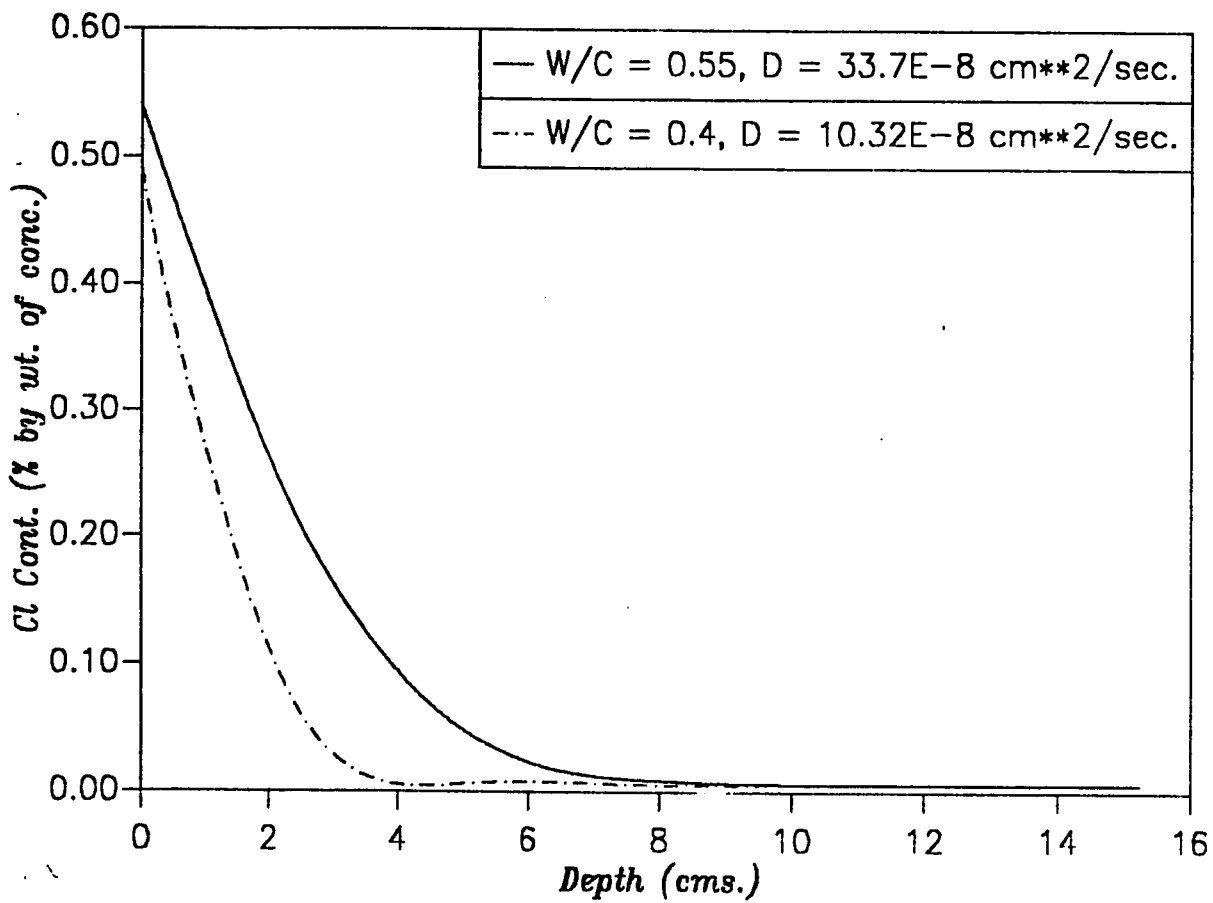


Figure 50: Effect of W/C Ratio on Chloride Diffusion: (CC=400 Kg/cum., 140 Days, 4% Chloride, Indoors)

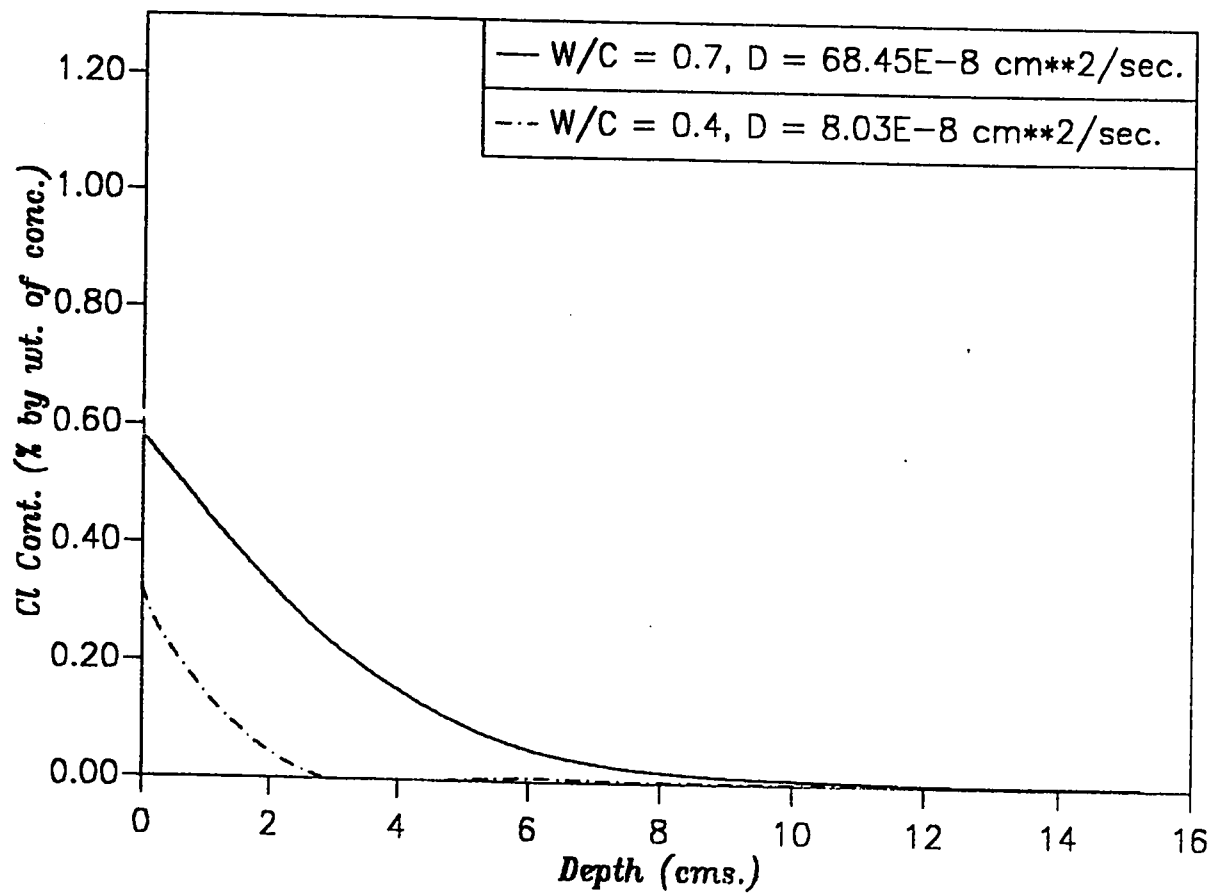


Figure 51: Effect of W/C Ratio on Chloride Diffusion: (CC=350 Kg/cum., 105 Days, 4% Chloride, Indoors)

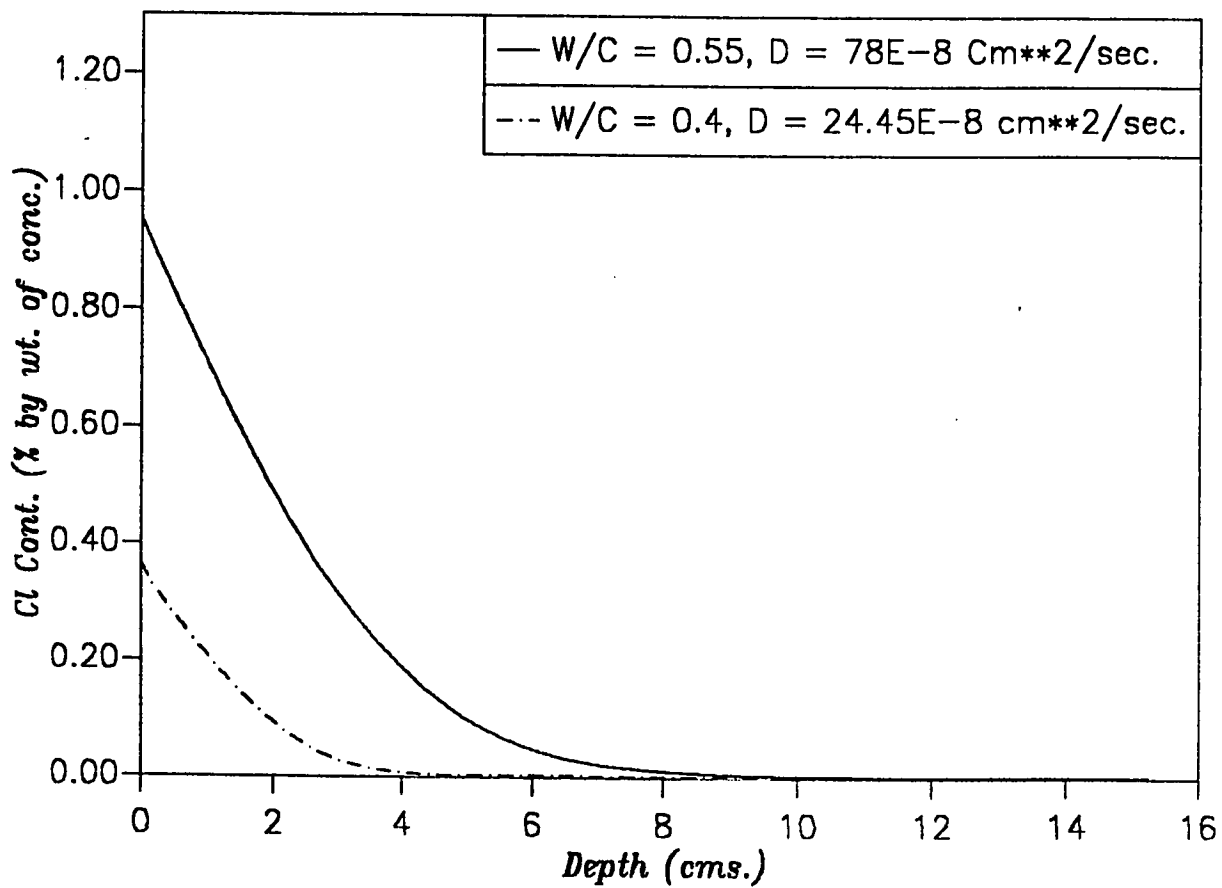


Figure 52: Effect of W/C Ratio on Chloride Diffusion: (CC=350 Kg/cum., 70 Days, 4% Chloride, Outdoors)

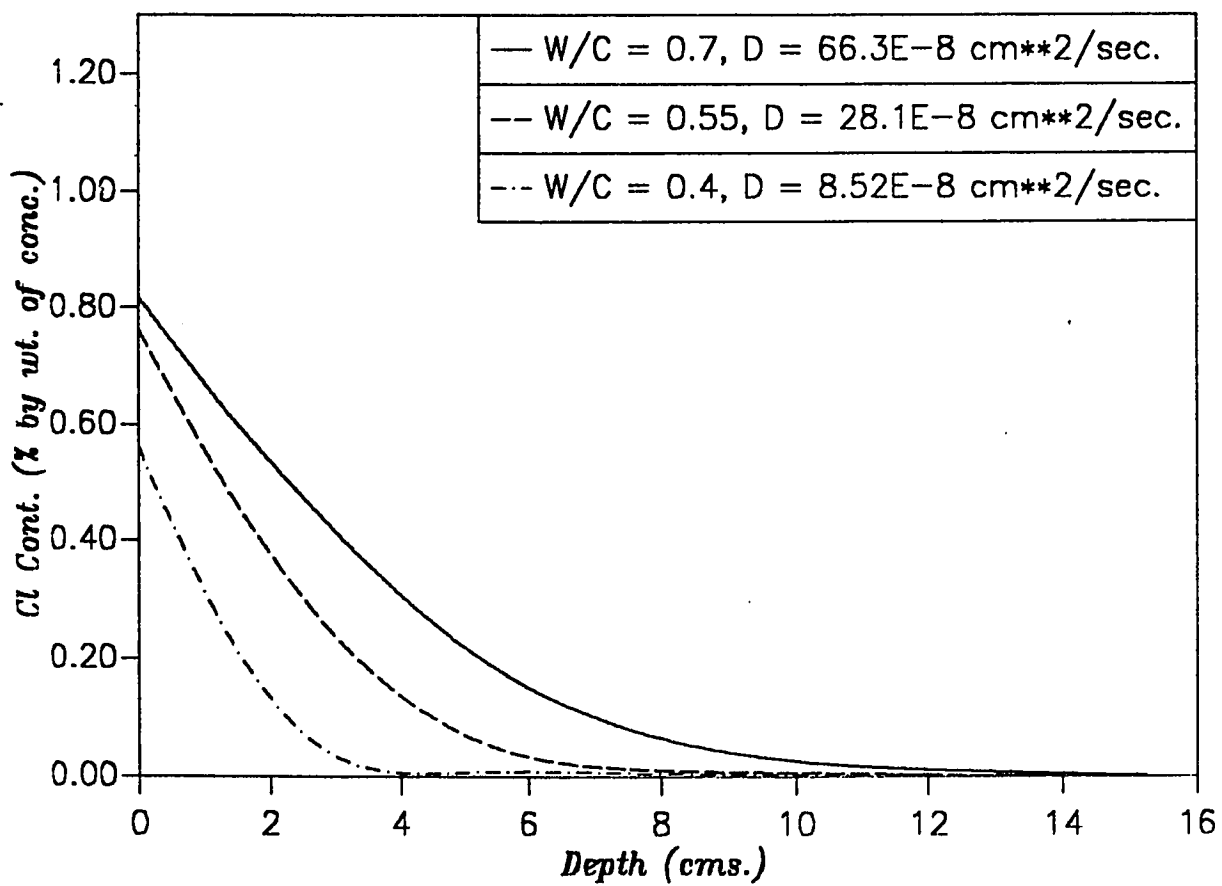


Figure 53: Effect of W/C Ratio on Chloride Diffusion: (CC=350 Kg/cum., 175 Days, 8% Chloride, Indoors)

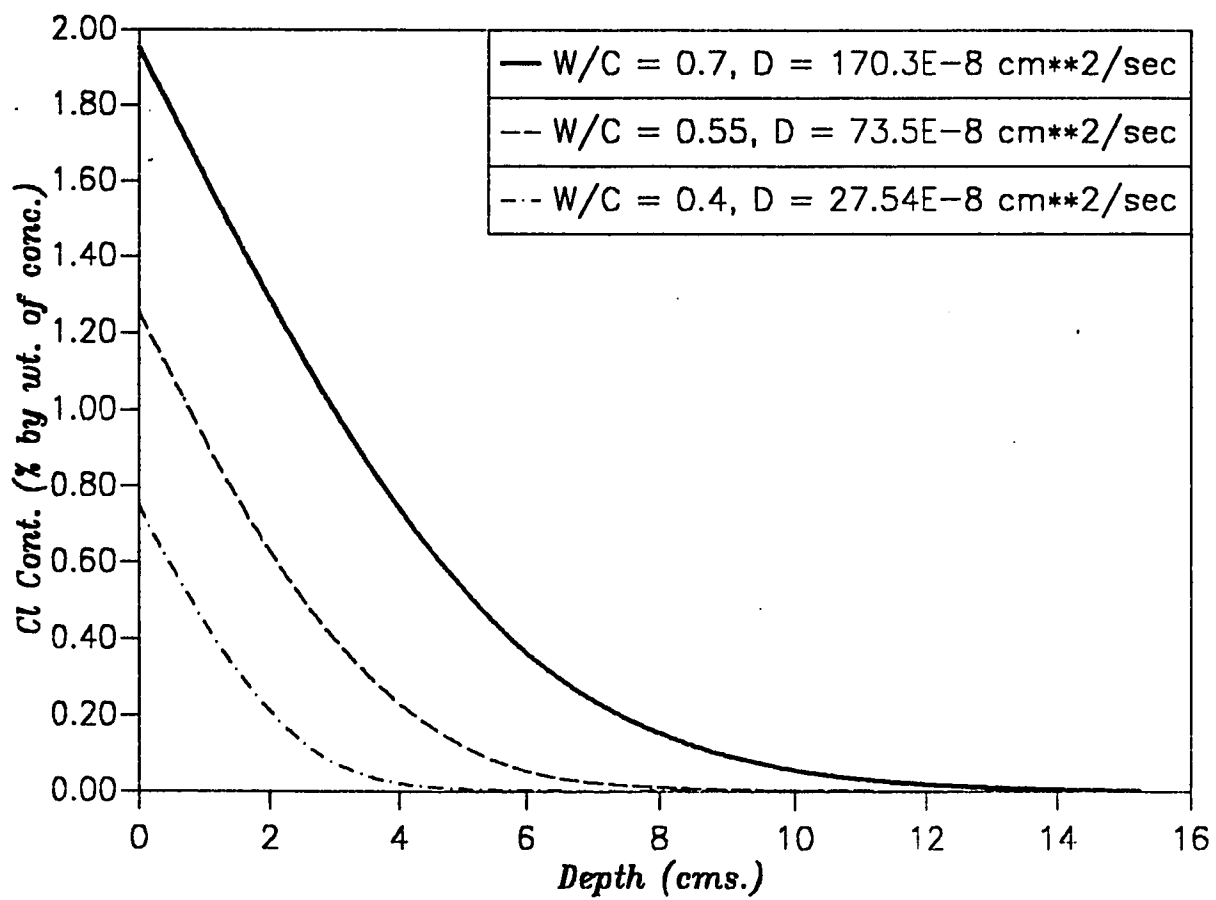


Figure 54: Effect of W/C Ratio on Chloride Diffusion: (CC=350 Kg/cum., 70 Days, 8% Chloride, Outdoors)

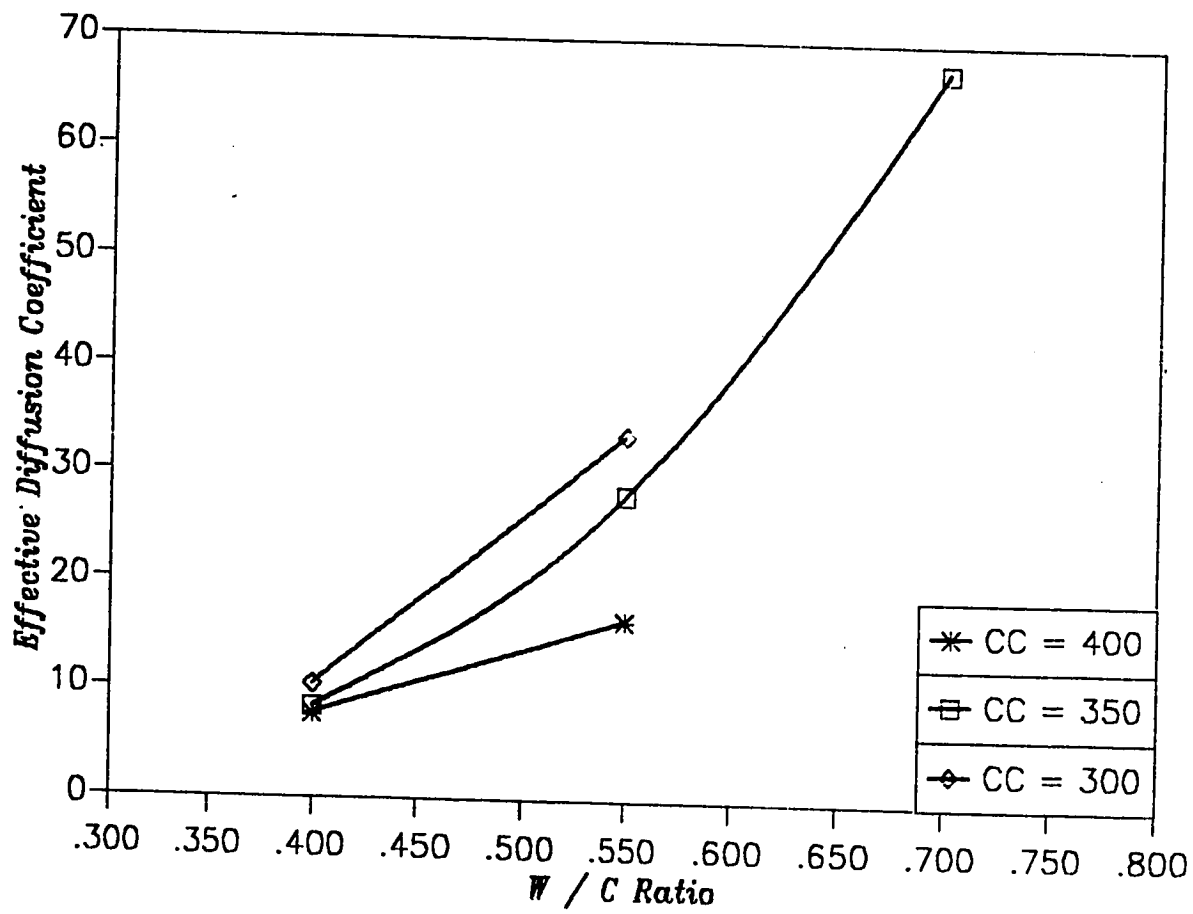


Figure 55: Variation of Effective Diffusion Coefficient with W/C Ratio

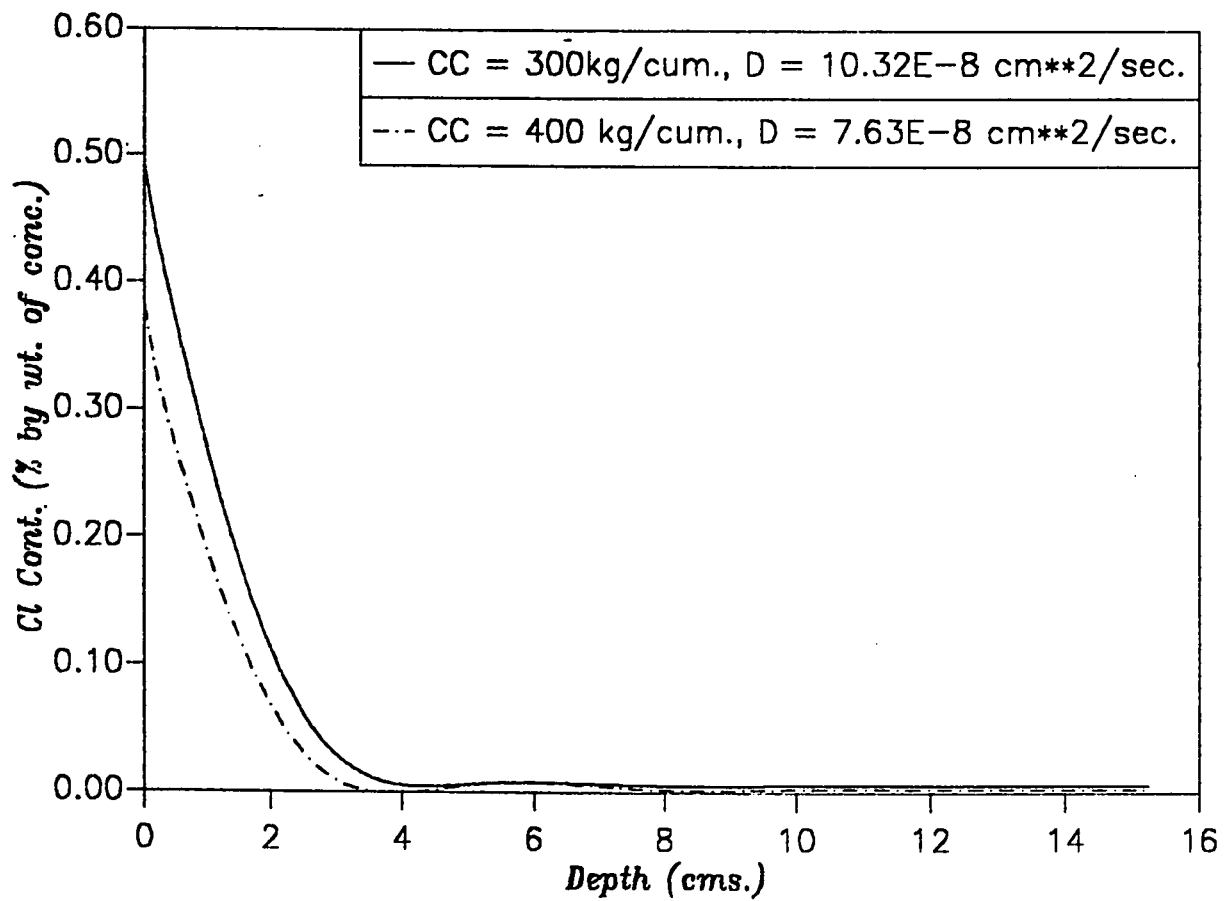


Figure 56: Effect of Cement Content on Chloride Diffusion: (W/C=0.4, 140 Days, 4% Chloride, Indoors)

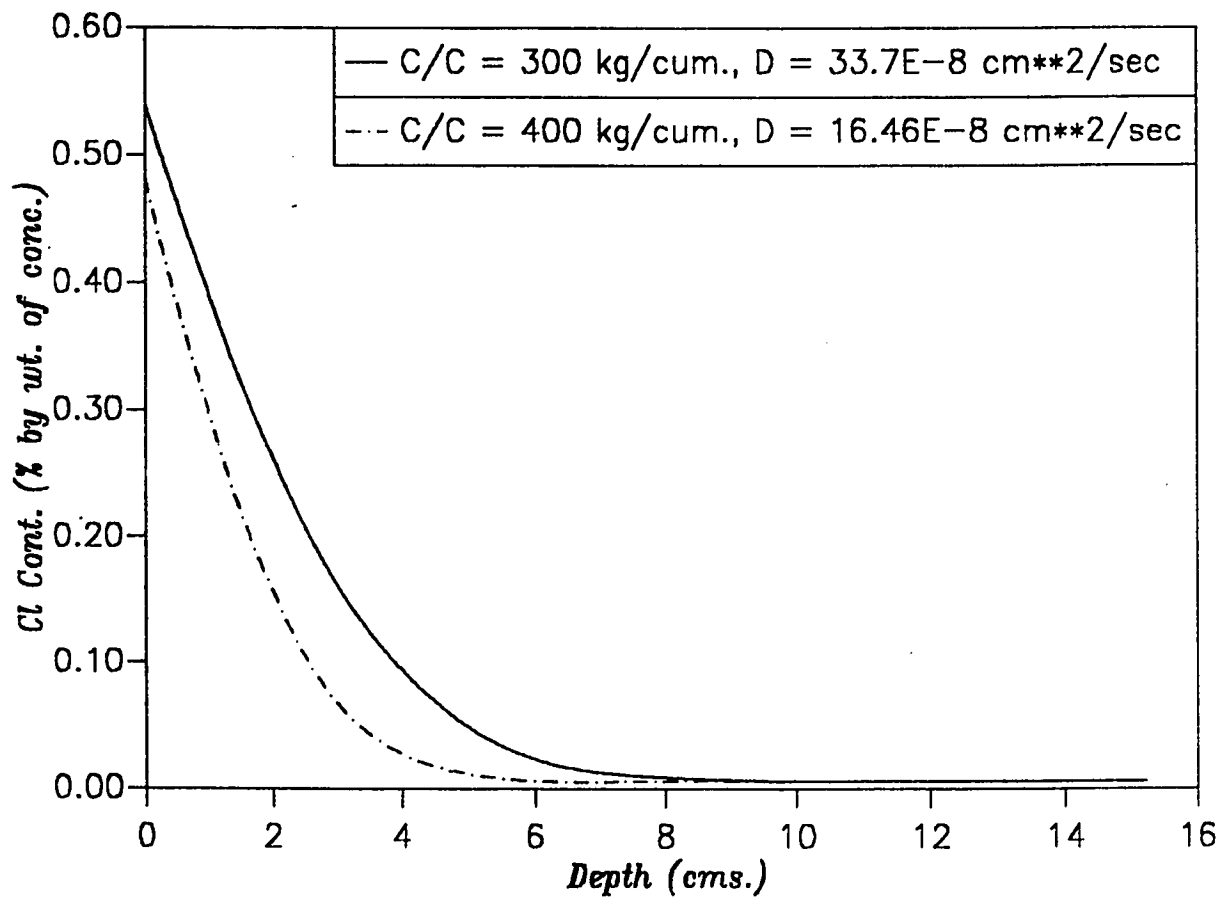


Figure 57: Effect of Cement Content Chloride Diffusion: (W/C=0.55, 140 Days, 4% Chloride, Indoors)

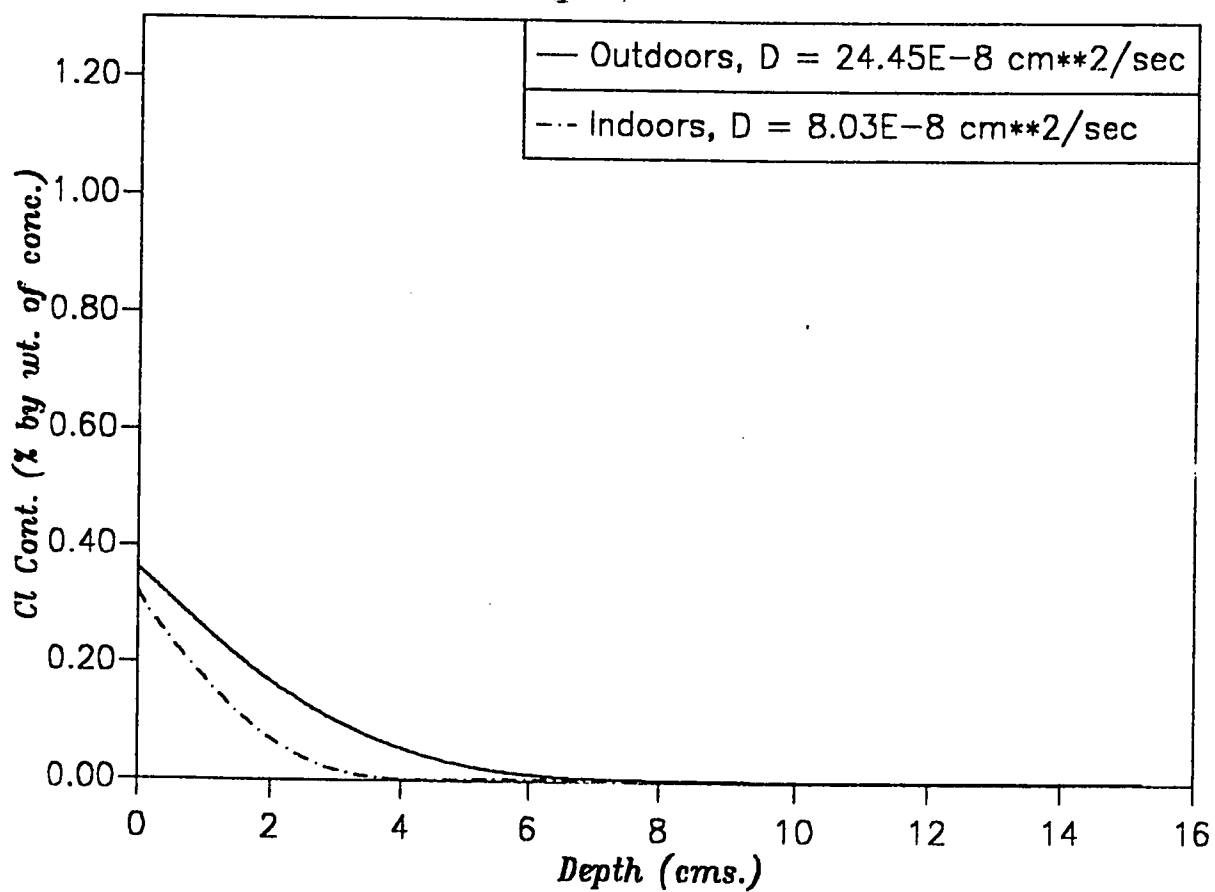


Figure 58: Effect of Exposure Conditions on Chloride Diffusion:
(CC=350 kg/cum., W/C=0.4, 4% Chloride, 175 Days)

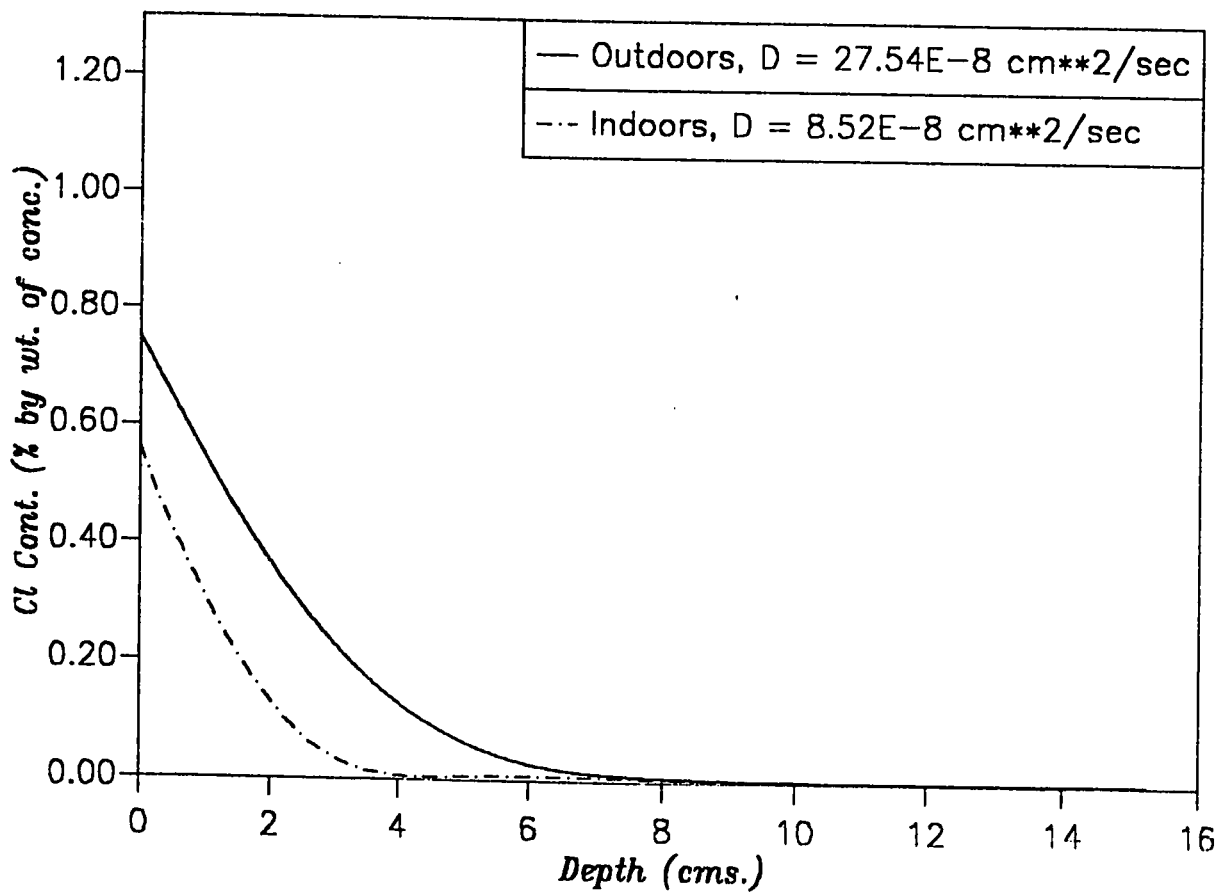


Figure 59: Effect of Exposure Conditions on Chloride Diffusion:
(CC=350 kg/cum., W/C=0.4, 8% Chloride, 175 Days)

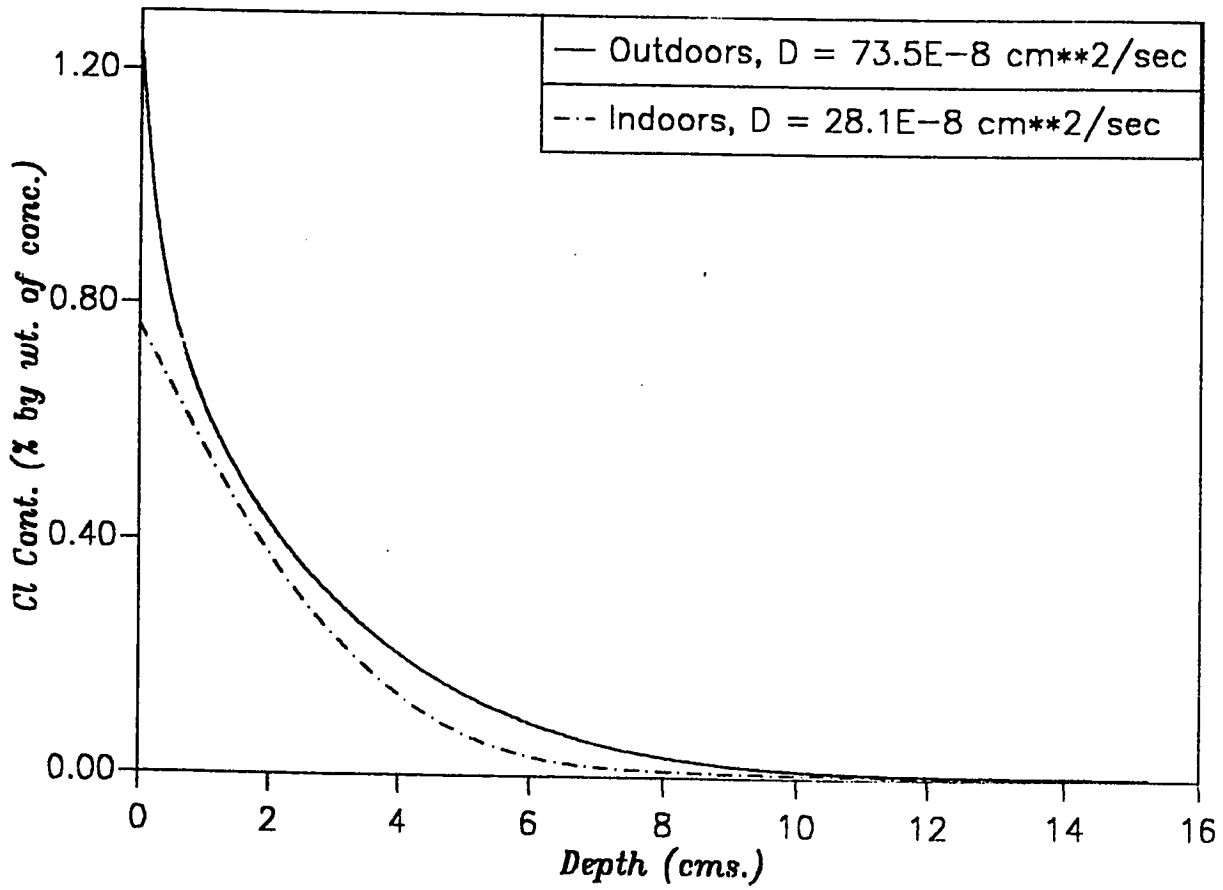


Figure 60: Effect of Exposure Conditions on Chloride Diffusion:
(CC=350 kg/cum., W/C=0.55, 8% Chloride, 175 Days)

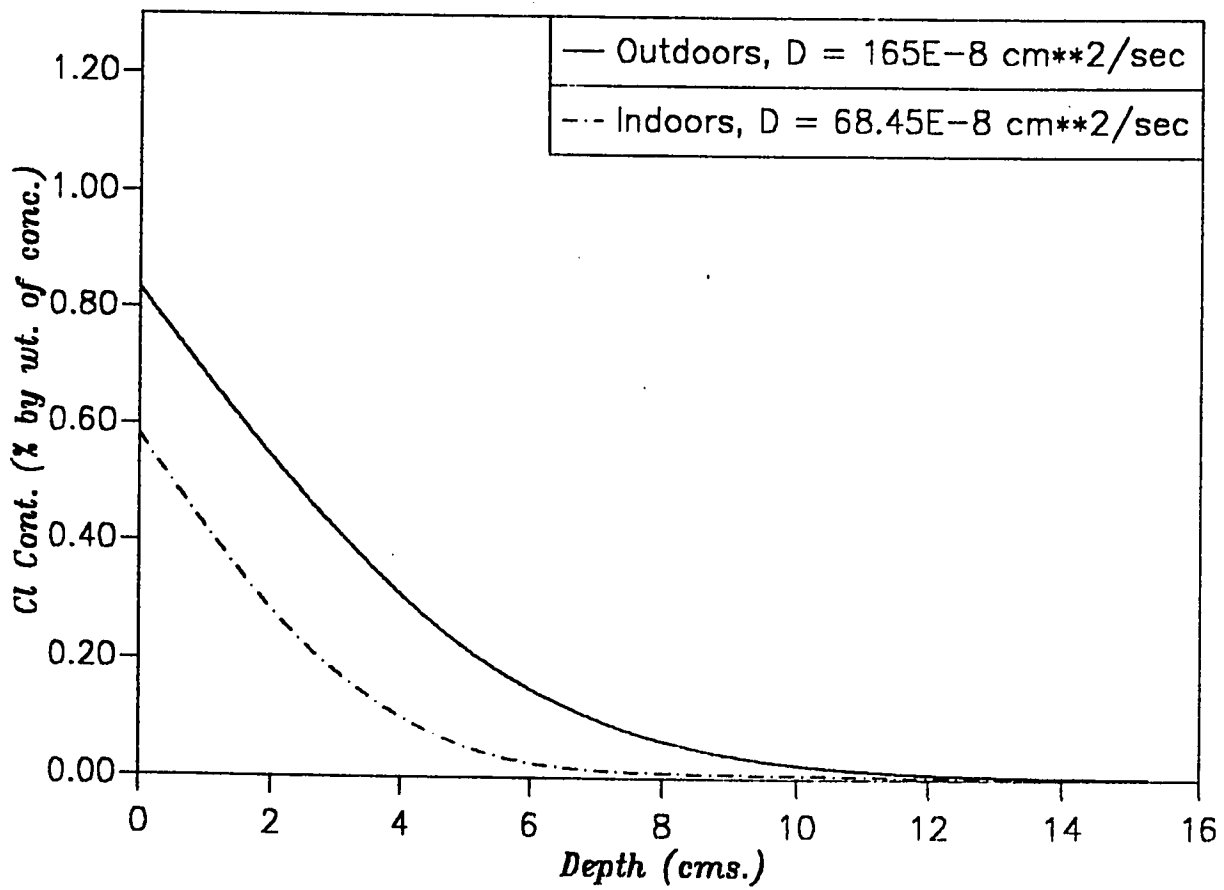


Figure 61: Effect of Exposure Conditions on Chloride Diffusion:
(CC=350 kg/cum., W/C=0.7, 4% Chloride, 70 Days)

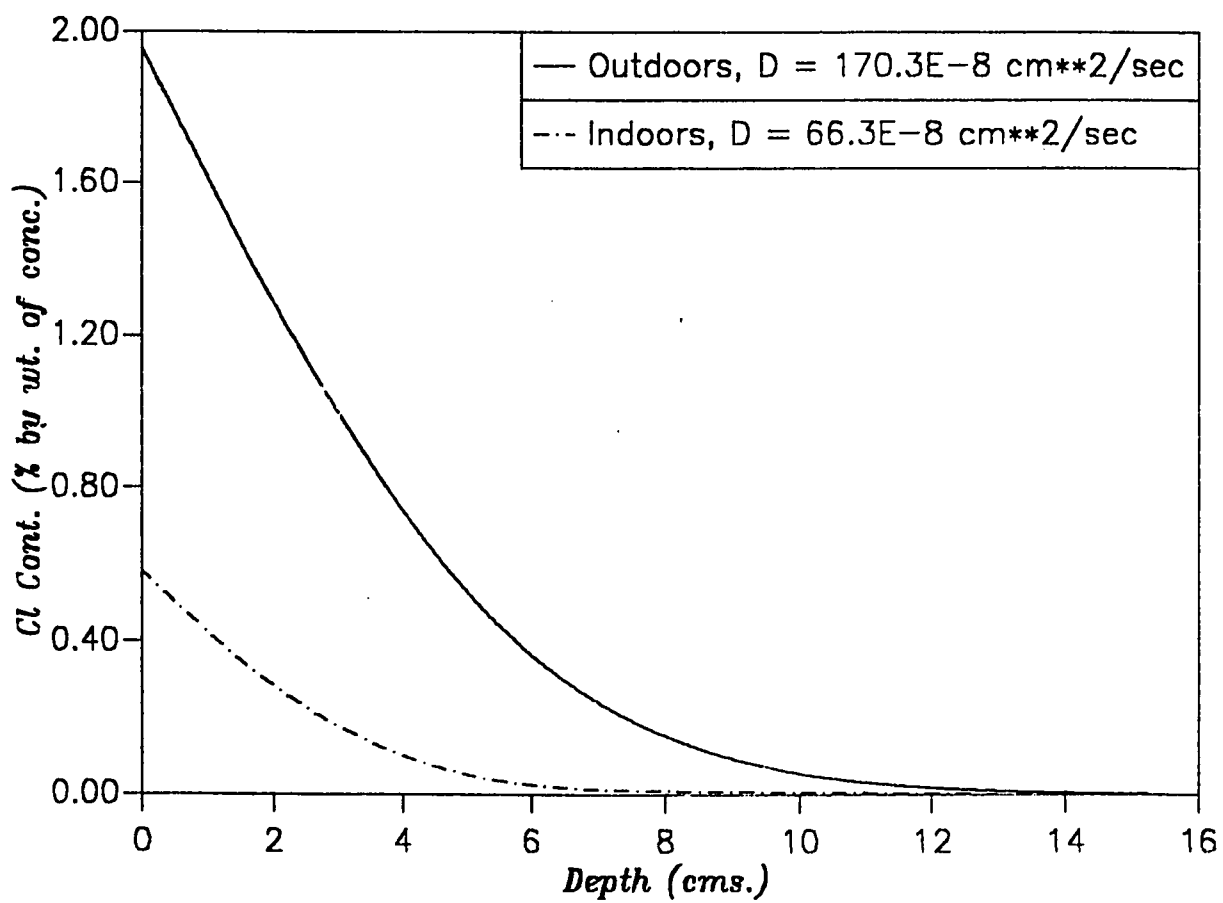


Figure 62: Effect of Exposure Conditions on Chloride Diffusion:
(CC=350 kg/cum., W/C=0.7, 8% Chloride, 70 Days)

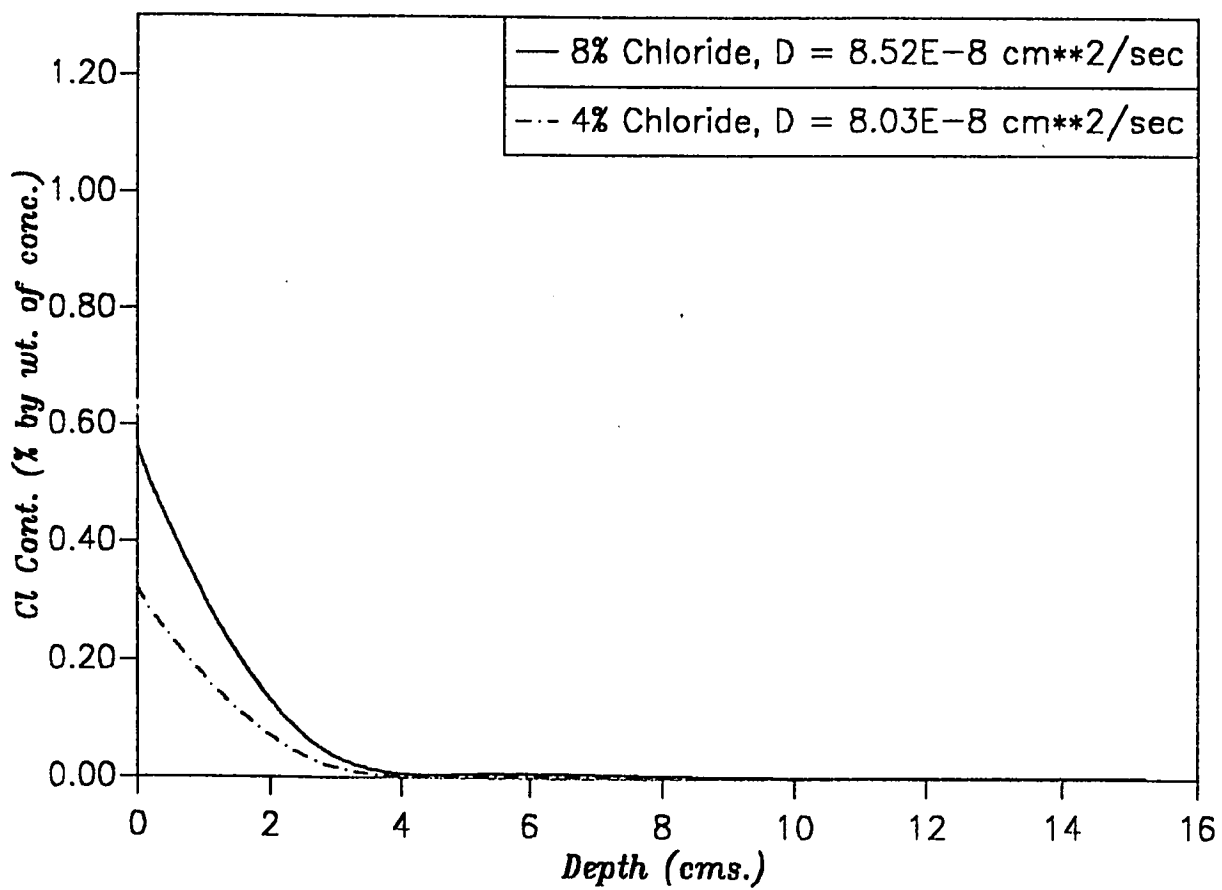


Figure 63: Effect of Exposure Solution Concentration on Chloride Diffusion: (W/C=0.4, 175 Days, Indoors)

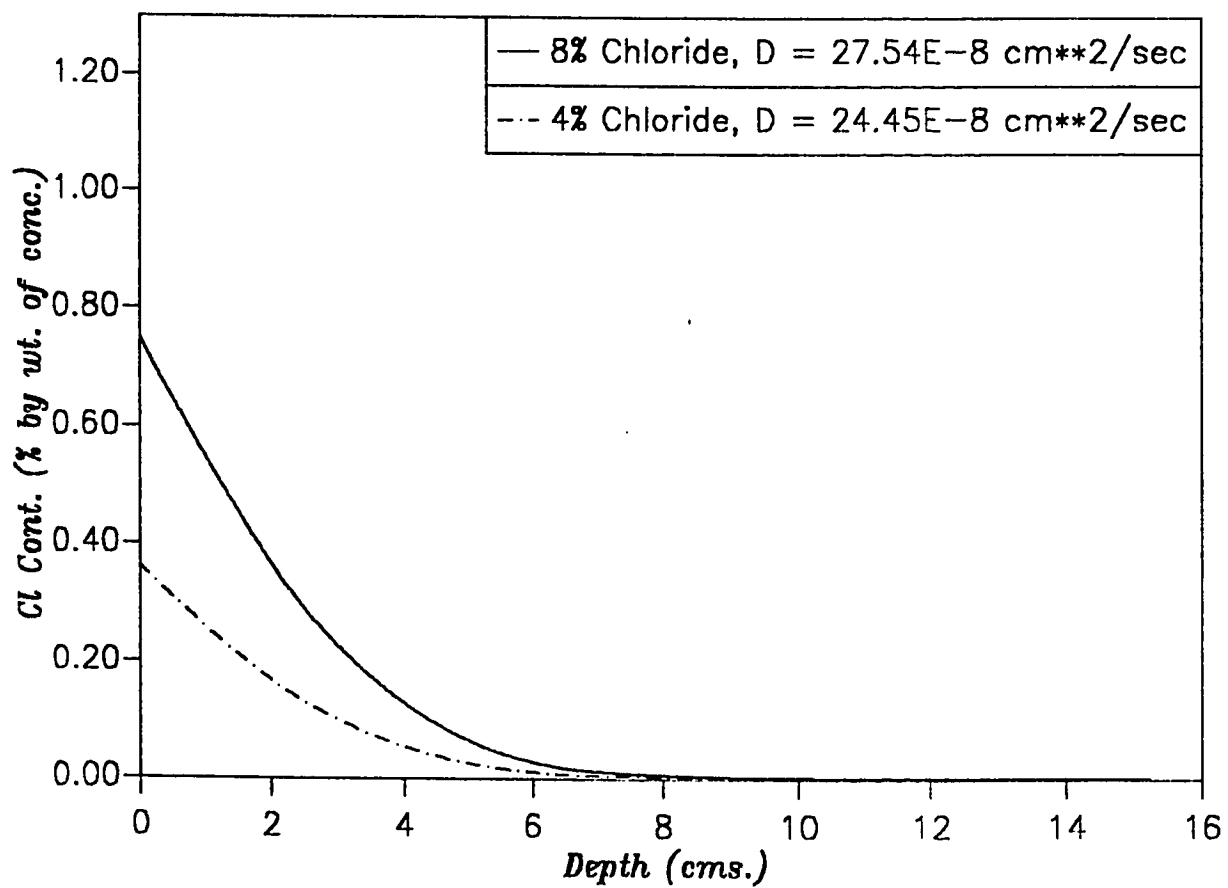


Figure 64: Effect of Exposure Solution Concentration on Chloride Diffusion: (W/C=0.4, 175 Days, Outdoors)

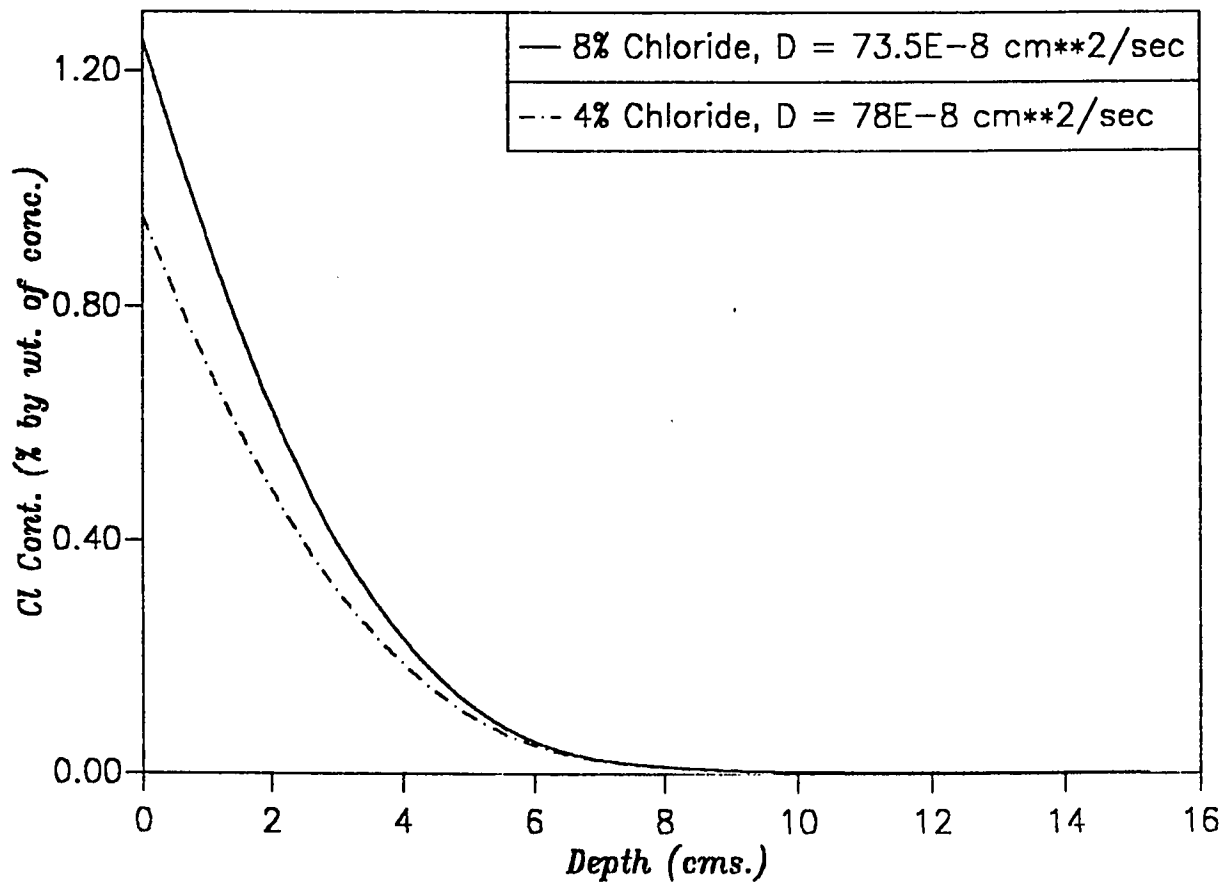


Figure 65: Effect of Exposure Solution Concentration on Chloride Diffusion: (W/C=0.55, 70 Days, Outdoors)

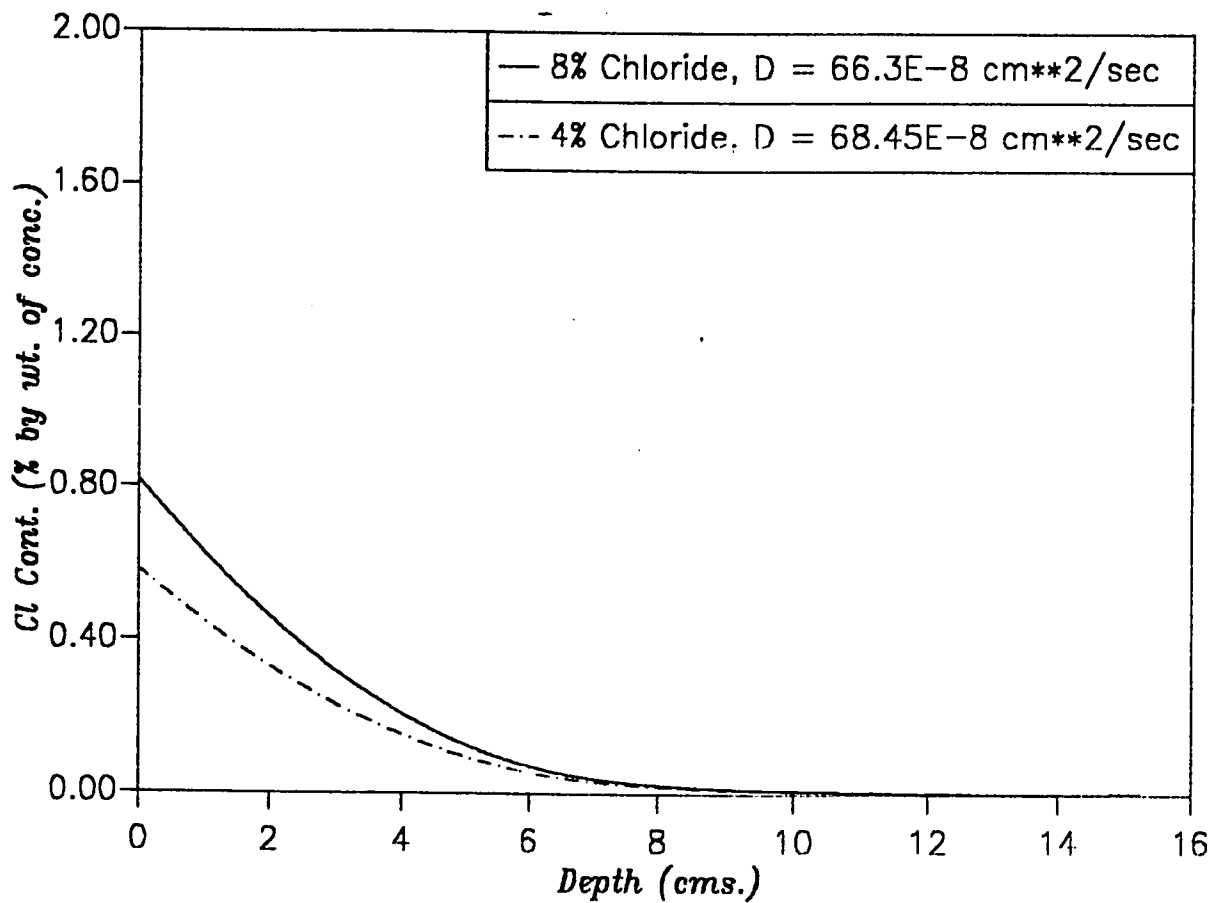


Figure 66: Effect of Exposure Solution Concentration on Chloride Diffusion: (W/C=0.7, 105 Days, Indoors)

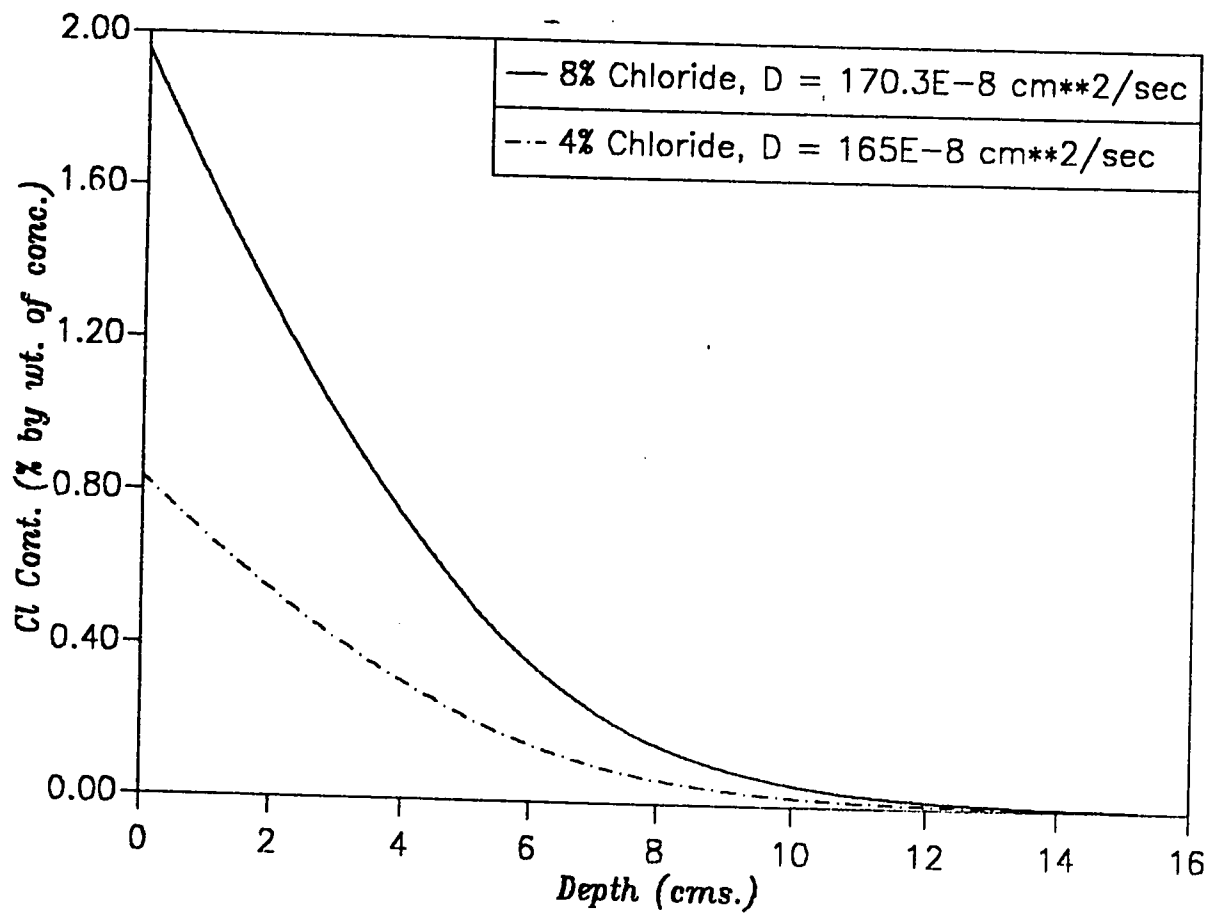


Figure 67: Effect of Exposure Solution Concentration on Chloride Diffusion: (W/C=0.7, 70 Days, Outdoors)

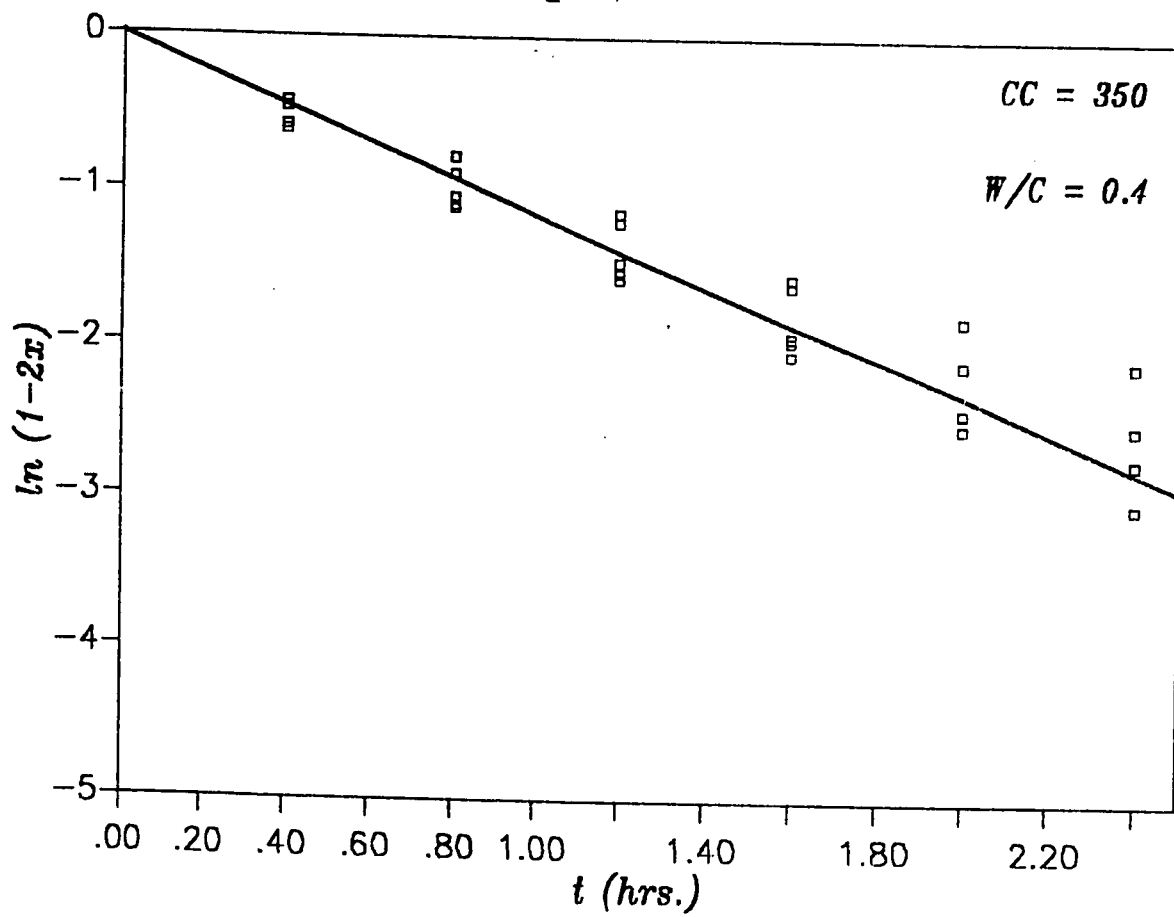


Figure 68: Fit for $\ln(1-2x)$ Vs t : (CC=350 kg/cum., W/C=0.4)

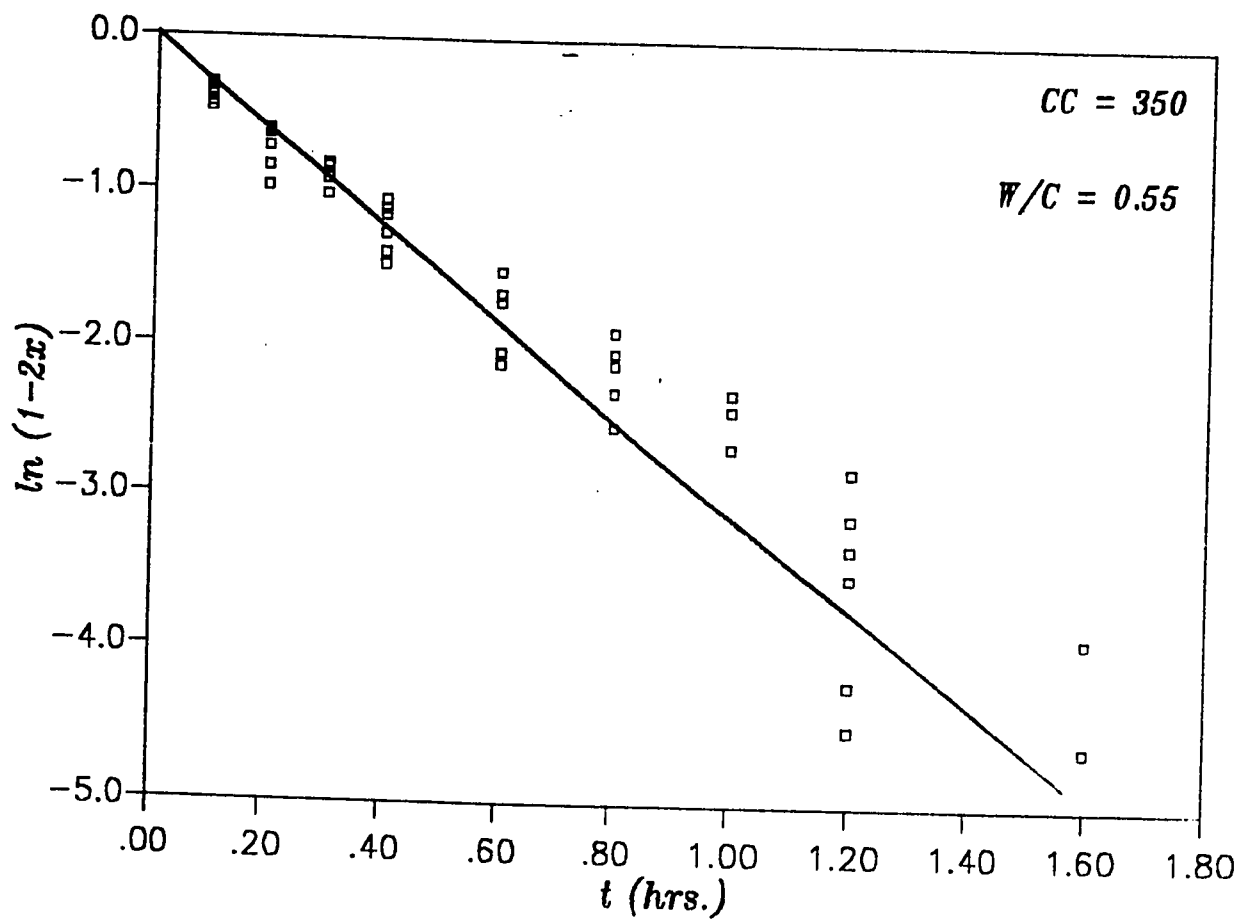


Figure 69: Fit for $\ln(1-2x)$ Vs t : (CC=350 kg/cum., W/C=0.55)

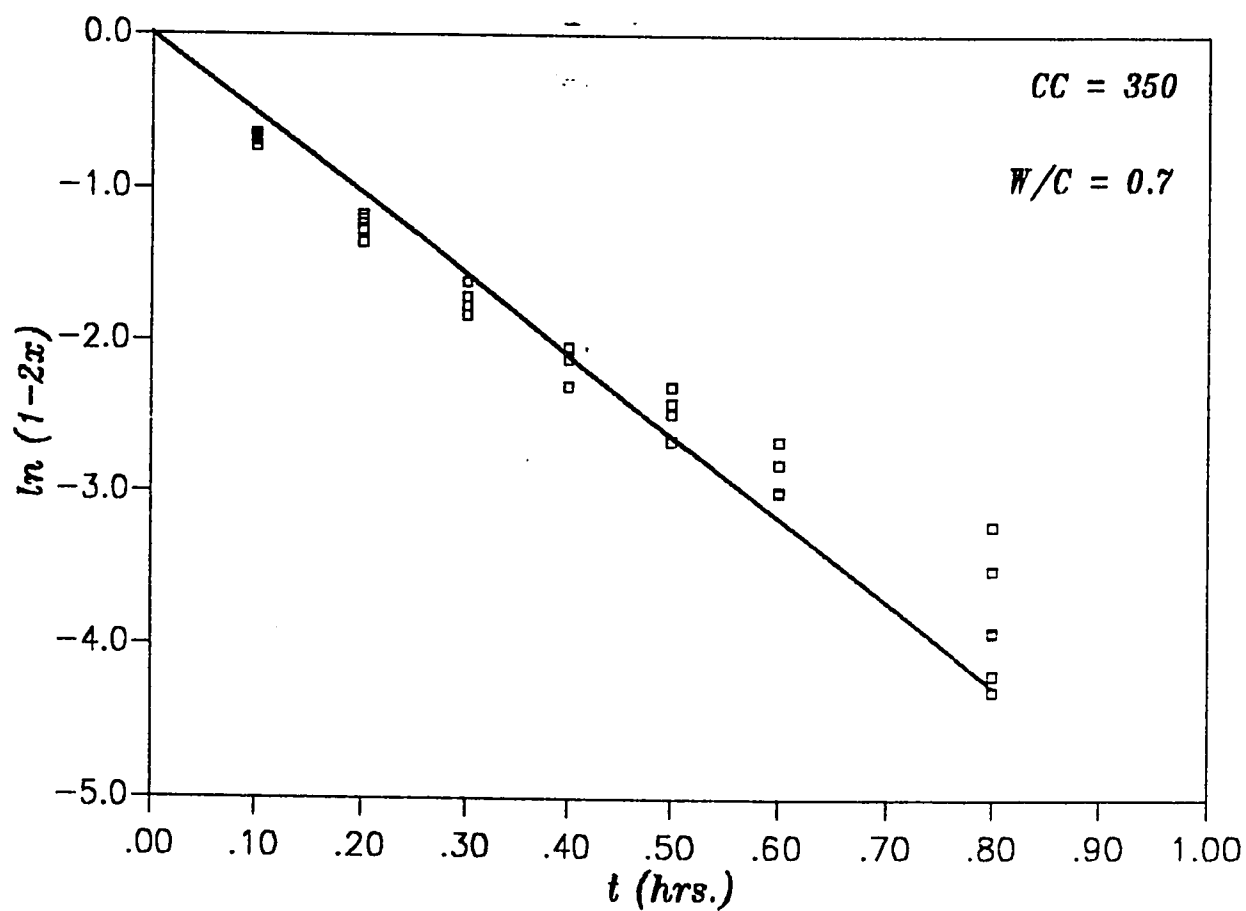


Figure 70: Fit for $\ln(1-2x)$ Vs t : (CC=350 kg/cum. W/C=0.7)

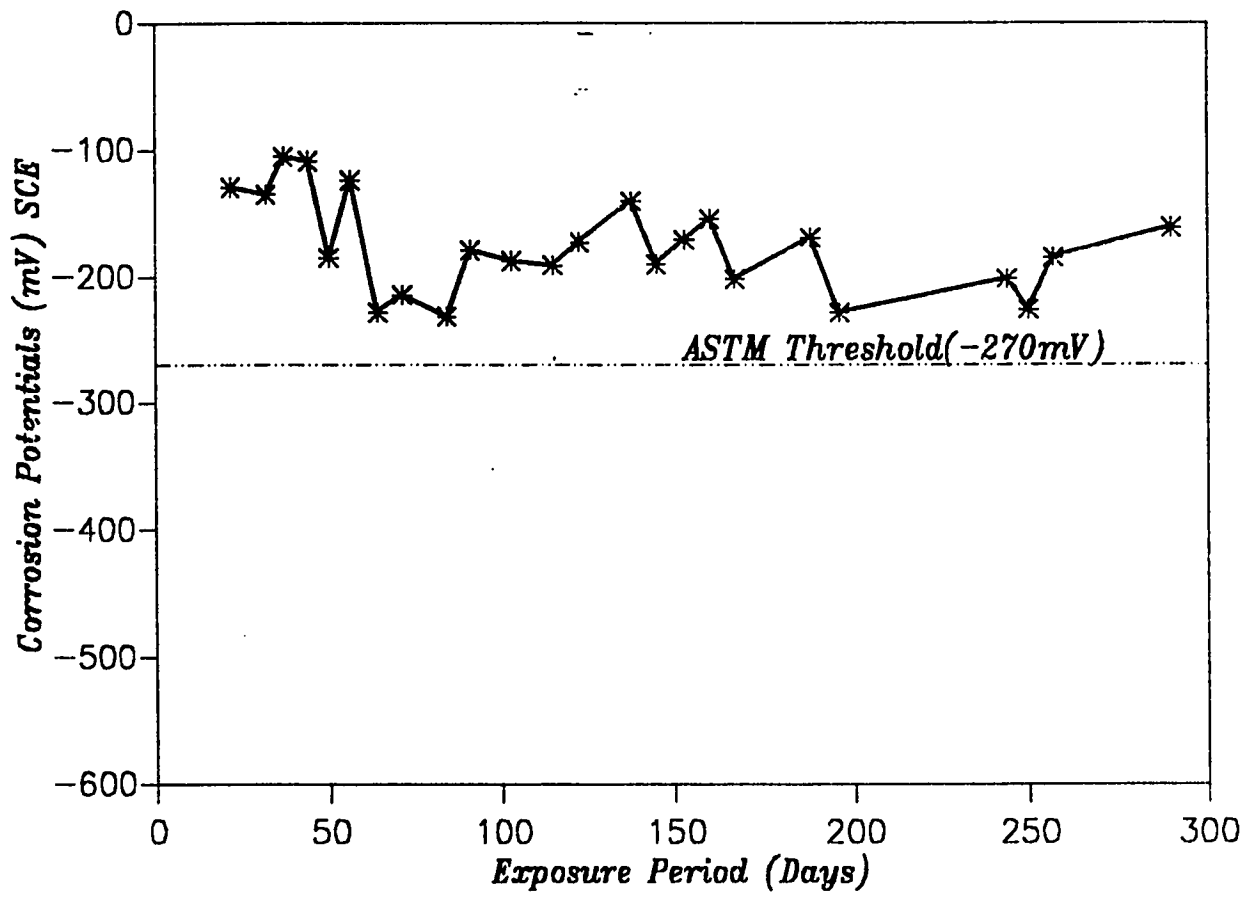


Figure 71: Corrosion Potentials: (W/C=0.4, 4% Chloride, Cover=4")

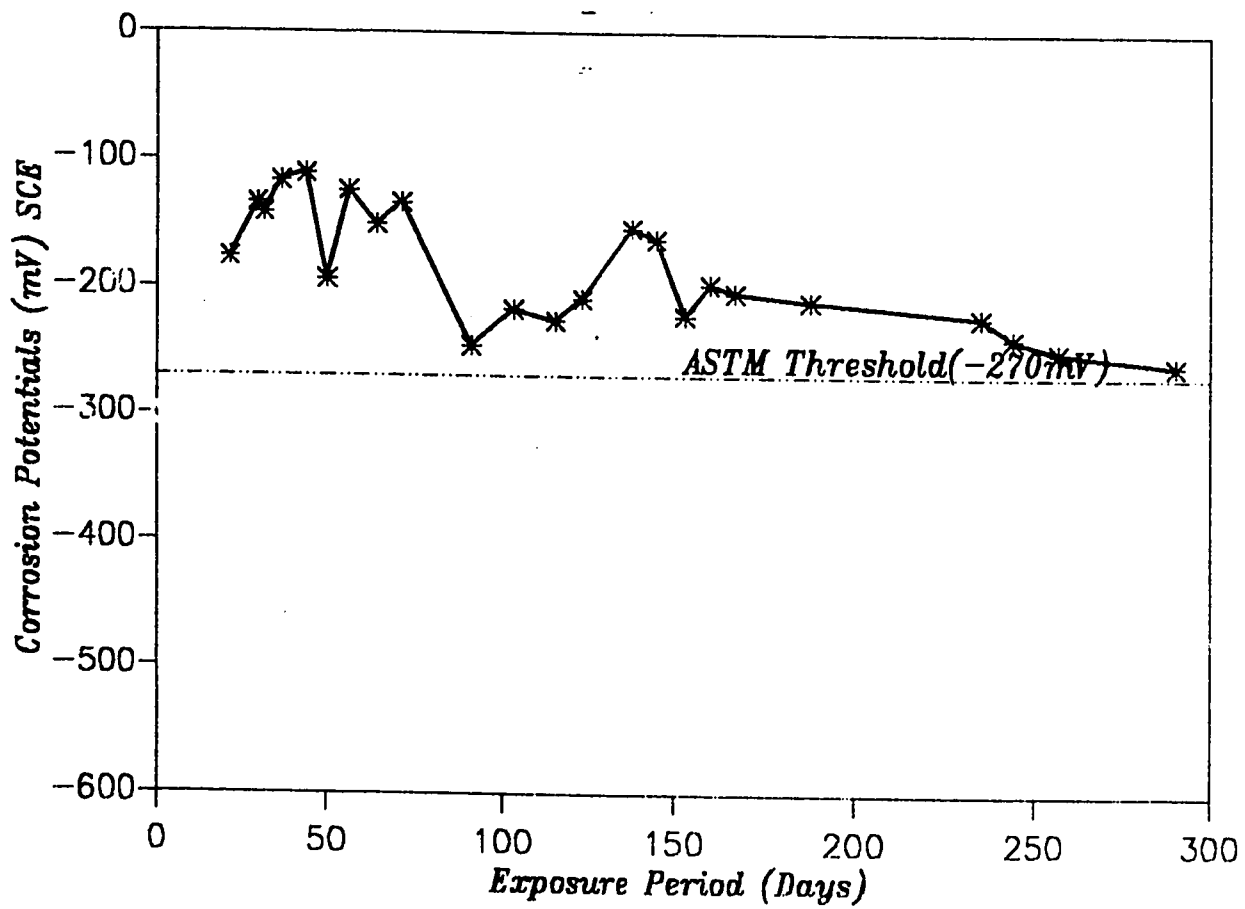


Figure 72: Corrosion Potentials: (W/C=0.4, 4% Chloride, Cover=3")

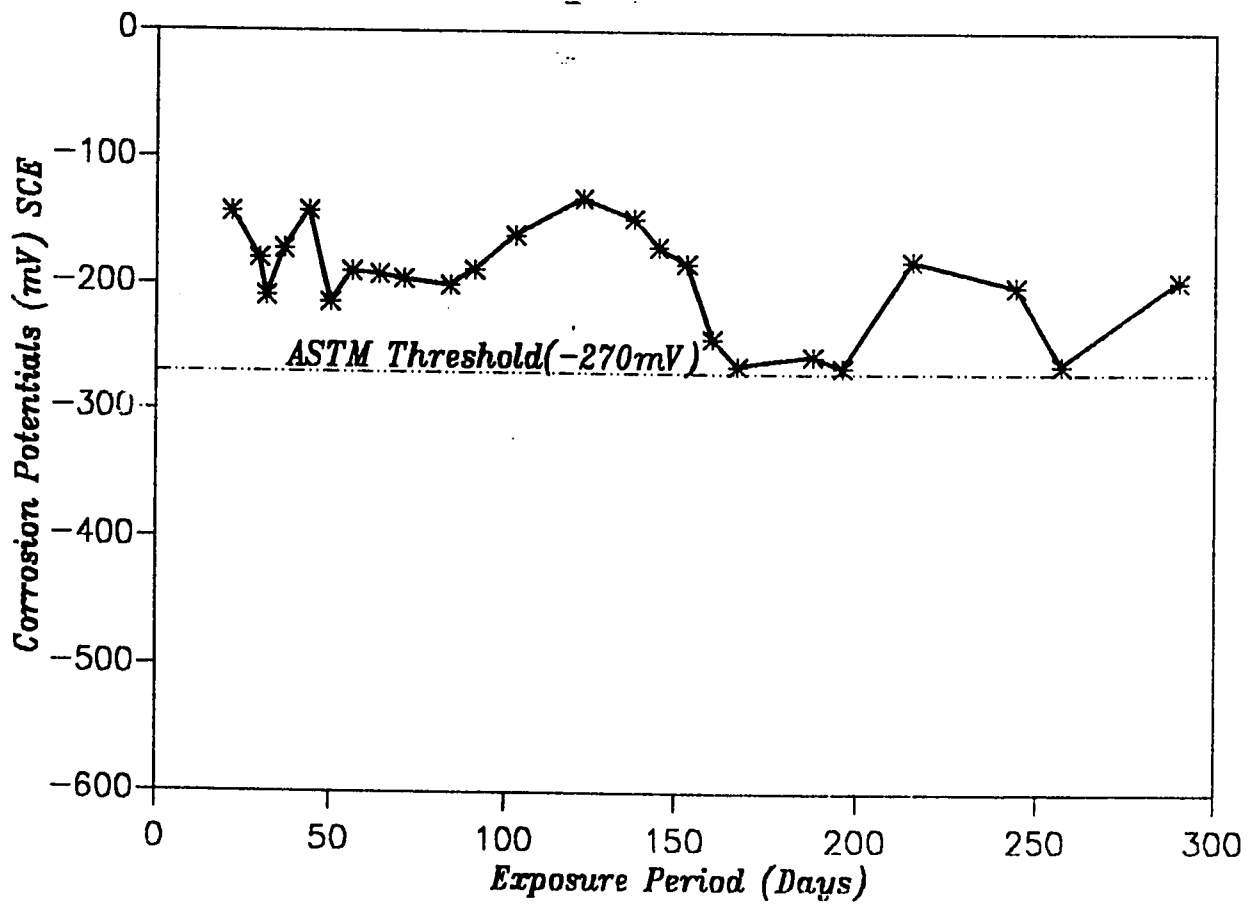


Figure 73: Corrosion Potentials: (W/C=0.4, 4% Chloride, Cover=1.5")

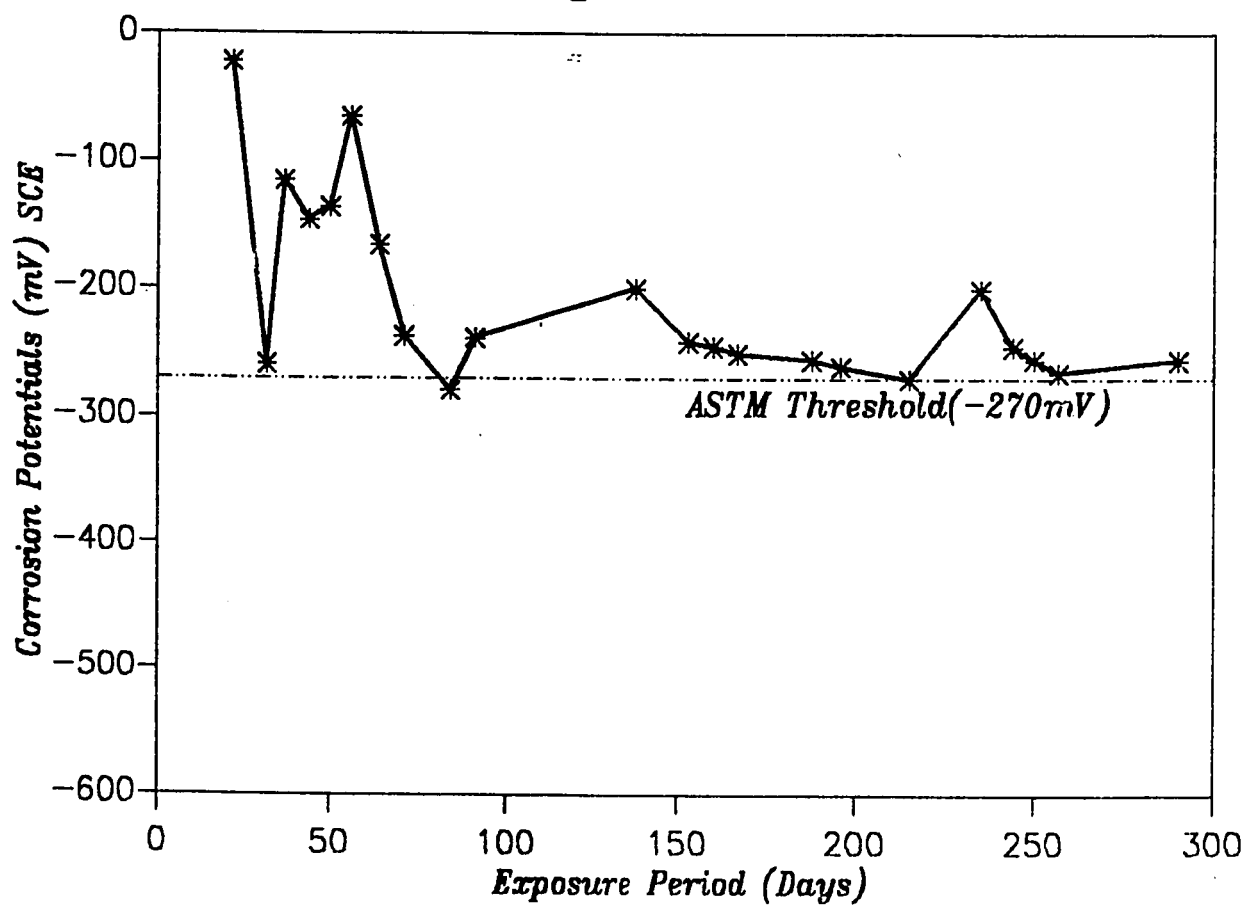


Figure 74: Corrosion Potentials: (W/C=0.55, 4% Chloride, Cover=4")

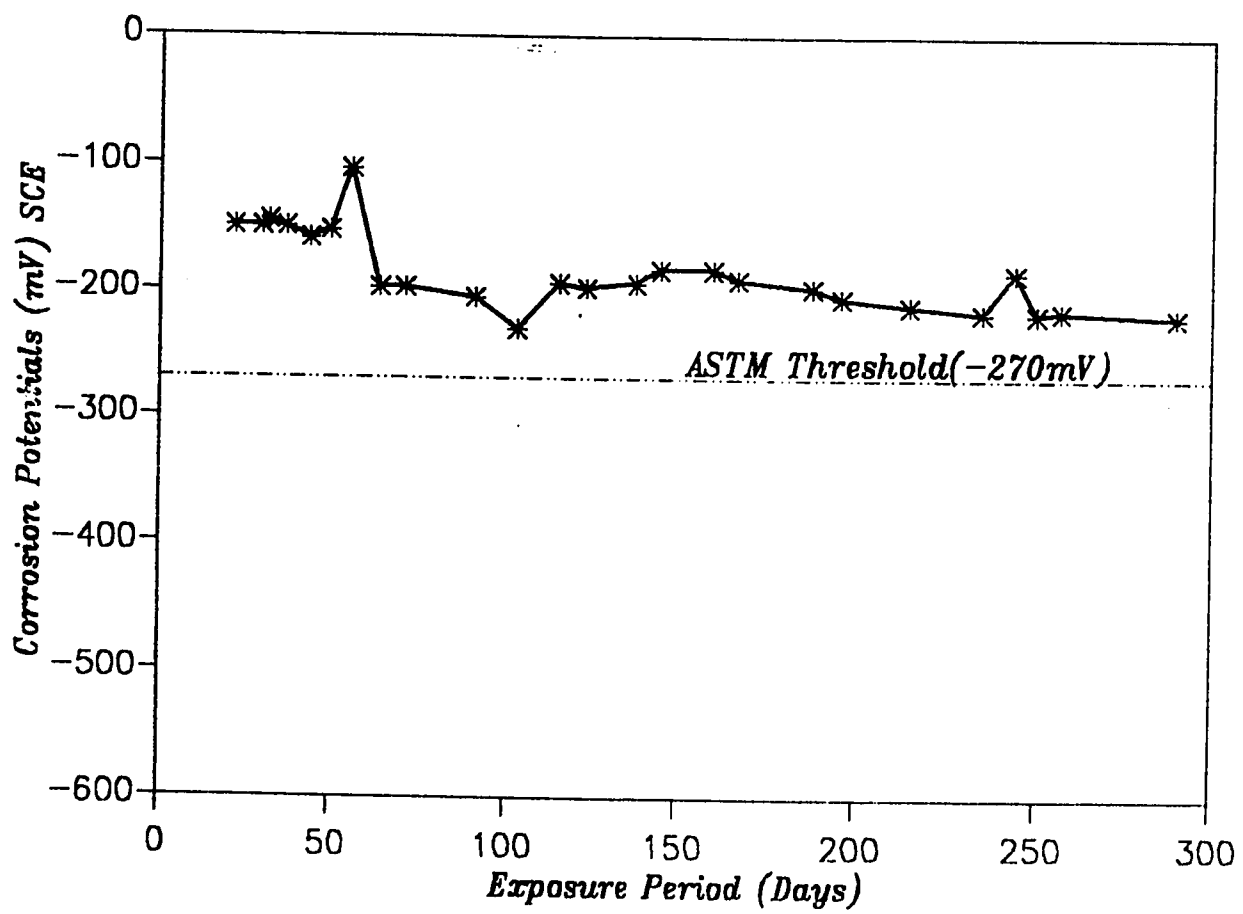


Figure 75: Corrosion Potentials: (W/C=0.55, 4% Chloride, Cover=3")

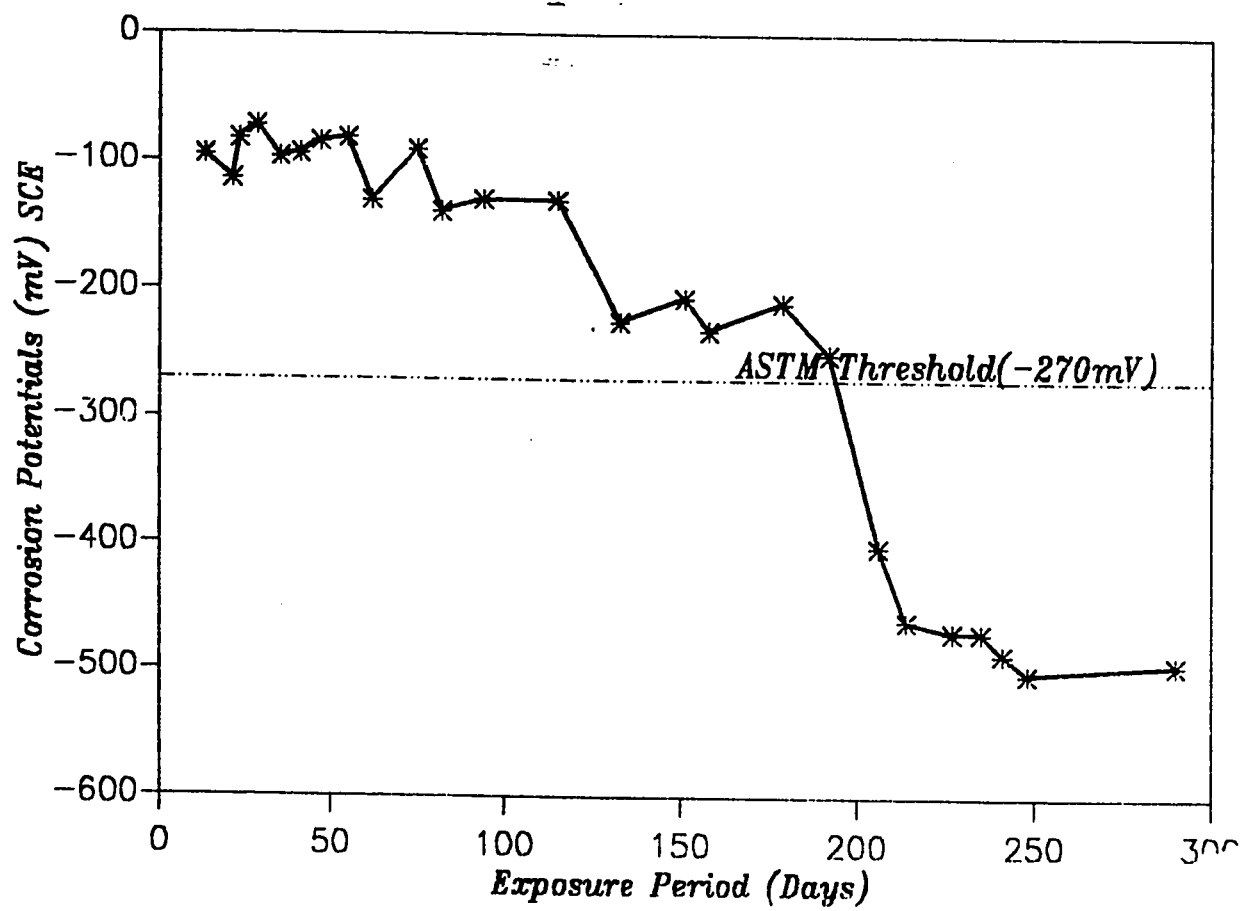


Figure 76: Corrosion Potentials: (W/C=0.55, 4% Chloride, Cover=1.5")

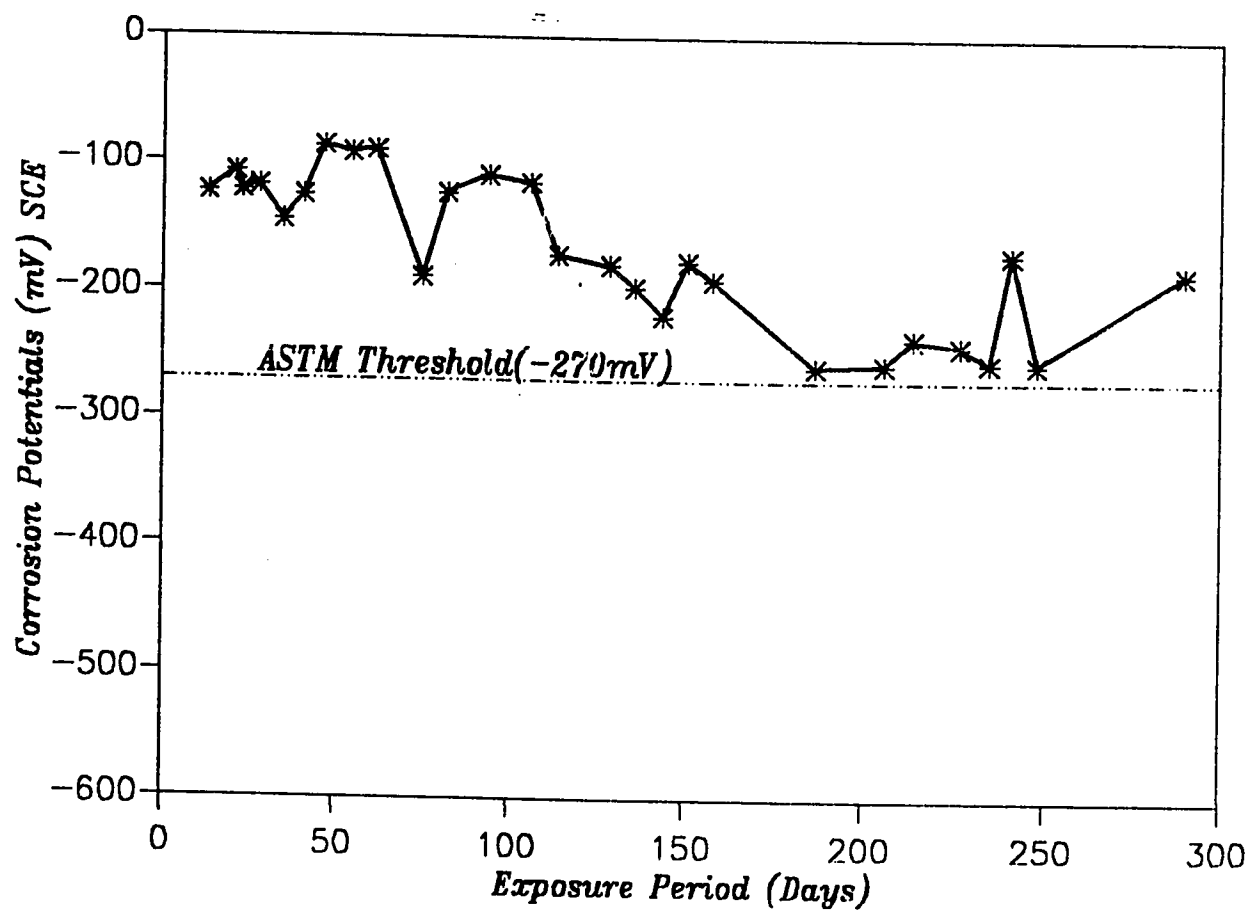


Figure 77: Corrosion Potentials: (W/C=0.4, 8% Chloride, Cover=4")

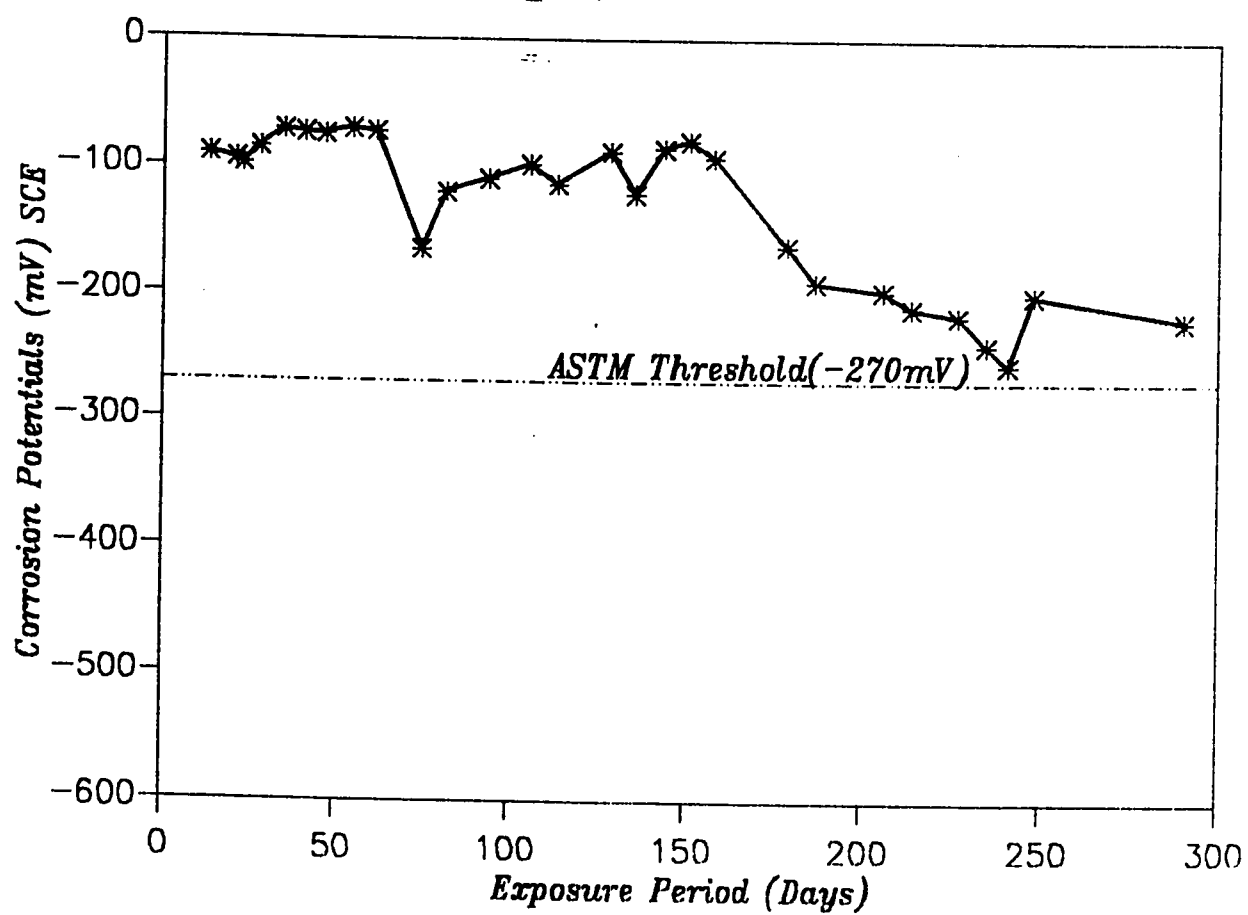


Figure 78: Corrosion Potentials: (W/C=0.4, 8% Chloride, Cover=3")

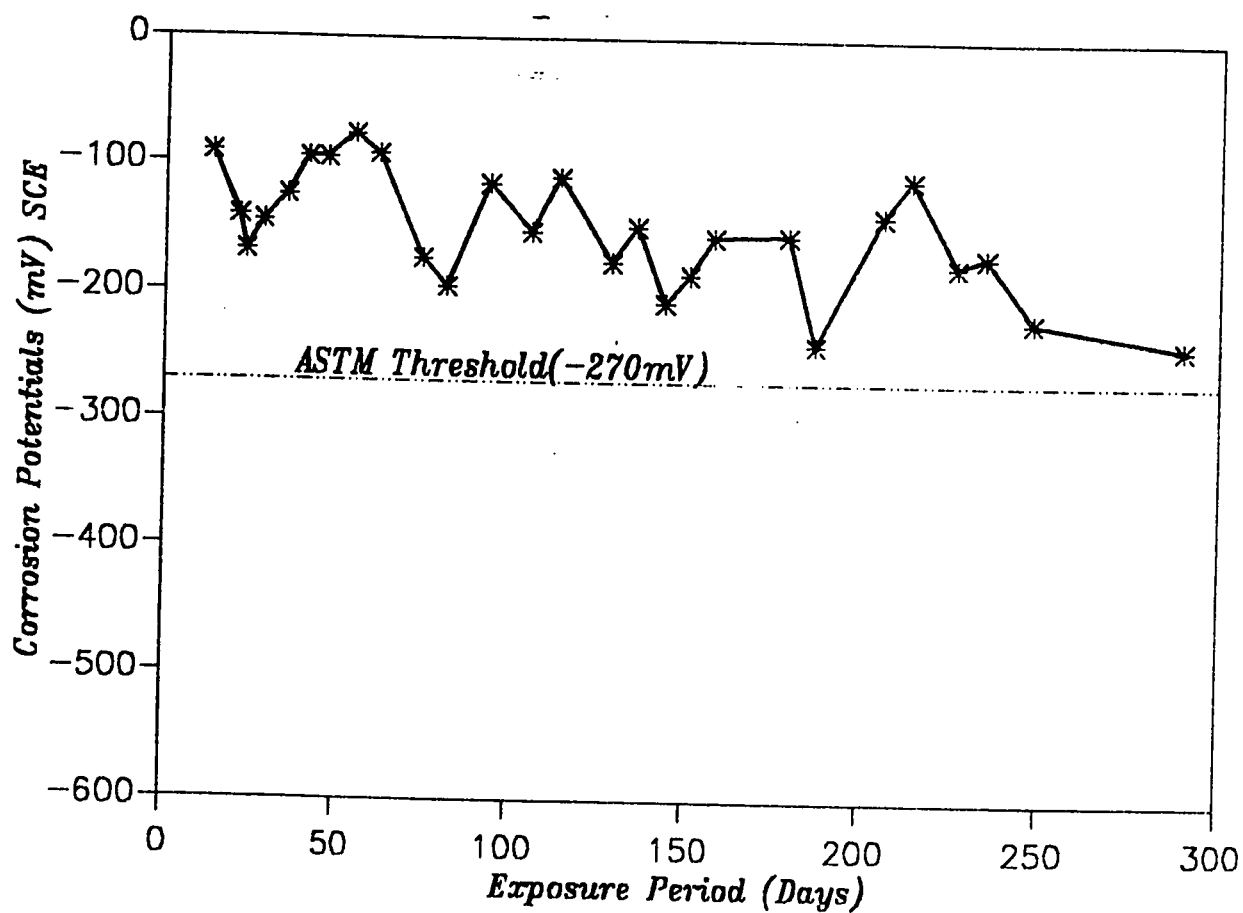


Figure 79: Corrosion Potentials: (W/C=0.4, 8% Chloride, Cover=1.5")

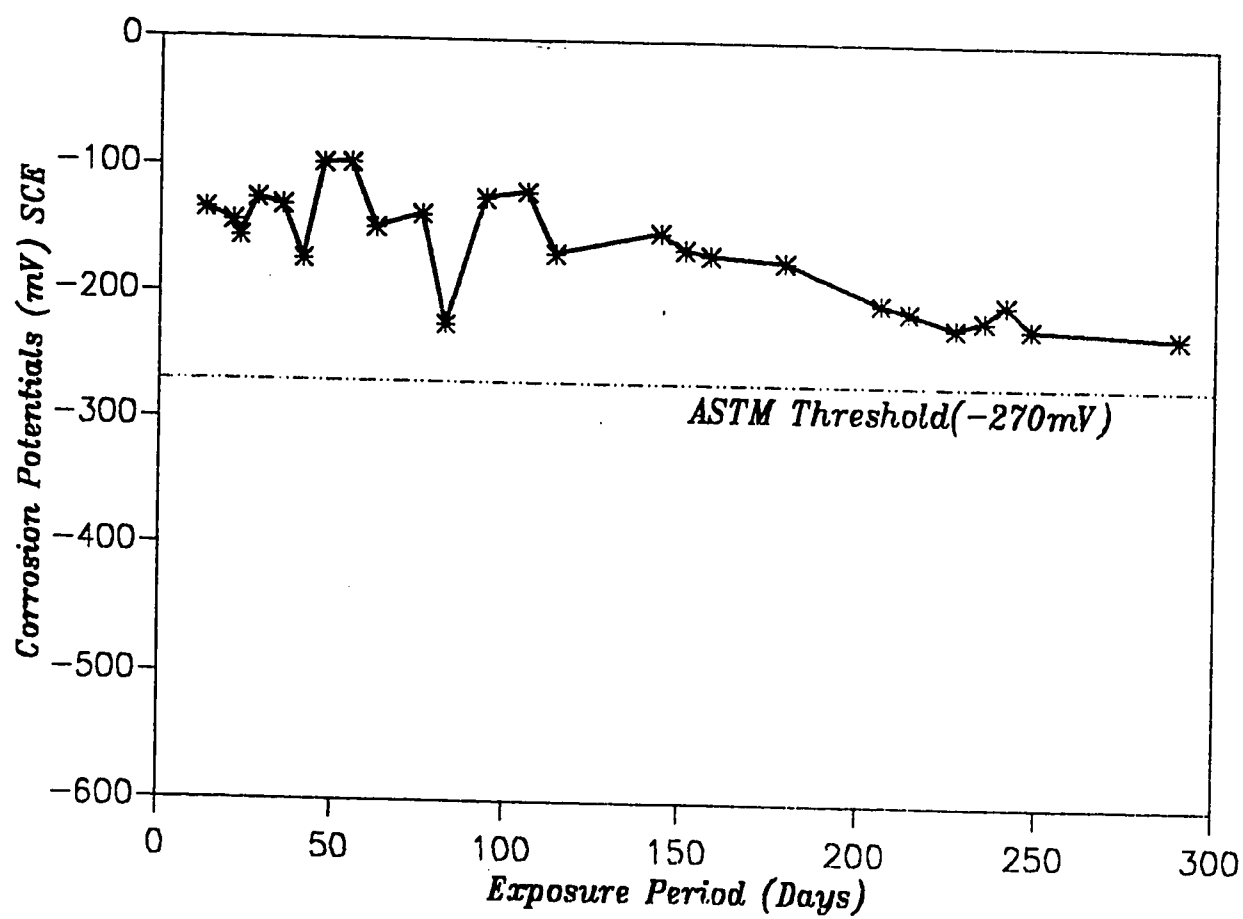


Figure 80: Corrosion Potentials: (W/C=0.55, 8% Chloride, Cover=4")

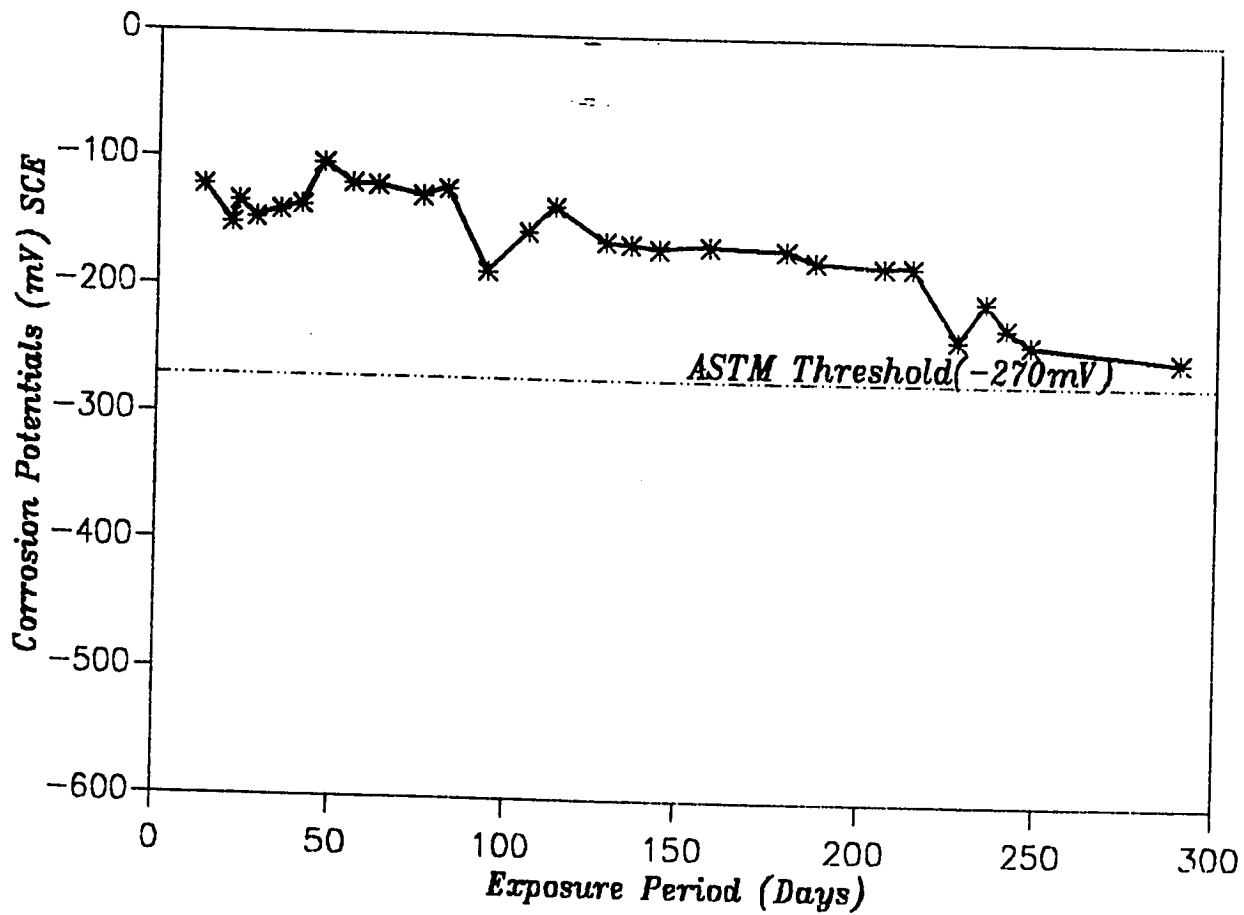


Figure 81: Corrosion Potentials: (W/C=0.55, 8% Chloride, Cover=3")

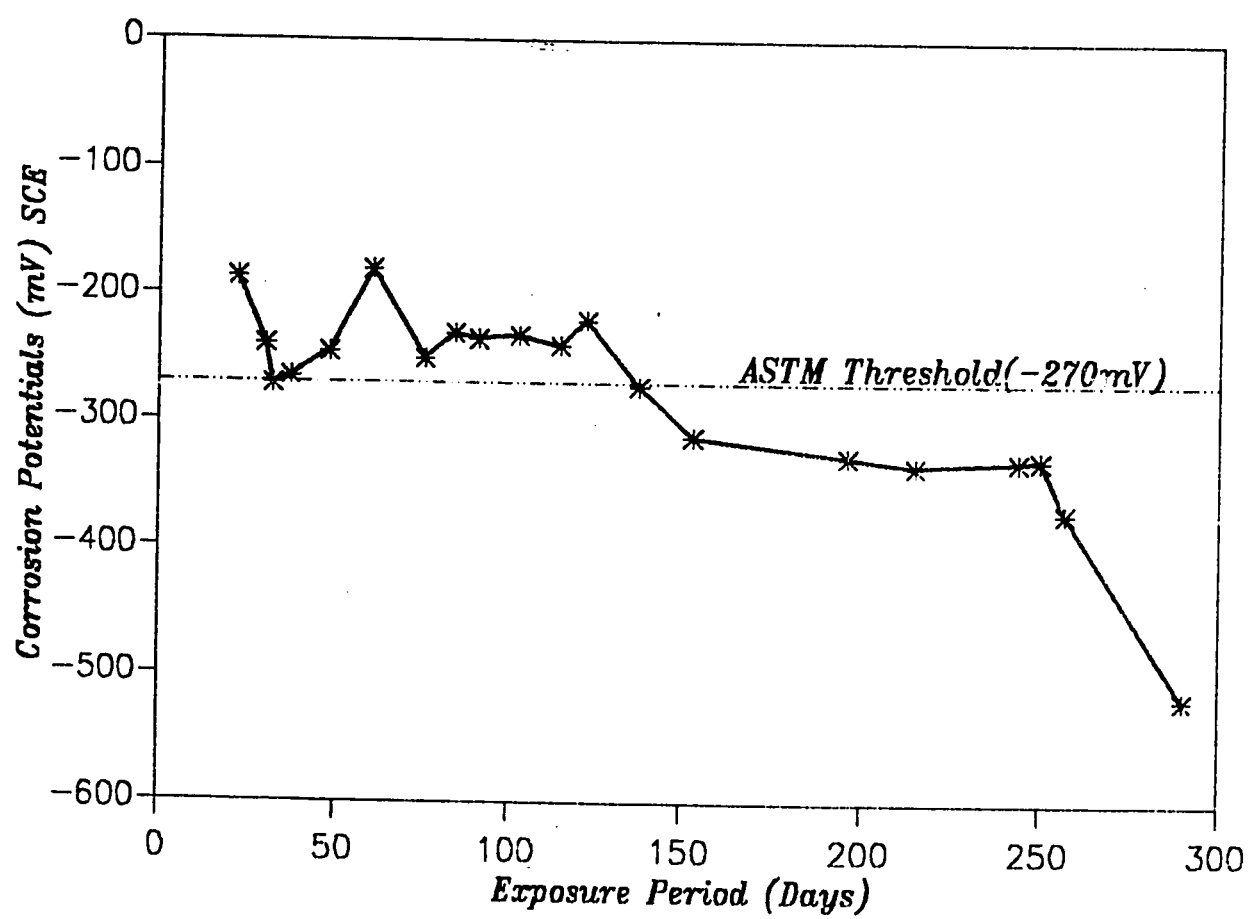


Figure 82: Corrosion Potentials: (W/C=0.55, 8% Chloride, Cover=1.5")

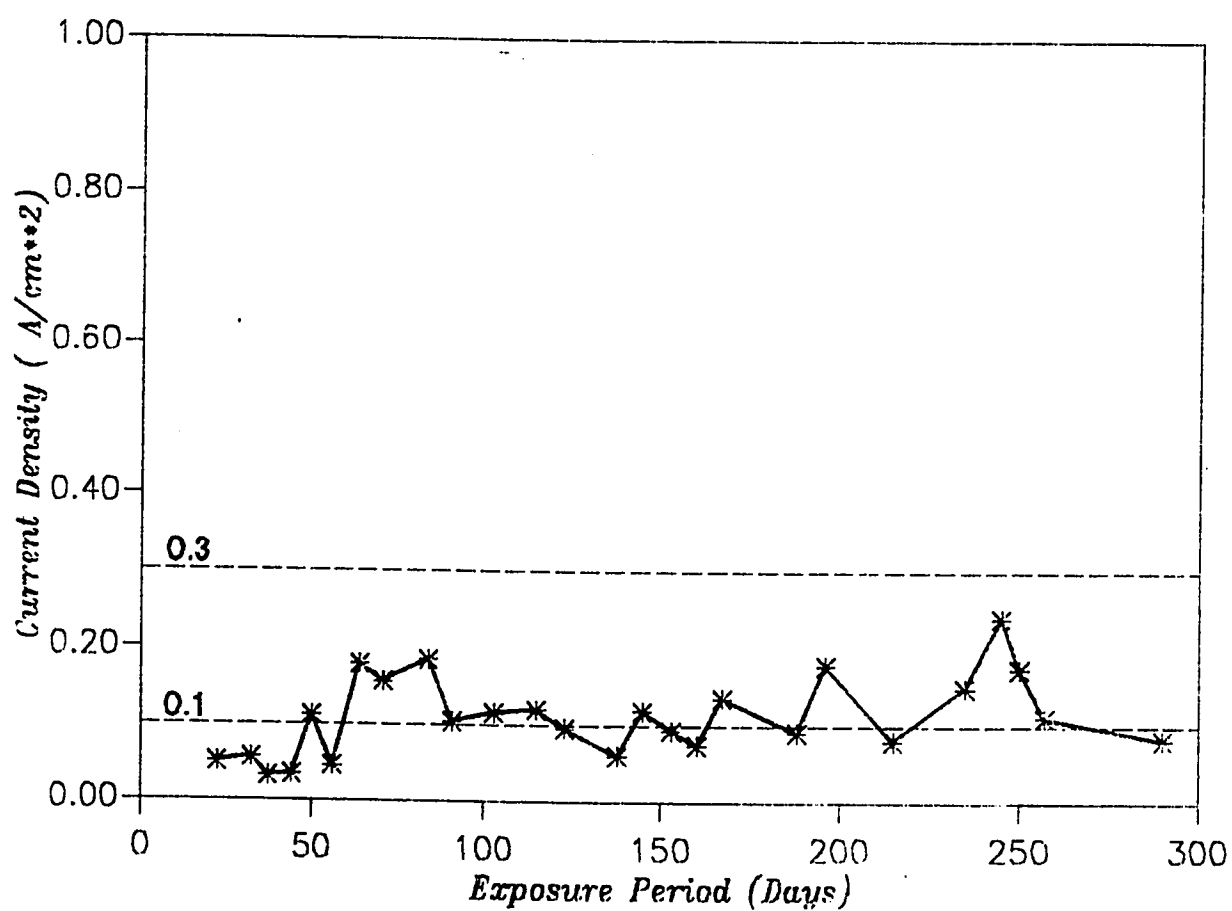


Figure 83: Corrosion Current Densities: (W/C=0.4, 4% Chloride, Cover=4")

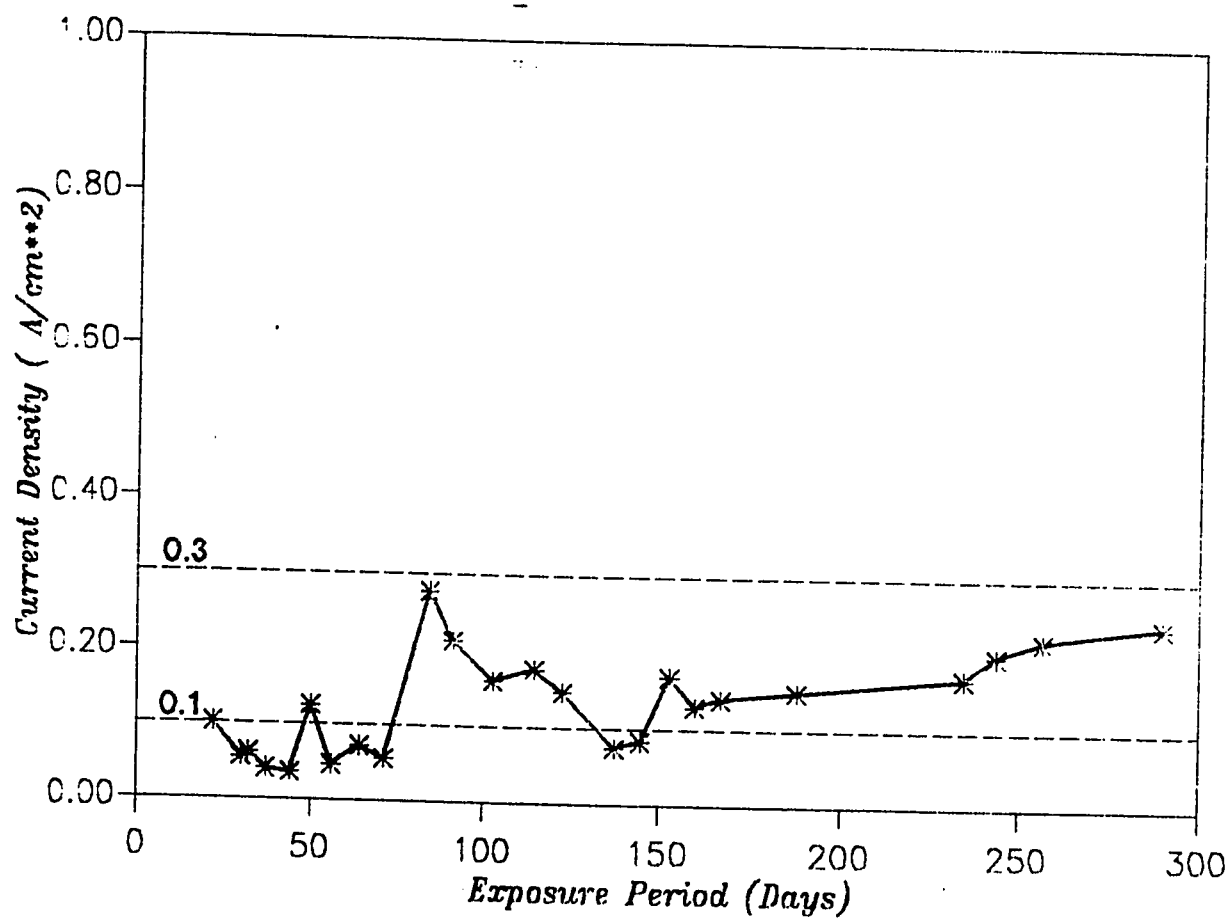


Figure 84: Corrosion Current Densities: (W/C=0.4, 4% Chloride, Cover=3")

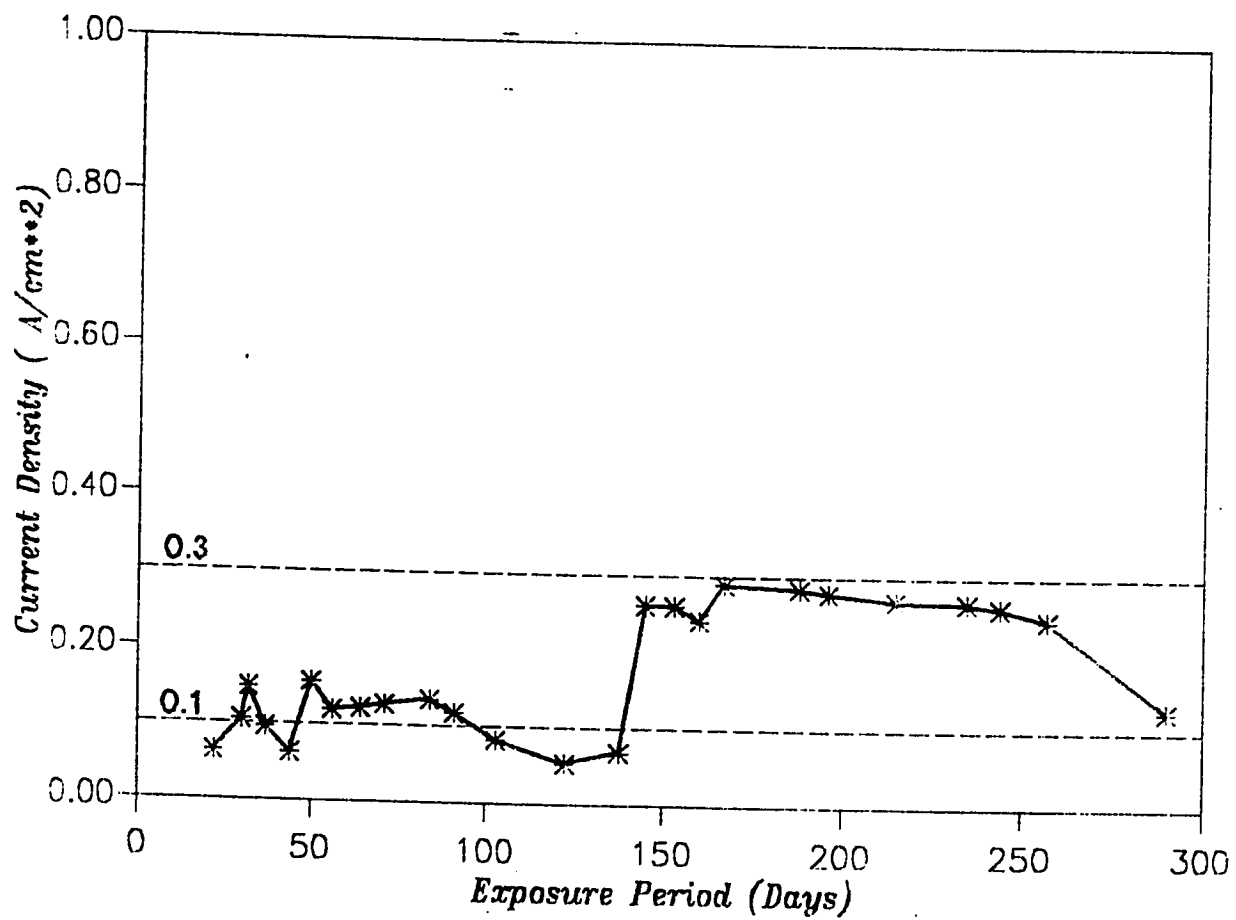


Figure 85: Corrosion Current Densities: (W/C=0.4, 4% Chloride, Cover=1.5")

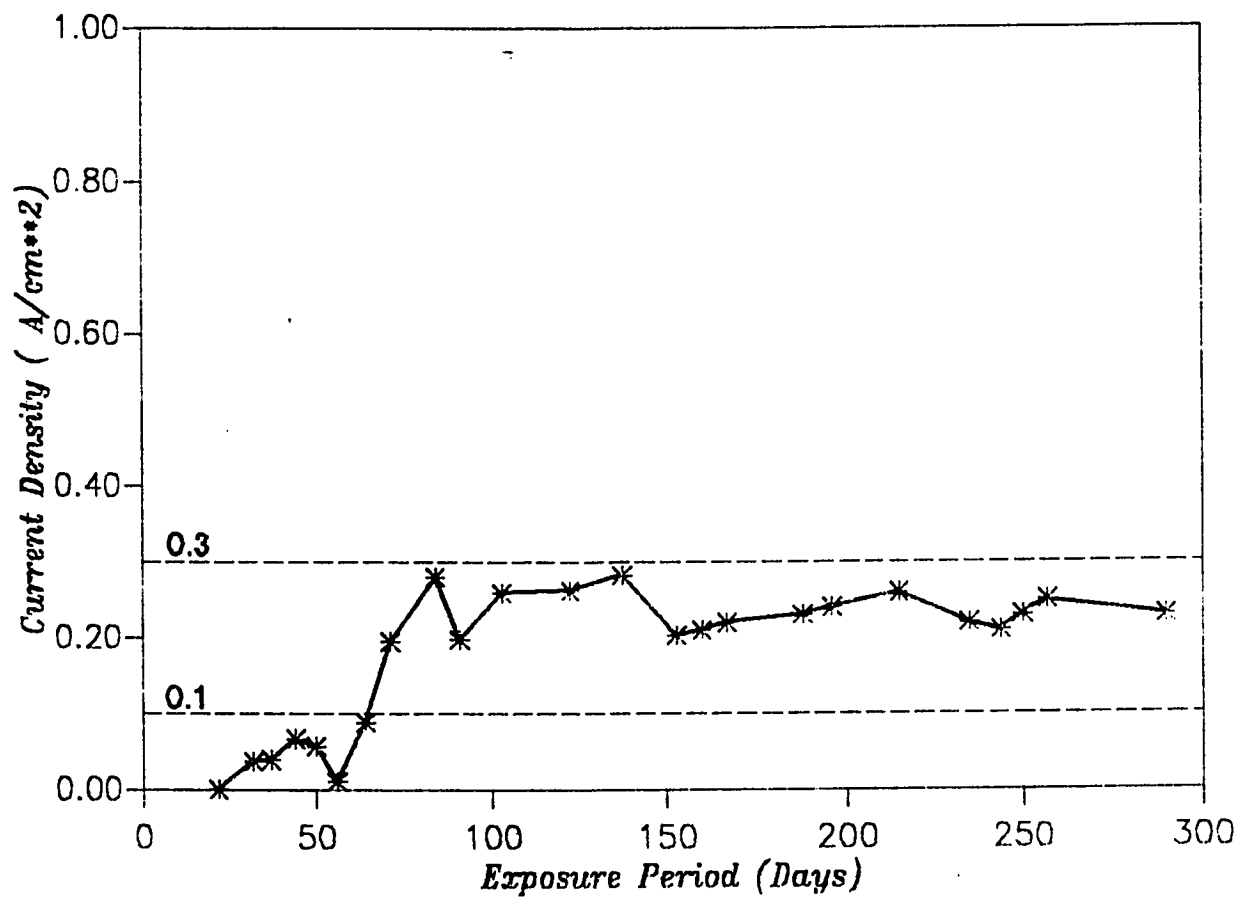


Figure 86: Corrosion Current Densities: (W/C=0.55, 4% Chloride, Cover=4")

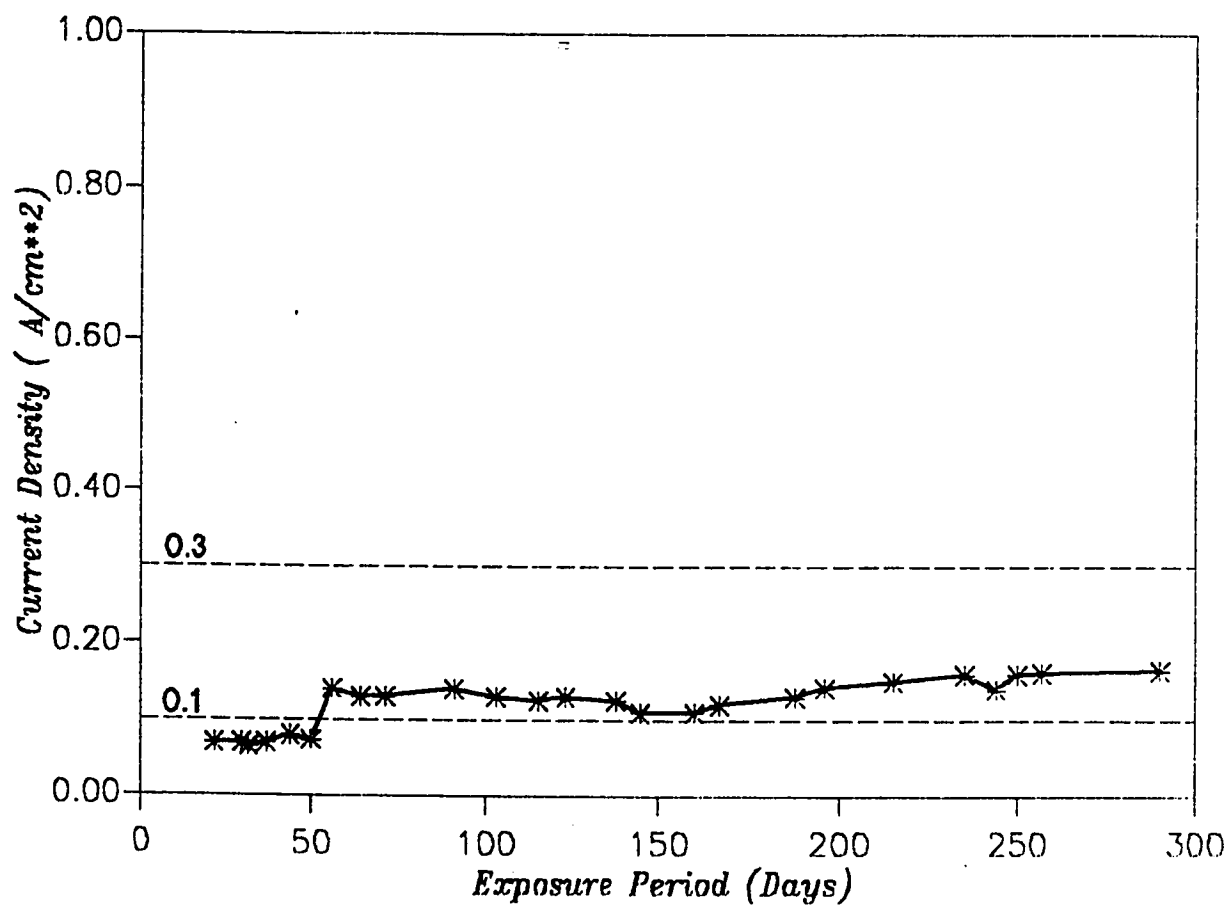


Figure 87: Corrosion Current Densities: (W/C=0.55, 4% Chloride, Cover=3")

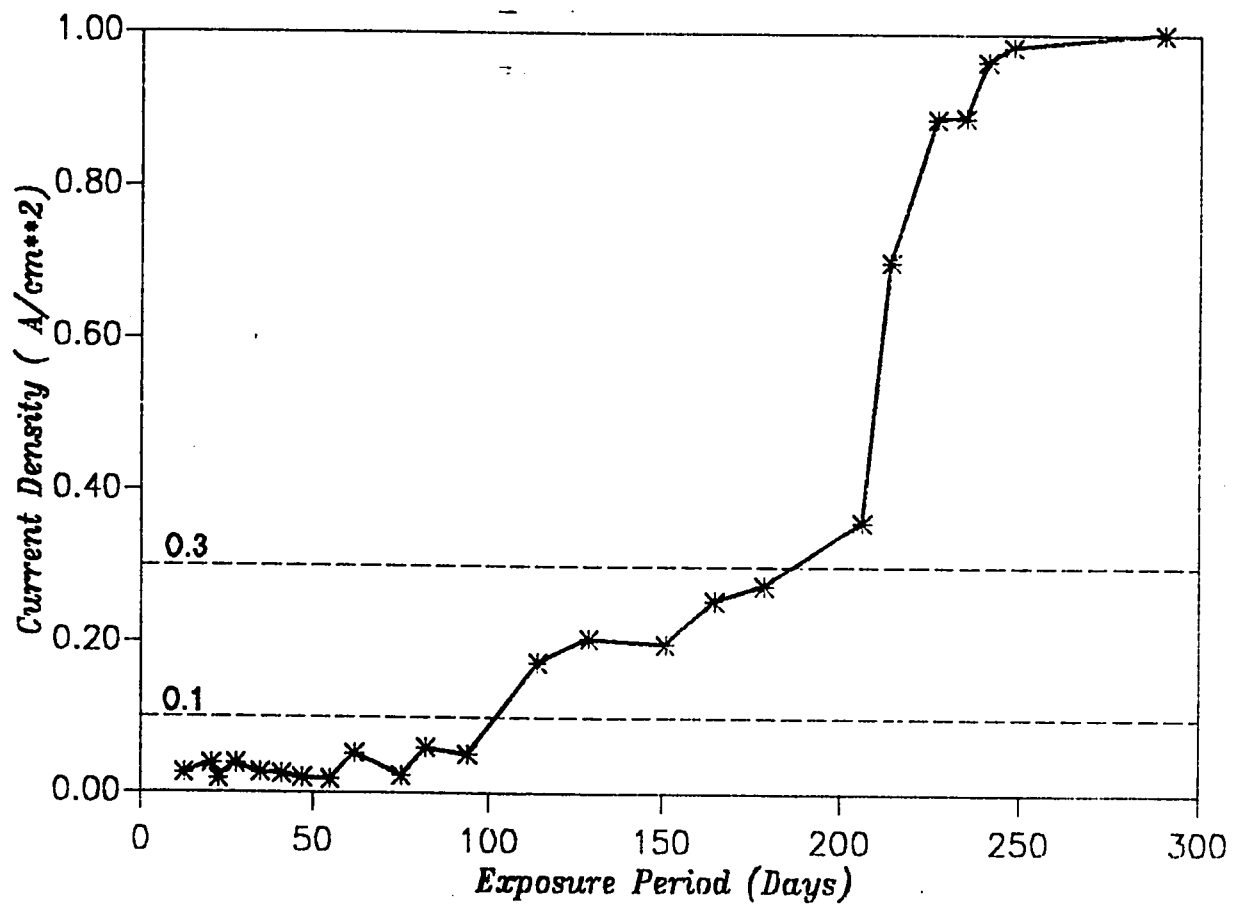


Figure 88: Corrosion Current Densities: (W/C=0.55, 4% Chloride, Cover=1.5")

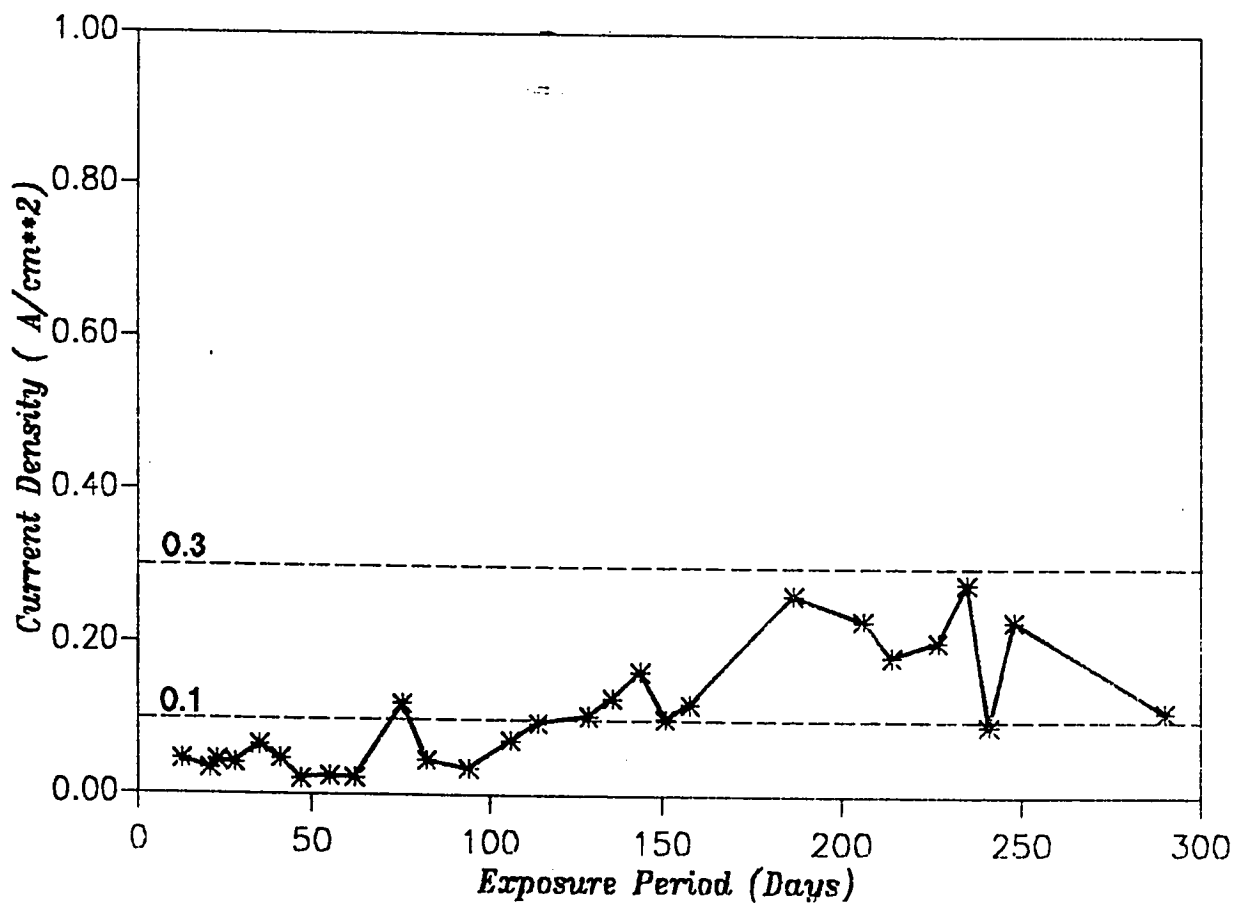


Figure 89: Corrosion Current Densities: (W/C=0.4, 8% Chloride, Cover=4")

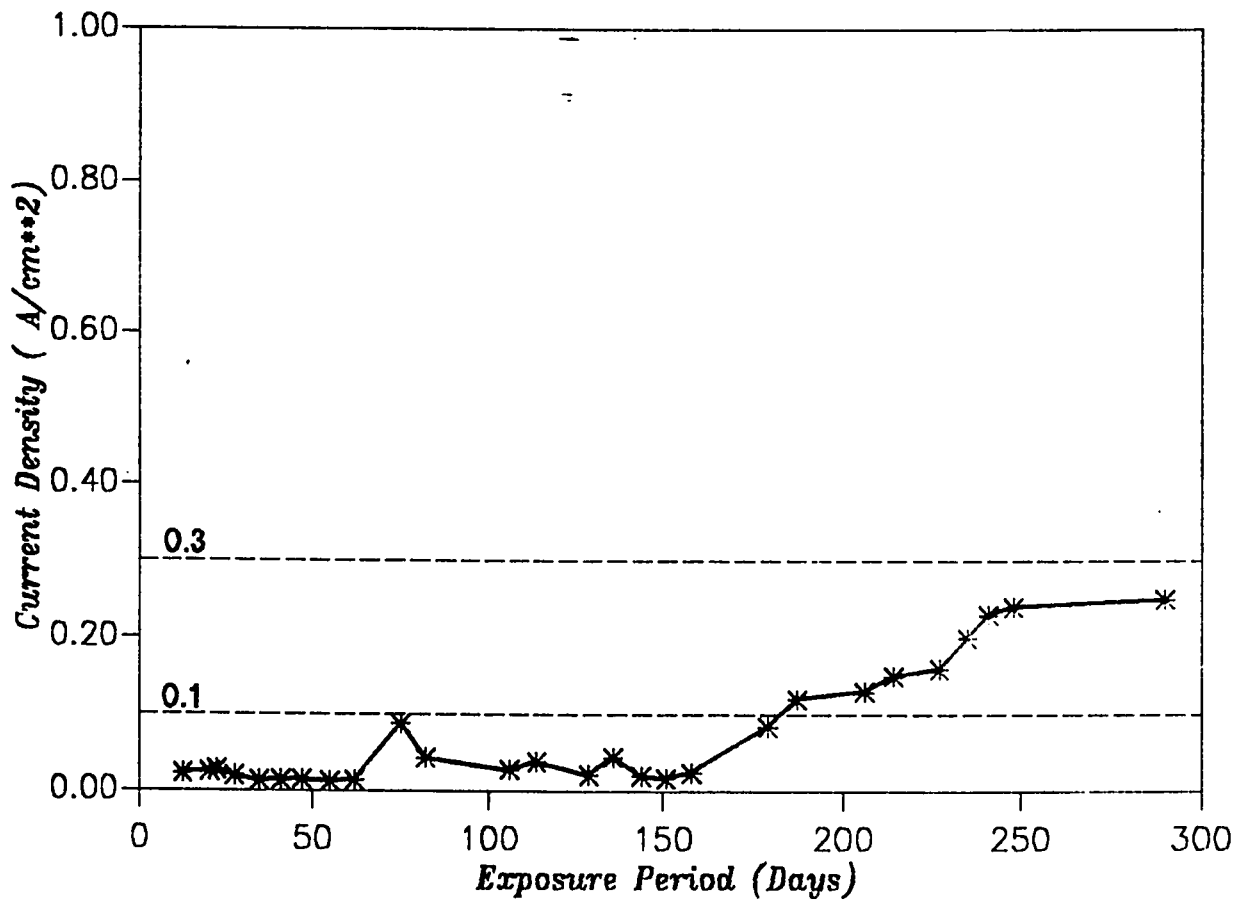


Figure 90: Corrosion Current Densities: (W/C=0.4, 8% Chloride, Cover=3")

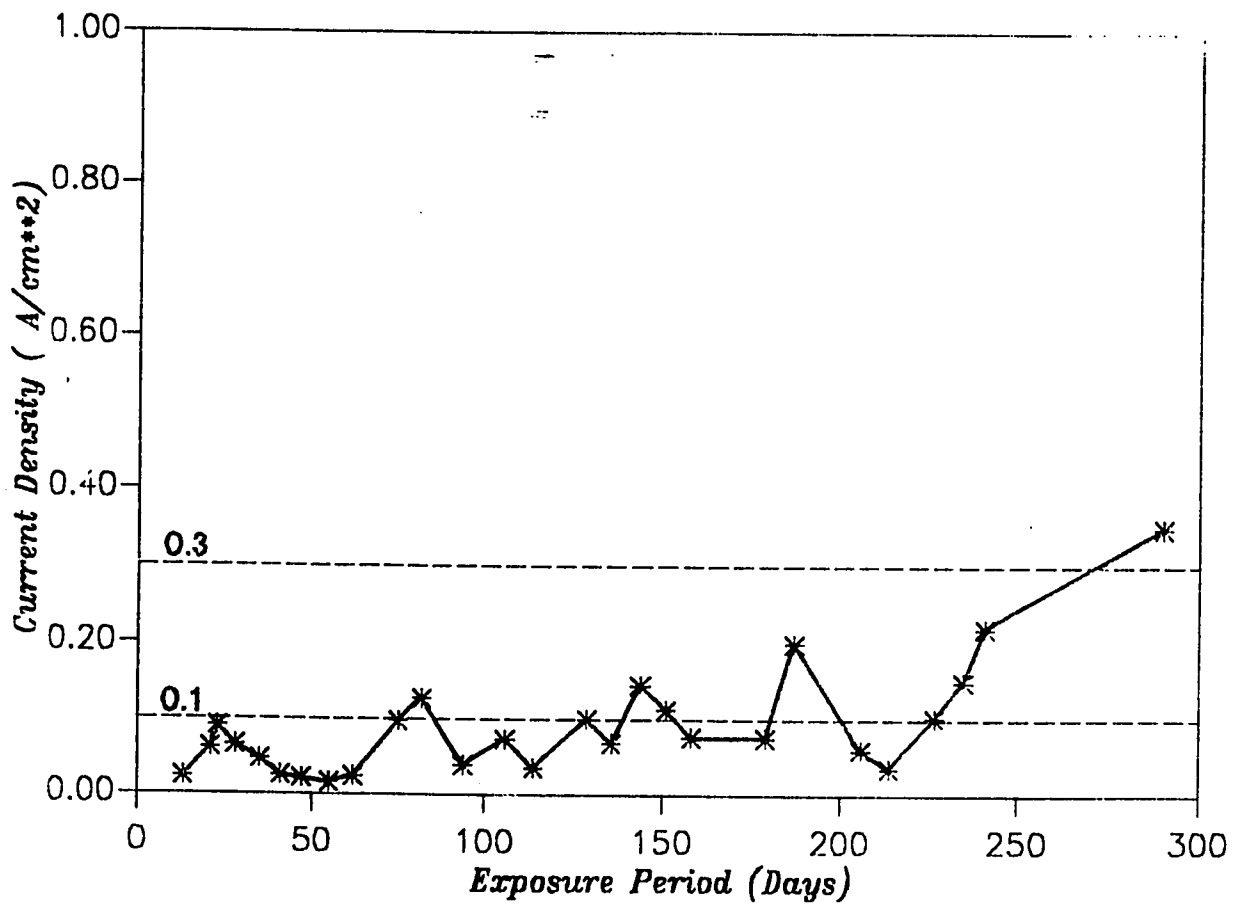


Figure 91: Corrosion Current Densities: (W/C=0.4, 8% Chloride, Cover=1.5")

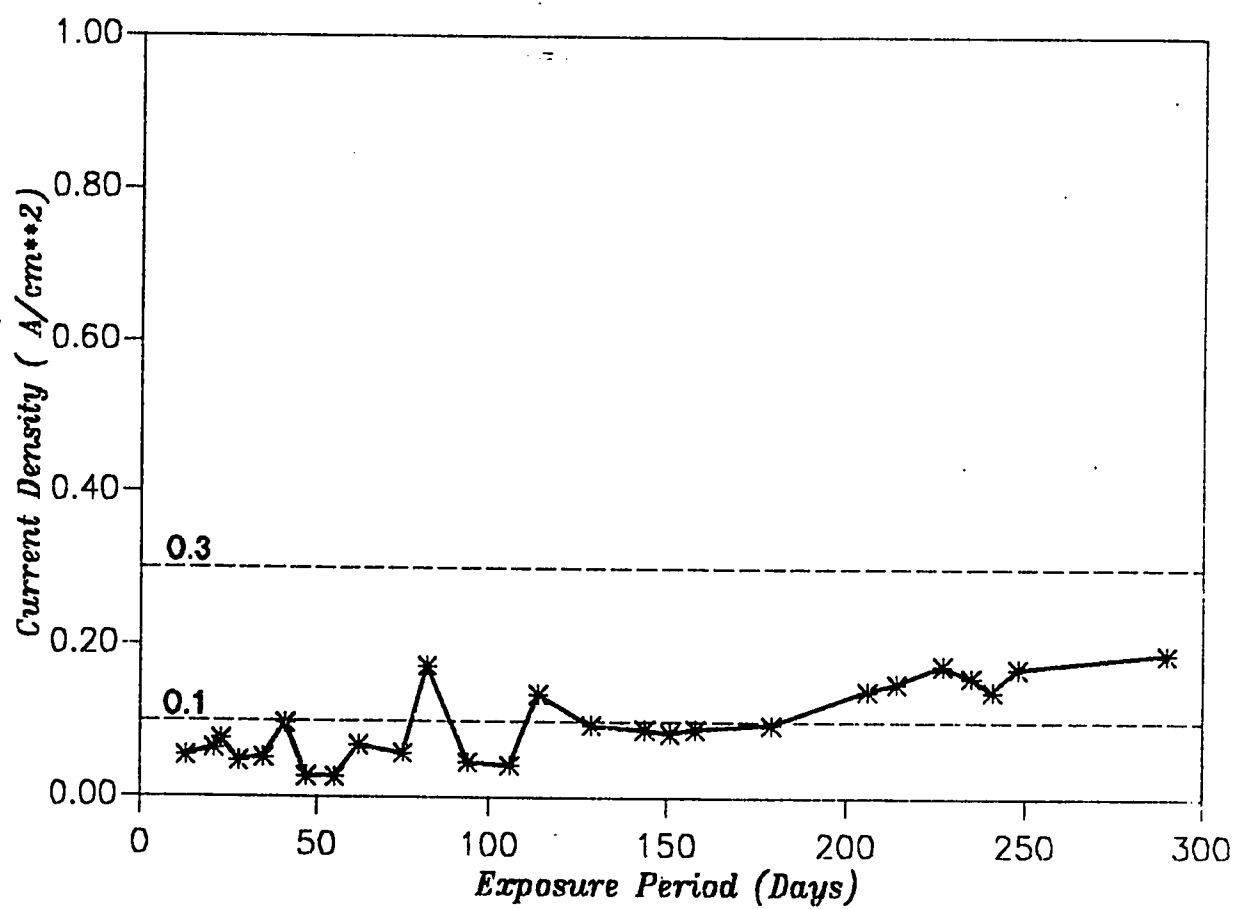


Figure 92: Corrosion Current Densities: (W/C=0.55, 8% Chloride, Cover=4")

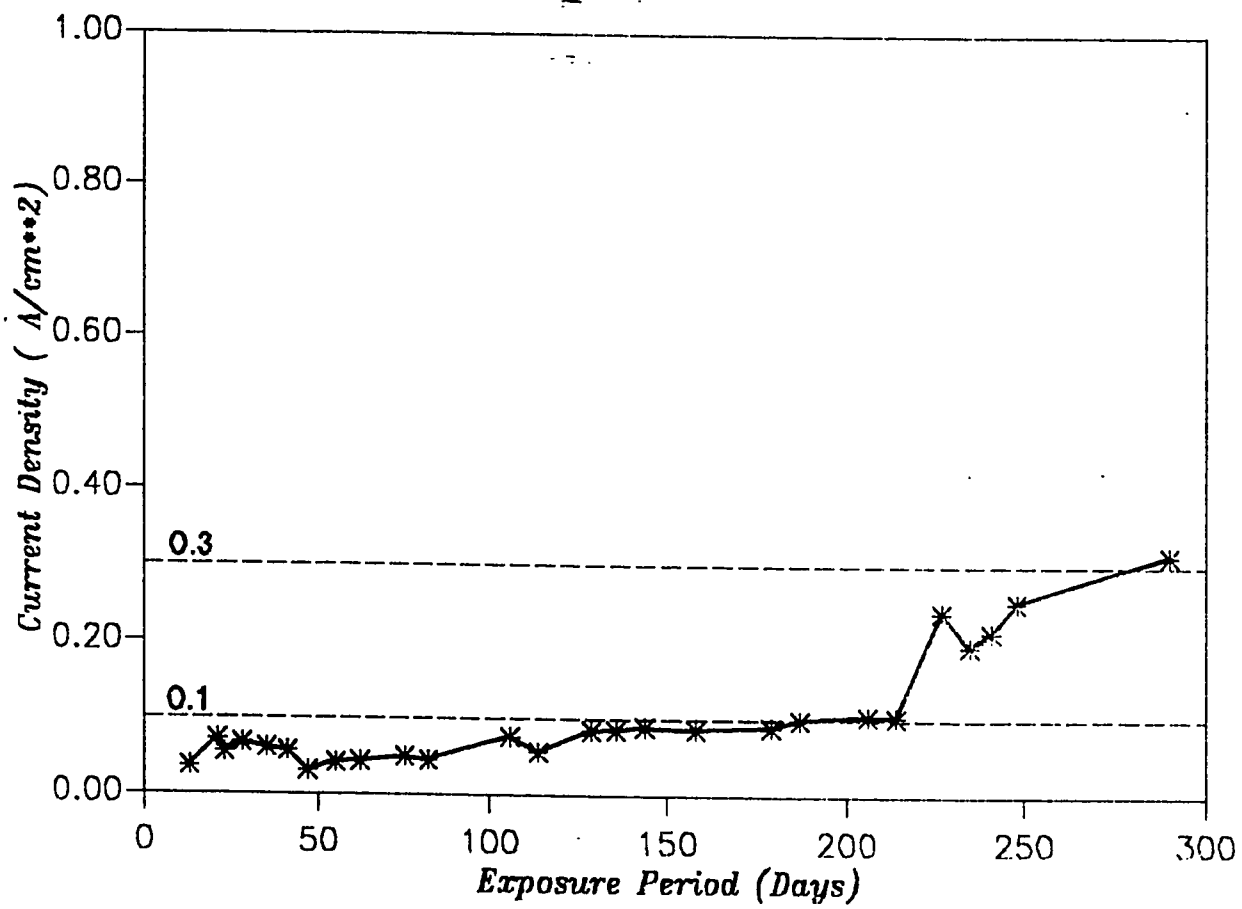


Figure 93: Corrosion Current Densities: (W/C=0.55, 8% Chloride, Cover=3")

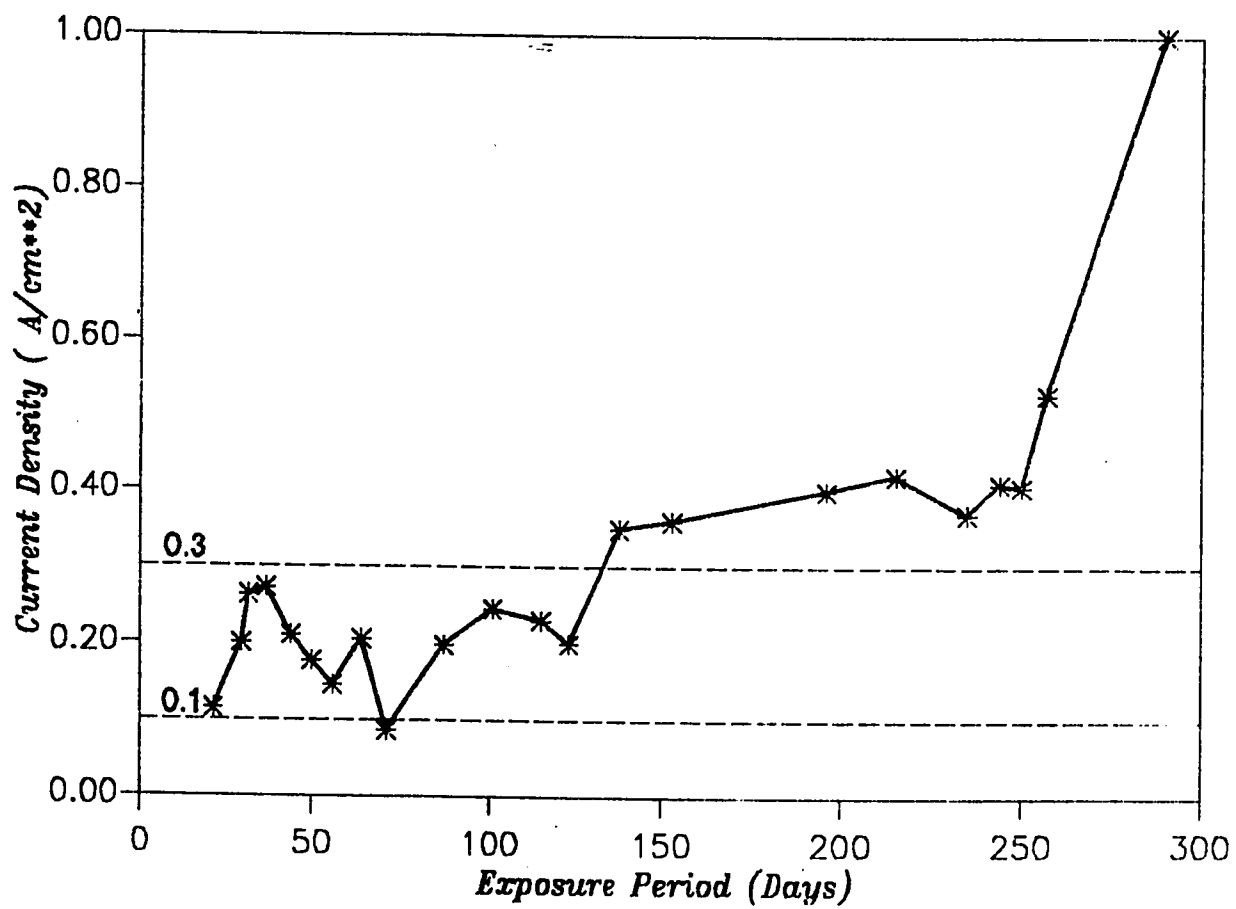


Figure 94: Corrosion Current Densities: (W/C=0.55, 8% Chloride, Cover=1.5")

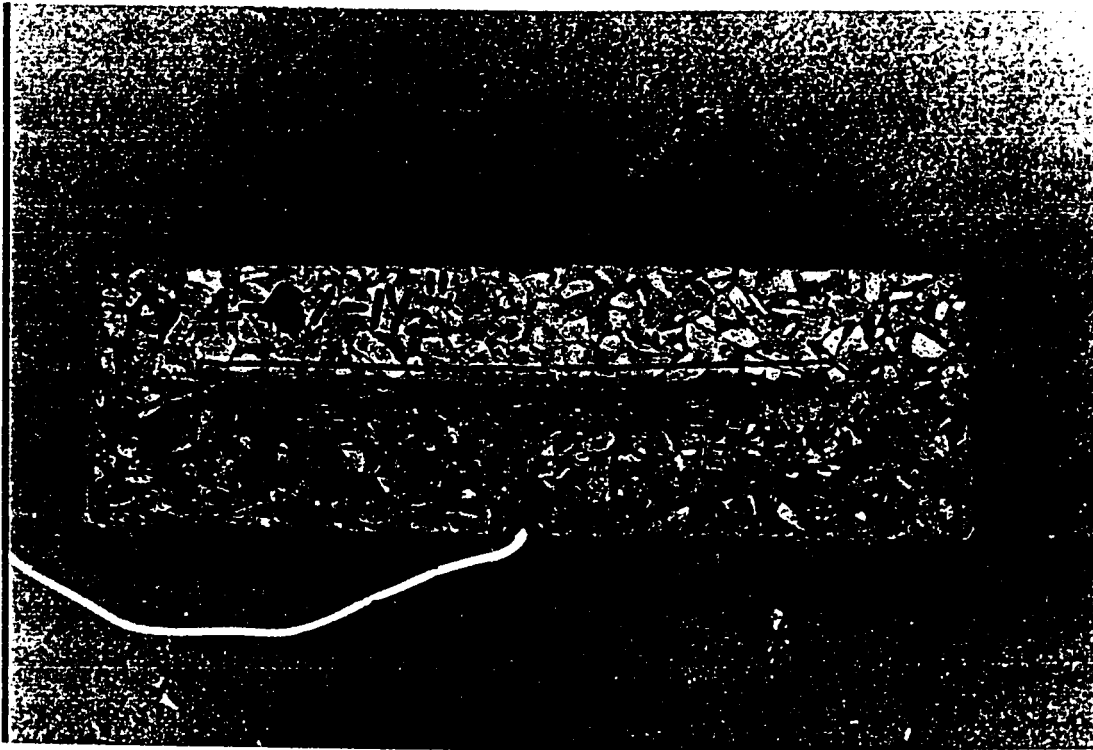


Figure 95: Specimens Showing no Signs of Corrosion: (W/C=0.4, 4% Chloride, Cover=1.5")

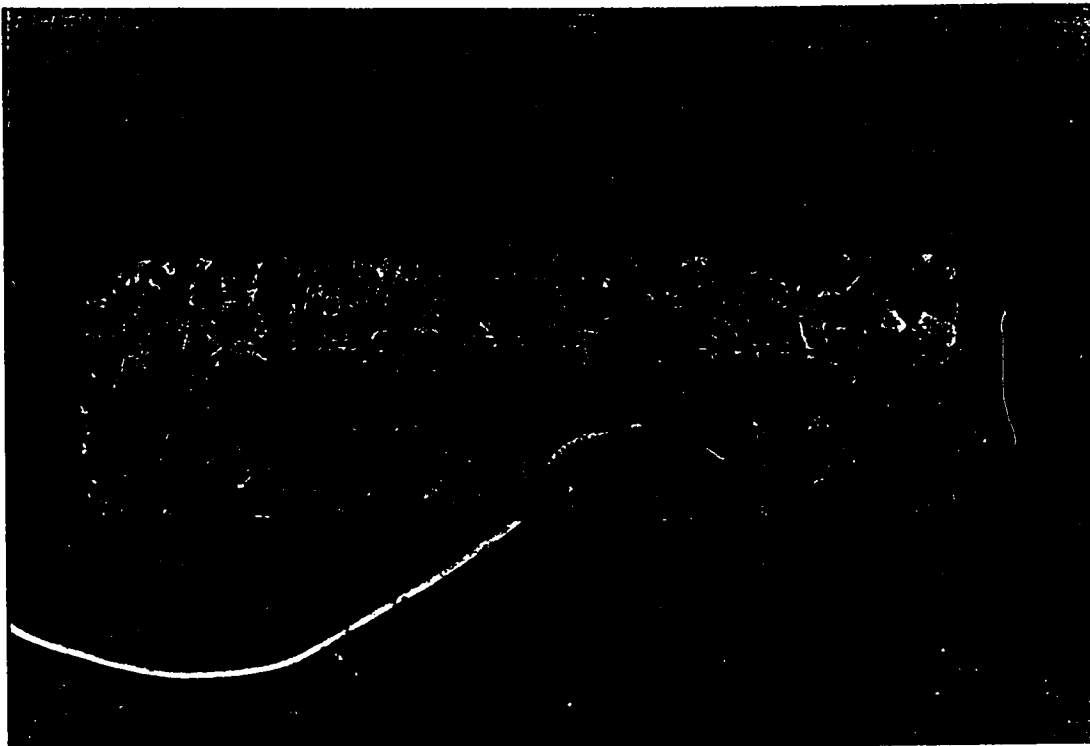


Figure 96: Block Showing Initiation: (W/C=0.4, 8% Chloride, Cover=1.5")

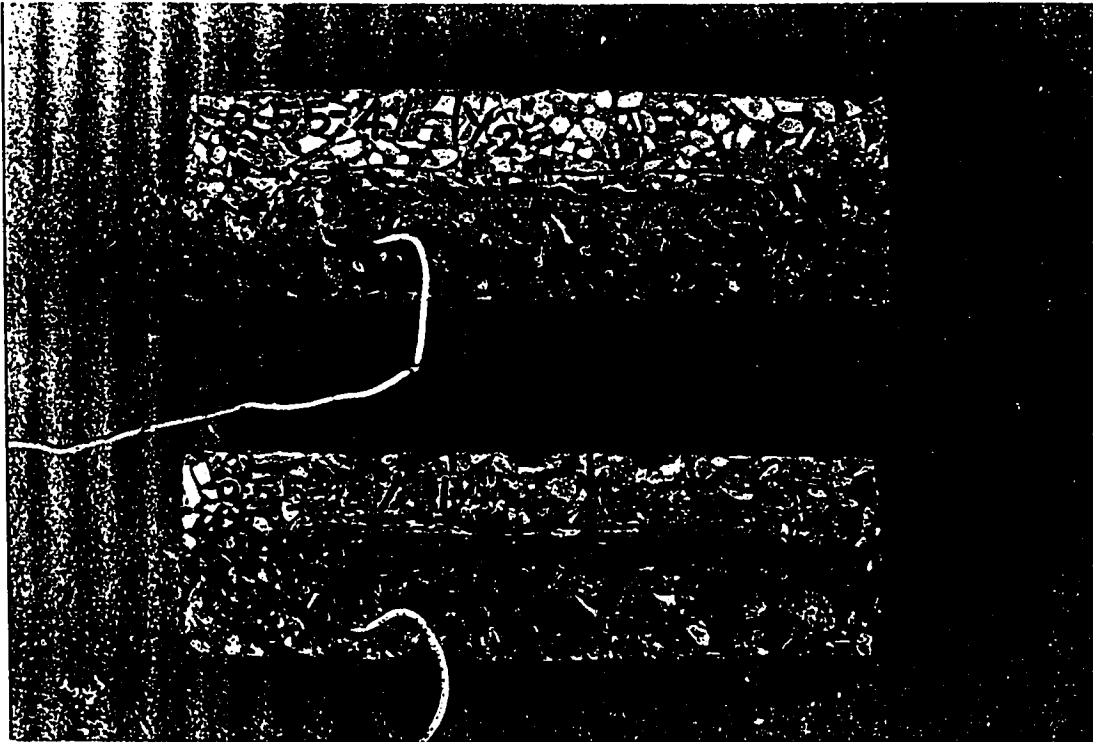


Figure 97: Blocks Showing Active Corrosion: (W/C=0.55, Cover=1.5")

Chapter VI

PREDICTION OF THE TIME TO INITIATION OF CORROSION

6.1 General

In this chapter, an attempt is made to use the experimentally generated test data to arrive at a model for predicting the time to initiation of corrosion in reinforced concrete structures. From statistical analysis of the experimental results, an empirical relationship is developed for diffusion coefficient as a function of w/c ratio and cement content. Then using the solution to Fick's second law (Eqn. 6.1) for the appropriate boundary conditions, the initiation time for corrosion can be predicted assuming a certain threshold value of chloride concentration.

6.2 Basic Prediction Equation

The basic equation used for prediction is

$$\frac{C_{th} - C_i}{C_s - C_i} = 1 - \operatorname{erf} \frac{x}{2\sqrt{D_e t_i}} \quad (6.1)$$

where

C_i is the chloride concentration which was present at the time of

casting, also called the primary chlorides

C_{th} is the threshold chloride concentration needed to initiate corrosion for the given concrete

C_s is the surface chloride concentration

erf is the error function and can be determined from standard tables

D_e is the effective diffusion coefficient

t is the time required to initiate corrosion

6.3 Surface Chloride Concentration

A prior knowledge of surface chloride concentration C_s is needed for prediction purposes. The success of the prediction depends to a great deal on the accuracy of the C_s value assumed. This has to come from engineering judgement and experience. Taking a few samples very close to the surface would also help in making a reasonably good guess. However it should be borne in mind that the seasonal variation of C_s cannot be taken while using the prediction equations. But for all practical purposes, assuming a constant C_s will give reasonably good estimates of the corrosion initiation time. For this prediction the values of C_s obtained from the optimization run are used.

6.4 Threshold Chloride Concentration

Threshold chloride concentration can be defined as the concentration of chlorides at the rebar level, which will lead to the de-passivation and eventually the corrosion of the rebar. From a literature survey (Chap. 2) it was seen that a threshold of 0.35 % of chlorides by weight of cement (app. 0.05% by weight of concrete) can safely be used as the threshold chloride concentration. Moreover, from the chloride analysis of concrete samples taken at the rebar level, it was observed that the chloride concentration was very close to 0.35% by weight of cement for the specimens showing signs of initiation.

6.5 Expression for Effective Diffusion Coefficient

For the various concrete mixes, effective diffusion coefficients obtained from the exposure test was used to develop a regression model for D_e as a function of w/c ratio and cement content. Using a SAS program, non linear regression analysis was performed trying various models for this purpose. The final model which gave a good correlation with the limited data available is

$$D_e * 10^8 = 82.74 - 425.9 (W/C) + 568.42 (W/C)^2 + 4.26 (C)^6 \quad (6.2)$$

where

W/C is the water-cement ratio

C is the normalized cement content obtained by dividing the

cement content in kg/m^3 by 350

D_e is the effective diffusion coefficient in cm^2/sec .

The deviation between the calculated and the experimental value is shown in Fig. 98. Because of time constraints, the effect of cement content was studied only for the indoors exposure. Hence the relationship for D_e shown above is valid only for indoor exposure conditions. However, from experiments like those pursued in this research, similar relationships can also be developed for any type of exposure conditions. Appendix D presents the details of the SAS analysis for the indoor exposure samples. Using the expression of Eqn. 6.2, D_e values are calculated for the different concretes used as listed in Table 14, together with the previously evaluated C_e values.

6.6 Results and Discussion

Based on the diffusivity values calculated from Eqn. (6.2), the C_e values obtained from the optimization run and for an assumed chloride threshold level of 0.35% by weight of cement (app. 0.052% by weight of concrete) the time to initiation of corrosion can be predicted using Eqn. 6.1. The predicted time to corrosion initiation for the different concrete mixes and rebar covers are given in Table 15. A comparison of the predicted and the actual time to corrosion initiation is also shown in

Table 15. The results show quite a reasonable correlation. The variation between the predicted and the actual initiation times does not indicate any definite trend. Depending on whether the predicted D_r was greater than or smaller than the actual value, the time to initiation also varied. However, if experiments are conducted considering a more wider range for the two variables considered, viz. w/c ratio and cement content, a model which would be of more general application could be developed using the same approach.

6.7 MIX DESIGN CONSIDERATIONS

One of the means of transportation of chloride ions in concrete is by diffusion. Therefore, for chloride contaminated environments, concrete mix proportioning has to be based on an acceptable value of D_r . In situations where Fick's laws of diffusion will be applicable with sufficient accuracy, one can predict the time to initiation of corrosion based on an idealized condition and assumed parameters. For a desired time of corrosion free life of a structure, once the cover to rebar is decided, the required value of D_r can be determined from Eqn. 6.1. Once this value of D_r is obtained, the concrete mix can be proportioned to yield the desired value of D_r . From a broad based study, it would be possible to establish a function of D_r in terms of important parameters as indicated in Eqn. 6.2. If such an equation is obtained, the mix design parameters can easily be determined for a target value of D_r .

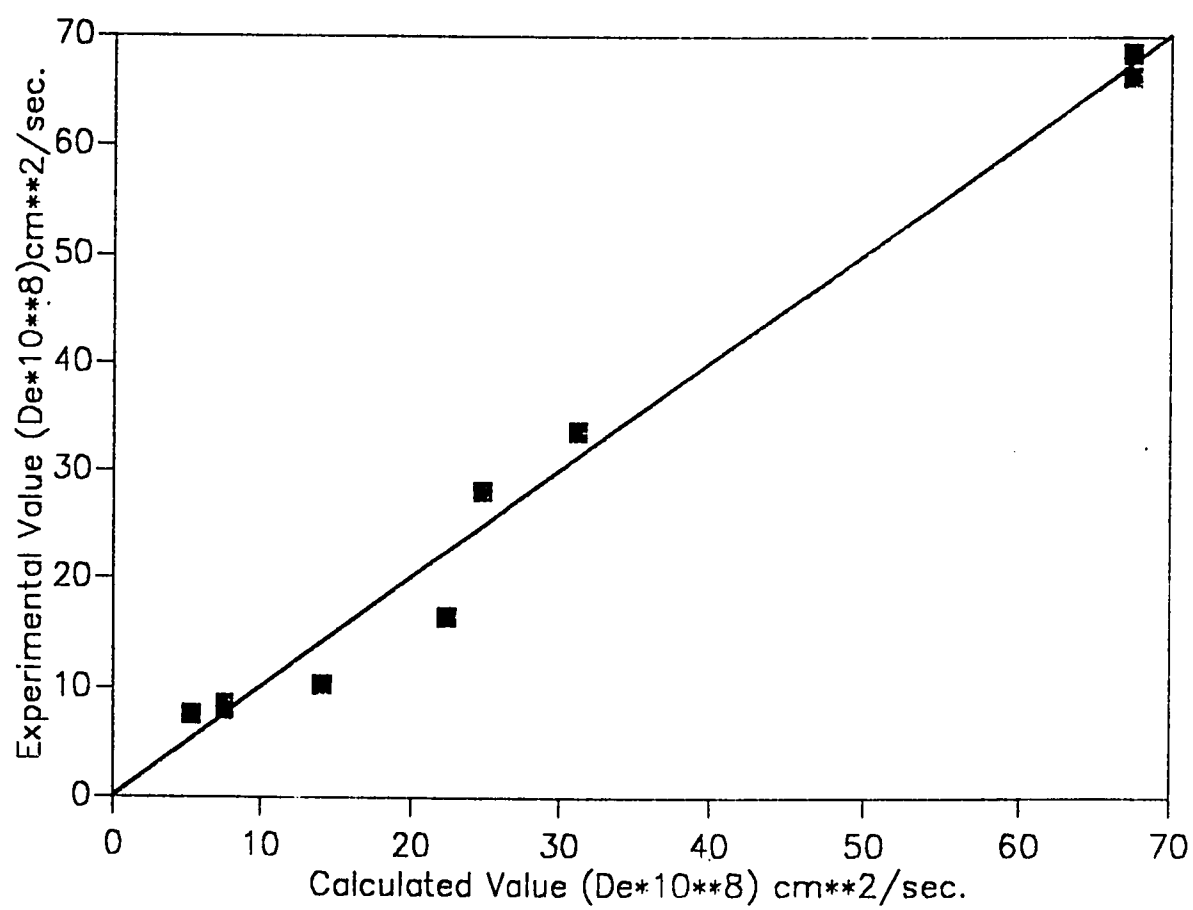


Figure 98: Experimental and Calculated Values of D_e

Table 14: C_s and D_e Values Used for Predicting the Initiation of Corrosion

CC	W / C	Chloride	D_e *	C_s #
300	0.40	4 %	14.09	0.49
	0.55	4 %	31.20	0.54
350	0.40	4 %	7.59	0.32
		8 %	7.59	0.56
	0.55	8 %	24.70	0.76
	0.70	4 %	67.40	0.58
		8 %	67.40	0.815
400	0.40	4 %	5.24	0.38
	0.55	4 %	22.35	0.49

* $10^8 \text{ cm}^2 / \text{sec.}$

% by weight of concrete

Table 15: Predicted Time to Initiation of Corrosion

		Cover to Reinforcement		
		4 "	3 "	1.5 "
W / C	Chloride	Time to Initiation in Days (Years)		
0.4	4 %	3887 (10.6)	2186 (6.0)	547 (1.50)
	8 %	2700 (7.3)	1519 (4.20)	380 (1.04) 280 (0.787)*
0.55	4 %	1015 (2.8)	571 (1.6)	143 (0.39) 200 (0.548)*
	8 %	709 (1.9)	399 (1.10) 285 (0.781)*	100 (0.27) 120 (0.329)*

* experimental time to initiation of corrosion

Chapter VII

CONCLUSIONS AND RECOMMENDATIONS

7.1 Conclusions

Chloride ion diffusion coefficients are determined for concrete made from the local materials using the conventional ponding technique and a gas diffusion technique, which for the first time tried on concrete. The gas diffusion technique appears to be quite a rapid and promising method for evaluating the diffusion coefficients for any ion in concrete. Based on the test results generated, an attempt was also made to predict the time to corrosion initiation of the steel reinforcement in concrete. The following conclusions are drawn from this study:

1. The chloride diffusion coefficients for Sulphate Resisting Portland Cement concrete made with local materials appears to be greater than values reported so far in literature.
2. Diffusion coefficient D_c is found to be strongly influenced by the water-cement ratio. The value of D_c increases with increasing w/c ratio.
3. The values of D_c for concretes exposed to outdoor environment are expected to be much higher than the values for identical

concretes in indoors.

4. The chloride diffusion coefficient decreases with an increase in the cement content. This effect is more pronounced for higher w/c ratios.
5. The chloride diffusion coefficient is independent of the exposure chloride concentration. However, as the amount of chlorides within the concrete is directly proportional to the surface concentration, higher surface concentration is detrimental from the view point of durability as it will lead to an earlier initiation of corrosion.
6. Threshold chloride level of 0.35% by weight of cement (0.05% by weight of concrete) for the initiation of chloride induced corrosion appears to hold good for the local concrete.
7. It appears that in an idealized condition, Fick's second law of diffusion can be used to predict the corrosion initiation time, if the chloride exposure condition can be modelled with sufficient accuracy.
8. This study has shown that for the first time that the chloride diffusion coefficient in concrete can be determined from the measurement of the ratio of porosity to tortuosity $\frac{\varepsilon}{\tau}$ which is a characteristic material property of a porous media. The gas diffusion test therefore appears to be a rapid and reliable method for evaluating D_c .

7.2 Recommendations

The following recommendations are made as a continuing and complementary study of this problem.

1. In this study, the surface chloride concentration C_s was maintained constant throughout the period of exposure. In actual exposure conditions, this is not the case. Therefore an effort has to be made to idealize the C_s value for the various exposure conditions relevant to the area, so that the prediction model would be reasonably valid.
2. The expression obtained for D_c of chloride ion in concrete was based on the limited variables considered in this study. Tests have to be conducted considering a much wider range of the different parameters, which would help in arriving at a more general expression which could be of great practical use.
3. The gas diffusion test, which for the first time was conducted on concrete, appears to be quite a promising rapid technique for evaluating the D_c of any ion in concrete. Attempts should therefore be made to standardize this test.

REFERENCES

1. Report- ACI Committee 222, "Corrosion of Metals In Concrete", *ACI Materials Journal* , Jan/Feb 1985, pp. 3-32.
2. Figg, J.W., "Rusting Reinforcement, No. 1 Problem of Concrete Durability", *Concrete* , May 1980, pp. 34-36.
3. Al-Tayyib, A.J., Baluch, M.H., Alfarabi Sharif and Mahamud, M.M., "The Effect of Thermal Cycling on the Durability of Concrete Made From Local Materials in the Arabian Gulf Countries", *Journal of Material in Civil Engineering* , ASCE, Vol. 1, No. 3, Aug. 1989, pp. 35-45.
4. Alfarabi Sharif, "Confirmation of TICC Damage Hypothesis- A Petrographic Study", *Journal of Material in Civil Engineering* , ASCE, Vol. 3, No. 3, Aug. 1991, pp. 179-188.
5. Garrels, R.M., Dreyer, R.M., and Howard, A.L., "Diffusion of Ions through Intergranular Spaces in Water Saturated Rocks", *Bulletin, Geological Society of America* , Vol. 60, 1949, pp. 1809-1828.
6. Colleparidi, M., Marcialis, A., and Turriaziani, R., "Kinetics of Penetration Chloride Ions in Concrete", *IL Cemento* , Vol. 4, 1967, pp. 157-163.

7. Gjorv, O.E. and Vennesland, O., "Diffusion of Chloride Ions From Sea Water into Concrete", *Cement and Concrete Research* , Vol. 9, No. 2, 1979, pp. 229-238.
8. Page, C.L., Short, N.R. and Tarras, A., "Diffusion of Chloride Ions in Hardened Cement Pastes", *Cement and Concrete Research* , Vol. 11 , No. 3 , May 1981, pp. 395-406.
9. Goto, S. and Roy, D.M., "Diffusion of Ions through Hardened Cement Pastes", *Cement and Concrete Research*, Vol. 11, No: 51, 1981, pp. 751-759.
10. Page, C.L. , Short, N.R. and Holden, W.R. , "The Influence of Different Cements on Chloride-Induced Corrosion of Reinforcing Steel" , *Cement and Concrete Research*, Vol. 16, No. 1, 1986, pp. 79-86.
11. Diab, H, , Bentur, A. , Wirguin, C.H. and Ben-Dor, L. , "Diffusion of Cl Ions Through Portland Cement and Portland Cement Polymer Pastes", *Cement and Concrete Research*. Vol. 18, No. 5, 1988, pp. 715-722.
12. Dhir, R.K., Jones, M.R. and Elghaly, A.E., "PFA Concrete: Exposure Temperature Effects on Chloride Diffusion", *Cement and Concrete Research*, Vol. 23, No. 5, 1993, pp. 1105-1114.
13. Byfors, K, , "Influence of Silica Fume and Pulverized Fly Ash on Chloride Diffusion and pH Levels in Cement Paste", *Cement Construction Research*, Vol. 17, No. 1, 1987, pp. 115-130.

14. Midgley, H.G. and Illston, J.M., "The Penetration of Chlorides into Hardened Cement Pastes", *Cement and Concrete Research*, Vol. 14, 1984, pp. 546-558.
15. Ost, B. and Monfore, G.E., "Penetration of Chlorides into Concrete", *Journal of PCA Research and Development Laboratories*, No. 1, 1986, pp. 46-52.
16. Hansson, C.M., Frolund, T.H. and Markussen, J.B. , "Effect of Chloride Cation Type on the Corrosion of Steel in Concrete by Chloride Salts", *Cement and Concrete Research*, Vol. 15, No. 1, 1985, pp. 65-72.
17. Arup, H., "The Mechanisms of Protection of Steel by Concrete", *Corrosion of Reinforcement in Concrete*, Ellis Horwood Ltd., 1983, pp. 151-157.
18. Volkwein, A. and Springenschlund, R., "Proc. 2nd International Conf. on Durability of Building Materials and Components", *National Bureau of Standards 1981*, pp.199-209.
19. West, R. E. and Hime , W. G. , "Chloride Profiles in Salty Concrete", *National Association of Corrosion Engineers*, July 1985 , pp. 29-35.
20. Browne, R.D. and Geoghegan, M.P., "Mechanism of Corrosion of Steel in Concrete in Relation to Design, Inspection and Repair of Offshore and Coastal Structures", *Performance of Concrete in Marine Environment*, ACI SP-65, American Concrete Institute, 1985, pp. 169-204.

21. Tutti, K. , "Service Life of Structures with regard to Corrosion of Embedded Steel", *Performance of Concrete in Marine Environment*, ACI SP-65, American Concrete Institute, Detroit, 1985, pp. 223-236.
22. Bruenfield, N., "Chlorides in Concrete", *Concrete Repairs*, Palladian, Vol. 2, 1986, pp. 24-27.
23. Verbeck, G.J, "Mechanism of Corrosion of Steel in Concrete", *Corrosion of Metals in Concrete*, ACI SP-49, American Concrete Institute , 1975, pp. 24-38.
24. Raharinaivo, A. and Jean-Marie, G. , "On the Corrosion of Reinforcing Steel in Concrete in the Presence of Chlorides", *Materiales de Construcción*, Vol. 36, No. 294, Oct./Nov./Dec. 1986, pp. 5-16.
25. Gau, Y. and Cornet, I. , "Penetration of Hardened Concrete by Sea Water Chlorides with and without Impressed Current", *Corrosion*, Vol. 41, No. 2, Feb. 1985, pp. 93-100.
26. Kayyali, O.A. and Haque, M.N. , "Chloride Penetration and the Ratio of Cl/OH^- in the Pores of Cement Paste", *Cement and Concrete Research*, Vol. 18 , No. 6, 1988, pp. 895-900.
27. Weyers, R.E. and Smith, D.G., "Chloride Diffusion Constant for Concrete", *Structural Materials*, The Society, New York, 1989, pp. 106-115.
28. Jaegerman, C. , "Effect of W/C Ratio and Curing on Chloride Penetration into Concrete Exposed to the Mediterranean Sea",

- ACI Materials Journal*, Vol.87, No.4, July/Aug. 1990, pp. 333-339.
29. Dhir, R.K., Jones, M.R. and Ahmed, H.E.H., "Concrete Durability: Estimation of Chloride Concentration During Design Life", *Magazine of Concrete Research*, No. 54, March 1991, pp. 37-44.
 30. Crank, J., *"The Mathematics of Diffusion"*, 2nd ed., Clarendon Press, Oxford, 1975
 31. Mustafa, M.A. and Yusof, K.M., "Atmospheric Chloride Penetration into Concrete in Semi-Tropical Marine Environment", *Cement and Concrete Research*, Vol. 24, No. 4, 1994, pp. 661-670.
 32. Sergi, G., Yu, S.W. and Page, C.L., "Diffusion of Chloride and Hydroxyl Ions in Cementitious Materials Exposed to a Saline Environment", *Magazine of Concrete Research*, No. 158, March 1992, pp. 63-69.
 33. Teng, S.P. and Lee, C.H., "Numerical Analysis through Diffusion Experimental Results", *Cement and Concrete Research*, Vol. 22, No. 2/3, 1992, pp. 445-450.
 34. Funahasi, M., "Predicting Corrosion Free Service Life of a Concrete Structure in a Chloride Environment", *ACI Materials Journal*, Nov./Dec. 1990, pp. 581-587.
 35. Liam, K.C., Roy, S.K. and Northwood, D.C., "Chloride Ingress Measurements and Corrosion Potential Mapping Study of a 24-year old Reinforced Concrete Jetty Structure in a Tropical

- Marine Environment", *Magazine of Concrete Research*. Vol. 44, No. 160, Sept. 1992, pp. 205-215.
36. Nagano, H. and Naito, T., "Application of Diffusion Theory to Chloride Penetration into Concrete Located in Splashing Zone", *Transactions of the Japan Concrete Institute*. Vol. 7, 1985, pp. 157-164
37. Whiting, D., "Rapid Measurements of Chloride Permeability of Concrete", *Public Roads*, Vol. 45, No. 3, Dec. 1981, pp. 101-112.
38. "Standard Method of Test for Rapid Determination of the Chloride Permeability of Concrete", *AASHTO T 277-83*, American Association of Highway and Transport Officials, Washington, D.C., 1983.
39. Andrade, C. and Sanjuan, M.A., "Experimental Procedure for the Calculation of Diffusion Coefficients in Concrete from Migration Tests", *Advances in Cement Research*. Vol. 6, No. 23, 1994, pp. 127-134.
40. Dhir, R.K., Jones, M.R., Ahmed, H.E.H. and Seneviratne, A.M.G., "Rapid Estimation of Chloride Diffusion in Concrete", *Magazine of Concrete Research*, Vol. 42, No. 152, Sept. 1990, pp. 177-185.
41. Tang, L. and Nilsson, L., "Rapid Determination of Chloride Diffusivity in Concrete by Applying an Electrical Field", *ACI Materials Journal*, Jan/Feb 1992, pp. 49-53.

42. Masuda, Y., "Penetration Mechanism of Chloride Ion into Concrete", *Proc.-RILEM 1st International Congress- Materials Science to Materials Engg.*, Versailles, 1987, pp. 935-942.
43. Cavalier, P.G. and Vassie, P.R., "Investigation and Repair of Reinforcement Corrosion in a Bridge Deck", *Proceedings-Institution of Civil Engineers*, London Vol. 70, Aug. 1981, pp. 461-480.
44. Arup, H., "The Mechanisms of Protection of Steel by Concrete", *Corrosion of Reinforcement in Concrete*, Ellis Horwood Ltd., 1983, pp. 151-157.
45. Comite Euro-International Du Beton, "Durability of Concrete Structures- State of the Art Report", *Bulletin D'Information No.148*, Paris, 1982.
46. Rasheeduzzafar, Dakhil, F.H. and Al-Gahtani, A.S., "Deterioration of Concrete Structures in the Environment of the Middle East", *ACI Materials Journal*, Jan/Feb 1984, pp. 13-20.
47. ACI Committee 210, "Guide to Durable Concrete", (ACI 201.2R-77) (Reaffirmed 1982), American Concrete Institute, Detroit, 1977, pp.37.
48. Weigler, H. and Segmuller, E., "Action of Chlorides on Concrete", *Betonwerk and Fertigeteil-Technik (Weishaden)*. No. 8, 1973, pp. 577-584.
49. Stratful, R.F., Jurkovich, W.J. and Spellman, D.L., "Corrosion Testing of Bridge Decks", *Transportation Research Record*, No. 539, 1975, pp. 50-59.

50. Clear, K.C., "Time to Corrosion of Reinforcing Steel in Concrete, Performance after 830 days of Daily Salt Applications", *Report No. FHWA-RD-76-70*. Federal Highway Administration, Washington.D.C., April 1976, p. 64.
51. Knofel, D., "*Corrosion of Building Materials*", Van Nostrand Reinhold Company, New York, 1975, p. 39.
52. Hausmann, D.A., "Steel Corrosion in Concrete", *Materials Protection*, Vol. 6, No. 11, 1967, pp. 19-23.
53. Lewis, D.A., "Some Aspects of the Corrosion of Steel in Concrete", *Proc- 1st International Congress on Metallic Corrosion (London 1962)*. Butterworths, Washington.D.C., 1962, pp. 547-555.
54. Everett, L.M. and Treadway, K.W.J., "Deterioration Due to Corrosion in Reinforced Concrete", *Building Research Establishment Information Paper*, IP 12/18, 1980.
55. Hansson, C.M. and Sorensen, B. , "The Threshold Concentration of Chloride in Concrete for the Initiation of Reinforcement Corrosion", *ASTM Special Technical Publication 1065*, Aug. 1990, pp. 3-16.
56. Browne, R.D. , "Design Prediction of the Life for Reinforced Concrete in Marine and Other Chloride Environment", *Durability of Building Materials (Amsterdam)*, No. 1, 1982, pp. 113-125.
57. Geankoplis, C.J., "*Mass Transport Phenomena*". Holt, Rinehart & Winston, Inc., U.S.A., 1972.
58. Satterfield, C.N., "*Mass Transfer in Hetrogeneous Catalysis*", 1971.

59. Hirschfelder, J.O., Curtiss, C.F. and Bird, R.B., *"Molecular Theory of Gases and Liquids"*, John Wiley and Sons, New York, 1954.
60. Krishna, R., "A Unified Approach to the Modelling of Intraparticle Diffusion in Adsorption Processes" *Gas Separation and Purification*, Vol. 7, No. 2, 1993, pp. 91-104.
61. Satterfield, C.N. and Sherwood, T.K., *"The Role of Diffusion in Catalysis"*, Addison-Wesley Publishing Company, Inc., London, 1963.
62. Basset, J., Denney, R.C., Jeffery, G.H. and Mendham, J., *"Vogel's Text Book of Quantitative Inorganic Analysis"*, Longman, London, 1985, p. 754.
63. Dogu, G. and Smith, J.M., "Rate Parameters from Dynamic Experiments with Single Catalyst Pellet", *Chemical Engineering Science*, Vol. 31, 1976, pp. 123-135.
64. Marrero, T.R. and Mason, E.A., "Gaseous Diffusion Coefficients" *Journal of Physical and Chemical Reference Data*, Vol. 1, No. 1, 1972, pp. 3-118.
65. Escalante, E., Ito, S. and Cohen, M., "Measuring the Rate of Corrosion of Steel in Concrete", *Annual Report NBSIR 80-2012*, National Bureau of Standards, Gaithersburg, Md., March 1980, pp. 1-26.
66. Escalante, E., Whitenton, E. and Qui, F., "Measuring the Rate of Corrosion of Reinforcing Steel in Concrete", *Final Report NBSIR*

- 86-3456, National Bureau of Standards, Gaithersburg, Md., Oct. 1986, pp. 1-27.
67. Clear, K.C., "Measuring Rate of Corrosion of Steel in Field Concrete Structures", *Transportation Research Record*, 1211, pp. 28-36.
68. Maslehuddin, M. and Omar, S.B.A., "Corrosion of Reinforcement in Concrete- Its Monitoring and Prevention". :ecit, Personal communication, 1992.
69. Stern, M. and Geary, A.L., "A Theoretical Analysis of the Shape of the Polarizing Curves", *Journal of Electrochemical Society*, Vol. 104, 1957, pp. 56-63.
70. Mansfield, F., "Polarization Resistance Measurements: Experimental Procedure and Evaluation of the Data", *Electrochemical Techniques for Corrosion*, NACE, Houston, 1977, pp. 18-26.
71. Gonzalez, A.J., Feliu, S., Andrade, C. and Rodriguez, I., "On-site Detection of Corrosion of Reinforced Concrete Structures", *Materials and Structures*, Vol.24, 1991, pp. 346-350.
72. Smith, J.M., "Chemical Engineering Kinetics", Mc Graw Hill Inc., N.Y., 1981, p. 347.
73. DIN 1048 Part 1, *Test Mehtods For Concrete*, pp.9-10.
74. Colleparidi, M., Marcialis, A., and Turriaziani, R., "Penetration of Chloride ions into Cement Pastes and Concrete", *Journal of the American Ceramic Society*, Vo., 55, No. 10, 1972, pp.534-536.

75. Maslehuddin, M., Rasheeduzzafar, Page, C.L., Al-Mana, A.I. and Al-Tayyib, A.J., "Effect of Temperature and Sulphate Contamination on the Chloride Binding Capacity on Cements", *Proc. 4th. International Conference on Deterioration and Repair of Reinforced Concrete in the Arabian Gulf, Bahrain, 10-13 October, 1993.*
76. Welty, J.R., Wilson, R.E., and Wicks, C.E., *Fundamentals of Momentum, Heat and Mass Transfer*, John Wiley & Sons, Inc., USA, 1976.

Appendix A

VOLUMETRIC CALIBRATION OF THE DIFFUSION CELL

A gas expansion test was conducted on the diffusion cells to determine the volume of the two chambers of the diffusion cell. Figure 99 shows the flow diagram used for the test.

A.1 Top Half Cell with the Sensor

Table 16 shows the pressures recorded on conducting the test on the top half of the chamber.

$$P_{atm} = 762.75 \text{ mm of Hg}$$

$$V_A = 125 \text{ cc.}$$

$$Temp = 23^\circ C = 296^\circ K$$

$$\begin{aligned} n_{AO} &= \frac{P V_A}{R T} \\ &= \frac{762.75 \cdot 125}{62.361 \cdot 296} = 5.1652 \text{ mmoles} \end{aligned}$$

Calculation of V_{BCD}

Table 16: Test on the Top Chamber

Pa (mm of Hg)	Pb (mbar)	Pc (mbar)	Pd (mbar)
atm	518	518	518
775.7	775.7	775.7	775.7
atm	atm	518	518
786	786	786	786
atm	atm	atm	518
959.3	959.3	959.3	959.3

$$n_A + n_{BCD} = n_{BCD} \quad (\text{A.1})$$

$$5.1652 + \frac{518 \cdot V_{BCD}}{83.14 \cdot 296} = \frac{775.7 \cdot (125 + V_{BCD})}{83.14 \cdot 296}$$

$$127112 + 518 V_{BCD} = 775.7 (125 + V_{BCD})$$

$$245.38 + V_{BCD} = 187.19 + 1.497 V_{BCD}$$

$$V_{BCD} = 117 \text{ cc} \quad (\text{A.2})$$

$$V_B + V_C + V_D = 117 \quad (\text{A.3})$$

$$V_B + V_{CD} = 117 \quad (\text{A.4})$$

Calculation of V_B

$$n_A + n_B + n_{CD} = n_{ABCD} \quad (\text{A.5})$$

$$5.1652 + \frac{762.75 \cdot V_B}{62.361 \cdot 296} + \frac{518 \cdot V_{CD}}{83.14 \cdot 296} = \frac{786 \cdot (125 + V_B + V_{CD})}{83.14 \cdot 296} \quad (\text{A.6})$$

$$V_B - 1.13 V_{CD} = -123.5 \quad (\text{A.7})$$

From (A.4)

$$V_{CD} = 117 - V_B \quad (\text{A.8})$$

Substituting in (A.7)

$$V_B = 4.09 \text{ cc}$$

Calculation of V_C and V_D

$$n_A + n_B + n_C + n_D = n_{ABCD} \quad (\text{A.9})$$

$$5.1652 + \frac{762.75 \cdot V_B}{62.361 \cdot 296} + \frac{762.75 \cdot V_C}{62.361 \cdot 296} + \frac{518 \cdot V_D}{83.14 \cdot 296} = \frac{959.3 \cdot (125 + V_B + V_C + V_D)}{83.14 \cdot 296} \quad (\text{A.10})$$

On solving the equations we get

$$V_B = 4.09 \text{ cc.}$$

$$V_C = 85.05 \text{ cc.}$$

$$V_D = 27.86 \text{ cc.}$$

A.2 Bottom Half Cell

Table 17: Test on the Bottom Chamber

Pa (mm of Hg)	Pb (mbar)	Pc (mbar)	Pd (mbar)
atm	500	500	500
763.3	763.3	763.3	763.3
atm	atm	518	518
769	769	769	769
atm	atm	atm	497.5
950	950	950	950

$$P_{atm} = 764.45 \text{ mm of Hg}$$

$$V_A = 125 \text{ cc.}$$

$$Temp = 23^\circ C = 296^\circ K$$

$$\begin{aligned}
 n_{AO} &= \frac{PV_A}{RT} \\
 &= \frac{764.4 \cdot 125}{62.361 \cdot 296} = 5.1764 \text{ mmoles}
 \end{aligned}$$

Calculation of V_{BCD}

$$n_A + n_{BCD} = n_{ABCD} \quad (A.11)$$

$$5.1764 + \frac{500 \cdot V_{BCD}}{83.14 \cdot 296} = \frac{763.3 \cdot (125 + V_{BCD})}{83.14 \cdot 296}$$

$$127388 + 500 V_{BCD} = 763.3 (125 + V_{BCD})$$

$$254.78 + V_{BCD} = 190.83 + 1.53 V_{BCD}$$

$$V_{BCD} = 120.66 \text{ cc} \quad (\text{A.12})$$

$$V_B + V_C + V_D = 120.66 \quad (\text{A.13})$$

$$V_B + V_{CD} = 120.66 \quad (\text{A.14})$$

Calculation of V_B

$$n_A + n_B + n_{CD} = n_{ABCD} \quad (\text{A.15})$$

$$5.1652 + \frac{764.4 \cdot V_B}{62.361 \cdot 296} + \frac{496.7 \cdot V_{CD}}{83.14 \cdot 296} = \frac{768.8 \cdot (125 + V_B + V_{CD})}{83.14 \cdot 296} \quad (\text{A.16})$$

$$0.92 \cdot V_B - V_{CD} = -123.5 \quad (\text{A.17})$$

From (A.4)

$$V_{CD} = 120.66 - V_B \quad (\text{A.18})$$

Substituting in (A.7)

$$V_B = 3.15 \text{ cc}$$

Calculation of V_C and V_D

$$n_A + n_B + n_C + n_D = n_{ABCD} \quad (\text{A.19})$$

$$5.1764 + \frac{764.4 \cdot V_B}{62.361 \cdot 296} + \frac{764.4 \cdot V_C}{62.361 \cdot 296} + \frac{518 \cdot V_D}{83.14 \cdot 296} = \frac{950 \cdot (125 + V_B + V_C + V_D)}{83.14 \cdot 296} \quad (\text{A.20})$$

On solving the equations we get

$$V_B = 3.15 \text{ cc.}$$

$$V_C = 84.7 \text{ cc.}$$

$$V_D = 32.81 \text{ cc.}$$

It can be that the volume of the two chambers are nearly the same.

Therefore adopting an average value, we get

$$V_C = \frac{84.7 + 85.05}{2} = 84.88 \text{ cc.}$$

where

V'_A is the volume of the calibrated tube (125 cc.)

V_B is the volume of section B in cc.

V_C is the volume of section C in cc.

V_D is the volume of section D in cc.

V_{CD} is the volume of sections C and D combined in cc

V_{BCD} is the volume of sections B,C and D combined in cc.

V_{ABCD} is the volume of sections A,B,C and D combined in cc.

- n_A is the number of mmoles of the gas in section A
 n_B is the number of mmoles of the gas in section B
 n_C is the number of mmoles of the gas in section C
 n_D is the number of mmoles of the gas in section D
 n_{CD} is the number of mmoles of the gas in C and D combined
 n_{BCD} is the number of mmoles of the gas in B,C and D combined
 n_{ABCD} is the number of mmoles of the gas in A,B,C and D combined
 P is the pressure in mbars
 R is the universal gas constant = $0.8314 \text{ (bar lts.) / (gmole K)}$
 or $62.361 \text{ (mm of Hg lts.) / (gmole K)}$

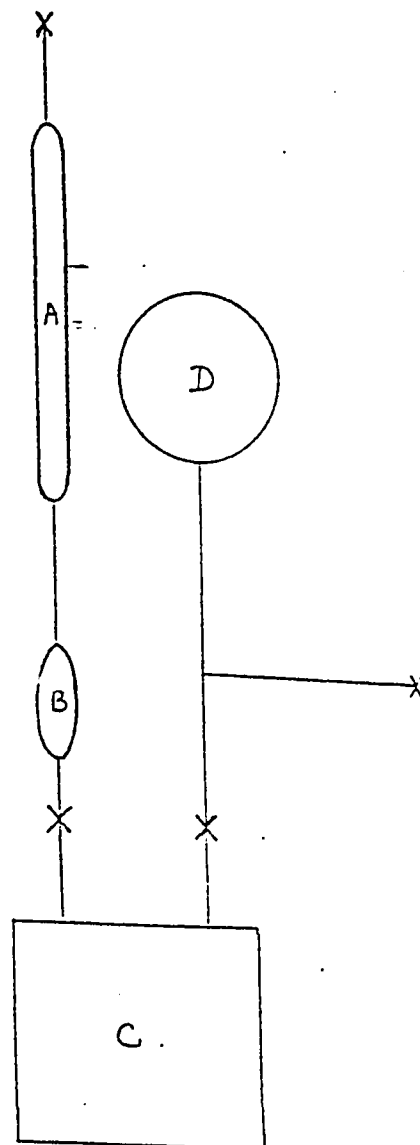


Figure 99: Flow Diagram for the Gas Expansion Test

Appendix B

OPTIMIZATION OUTPUT

FILE: CONCRETE OUTPUT1 A1 KING FAHD UNIVERSITY OF PETROLEUM AND MINERALS,

1

 * OPTIMIZATION RESULTS *

 W/C RATIO : 0.4
 EXPOSURE : INDOORS
 CHLORIDE : 8%
 REFERENCE : NAVAZ .C.M.
 FILE NAME : 4IOPTA

TIME OF PROGRAM RUN 11:42:11
 DATE OF PROGRAM RUN 3/ 7/1994

 CHLORIDE CONCENTRATION = 8%
 EXPOSURE DAYS = 70

MIN. SUM OF SQUARES ERROR = 0.71675843E-03 AT ITERATION NO. 0

MIN. SUM OF SQUARES ERROR = 0.71675843E-03 AT ITERATION NO. 1

NO FUNCTION IMPROVEMENT POSSIBLE

MIN. SUM OF SQUARES ERROR = 0.71675843E-03 AT ITERATION NO. 2

SOLUTION OF THE EQUATION :

CS = 0.5600 % CHLORIDE
 D = 8.520E-8 CM**2/SEC

DIFFUSIVITY = 8.520E-8 CM**2/SEC

X CMS.	EXPT CONCENTRATION % CHLORIDE	CAL. CONCENTRATION % CHLORIDE
0.63500	0.27400	0.30053
2.54000	0.01000	0.01284
5.08000	0.00500 ✓	0.00600
7.62000	0.00400	0.00600

 * OPTIMIZATION RESULTS *

 W/C RATIO : 0.4
 EXPOSURE : INDOORS
 CHLORIDE : 8%
 REFERENCE : NAVAZ .C.M.
 FILE NAME : 4IOPTA

TIME OF PROGRAM RUN 11:42:38
 DATE OF PROGRAM RUN 3/ 7/1994

 CHLORIDE CONCENTRATION = 8%
 EXPOSURE DAYS = 105

MIN. SUM OF SQUARES ERROR = 0.23233815E-03 AT ITERATION NO. 0

MIN. SUM OF SQUARES ERROR = 0.23233815E-03 AT ITERATION NO. 1

NO FUNCTION IMPROVEMENT POSSIBLE

MIN. SUM OF SQUARES ERROR = 0.23233815E-03 AT ITERATION NO. 2

SOLUTION OF THE EQUATION :

CS = 0.5600 % CHLORIDE
 D = 8.520E-8 CM**2/SEC

DIFFUSIVITY = 8.520E-8 CM**2/SEC

X CMS.	EXPT CONCENTRATION % CHLORIDE	CAL. CONCENTRATION % CHLORIDE
0.63500	0.33900	0.34369
2.54000	0.02500	0.02875
5.08000	0.02000	0.00602
7.62000	0.00500 /	0.00600

 * OPTIMIZATION RESULTS *

 W/C RATIO : 0.4
 EXPOSURE : INDOORS
 CHLORIDE : 8%
 REFERENCE : NAVAZ .C.M.
 FILE NAME : 4IOPTA

TIME OF PROGRAM RUN 11:42:38
 DATE OF PROGRAM RUN 3/ 7/1994

 CHLORIDE CONCENTRATION = 8%
 EXPOSURE DAYS = 175

MIN. SUM OF SQUARES ERROR = 0.90607023E-03 AT ITERATION NO. 0

MIN. SUM OF SQUARES ERROR = 0.90607023E-03 AT ITERATION NO. 1

NO FUNCTION IMPROVEMENT POSSIBLE

MIN. SUM OF SQUARES ERROR = 0.90607023E-03 AT ITERATION NO. 2

SOLUTION OF THE EQUATION :

CS = 0.5600 % CHLORIDE
 D = 8.520E-8 CM**2/SEC

DIFFUSIVITY = 8.520E-8 CM**2/SEC

X . EXPT CONCENTRATION CMS.	% CHLORIDE	CAL. CONCENTRATION % CHLORIDE
0.63500	0.41000	0.38959
2.54000	0.08000	0.06891
5.08000	0.02600	0.00686
7.62000	0.00600	0.00500

TOTAL SUM OF SQUARES ALL DATA SETS = 0.18551666E-02

Appendix C

SAMPLE CALCULATION FOR THE STATIC TEST

A sample calculation is shown for the concrete with the following details

$$CC = 350 \text{ kg/m}^3$$

$$W/C = 0.55$$

Effective pore radius = 135 Angstroms

C.1 Molecular Diffusion Coefficient

The expression used to determine the bulk diffusion coefficient for the helium/nitrogen system is

$$D_{12} = \frac{0.001858 T^{3/2} \left[\frac{1}{M_1} + \frac{1}{M_2} \right]^{1/2}}{P \sigma_{12}^2 \Omega_p} \quad (\text{A.12})$$

Different parameters required for calculating D_{12} were obtained from ref [76].

To find σ_{12}

Helium

$$\frac{\epsilon_A}{k} = 33.3$$

$$\text{Therefore } \sigma_1 = 2.968$$

Nitrogen

$$\frac{\epsilon_A}{k} = 91.5$$

$$\text{Therefore } \sigma_2 = 3.681$$

$$\sigma_{12} = \frac{2.968 + 3.681}{2} = 3.325$$

To find $\Omega_{D,12}$

$$\begin{aligned} \frac{\epsilon_{12}}{k} &= \sqrt{\left\{ \frac{\epsilon_1}{k} * \frac{\epsilon_2}{k} \right\}} \\ &= \sqrt{33.3 * 91.5} = 55.2 \end{aligned}$$

$$T = 18^\circ C = 18 + 273 = 291^\circ K$$

$$\frac{\epsilon_{12}}{k T} = \frac{55.2}{291} = 0.1897$$

$$\frac{k T}{\epsilon_{12}} = 5.272$$

$$\Omega_{D,12} = 0.919$$

$$M_{\text{helium}} = 4.006$$

$$M_{\text{nitrogen}} = 28.02$$

$$D_{12} = \frac{0.001858 \cdot 291^{3/2} \left[\frac{1}{4.006} + \frac{1}{28.02} \right]^{1/2}}{1 \cdot 3.325^2 \cdot 0.919} = 0.485 \text{ cm}^2/\text{sec.}$$

C.2 Knudsen Diffusion Coefficients

The expression for Knudsen diffusion coefficient is

$$D_k = 9700 \cdot r_c \cdot \sqrt{\left(\frac{T}{M} \right)} \quad (\text{A.13})$$

For Helium

$$D_{1k} = 9700 \cdot 135 \cdot 10^{-8} \sqrt{\left[\frac{291}{4.006} \right]} = 0.112 \text{ cm}^2/\text{sec.}$$

For Nitrogen

$$D_{1k} = 9700 \cdot 135 \cdot 10^{-8} \sqrt{\left[\frac{291}{28.02} \right]} = 0.042 \text{ cm}^2/\text{sec.}$$

C.3 Evaluation of epsilon / tau

The mass balance equation for the system is

$$\begin{aligned} 0 = & -\frac{1}{2} \left[1 + \frac{D_{12}}{D_{1K}} \right] \ln(1 - 2x_1) + \frac{1}{4} \left[1 - \frac{D_{2K}}{D_{1K}} \right] \ln(1 - 2x_1) \\ & + \frac{1}{2} \left[1 - \frac{D_{2K}}{D_{1K}} \right] (x_1) \end{aligned} \quad (\text{A.14})$$

where

$$0 = \frac{AD_{12}ct}{V\tau L} \quad (\text{A.15})$$

Substituting the values for D_{12} , D_{1k} and D_{2k} , for 0.005 step increments in the value of x_1 , the corresponding values of θ are generated using a computer program (Table 18).

For example, for $x_1 = 0.825$, from Table 18, $\theta = 1.026$.

For Eqn. (A.15),

$$V = 84.88 \text{ cc}$$

$$A = 20.24 \text{ cm}^2$$

$$L = 1 \text{ cm}$$

$$t = 0.1 \text{ hr}$$

Therefore

$$\frac{\varepsilon}{\tau} = \frac{1.026 \cdot 84.88 \cdot 1}{20.24 \cdot 0.485 \cdot 0.1 \cdot 60 \cdot 60} = 0.025$$

Likewise $\frac{\varepsilon}{\tau}$ can be determined for each x_1 . Table 19 collectively

ly shows the $\frac{\varepsilon}{\tau}$ values for all the concretes tested. For this

concrete, the average $\frac{\varepsilon}{\tau} = 0.0179$.

We know,

$$D_c = D_{NaCl/H_2O} * \frac{\varepsilon}{\tau}$$

$$D_r = 1.26 \cdot 10^5 * 0.0179 = 22.55 \cdot 10^8 \text{ cm}^2/\text{sec}.$$

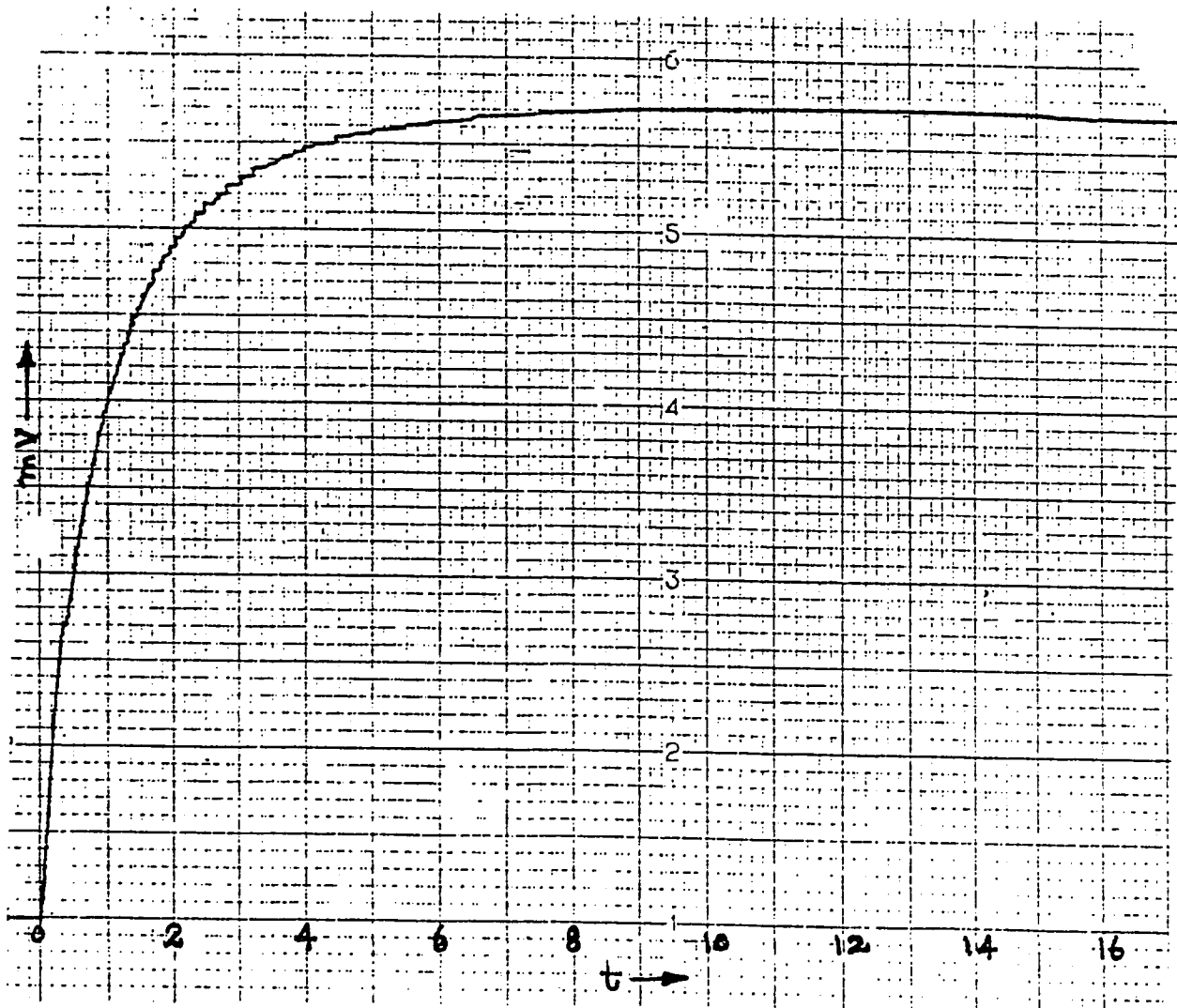


Figure 100: Diffusion Curve Obtained From the Static Test

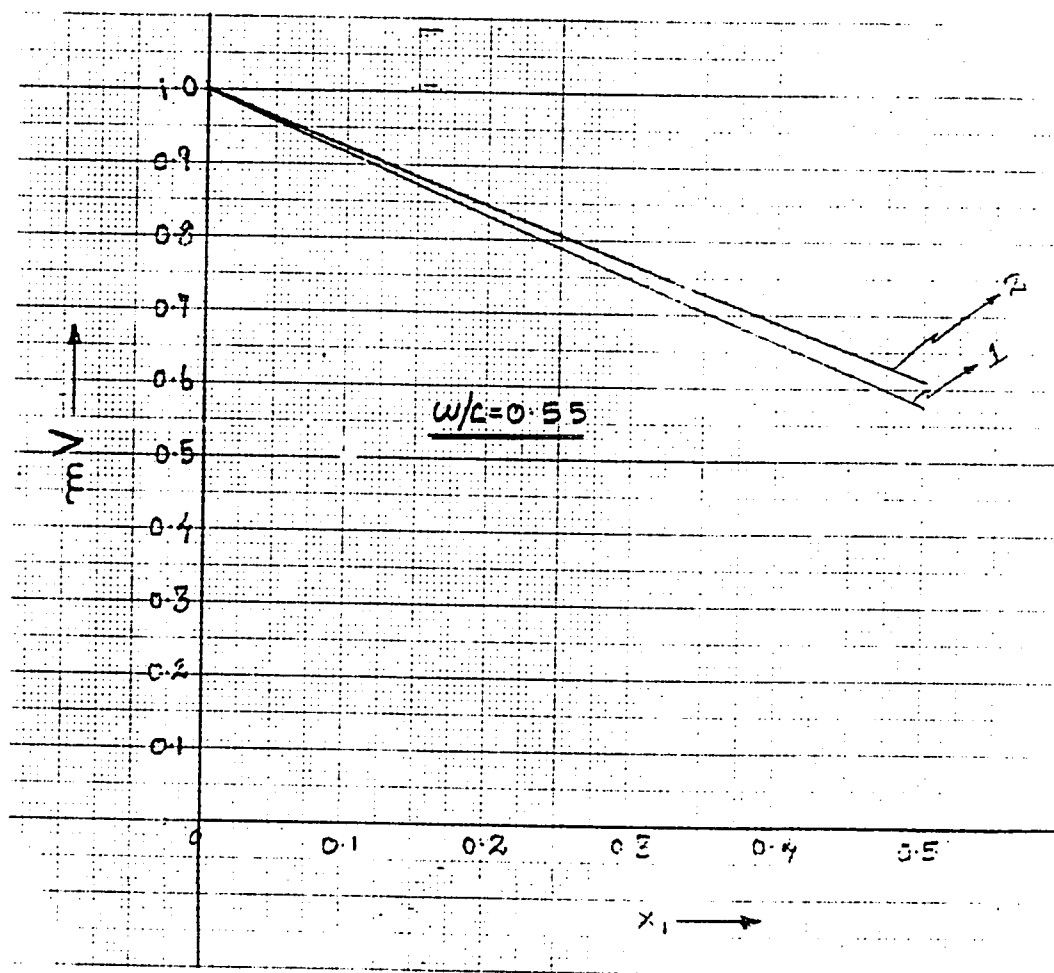


Figure 101: Plot of Concentration Ratio Vs Time

Table 18: Computer Generated Theta Values

206

C/C = 350 KG/CUM. W/C = 0.55

X1	THETA
.00500	0.02677803
.01000	0.05381208
.01500	0.08110732
.02000	0.10866922
.02500	0.13650346
.03000	0.16461569
.03500	0.19301170
.04000	0.22169822
.04500	0.25068104
.05000	0.27996665
.05500	0.30956227
.06000	0.33947450
.06500	0.36971051
.07000	0.40027827
.07500	0.43118525
.08000	0.46243954
.08500	0.49404937
.09000	0.52602339
.09500	0.55837077
.10000	0.59110039
.10500	0.62422210
.11000	0.65774590
.11500	0.69168204
.12000	0.72604150
.12500	0.76083511
.13000	0.79607505
.13500	0.83177316
.14000	0.86794204
.14500	0.90459496
.15000	0.94174564
.15500	0.97940844
.16000	1.01759720
.16500	1.05632877
.17000	1.09562111
.17500	1.13548756
.18000	1.17595005
.18500	1.21702385
.19000	1.25872993
.19500	1.30108833
.20000	1.34412098
.20500	1.38785172
.21000	1.43230343
.21500	1.47750092
.22000	1.52346897
.22500	1.57023907
.23000	1.61783886
.23500	1.66629791

.24000	1.71565056
.24500	1.76593208
.25000	1.81717682
.25500	1.86942673
.26000	1.92272186
.26500	1.97710609
.27000	2.03262520
.27500	2.08933067
.28000	2.14727688
.28500	2.20651817
.29000	2.26711655
.29500	2.32913780
.30000	2.39265251
.30500	2.45773602
.31000	2.52446842
.31500	2.59294033
.32000	2.66324425
.32500	2.73548317
.33000	2.80977345
.33500	2.88623428
.34000	2.96500206
.34500	3.04621887
.35000	3.13004780
.35500	3.21666622
.36000	3.30626965
.36500	3.39907646
.37000	3.49532700
.37500	3.59528923
.38000	3.69927120
.38500	3.80761242
.39000	3.92070198
.39500	4.03898048
.40000	4.16295052
.40500	4.29320526
.41000	4.43041706
.41500	4.57538605
.42000	4.72904968
.42500	4.89253235
.43000	5.06719398
.43500	5.25468540
.44000	5.45707035
.44500	5.67693520
.45000	5.91762066
.45500	6.18352222
.46000	6.48059082
.46500	6.81717014
.47000	7.20548153
.47500	7.66446590
.48000	8.22586823
.48500	8.94918537
.49000	9.96799088
.49500	11.70848846
.50000	34.93734741

Table 19: Epsilon / Tau Values

CC=350 kg/m³, W/C=0.40

mV	t (cms.)	t (hrs.)	x ₁	θ	R=ε/τ	(R _{avg} -R) ² •10 ⁵	ln(1-2x ₁)
0.820	2	0.4	0.220	1.62	0.010	529	-0.58
0.735	4	0.8	0.324	2.91	0.009	169	-1.04
0.684	6	1.2	0.384	4.05	0.008	9	-1.46
0.650	8	1.6	0.428	5.21	0.008	9	-1.94
0.630	10	2.0	0.456	6.65	0.008	9	-2.43
0.618	12	2.4	0.468	7.50	0.008	9	-2.75
0.608	14	2.8	0.480	8.77	0.007	49	-3.22
0.600	16	3.2	0.492	11.22	0.008	9	-4.13
0.820	2	0.4	0.220	1.62	0.018	529	-0.58
0.730	4	0.8	0.332	3.02	0.009	169	-1.09
0.680	6	1.2	0.392	4.22	0.008	9	-1.53
0.650	8	1.6	0.430	5.40	0.008	9	-1.97
0.630	10	2.0	0.456	6.65	0.008	9	-2.43
0.618	12	2.4	0.468	7.50	0.008	9	-2.75
0.610	14	2.8	0.480	8.77	0.008	9	-3.22
0.605	16	3.2	0.488	10.14	0.008	9	-3.22
0.830	2	0.4	0.228	1.70	0.010	529	-0.61
0.745	4	0.8	0.336	3.09	0.009	169	-1.11
0.700	6	1.2	0.396	4.33	0.009	169	-1.57
0.670	8	1.6	0.436	5.64	0.008	9	-2.06
0.650	10	2.0	0.460	6.90	0.008	9	-2.53
0.635	12	2.4	0.476	8.28	0.008	9	-3.04
0.630	14	2.8	0.488	10.14	0.009	169	-3.73
0.620	16	3.2	0.496	13.08	0.009	169	-4.83
0.855	2	0.4	0.200	1.43	0.009	169	-0.51
0.775	4	0.8	0.315	2.76	0.008	9	-0.999
0.730	6	1.2	0.375	3.83	0.008	9	-1.39
0.700	8	1.6	0.420	5.04	0.008	9	-1.83
0.680	10	2.0	0.450	6.30	0.008	9	-2.30
0.670	12	2.4	0.465	7.26	0.007	49	-2.66
0.660	14	2.8	0.475	8.17	0.007	49	-3.00
0.650	16	3.2	0.490	10.63	0.008	9	-3.91
0.860	2	0.4	0.205	1.48	0.009	169	-0.53
0.790	4	0.8	0.305	2.62	0.008	9	-0.94
0.745	6	1.2	0.375	3.83	0.008	9	-1.39
0.720	8	1.6	0.415	4.87	0.007	49	-1.77
0.700	10	2.0	0.440	5.81	0.007	49	-2.12
0.690	12	2.4	0.455	6.30	0.006	289	-2.41

0.680	14	2.8	0.470	7.68	0.007	49	-2.81
0.675	16	3.2	0.480	8.77	0.007	49	-3.22
0.670	18	3.6	0.490	10.63	0.007	49	-3.91
0.870	2	0.4	0.175	1.21	0.007	49	-0.43
0.800	4	0.8	0.270	2.16	0.006	289	-0.78
0.750	6	1.2	0.340	3.16	0.006	289	-1.14
0.715	8	1.6	0.395	4.17	0.006	289	-1.56
0.690	10	2.0	0.420	5.04	0.006	289	-1.83
0.675	12	2.4	0.440	5.81	0.006	289	-2.12
0.665	14	2.8	0.455	6.59	0.006	289	-2.41
0.655	16	3.2	0.470	7.68	0.006	289	-2.81
0.645	20	4.0	0.485	9.54	0.006	289	-3.51
0.640	24	4.8	0.490	10.63	0.005	729	-3.91
0.880	2	0.4	0.185	1.29	0.008	9	-0.46
0.815	4	0.8	0.295	2.48	0.007	49	-0.89
0.770	6	1.2	0.350	3.33	0.007	49	-1.20
0.740	8	1.6	0.400	4.43	0.007	49	-1.61
0.720	10	2.0	0.440	5.81	0.007	49	-2.12
0.705	12	2.4	0.460	6.90	0.007	49	-2.53
0.690	14	2.8	0.475	8.17	0.007	49	-3.00
0.685	16	3.2	0.485	9.54	0.007	49	-3.51
0.680	20	4.0	0.490	10.63	0.006	289	-3.91

Average $\epsilon/\tau=0.0077$

Std. Deviation=0.0011

CC=350 kg/m³, W/C=0.55

mV	t (cms.)	t (hrs.)	x_1	θ	$R=\epsilon/\tau$	$(R_{avg}-R)^2 \cdot 10^4$	$\ln(1-2x_1)$
0.850	0.5	0.1	0.175	1.14	0.027	6084	-0.43
0.760	1	0.2	0.310	2.52	0.030	11664	-0.97
0.680	2	0.4	0.375	3.60	0.022	784	-1.39
0.630	3	0.6	0.440	5.46	0.022	784	-2.12
0.610	4	0.8	0.450	5.92	0.018	114	-2.30
0.590	6	1.2	0.482	8.49	0.017	484	-3.32
0.580	8	1.6	0.495	11.71	0.018	144	-4.61
0.860	0.5	0.1	0.185	1.22	0.029	9604	-0.46
0.780	1	0.2	0.285	2.21	0.027	6084	-0.84
0.70	2	0.4	0.385	3.81	0.023	1444	-1.47
0.660	3	0.6	0.435	5.25	0.021	324	-2.04
0.640	4	0.8	0.460	6.48	0.019	4	-2.53
0.620	6	1.2	0.485	9.22	0.018	144	-3.51
0.850	0.5	0.1	0.160	1.02	0.025	3364	-0.39
0.760	1	0.2	0.255	1.87	0.022	784	-0.71
0.700	1.5	0.3	0.320	2.66	0.021	324	-1.02

0.660	2	0.4	0.360	3.31	0.020	64	-1.27
0.610	3	0.6	0.405	4.29	0.017	484	-1.66
0.580	4	0.8	0.444	5.46	0.016	1024	-2.12
0.550	6	1.2	0.480	8.23	0.016	1024	-3.12
0.850	0.5	0.1	0.135	0.83	0.020	64	-0.31
0.760	1	0.2	0.225	1.57	0.019	4	-0.60
0.690	1.5	0.3	0.285	2.21	0.018	144	-0.84
0.640	2	0.4	0.335	2.89	0.017	484	-1.11
0.580	3	0.6	0.390	3.92	0.016	1024	-1.51
0.540	4	0.8	0.425	4.89	0.015	1764	-1.90
0.510	5	1.0	0.450	5.92	0.014	2704	-2.30
0.490	6	1.2	0.470	7.21	0.014	2704	-2.81
0.470	10	2.0	0.490	9.97	0.012	5184	-3.91
0.870	0.5	0.1	0.15	0.94	0.023	1444	-3.60
0.790	1	0.2	0.235	1.67	0.020	64	-0.63
0.740	1.5	0.3	0.300	2.39	0.019	4	-0.92
0.700	2	0.4	0.340	2.96	0.018	144	-1.14
0.640	3	0.6	0.410	4.43	0.018	144	-1.71
0.610	4	0.8	0.435	5.25	0.016	1024	-2.04
0.590	5	1.0	0.465	6.82	0.016	1024	-2.66
0.580	5	1.2	0.475	7.66	0.015	1764	-3.00
0.870	0.5	0.1	0.140	0.87	0.021	324	-0.33
0.790	1	0.2	0.230	1.62	0.019	4	-0.62
0.740	1.5	0.3	0.280	2.15	0.017	484	-0.82
0.700	2	0.4	0.325	2.74	0.016	1024	-1.05
0.640	3	0.6	0.390	3.92	0.016	1024	-1.51
0.600	4	0.8	0.435	5.25	0.016	1024	-2.04
0.580	5	1.0	0.455	6.18	0.015	1764	-2.41
0.570	6	1.2	0.470	7.21	0.014	2704	-2.81
0.550	8	1.6	0.490	9.97	0.015	1764	-3.91
0.540	10	2.0	0.495	11.71	0.014	2704	-4.61

Average $\varepsilon/\tau=0.0192$

Std. Deviation=0.0046

CC=350 kg/m³, W/C=0.70

mV	t (cms.)	t (hrs.)	x_1	θ	$R=\varepsilon/\tau$	$(R_{avg}-R)^2 \cdot 10^6$	$\ln(1-2x_1)$
0.760	0.5	0.1	0.245	1.61	0.039	88.4	-0.67
0.650	1	0.2	0.355	2.94	0.035	29.2	-1.24
0.600	1.5	0.3	0.405	3.92	0.031	1.96	-1.66
0.570	2	0.4	0.440	4.98	0.030	0.16	-2.12
0.550	2.5	0.5	0.460	5.91	0.028	2.56	-2.53
0.535	3	0.6	0.475	6.99	0.028	2.56	-3.00
0.520	4	0.8	0.490	9.09	0.027	6.76	-3.91

0.750	0.5	0.1	0.250	1.66	0.031	10.82	-0.69
0.650	1	0.2	0.350	2.86	0.040	19.36	-1.20
0.590	1.5	0.3	0.410	4.04	0.034	5.76	-1.71
0.560	2	0.4	0.440	4.98	0.032	0.16	-2.12
0.540	2.5	0.5	0.458	5.80	0.030	2.56	-2.48
0.525	3	0.6	0.475	6.99	0.028	2.56	-3.00
0.510	4	0.8	0.490	9.09	0.027	6.76	-3.91
0.780	0.5	0.1	0.240	1.57	0.038	70.56	-0.65
0.680	1	0.2	0.345	2.78	0.033	11.56	-1.17
0.630	1.5	0.3	0.400	2.80	0.022	57.76	-1.61
0.600	2	0.4	0.435	4.80	0.029	0.36	-2.04
0.580	2.5	0.5	0.450	5.40	0.026	12.96	-2.30
0.570	3	0.6	0.465	6.22	0.025	21.16	-2.66
0.555	4	0.8	0.480	7.50	0.023	43.56	-3.22
0.545	6	1.2	0.493	9.90	0.020	92.16	-4.27
0.750	0.5	0.1	0.260	1.76	0.042	153.8	-0.73
0.650	1	0.2	0.360	3.02	0.036	0.16	-1.27
0.605	1.5	0.3	0.410	4.04	0.032	5.76	-1.71
0.580	2	0.4	0.440	4.98	0.030	0.16	-2.12
0.560	2.5	0.5	0.455	5.64	0.027	6.76	-2.41
0.545	3	0.6	0.470	6.57	0.026	12.96	-2.81
0.535	4	0.8	0.480	7.50	0.023	43.56	-3.22
0.780	0.5	0.1	0.250	1.66	0.040	108.1	-0.69
0.690	1	0.2	0.350	2.86	0.030	19.36	-1.20
0.640	1.5	0.3	0.410	4.04	0.032	5.76	-1.71
0.610	2	0.4	0.440	4.98	0.030	0.16	-2.12
0.595	2.5	0.5	0.458	5.80	0.028	2.56	-2.48
0.580	3	0.6	0.475	6.99	0.028	2.56	-3.00
0.570	4	0.8	0.485	8.16	0.024	31.36	-3.51
0.780	0.5	0.1	0.200	1.23	0.029	0.36	-0.51
0.660	1	0.2	0.310	2.31	0.028	2.56	-0.97
0.600	1.5	0.3	0.363	3.07	0.025	21.16	-1.29
0.555	2	0.4	0.405	3.92	0.024	31.40	-1.66
0.530	2.5	0.5	0.425	4.47	0.021	73.96	-1.89
0.510	3	0.6	0.435	4.80	0.019	112.4	-2.04
0.485	4	0.8	0.465	6.22	0.019	112.4	-2.66
0.470	5	1.0	0.485	8.16	0.020	92.16	-3.51
0.460	6	1.2	0.490	9.09	0.018	134.6	-3.91
0.770	0.5	0.1	0.250	1.66	0.040	10.82	-0.69
0.670	1	0.2	0.360	3.02	0.036	40.96	-1.27
0.620	1.5	0.3	0.415	4.18	0.033	11.56	-1.77
0.590	2	0.4	0.445	5.18	0.031	1.96	-2.21
0.575	2.5	0.5	0.465	6.22	0.030	0.16	-2.66

0.565	3	0.6	0.475	6.99	0.028	2.56	-3.00
0.550	4	0.8	0.490	9.09	0.027	6.76	-3.91
0.545	6	1.2	0.495	10.67	0.027	73.96	-4.61
0.760	0.5	0.1	0.245	1.61	0.039	88.4	-0.67
0.640	1	0.2	0.370	3.19	0.038	70.6	-1.35
0.590	1.5	0.3	0.420	4.32	0.035	29.2	-1.83
0.560	2	0.4	0.450	5.40	0.032	57.6	-2.30
0.545	2.5	0.5	0.465	6.22	0.030	0.16	-2.66
0.535	3	0.6	0.475	6.99	0.028	2.56	-2.99
0.520	4	0.8	0.490	9.09	0.027	6.76	-3.92

Average $\epsilon/\tau=0.0296$

Std. Deviation=0.0052

CC=300 kg/m³, W/C=0.40

mV	t (cms.)	t (hrs.)	x_1	θ	$R=\epsilon/\tau$	$(R_{avg}-R)^2 \cdot 10^4$
0.695	2	0.4	0.345	2.05	0.012	9
0.625	4	0.8	0.420	3.16	0.009	0
0.590	6	1.2	0.460	4.32	0.009	0
0.575	8	1.6	0.475	5.11	0.008	1
0.560	12	2.4	0.490	6.63	0.007	4
0.710	2	0.4	0.355	2.16	0.013	16
0.660	4	0.8	0.415	3.06	0.009	0
0.625	6	1.2	0.460	4.32	0.009	0
0.615	8	1.6	0.475	5.11	0.008	1
0.600	12	2.4	0.485	5.95	0.006	9

Average $\epsilon/\tau=0.009$

Std. Deviation=0.0021

CC=300 kg/m³, W/C=0.55

mV	t (cms.)	t (hrs.)	x_1	θ	$R=\epsilon/\tau$	$(R_{avg}-R)^2 \cdot 10^4$
0.850	1	0.2	0.180	1.28	0.015	127.7
0.670	2	0.4	0.400	4.54	0.027	0.49
0.630	3	0.6	0.445	6.41	0.026	0.09
0.610	4	0.8	0.470	7.87	0.024	5.29
0.590	6	1.2	0.495	12.79	0.026	0.09
0.760	1	0.2	0.310	2.75	0.033	44.89
0.680	2	0.4	0.410	4.83	0.029	7.29
0.645	3	0.6	0.455	6.75	0.027	0.49
0.630	4	0.8	0.475	8.37	0.025	1.69
0.615	6	1.2	0.490	10.89	0.022	18.49
0.750	1	0.2	0.280	2.34	0.028	2.89
0.660	2	0.4	0.385	4.15	0.025	1.69
0.615	3	0.6	0.435	5.74	0.023	10.89
0.590	4	0.8	0.465	7.44	0.022	18.49

0.570	6	1.2	0.490	10.89	0.022	18.49
0.565	8	1.6	0.495	12.79	0.019	53.29
0.760	1	0.2	0.300	2.61	0.031	22.1
0.680	2	0.4	0.400	4.83	0.029	7.29
0.645	3	0.6	0.445	6.20	0.025	1.69
0.625	4	0.8	0.470	7.87	0.024	5.29
0.610	6	1.2	0.490	10.89	0.022	18.49
0.750	1	0.2	0.285	2.41	0.029	7.29
0.660	2	0.4	0.390	4.28	0.026	0.09
0.615	3	0.6	0.445	6.20	0.025	1.69
0.590	4	0.8	0.470	7.87	0.024	5.29
0.570	6	1.2	0.495	12.79	0.026	0.09
0.740	1	0.2	0.325	2.98	0.036	94.1
0.660	2	0.4	0.425	5.34	0.032	32.5
0.610	4	0.8	0.485	9.78	0.029	9.29
0.780	1	0.2	0.300	2.61	0.031	22.1
0.700	2	0.4	0.400	4.54	0.027	0.49
0.650	4	0.8	0.470	7.87	0.024	5.29
0.638	6	1.2	0.490	10.89	0.022	18.49

Average $\epsilon/\tau=0.0263$
Std. Deviation=0.0042

CC=400 kg/m³, W/C=0.40

mV	t (cms.)	t (hrs.)	x_1	θ	$R=\epsilon/\tau$	$(R_{avg}-R)^2 \cdot 10^6$
0.730	2	0.4	0.325	2.21	0.013	36
0.680	4	0.8	0.390	3.16	0.009	4
0.650	6	1.2	0.425	3.94	0.008	1
0.635	8	1.6	0.445	4.56	0.007	0
0.610	12	2.4	0.475	6.15	0.006	1
0.600	16	3.2	0.485	7.18	0.005	4
0.870	2	0.4	0.150	0.76	0.005	4
0.685	4	0.8	0.375	2.90	0.008	1
0.650	6	1.2	0.415	3.68	0.007	0
0.630	8	1.6	0.435	4.23	0.006	1
0.605	12	2.4	0.470	5.79	0.006	1
0.590	16	3.2	0.485	7.18	0.005	4
0.585	20	4.0	0.490	8.00	0.005	4

Average $\epsilon/\tau=0.007$
Std. Deviation=0.0023

CC=400 kg/m³, W/C=0.55

mV	t (cms.)	t (hrs.)	x ₁	θ	R=ε/τ	(R _{avg} -R) ² •10 ⁶
0.880	0.5	0.1	0.125	0.62	0.015	16
0.810	1	0.2	0.195	1.06	0.013	4
0.760	1.5	0.3	0.245	1.44	0.012	1
0.720	2	0.4	0.285	1.80	0.011	0
0.675	3	0.6	0.330	2.29	0.009	4
0.635	4	0.8	0.370	2.85	0.009	4
0.580	6	1.2	0.425	3.98	0.008	9
0.550	8	1.6	0.455	5.03	0.008	9
0.525	12	2.4	0.485	7.27	0.007	16
0.880	0.5	0.1	0.125	0.62	0.015	16
0.810	1	0.2	0.195	1.06	0.013	4
0.755	1.5	0.3	0.250	1.48	0.012	1
0.720	2	0.4	0.285	1.80	0.011	0
0.650	3	0.6	0.355	2.62	0.010	1
0.610	4	0.8	0.395	3.29	0.010	1
0.550	6	1.2	0.455	5.03	0.010	1
0.520	8	1.6	0.490	8.09	0.012	1

Average ε/τ=0.011
Std. Deviation=0.0023

Appendix D

SAS PROGRAM AND THE OUTPUT OF THE REGRESSION ANALYSIS

D.1 SAS Program

```

*** WIDTH 50 DEPTH 60 ***;
*****
***** DOTS SHOULD NOT BE USED IN OPTIONS *****;
*****
*GOPTIONS NOTEXT82 BORDER VSIZE=7 HSIZE=8;
*****
*          TO VIEW THE OUTPUT ON THE SCREEN
*****
*GOPTIONS DEVICE=IBM3179;
*****
*-----
*          HARDCOPY ON SAS PRINTER + ADMPRINT FILE
*-----
*GOPTIONS DEVICE=GDDM87 DEVADDR=(...,'MOD2');
*=====
*          HARDCOPY ON SAS PRINTER
*=====
*GOPTIONS DEVICE=IBM3287 DEVADDR='4FF';
*****
*          HARDCOPY ON CALCOMP PLOTTER
*****
*GOPTIONS DEVICE=CALCPSAS VSIZE=15 HSIZE=20;
*****
*          HARDCOPY ON PAGE PRINTER
*****
*GOPTIONS DEVICE=GDDMFAM4 GDDMN=IBM3812 GDDMT=IMG24OX;
*GOPTIONS NOTEXT82 BORDER;
*****
CMS FI IN DISK DIF DATA A1;

DATA ONE;
  INFILE IN;

  *INPUT X S ;
  INPUT X Y S;
DATA TWO;
  SET ONE;
  *SL=LOG(S) ;
  PROC NLIN METHOD=DUD;
  *;
  PARMs C1=0.1 C2=0.1 C3=0.1 C4=0.1 ;
  *PARMS C1=0.1 C2=0.1 C3=0.1 ;
  *PARMS C1=2.0 ;
  *;
  *DATA NEW2 SET NEW1;
  *C1=0.1;
  *C2=0.2;
  *PROC GLM DATA=NEW1;
  *MODEL S = C1 + C2*(X*Y)**C3 + C4*Y**C5 ;
  *          C5*(WC*CC)**C7 ;
  *MODEL D = C1 + C2*CC**C3 + C4*(WC/CC)**C5 ;
  *MODEL S=C1+C2*X+C3*X**2+C4*X**3 +C5*COS(X) + C6*EXP(-X) ;
  *MODEL S=C1+C2*X+C3*X**2+C4*X**3 +C5*EXP(-X) ;
  *MODEL S=C1+C2*X+C3*X**2+C4*(Y**2);
  *MODEL S=C1+C2*X+C3*X**2+C4*(Y**6);
  *MODEL S=C1+C2*X+C3*X**2+C4*(Y**2);

```

```

*MODEL S=-33.5 -372.39*X +515.44*X**2 +180.89*(Y**-1) -71.88*(Y**-1);
*MODEL S=C1*X+C2*X**2+C3*(Y**-1);
*MODEL S=(C1+C2*X+C3*X**2)*C7+ (C4+C5*Y+C6*Y**2)*C8;
*MODEL S=C1*COS(C2*X) ;
*MODEL S=C1*(TAN(X))**-1 ;
*MODEL S=C1+C2*EXP(X**2) ;
*MODEL S=C1+C2*(EXP(-X)) ;
*MODEL S=C1+C2*X+C3*X**2 ;
*MODEL S=C1+C2*(Y**-0.095)+C3*((X/Y)**0.25);
*MODEL S=C1+C2*(Y**-0.095)+C3*((X*Y)**0.25);
*MODEL S=C1+ C2*(Y**C3 )+C4*((X*Y)**C5);
*MODEL S=C1+C2*X ;
*MODEL S=C1*X**(C2);
*MODEL S=C1*LOG(X) ;
*MODEL S=C1+ C2*X**(.5)+C3*X**0.33+ C4*X**.25 + C5*X**0.15 ;
*MODEL S=C1+ C2*X**(C3)+C4*X**(C5)+ C6*X**(C7);
*MODEL S=C1*X**(C2);
*MODEL S=C1*X**(0.70);
*MODEL S=C1*(EXP(X));
*
*OUTPUT OUT=A PARMS=C1
* P=TT ;
OUTPUT OUT=A PARMS=C1 C2 C3 C4
P=TT ;

DATA THREE;
SET ONE;
SET TWO;
SET A;
CALC=TT ;
*
DEV =(CALC-S)*100.0/S;
KEEP X Y S CALC DEV ;
*KEEP WC CC D CALC DEV ;
PROC PRINT;
*
DATA FOUR;
SET THREE;
DEV=ABS(DEV);
KEEP DEV;
*
*-----CALCULATES AVERAGE ABSOLUTE DEVIATION-----
*
DATA FIVE;
PROC MEANS DATA=FOUR;
OUTPUT OUT=B ;
PROC GLM DATA=THREE;
PROC PRINT ;
*
*-----PROCEDURE GLOT IS CALLED TO PLOT-----
*
DATA SIX;
SET ONE;
SET TWO;
SET THREE;
PROC GLOT;

```

```

*PLOT S*X CALS*X /OVERLAY;
*PLOT S*X CALS*X /OVERLAY CAXIS=BLACK;
PLOT S*Y CALS*Y /OVERLAY;
SYMBOL1 C=RED I=NONE V=CIRCLE;
SYMBOL2 C=BLUE I=NONE V=STAR;
*SYMBOL2 C=BLUE I=SPLINE V=CIRCLE;
*TITLE1 C=BLUE 'DIFFUSION COEFFICIENT';
TITLE2 C=BLUE 'DIFFUSION COEFFICIENT';
TITLE6 H=1.0 C=BLUE 'O-EXP. VALUES *-CALC. VALUES';
*TITLE6 J=C H=1.0 C=B '*-EXP. VALUES #-CALC. VALUES';
*TITLE3 C=BLUE 'INDOORS CC=350 KG/CUM.';
  LABEL S='DIFF COEFF'
    X='WATER CEMENT RATIO'
    Y='NORMALIZED CEMENT CONTENT';
*FOOTNOTE1 J=C H=0.2 C=BLACK
*F=TITALIC 'DIAMOND FOR EXPERIMENTAL VALUES';
FOOTNOTE1 J=C H=2.0 C=BLACK
F=TITALIC 'MODEL IS  $D = -82.4 - 425.9(WC) + 568.42(WC)**2 + 4.26(C)**2$ ';
FOOTNOTE2 J=C H=2.0 C=BLACK
F=TITALIC 'FIGURE ( ): PREDICTED AND ACTUAL VALUES OF DIFFUSION C

```

D.2 SAS Output for the Regression Analysis

FILE: MOD2 LISTING A1 KING FAHD UNIVERSITY OF PETROLEUM AND MINERALS, DHAHRAN

PAGE 00001

The SAS System

09:55 Wednesday, 11/1/2011

Non-Linear Least Squares Initialization				Dependent Variable S	
DUD	C1	C2	C3	C4	Sum of Squares
-5	0.100000	0.100000	0.100000	0.100000	11427.754781
-4	0.110000	0.100000	0.100000	0.100000	11422.858727
-3	0.100000	0.110000	0.100000	0.100000	11424.759359
-2	0.100000	0.100000	0.110000	0.100000	11425.865560
-1	0.100000	0.100000	0.100000	0.110000	11421.804550

Non-Linear Least Squares Iterative Phase				Dependent Variable S		Method: DUD
Iter	C1	C2	C3	C4	Sum of Squares	
0	0.100000	0.100000	0.100000	0.110000	11421.804550	
1	82.736189	-425.895524	568.424611	4.262618	75.890524	
2	82.736189	-425.895524	568.424611	4.262618	75.890524	

NOTE: Convergence criterion met.

Non-Linear Least Squares Summary Statistics Dependent Variable S

Source	DF	Sum of Squares	Mean Square
Regression	3	11510.071676	3836.690559
Residual	6	75.890524	12.648421
Uncorrected Total	9	11585.962200	
(Corrected Total)	8	4776.411800	

NOTE: The Jacobian is singular.

Parameter	Estimate	Asymptotic Std. Error	Asymptotic 95 % Confidence Interval	
			Lower	Upper
C1	82.7361891	3.538486955	74.07781715	91.39456098
C2	-425.8955237	18.600491653	-471.40931997	-380.38172735
C3	568.4246109	0.000000000	568.42461088	568.42461088
C4	4.2626182	1.630204583	0.27364637	8.25158796

Asymptotic Correlation Matrix

Corr	C1	C2	C3	C4
C1	1	-0.6533416	.	-0.549275114
C2	-0.6533416	1	.	-0.078347335
C3	.	.	1	.
C4	-0.549275114	-0.078347335	.	1

The SAS System

09:55 Wednesday, 11/1/2011

OBS	X	Y	S	CALS	DEV
1	0.40	1.143	7.63	5.2375	-31.3561
2	0.40	1.000	8.03	7.5885	-5.4977
3	0.40	1.000	8.52	7.5885	-10.9327
4	0.40	0.857	10.32	14.0854	36.4865
5	0.55	1.143	16.46	22.3537	35.8062
6	0.55	1.000	28.10	24.7047	-12.0829
7	0.55	0.857	33.70	31.2016	-7.4137
8	0.70	1.000	68.50	67.4000	-1.6058
9	0.70	1.000	66.30	67.4000	1.6591

The SAS System

09:55 Wednesday, 11/1/2011

Analysis Variable : DEV

N	Mean	Std Dev	Minimum	Maximum
9	15.8711933	14.5152533	1.6058394	36.4864605

The SAS System

09:55 Wednesday, 11/1/2011

VITAE

Name : Navaz Cheriya Malikakkal

Family Name : Cheriya Malikakkal

Date of Birth : 10 October, 1967

Permanent Address : Subaighar,
Chirakkal. P.O.
Cannanore-670 011
Kerala
India.

Schools Attended : St. Michael's Anglo-Indian Boys High School
Cannanore, Kerala.

Colleges Attended : Sree Narayana College
Thotada, Cannanore,
Kerala.

Tangal Kunju Musaliar College of Engg.
Quilon, Kerala.

King Fahd University of Petroleum & Minerals
Dhahran, Saudi Arabia.